

***Ex vivo* and *in vitro* characterization of natural killer
cell functions and receptor expression profiles
in obesity**

DISSERTATION

zur Erlangung des Doktorgrades der Naturwissenschaften
Doctor rerum naturalium (Dr. rer. nat.)

der

Naturwissenschaftlichen Fakultät I
– Biowissenschaften –
der Martin-Luther-Universität Halle-Wittenberg

vorgelegt

von Frau M.Sc. WIEBKE NAUJOKS

geb. am 15. Oktober 1985 in Magdeburg

Gutachter:

Prof. Dr. Stefan Hüttelmaier

Prof. Dr. Heike Kielstein

Prof. Dr. Roland Jacobs

Datum der Einreichung: 26.11.2019

Datum der Verteidigung: 06.07.2020

Eidesstattliche Erklärung

Hiermit versichere ich, WIEBKE NAUJOKS, an Eides statt, dass ich mich mit der vorliegenden Promotionsschrift erstmals um die Erlangung des Doktorgrades bewerbe und die Arbeit weder in gleicher noch ähnlicher Form einer anderen Prüfungskommission zur Begutachtung vorgelegt habe. Diese Promotionsschrift habe ich selbstständig und nur unter Verwendung der angegebenen Quellen und Hilfsmittel verfasst. Alle wörtlich und inhaltlich entnommenen Angaben wurden als solche kenntlich gemacht.

HALLE (SAALE), DEN

.....

WIEBKE NAUJOKS

Abstract

Obesity is associated with an increased risk for several cancer types and an impairment of the functionality of natural killer (NK) cells. This study aimed to investigate the impact of the body weight on NK cell receptor profiles and on NK cell cytotoxicity against colorectal and breast cancer cells in mice and humans by conducting two studies. Therefore, C57BL/6 mice received a high-fat diet (35% fat) to induce obesity or a normal-fat diet (4% fat) under restrictive and *ad libitum* feeding regimes. In the human study, peripheral blood mononuclear cells were isolated from normal weight, overweight and obese healthy blood donors.

Flow cytometric analysis revealed alterations in obese mice and humans, including the frequency of immune cell populations, the expression of activating and inhibitory NK cell receptors, and other NK cell-related markers on total NK cells and NK cell subsets compared to normal weight controls. Furthermore, the cytolytic NK cell activity against colorectal cancer cells was reduced in obese and overweight subjects as well as in obese mice.

The present study gives new insights into the influence of high-fat feeding on NK cell characteristics in mice. Furthermore, data revealed an altered NK cell phenotype, an impaired NK cell effector function against colon cancer cells, and NK cell subset alterations in obese and overweight individuals. These NK cell alterations and dysfunction might be an explanation for the higher colorectal cancer risk in obesity.

Keywords

Obesity · Overweight · Human natural killer cells · High-fat diet · Diet-induced obesity · Murine natural killer cells · Colorectal cancer · Postmenopausal breast cancer · NK cell phenotyping

Kurzfassung

Adipositas ist mit einem erhöhten Risiko für mehrere Krebsarten verbunden. Darüber hinaus wurde beschrieben, dass die Funktionalität von Natürlichen Killerzellen (NK- Zellen) unter Adipositas beeinträchtigt ist. Ziel dieser Arbeit war es, den Einfluss des Körpergewichts auf die NK-Zellrezeptorausstattung und auf die NK-Zellzytotoxizität gegenüber Darm- und Brustkrebszellen bei Mäusen und Menschen zu untersuchen. Dazu wurden C57BL/6-Mäuse zur Induktion einer Adipositas mit einer fettreichen Diät (35% Fett) gefüttert oder sie erhielten eine fettarme Diät (4% Fett) unter restriktiven und *ad libitum* Ernährungsregimen. Im Rahmen der Humanstudie wurden mononukleäre Zellen des peripheren Blutes aus gesunden normalgewichtigen, übergewichtigen und adipösen Blutspendern isoliert.

Die durchflusszytometrische Analyse der Blutzellen der adipösen Individuen im Vergleich zu den normalgewichtigen Individuen, zeigte Veränderungen bezüglich der Zellzahl verschiedener Immunzellpopulationen, der Expression von aktivierenden und hemmenden NK-Zellrezeptoren und anderen NK-Zell-bezogenen Markern auf den NK-Zellen und NK-Zell-Subpopulationen. Darüber hinaus war die zytolytische NK-Zellaktivität gegen Darmkrebszellen bei adipösen und übergewichtigen Spendern sowie bei adipösen Mäusen reduziert.

Die vorliegende Arbeit liefert zum einen neue Erkenntnisse zum Einfluss einer fettreichen Ernährung auf die Eigenschaften der NK-Zellen bei Mäusen. Darüber hinaus geben die Daten Hinweise auf eine Beeinträchtigung des NK-Zellphänotyps und der NK-Zell-Effektorfunktion gegen Darmkrebszellen bei adipösen und übergewichtigen Personen. Diese beobachteten Veränderungen und Dysfunktionen von NK-Zellen können zur Aufklärung des höheren Darmkrebsrisikos bei Adipositas beitragen.

Schlüsselwörter

Adipositas · Übergewicht · Humane Natürliche Killerzellen · Hoch-Fett-Diät · Diät-induzierte Adipositas · Murine Natürliche Killerzellen · Darmkrebs · Postmenopausaler Brustkrebs · NK-Zell-Phänotypisierung

Contents

EIDESSTATTLICHE ERKLÄRUNG.....	I
ABSTRACT	II
KURZFASSUNG.....	III
CONTENTS	IV
1 INTRODUCTION	1
1.1. Obesity prevalence and health consequences	1
1.2. Adipose tissue and metaflammation.....	2
1.3. The immune system	3
1.4. Natural killer cells in mice and man.....	3
1.4.1. Cytotoxic and regulatory phenotypes of NK cell subsets	3
1.4.2. NK cell regulation.....	4
1.4.3. NK cell receptors.....	6
1.4.4. NK cell effector responses	9
1.5. Obesity, NK cells and cancer.....	10
1.6. Aims and objectives	13
2 MATERIALS.....	14
2.1. Equipment and supplies.....	14
2.2. Chemicals and biological reagents	15
2.3. Buffers, media and solutions	15
2.4. Antibodies	16
2.5. Kits	18
2.6. Cell lines.....	19
2.7. Mouse strain.....	19
2.8. Animal diets	19
2.9. Software.....	19
3 METHODS	20
3.1. Cell lines and cell culture	20
3.2. Cell count and viability determination	21
3.3. Mouse husbandry, feeding regimes and experimental setup.....	21
3.4. Mouse anesthesia, sacrificing and probe sampling.....	22
3.5. Multiplex immunoassay of murine plasma cytokines	22
3.6. Buffy coat sample acquisition from human blood donors	23
3.7. Separation of peripheral blood mononuclear cells (PBMCs) from human buffy coats...23	

3.8. Cryopreservation and thawing of human PBMCs	23
3.9. Flow cytometric analysis.....	24
3.9.1. Principles of flow cytometry	24
3.9.2. Multicolor flow cytometry of murine peripheral blood immune cells	25
3.9.3. Multicolor flow cytometric analysis of human PBMCs.....	27
3.9.4. Flow cytometric measurements and gating strategies	32
3.10. Magnetic activated cell sorting (MACS).....	36
3.11. Real-time cell analysis systems xCELLigence and iCELLigence	36
3.11.1. Principles of the real-time cell analysis system.....	36
3.11.2. Cell proliferation assays	39
3.11.3. Cytotoxicity assays	40
3.12. Statistical analysis	41
4 RESULTS.....	42
4.1. Murine study.....	42
4.1.1. Dietary intakes.....	42
4.1.2. Body weights, visceral fat masses and organ weights.....	42
4.1.3. Cytokine plasma concentrations.....	44
4.1.4. Immune cell populations in murine blood	45
4.1.5. Phenotypes of primary murine peripheral blood NK cells.....	47
4.1.6. Determination of the optimal cell seeding number of CT26.WT target cells.....	48
4.1.7. Cytolytic activity of primary murine splenic NK cells against murine colon cancer cell line CT26.WT.....	49
4.2. Human study	51
4.2.1. Study population	51
4.2.2. Immune cell populations in peripheral blood mononuclear cells (PBMCs)	51
4.2.3. Expression of killer-cell immunoglobulin-like receptors (KIRs) on NK cells	53
4.2.4. Expression of natural cytotoxicity receptors (NCRs) on NK cells	54
4.2.5. Expression C-type lectin-like NKG2 receptors on NK cells	55
4.2.6. Expression of other inhibitory and activating receptors and adhesion molecules on NK cells	56
4.2.7. Expression of functional markers on NK cells.....	60
4.2.8. Co-expression analysis of different NK surface markers.....	66
4.2.9. Expression of intracellular NK cell markers	67
4.2.10. CD107a degranulation	70
4.2.11. Determination of the optimal cell seeding number of the human cancer target cells DLD-1 and MCF-7.....	71

4.2.12.	Determination of the appropriate effector to target (E:T) ratio	72
4.2.13.	Cytolytic activity of primary human NK cells against the human colon cancer cell line DLD-1	73
4.2.14.	Cytolytic activity of primary human NK cells against the human breast cancer cell line MCF-7.....	75
5	DISCUSSION	78
5.1.	Diet-induced obesity in C57BL/6 mice.....	78
5.1.1.	Dietary phenotypes.....	79
5.1.2.	DIO-impact on cytokine plasma levels.....	80
5.1.3.	DIO-impact on immune cell populations.....	80
5.1.4.	DIO-impact on murine NK cell population and NK cell subsets	82
5.1.5.	DIO-impact on receptor profiles of murine NK cells	83
5.1.6.	DIO-impact on cytolytic activity of murine NK cells	84
5.1.7.	Summary I.....	84
5.2.	Human study: Impact of the human body weight on NK cell receptor profiles and NK cell functionality.....	85
5.2.1.	Study population	85
5.2.2.	Altered distribution of immune cell populations in obese subjects.....	86
5.2.3.	Altered NK cells phenotypes in overweight and obese subjects	87
5.2.4.	Real-time cytotoxicity assays of primary human NK cells against colon and breast cancer cells.....	96
5.2.5.	Summary II	99
5.3.	Comparison between mice and man	100
5.4.	Conclusion and outlook.....	101
	REFERENCES.....	103
	ABBREVIATIONS	VI
	LEBENS LAUF	VIII
	DANKSAGUNG.....	XI

1 Introduction

1.1. Obesity prevalence and health consequences

Obesity and overweight represent an immensely growing health problem worldwide. The prevalence of overweight and obesity nearly tripled between 1975 and 2016 [1], with the result that almost one third of the world's population is considered to be overweight or obese [2]. As a global pandemic, obesity caused four million deaths and 120 million disability-adjusted life-years in 2015 [3]. In Germany, two-third of man (67%) and half of women (53%) are overweight. Moreover, a quarter of men and women (23% and 24%, respectively) are even obese [4]. The World Health Organization (WHO) predicts a continued rising of the global obesity prevalence within the upcoming years with great negative impact on health and social welfare systems. Kelly and colleagues have estimated that by 2030 up to 57.8% of the world's adult population (3.3 billion people) will be either overweight or obese, if the current trends continue [5].

The WHO defines overweight and obesity as an abnormal or excessive fat accumulation. In most cases, it is a preventable result of chronic positive energy balance, as dietary intake exceeds energy expenditure. Overweight and obesity are most often classified by the body mass index (BMI). The BMI is the quotient of body weight (kg) through the square of height (m²). According to the WHO definitions, a BMI of 25 – 29.9 kg/m² is considered overweight, or also called pre-obese, and a BMI of ≥ 30 kg/m² is considered obese. Normal weight is defined as a BMI of 18.5 – 24.9 kg/m².

What makes obesity and overweight so negative? In addition to consequences in social life, mobility and quality of life, obesity and overweight are associated with an increased morbidity and mortality [6, 7]. The higher the BMI, the higher the risk for related chronic noncommunicable diseases (NCDs), such as type 2 diabetes mellitus [8], cardiovascular [9] and neurodegenerative diseases [10], non-alcoholic fatty liver disease [11], as well as musculoskeletal [12] and kidney disorders [13]. In addition, the susceptibility to infections is increased in obese individuals [14]. Moreover, overweight and obesity are major risk factors for the development of several cancer types [15]. Worldwide, up to 20% of all cancer cases are attributable to an excess body weight [16]. For 2018, about 440,373 new cancer cases in Germany have been estimated by the German Cancer Research Center (DKFZ). Of these, 30,567 cases (6.9%) have been predicted to be attributable to overweight [15], including the most common cancers among men and women – colorectal cancer (CRC) and postmenopausal breast cancer, respectively [17]. It has been estimated that in 2018 about 7,080 (23.2%) new cases of colorectal cancer and 4,958 (16.2%) new cases of postmenopausal breast cancer will be attributable to overweight. [15].

The risk of CRC among obese individuals is 1.33 times as high as among normal weight individuals [18]. Obese postmenopausal women have a 1.39 times higher risk of developing breast cancer compared to normal weight postmenopausal women [19]. In addition, obesity is also associated with a higher risk for men to develop breast cancer [20].

The underlying biological mechanisms that link obesity and cancer still remain unclear. In recent years, several studies have focused on the obesity-cancer connection. Besides genetic factors [21], effects of nutritional components [22], reduced physical activity [23], obesity-related insulin resistance [24], increased secretion of sex hormones and cytokines by adipose tissue [25], also the chronic low-grade inflammation [26] and obesity-associated alterations of immune cell function [27] are discussed as possible mechanisms underlying the increased risk for several cancer types under obesity.

1.2. Adipose tissue and metaflammation

As indicated above, in obesity and overweight, the excess of adipose tissue (AT) plays a crucial role. In mammals, there are mainly two types of AT: the brown AT and the white AT [28]. Brown AT (BAT) engages thermogenesis to maintain body temperature and is particularly abundant in newborns, but in adults it is present only in small amounts [28]. White AT (WAT), the major fat depot, stores energy in form of triglycerides and is subdivided into two main types: the subcutaneous AT (SAT) and the visceral AT (VAT) [29]. Apart from its function as an energy storage, WAT is a large metabolically and immunologically active endocrine organ composed of adipocytes, as well as fibroblasts, endothelial cells and a wide range of immune cells and it is capable to synthesize AT-derived factors, called adipocytokines, such as leptin, adiponectin, resistin and visfatin [30]. In normal weight subjects, adipocytokines act as hormones or soluble mediators maintaining metabolic homeostasis [25]. Excess fat accumulation especially in VAT in overweight and obese subjects results in hypoxia, apoptosis and cell stress leading to an altered AT environment and metabolic disturbances. Hence, the dysregulated secretion of adipocytokines, i.e. leptin and adiponectin, as well as the increased secretion of proinflammatory cytokines, i.e. interferon- γ (IFN- γ), interleukin-6 (IL-6) and tumor necrosis factor- α (TNF- α), leads to an infiltration in AT by inflammatory immune cells [31]. These obesity-induced metabolic inflammatory processes of AT are termed as ‘metaflammation’, with local and systemic effects. Therefore it is further defined as a systemic chronic low-grade inflammatory state [32, 33]. This generally accepted obesity-induced state is associated with dysfunctions of several immune cells, like macrophages [34], T lymphocytes [35] and B lymphocytes [36]. Furthermore, various studies have shown an impaired functionality of natural killer (NK) cells in obese subjects [37–40].

1.3. The immune system

The immune system is a complex, dynamic defense system and commonly classified into two categories of immune responses – the innate immunity and the adaptive immunity – each consisting of different immune cell types. The specific adaptive immune response is mainly composed of T lymphocytes and B lymphocytes, conducting cell-mediated and humoral responses, respectively. The major cellular components of the nonspecific or less specific innate immune response are granulocytes (neutrophils, eosinophils, basophils), macrophages (and their precursors monocytes), NKT (natural killer T) cells and NK cells.

Over the last decades, a new and growing family of immune cells has been discovered and is still being characterized – the innate lymphoid cells (ILCs). All members of this family lack adaptive antigen receptors. However, they mirror the functions of T lymphocytes and therefore break up the classical view of immune responses with its two categories. Especially NK cells, as a member of this family, are considered as innate counterparts of CD8⁺ cytotoxic T cells [41, 42]. In the ILC nomenclature, NK cells are currently classified as a distinct subgroup next to four other subgroups of ILCs [43]. All ILC subgroups share a common lymphoid progenitor and are present in both humans and mice [44].

1.4. Natural killer cells in mice and man

As mentioned above, NK cells are an integral component of the innate immune system. However, they also display characteristics of the adaptive immune system by acquiring immunological memory [45]. Additionally, it is well accepted that NK cells play roles bridging both innate and adaptive immune responses [46–48]. NK cells are large granular effector lymphocytes and poised for rapid killing of virus-infected and malignant transformed cells without prior sensitization while remaining tolerant of normal cells [49]. Human and murine NK cells constitute 5 - 15% of peripheral blood mononuclear cells (PBMCs). They are also distributed in various lymphoid organs and nonlymphoid peripheral tissues as tissue-resident NK cells [50].

1.4.1. Cytotoxic and regulatory phenotypes of NK cell subsets

1.4.1.1. Human NK cell subsets

Human NK cells are characterized phenotypically by the presence of the surface markers CD56 and CD16 (CD: cluster of differentiation), while the T cell receptor CD3 is absent [51]. CD56, which is an immunoglobulin (Ig) superfamily glycoprotein, is an isoform of the human neural cell adhesion molecule (NCAM). The functional importance of different expression levels of CD56 on human NK cells is largely unknown [51], although CD56 is thought to mediate interactions between NK cells and target cells [52]. CD16, which is a transmembrane glycoprotein of the Ig superfamily, acts as a Fc (fragment crystallizable)- γ receptor on the NK cell surface,

namely Fc γ RIII. The activating receptor CD16 binds with low-affinity to the Fc region of the IgG antibody and therefore facilitates the antibody-dependent cellular cytotoxicity (ADCC) by binding on IgG-opsonized target cells through CD16 [53].

Based on the expression density of CD56 and CD16 on the NK cell surface, several subpopulations can be distinguished: CD56^{bright}CD16^{dim}, CD56^{bright}CD16^{bright}, CD56^{dim}CD16^{dim}, CD56^{dim}CD16^{bright} and CD56^{dim}CD16^{bright} NK cells [54–56]. In this study, the focus of human peripheral NK cells was on the two following subsets: The CD56^{dim}CD16^{bright} NK cells subset, with low density of CD56 and high density of CD16, that represents the majority of NK cells in the peripheral blood (~90%). Furthermore, the CD56^{bright}CD16^{dim} NK cell subset, with high density of CD56 and low density of CD16, that represents about 10% of peripheral NK cells was investigated. Besides the different levels of CD56 and CD16 expression, the two subsets differ in their immunological functionality. The major CD56^{dim}CD16^{bright} NK cell subset display high cytotoxicity through abundant perforin and granzyme granules in their cytoplasm, whereas the minor CD56^{bright}CD16^{dim} NK cell subset has more immunoregulatory function through their ability to produce abundant cytokines, including IFN- γ , TNF- α , IL-10, IL-13 and granulocyte-macrophage colony-stimulating factor (GM-CSF) [55, 57].

1.4.1.2. Murine NK cell subsets

In contrast to human NK cells, murine NK cells do not express CD56, whereas CD16 is also expressed on murine NK cells. Due to the lack of CD56 expression other concepts to discriminate murine NK cell subsets have been established. Therefore, and in contrast to human NK cells, murine NK cells and NK cell subsets are identified according to the level of expression of the integrin family member CD11b and of the TNF receptor superfamily member CD27. On this basis four murine NK cell subsets are distinguishable: CD11b^{dim}CD27^{dim}, CD11b^{low}CD27^{bright}, CD11b^{bright}CD27^{bright} and CD11b^{bright}CD27^{dim} [58, 59]. The previous stated order of the four different subsets corresponds to the stages of their maturation. The four murine NK cell subsets differ in their cytotoxic capacity. As maturation progresses, NK cells produce less cytokines, but become more cytotoxic against target cells [58, 60, 61].

1.4.2. NK cell regulation

NK cells express a variety of receptors which allow them to distinguish healthy cells from virus-infected, stressed or malignant transformed cells and to eliminate the latter ones. The NK cell effector function is orchestrated by a family of inhibitory and activating surface receptors as well as by adhesion molecules and other functional markers [62]. Figure 1 illustrates the recognition of target cells by NK cells and the NK cell responses based on missing-self and induced-self theories, which are explained in the following.

The activating and inhibitory receptors recognize cell-surface and extracellular-secreted ligands, e.g. major histocompatibility complex class-I (MHC-I) and MHC-I-related molecules and some non-MHC molecules [63]. Inhibitory receptors identify MHC-I molecules (human leukocyte antigens [HLAs] in humans and H-2 in mice), which are constitutively expressed by nucleated healthy cells and get lost upon infection or malignant transformation. The loss of MHC-I leads to a predominance of activating signals and therefore to NK cell activation and target cell lysis. This mode of effector activation corresponds to the ‘missing-self recognition’ hypothesis, initially postulated by Ljunggren and Kärre [64]. Therefore, MHC-I expression leads to self-tolerance of healthy cells. The ‘missing-self’ hypothesis was later complemented by the ‘induced-self recognition’ hypothesis. In addition to the missing inhibitory signals due to the lack of MHC-I expression, the concurrent expression of activating ligands is necessary for target cell killing and cytokine production by NK cells. Activating ligands are expressed by stressed cells upon infection or cellular transformation [62, 65]. Thus, the balance and imbalance between activating and inhibitory signals dynamically regulate the effector function of the NK cell [49, 66].

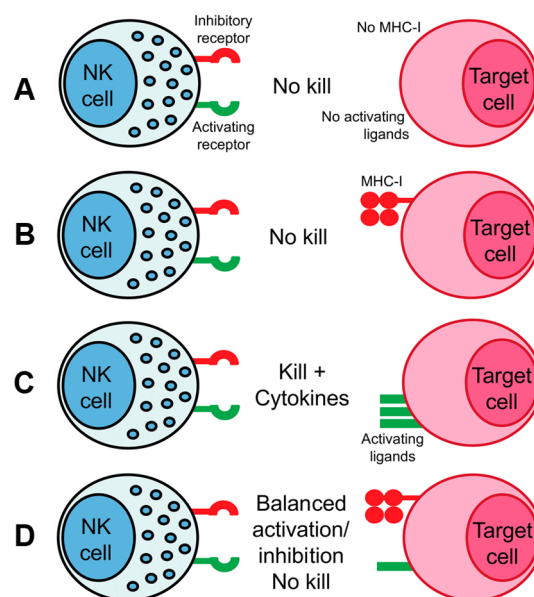


Figure 1: Recognition of target cells by NK cells: ‘missing-self’ and ‘induced-self’ theories. (A) NK cells do not respond if neither major histocompatibility complex class I (MHC-I) molecules nor activating ligands are expressed on target cells. This case usually applies for red blood cells. (B) NK cells do not respond if inhibitory receptors engage MHC-I molecules in the absence of ligands for activating receptors. This case usually applies for healthy cells. (C) Downregulation or loss of MHC-I and expression of activating ligands leads to potent NK cell activation resulting in target cell elimination either by direct killing through NK cell mediated cytotoxicity or indirectly through the secretion of pro-inflammatory cytokines, i.e. interferon- γ . This case usually applies to virus-infected or malignant transformed cells, known as ‘missing-self’ theory. (D) The outcome of NK cell responses depends on the balance of activating and inhibitory signaling. For example, ‘stressed’ cells can trigger NK cell activation by upregulation of ligands for activating receptors. Modified from [66].

1.4.3. NK cell receptors

Human and murine NK cells express a repertoire of various receptors. The majority is shared by human and mouse and some are expressed by only one species. However, the NK cell receptor repertoire essentially comprises three major receptor families: human killer immunoglobulin-like receptors (KIRs) and their murine counterparts, the lectin-like Ly49 receptors, as well as natural cytotoxicity receptors (NCRs) and C-type lectin-like receptors, which are described below.

Killer immunoglobulin-like receptors (KIRs)

Human KIRs belong to the Ig superfamily and bind MHC-I molecules. KIRs are highly polymorphic and encoded by the leukocyte receptor complex (LCR) on chromosome 19q13.4 [67]. The KIR family represents the leading group of negative regulators within the signaling pathways controlling NK cell lytic capacity [68]. It consists of twelve members and some allelic variants. The KIRs are type I transmembrane glycoproteins with two (KIR2D) or three (KIR3D) Ig-like extracellular domains with either a short (S) or long (L) cytoplasmic domain [69]. The length of the cytoplasmic domain determines the functional property of the KIRs. A long cytoplasmic domain mediates an inhibitory signal by the presence of one or two immunoreceptor tyrosine-based inhibitory motifs (ITIMs). In contrast, a short cytoplasmic domain mediates an activating signal through the receptor association with adaptor proteins bearing immunoreceptor tyrosine-based activating motifs (ITAMs) [69]. KIRs with two and three Ig domains bind to HLA-C/-G and HLA-A/-B molecules, respectively [63]. The most prominent inhibitory KIRs are KIR2DL1 (CD158a), KIR2DL2/DL3 (CD158b1/b2) and KIR3DL1/DL2 (CD158e/k), whereas KIR2DS4 is the most prominent activating KIR [70]. All four KIRs were analyzed in this study.

Ly49 receptors

Mice lack KIRs, but express structural divergent Ly49 receptors, which are functional homologs to human KIRs [63]. Ly49 receptors are type II transmembrane glycoproteins of the C-type lectin-like superfamily, the second major subfamily of NK cell receptors. They are encoded by a cluster of highly polymorphic and polygenic genes within the NK gene complex on mouse chromosome 6 [71]. The Ly49 gene family consists of two nomenclature systems, Ly49 and killer cell lectin-like receptor subfamily A (klra) [72]. Similarly to KIRs, Ly49 receptors also recognize MHC-I molecules, e.g. H2-D/ -K/ -L, and their inhibitory and activating function is characterized by the presence or absence of ITIM domains in their cytoplasmic tail. The Ly49 family comprises approximately 20 to 30 members, including several pseudogenes [72]. The type and level of Ly49 molecules are heterogeneously expressed in different mouse strains, such as C57BL/6 and BALB/c. The inhibitory Ly49 receptors, Ly49-C and Ly49-I as well as Ly49-F (expressed only by

C57BL/6) and the activating Ly49-H (expressed only by C57BL/6) were analyzed in the present study.

Natural cytotoxicity receptors (NCRs)

NCRs, including NKp30, NKp44, and NKp46 in humans and NKp46 in mice, are type I transmembrane glycoproteins of the Ig superfamily. All NCRs are activating and therefore they play a crucial role in the recognition and elimination of tumor cells by human and murine NK cells. NKp30 and NKp46 are constitutively expressed on all resting and activated NK cells, whereas NKp44 is only expressed on IL-2-activated NK cells [73, 74]. Although some interactions of the NCR with viral proteins have been described (e.g. NKp44 and NKp46 with influenza virus hemagglutinin), little is known about the NCR ligand specificities [75]. Among all receptors expressed by NK cells in mammals, NKp46 has been stated to be the best suitable and most specific NK cell marker [76, 77]. However, it is also expressed by a very small T cell subset [76]. NKp46 receptor has one Ig-like extracellular domain, while NKp30 and NKp44 have two Ig-like domains. All three NCRs contain positively charged amino acids in their transmembrane domain, which allow interaction with the ITAM-containing adapter molecules and thus deliver the activating signal [78].

C-type lectin-like receptors

The family of C-type lectin-like receptors comprises the subfamily of NK group 2 (NKG2) calcium-dependent lectin-like receptors, including CD94/NKG2 heterodimeric and NKG2D homodimeric receptors present on NK cells. They are type II transmembrane glycoproteins. The *CD94* and *NKG2*, also named *Klr* (killer cell lectin-like), genes are located on chromosome 12 in humans and chromosome 6 in mice and have, in contrast to *KIR* and *Ly49* genes, limited polymorphism [79]. The ligands of the NKG2 receptor family are non-classical MHC-I molecules (human HLA-E and murine Qa-1) [80, 81].

The heterodimeric C-type lectin-like receptors consist of a common subunit, CD94, which is disulfide-linked with either NKG2A, NKG2C, NKG2E (in humans and mice) or NKG2F (in humans) [79]. The inhibitory receptor CD94/NKG2A contains an ITIM in its cytoplasmic tail that mediates the inhibitory signal. Conversely, CD94/NKG2-C/-E/-F are activating members of this family with short cytoplasmic domains associated with adapter molecules bearing ITAM [82].

Another important member of the C-type lectin family is the homodimeric activating NK cell receptor NKG2D. Unlike the other NKG2 receptors, the NKG2D does not heterodimerize with CD94. NKG2D receptors, encoded by *Klrk1*, are known to recognize ligands with structural homology to MHC-1 molecules, e.g. human stress-induced ligands MHC-I chain-related (MIC)-A, MIC-B, and mouse ligands retinoic acid early inducible (REA)-1 and minor histocompatibility

complex H60 [79, 83, 84]. NKG2D is expressed on the surface of all mouse and human NK cells as well as on subsets of T and NKT cells [85]. In contrast to humans, in mice there are two isoforms of NKG2D – a short (NKG2D-S) and a long (NKG2D-L) form [86].

Other NK cell receptors and accessory molecules

In addition to the mentioned activating and inhibitory receptors of the Ig superfamily and the C-type lectin-like family, there are other receptors, such as co-receptors and adhesion molecules, which perform various functional tasks in the effector functions of the NK cell.

The surface markers CD2 (LFA-2: lymphocyte function-associated antigen 2), CD62L and CD226 (DNAM-1: DNAX accessory molecule 1) act as adhesion molecules and co-stimulators (CD2, CD226) on human and murine NK cells [87–89]. As a homing marker, CD62L (also known as L-selectin) plays an important role in the initial contact between NK cells in the bloodstream and the vascular endothelial cells during the migration and infiltration processes to lymph nodes as well as to normal and inflamed tissues [90, 91].

Further known co-stimulatory receptors are 2B4 (CD244) and NKp80, which are co-activating, as well as TIGIT (T-cell immunoreceptor with Ig and ITIM domains) and PD-1 (programmed cell death receptor-1), which are co-inhibitory [92–96]. These co-stimulatory receptors are all expressed in humans and mice, except for NKp80, which is absent in mice [93].

CD161 (also called NKRP1, NK1.1, KLRB1) is another C-type lectin-like receptor expressed by the majority of human and murine NK cells [63, 97]. In mice, five NKRP1 receptors have been described: NKRP1-A, -B, -C, -F, -G with either activating (-A, -C, -F) or inhibitory function (-B, -G) [63]. To date, only one NKRP1 receptor (NKRP1A) has been found in humans that inhibits NK cell-mediated cytotoxicity and cytokine secretion when bound to its ligand LLT-1 (lectin-like transcript-1) [98].

Markers for NK cell functionality are inhibitory receptor Siglec-7, which is absent in mice, and the activation-associated markers CD25, CD122, CD69 and CD107a, which are all expressed in humans and mice.

Siglec-7 engages sialic acid-containing ligands, which are often abundantly expressed on tumor cells protecting them from NK cell lysis [99]. CD25 and CD122 compose two of three subunits of the IL-2 receptor, namely the IL-2R α and IL-2R β chain, respectively. CD122 is constitutively expressed by NK cells to form the low-affinity IL-2 receptor composed of CD122 and CD132 (IL-2R γ chain), whereas CD25 expression is induced upon activation enabling the formation of the high-affinity IL-2 receptor, a trimeric receptor composed of CD25, CD122 and CD132 [100]. Binding of IL-2 stimulates NK cell proliferation and enhances NK cell cytotoxicity [101]. Therefore, CD25 expression was found to be positively correlated with NK cell cytotoxicity [102]. CD69 is an early activation marker in NK cells due to its rapid surface

expression after stimulation [103]. This stimulatory receptor triggers NK cell mediated cytolytic activity. Thus, it is used to identify functionally active NK cells [104]. Another important functional marker to identify NK cell activity is CD107a (LAMP-1: lysosomal-associated membrane protein-1). CD107a has found to be a marker of degranulation on NK cells. It is barely expressed on unstimulated NK cells, but it is highly upregulated upon stimulation of NK cells with MHC devoid cells, e.g. K562 leukemia cells, or with phorbol-12-myristate-13-acetate plus ionomycin. Furthermore, it has been demonstrated that both NK cell cytolytic activity and cytokine secretion correlate with CD107a surface expression [105, 106].

A number of NK cell markers, extra- and intracellular, are used to define the maturation and differentiation status by means of the different level of expression on or in the NK cell. Besides CD56 (only humans) and CD16 these include the surface receptors CD57 (only humans) and CD27 as well as the intracellular markers and transcription factors EOMES (eomesodermin), T-bet (T-cell associated transcription factor) and Blimp-1 (B lymphocyte-induced maturation protein-1). In mice, also the surface receptors CD11b, CD49b, and KLRG1 (killer cell lectin-like receptor G1) serve as maturation markers. Several studies have described five stages of NK cell maturation and differentiation in mice and humans, each characterized by a different composition and expression of the markers mentioned above [107–109]. A widely admitted hypothesis is that NK cell differentiation occurs as a linear multi-stage process, developing from NK cell precursors through immature $CD56^{\text{bright}}CD16^{\text{dim}}$ to the mature $CD56^{\text{dim}}CD16^{\text{bright}}$ NK cell subset [44, 54, 110]. $CD56^{\text{dim}}CD16^{\text{bright}}$ NK cells with high expression of CD57 are considered as terminally differentiated NK cells with high cytotoxic potential [111, 112]. In mice, immature NK cells express high levels of CD27 and lack KLRG1 and mature further in terminally differentiated $CD11b^+CD27^+KLRG1^+$ NK cells [113]. Recently, a sixth stage has been added defining the level of memory-like NK cells [44].

1.4.4. NK cell effector responses

As mentioned above, NK cells are essential for the elimination of carcinogenic and virus-infected cells. To perform this task, they secrete proinflammatory cytokines, i.e. IFN- γ and TNF- α , and they kill target cells upon activation. These two major functions are commonly attributed to distinct NK cell subsets – human $CD56^{\text{bright}}CD16^{\text{dim}}$ and $CD56^{\text{dim}}CD16^{\text{bright}}$ NK cell subsets and murine $CD11b^{\text{dim}}CD27^{\text{high}}$ and $CD11b^{\text{bright}}CD27^{\text{dim}}$ NK cell subsets, respectively.

Furthermore, NK cells are equipped with two direct killing mechanisms (Figure 2) [114]. Upon target cell recognition, NK cells form an immunological synapse – a extracellular space between NK and target cell – necessary to perform their cytolytic functions [115].

On the one hand, NK cells secrete their cytotoxic granules, stored in the cytoplasm, by exocytosis into the immunological synapse. These granules contain mainly pore-forming perforin and apoptosis-inducing granzyme B, but also granzyme A. The release of these cytolytic proteins subsequently induces target cell apoptosis by activating cell-death mechanisms. These include the activation of apoptotic cysteine proteases (caspases), but also caspase-independent apoptotic pathways. This granule-exocytosis pathway is mediated by the engagement of Fc γ CD16 receptor on an antibody-coated target cell or by the engagement of activating receptors on their cognate ligands on the target cell (Figure 2 A, B) [114, 116, 117].

On the other hand, direct target cell killing by NK cells is mediated by the stimulation of death receptors, e.g. Fas, on target cells by their corresponding ligands, e.g. Fas ligand (FasL), TNF-related apoptosis-inducing ligand (TRAIL), expressed on NK cells. This death receptor pathway potentially induces caspase-dependent apoptosis of the target cell (Figure 2 C-E) [114, 116, 118].

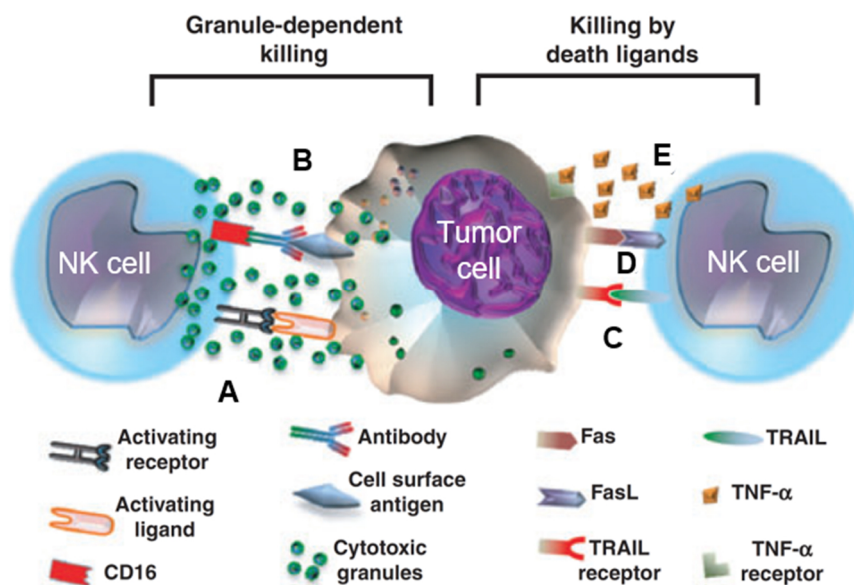


Figure 2: Two main direct killing mechanisms used by NK cells. The first cytotoxic mechanism is granule-dependent. Upon triggering of activation receptors by cognate ligands (A) or CD16 receptor engagement on antibody-coated target cell (B), the secretion of cytoplasmic granule toxins (perforin, granzymes) is induced by exocytosis. The second mechanism is mediated by binding of NK cell derived death-inducing ligands TRAIL (C) or FasL (D) or death-inducing cytokine TNF- α (E) on death receptors expressed on target cells. Both mechanisms potentially activate apoptosis pathways in target cells. Modified from [114]. TRAIL: Tumor necrosis factor-related apoptosis-inducing ligand. FasL: Fas ligand TNF- α : Tumor necrosis factor-alpha.

1.5. Obesity, NK cells and cancer

Many studies have shown that the incidence of obesity and overweight is associated with elevated susceptibilities for certain cancers, including endometrial cancer, esophageal adenocarcinoma, liver, prostate and kidney cancer as well as colorectal and post-menopausal breast cancer [15, 18, 19, 119–121]. The mechanisms underlying the increased tumor risk among obese

and overweight individuals are still poorly understood. Discussed causes are genetic predisposition, obesity-associated insulin resistance, elevated levels of AT-secreted hormones and cytokines, a low-grade inflammatory state and alterations in immune factors [122, 123]. Moreover, several studies have demonstrated that obesity is associated with an impaired NK cell functionality [37, 39, 40, 124–126].

In animal studies with diet-induced obese (DIO) and normal weight rats, alterations in the phenotype and tissue distribution pattern of NK cells in obese rats were observed. Interestingly, these obese-related alterations could be normalized by NK cell transfer into normal weight rats, indicating that the NK cell phenotype is strongly influenced by the metabolic environment [127]. A number of studies pointed out that the adipocytokine leptin plays a modulatory role on the innate and adaptive immune system [31, 38, 128, 129]. Obesity is associated with elevated plasma leptin levels [130]. In NK cells, leptin has both activation and regulatory functions [131]. *Ex vivo* studies on human and murine NK cells demonstrated that short-term stimulation with leptin enhances cytotoxicity and IFN- γ secretion of NK cells [37, 132]. In contrast, long-term stimulation with high leptin levels (comparable to obese conditions) reduced NK cell proliferation and functionality [132]. Further animal studies revealed negative impacts of a high-fat diet feeding on NK cell mediated target cell lysis [133–138]. For example, DIO rats with chemical induced colon cancer developed a higher tumor burden compared to normal weight rats, presumably mediated by the decreased expression of activating NKp46 and NKG2D receptors on splenic NK cells [137]. In addition, Spielmann *et al.* reported that DIO rats treated with breast cancer cells displayed a significantly reduced NK cell number and NK cell-tumor contacts in the lungs compared to the normal weight counterparts. Subsequently, decreased expression of the NKG2D on splenic NK cells was also determined and after three weeks significantly more lung metastasis were observed [138]. It could be shown that in obese rats, the reduced NK cell activity was associated with an impaired leptin-dependent signal transduction in NK cells [38]. Interestingly, the reduced cytotoxic NK cell activity in obese rats could be restored by energy restriction [139]. Analogous to animal experiments, human data similarly showed disturbed NK cell functionality in obese individuals. It has been demonstrated that AT NK cells as well as peripheral blood NK cells from obese subjects display an activated NK cell phenotype [39, 140]. However, despite the activated phenotype, NK cells showed less cytokine production and a reduced cytolytic activity against human myeloid leukemia cell line K562 and B cell lymphoma cell line Granta-519 *ex vivo* [39, 40]. In addition, reduced TRAIL expression as well as reduced degranulation activity in obese individuals have been demonstrated [37]. Moreover, an 11-year-follow-up study by Imai *et al.* indicated that a disturbed NK cell functionality is associated with an increased susceptibility for cancer in obese individuals [141]. However, the NK cell dysfunction in obesity seems to be partly

reversible after weight loss and fat mass reduction through a combined dietary and exercise program or after bariatric surgery [142, 143]. Furthermore, Barra and colleagues have shown that high intensity interval training (HIIT) can increase NK cell frequencies and restore NK cell functions in post-menopausal women and obese mice. Moreover, HIIT obese mice additionally challenged with breast cancer cells showed less metastatic tumor burden in their lungs [144].

In summary, both obese humans and animals display numerical and functional deficiencies in NK cells and exhibit an elevated risk of certain cancers. Since NK cells play an essential role in detection and elimination of cancerous cells, the altered function of NK cells may be a possible reason of the increased risk of cancer in obesity.

Until now, most of the few studies investigating the impact of obesity on NK cells have focused mainly on the total NK cell population in human and mice. Little research has been done on obesity-related impacts on the two main important human NK cell subpopulations CD56^{bright}CD16^{dim} and CD56^{dim}CD16^{bright} [125, 145]. Moreover, to date, scant has been paid to explore the impact of a pre-obese body weight on NK cell receptor expression and NK cell functionality. Furthermore, only a limited number of studies have addressed the link of obesity, NK cells and the elevated cancer risk [137, 138, 146]. Especially the elevated risk for the most frequent cancer among men and women - colorectal and postmenopausal breast cancer, respectively - in overweight and obese individuals has been largely overlooked. Previous research in examining the cytotoxicity of primary NK cells from obese individuals against human cancer cells has been mainly restricted to the myeloid leukemia cell line K562 [39, 40, 124, 126]. To date and to the author's knowledge, no study has investigated specifically the NK cell functionality of primary NK cells from overweight and obese subjects against human colon and breast cancer cell lines.

1.6. Aims and objectives

Obesity and overweight are global epidemics accompanied with life-threatening comorbidities. Actually, up to 49% of certain cancer types are associated with obesity and overweight [147], including colorectal cancer and postmenopausal breast cancer as the most common cancers among men and women, respectively [17]. However, the underlying pathophysiological mechanisms between overweight or obesity and the increased cancer risk remain unclear. NK cells display the first-line defense against virus-infected and malignant transformed cells. As mentioned above, several studies have explored the impact of obesity on NK cell functionality. Nevertheless, there is only limited research investigating the link of obesity, NK cells and cancer. To better understand the effect of elevated body weights on NK cells, murine and human models were used in this study.

The basic aims of this thesis were:

1. To explore the influence of *ad libitum* and restrictive feeding regimes of high-fat and normal-fat diets on phenotypes of C57BL/6 mice, with particular focus on possible differences in plasma cytokine levels, immune cell populations and receptor expression profiles of peripheral blood NK cells.
2. To investigate the impact of the human body weight on immune cell populations, NK cell receptor expression profiles and NK cell functionality of healthy blood donors with different body mass indexes (normal weight, overweight and obese).

In particular, the aim was to analyze the expression of relevant activating and inhibitory receptors and functional markers on the NK cells of the different diet/BMI groups in both models by multi-color flow cytometry. Moreover, the human study focused to analyze the expression of intra- and extracellular receptors, functional markers and accessory molecules on the CD56^{bright}CD16^{dim} and CD56^{dim}CD16^{bright} NK cell subsets. Additionally, the cytolytic activity of the isolated primary NK cells against colon and breast cancer cells should be investigated by real-time cell analysis systems.

2 Materials

2.1. Equipment and supplies

Table 1: Equipment and supplies.

Equipment	Company
Air flow cabinet, type: 'uniprotect'	EHRET Labor- und Pharmatechnik GmbH & Co. KG, Emmendingen, Germany
Anesthesia machine	UniVet porta, Groppler Medizintechnik Deggendorf, Germany
Bedding material (environmental enrichment)	LINOCREL FS 14, Altromin, Lage, Germany
Cell culture flasks CELLSTAR® (75 cm ²)	Greiner Bio-One GmbH, Frickenhausen, Germany
Cell strainer (70 µm)	Corning Science Mexico S.A. de C.V., Reynosa, Mexico
Centrifuge Heraeus Multifuge 4KR	Thermo Fisher Scientific Inc., Waltham, USA
Centrifuge Sigma 2-5	Sigma Laborzentrifugen GmbH, Osterode am Harz, Germany
CO ₂ incubator BINDER CB 210	BINDER GmbH, Tuttlingen, Germany
Flow cytometer LSR Fortessa™	Becton Dickinson GmbH, Heidelberg, Germany
Forma™ Series II water-jacketed CO ₂ Incubators	Thermo Fisher Scientific Inc., Marietta, USA
Inverted microscope Nikon Eclipse TS100	Nikon Instruments Inc., Melville, USA
Isoflurane induction chamber	UniVet porta, Groppler Medizintechnik Deggendorf, Germany
Isoflurane vaporizer	UniVet porta, Groppler Medizintechnik Deggendorf, Germany
Laminar flow cabinet Herasafe KS	Thermo Electron LED GmbH, Langenselbold, Germany
Leukosep® tubes	Greiner Bio-One GmbH, Frickenhausen, Germany
Luminex instrument	LiquiChip luminex 200 system (Qiagen, Hilden, Germany)
LUNA-fl™ Dual Fluorescence Cell Counter	Logos Biosystem, Annandale, USA
LUNA™ Cell Counting Slides	Logos Biosystem, Annandale, USA
MACS LS Column	Miltenyi Biotec GmbH, Bergisch Gladbach, Germany
Polycarbonate microisolator cage type 2, transparent	Zoonlab, Castrop-Rauxel, Germany
Polycarbonate-based igloo for mice (environmental enrichment)	Zoonlab, Castrop-Rauxel, Germany
QuadroMACS™ Separator	Miltenyi Biotec GmbH, Bergisch Gladbach, Germany
Round-bottom tubes (5 ml)	Corning Science Mexico S.A. de C.V., Reynosa, Mexico
RTCA iCELLigence™ 8-well E-Plate L8	ACEA Biosciences Inc., San Diego, USA
RTCA iCELLigence™ control unit (iPad with pre-installed analysis software)	ACEA Biosciences Inc., San Diego, & Apple Inc., Cupertino, USA
RTCA iCELLigence™ station	ACEA Biosciences Inc., San Diego, USA
RTCA xCELLigence™ control unit (laptop with pre-installed analysis software)	ACEA Biosciences Inc., San Diego, USA
RTCA xCELLigence™ station	ACEA Biosciences Inc., San Diego, USA
Trucount tubes	Trucount™ TubesBD Biosciences Inc., Sa Jose, USA

2.2. Chemicals and biological reagents

Table 2: Chemicals and biological reagents.

Name	Company
2-Mercaptoethanol (2-ME)	Merck KGaA, Darmstadt, Germany
7-AAD	Miltenyi Biotec GmbH, Bergisch Gladbach, Germany
Acridine orange (AO)/ Propidium iodide (PI) staining	Logos Biosystem, Annandale, USA
Ampuwa® (sterile injection-grade H ₂ O)	Fresenius Kabi Deutschland GmbH, Bad Homburg, Germany
Biocoll (Density: 1.077 g/ml)	Merck KGaA, Darmstadt, Germany
Dimethyl sulfoxide (DMSO)	Sigma-Aldrich Inc., St. Louis, USA
Dulbecco's Phosphate Buffered Saline (DPBS); w/o Ca ²⁺ , w/o Mg ²⁺	Merck KGaA, Darmstadt, Germany
eBioscience™ Brefeldin A solution (1000X)	Life Technologies GmbH, Darmstadt, Germany
Ethylenediaminetetraacetic acid tetrasodium salt (EDTA-Na ₄)	Carl Roth GmbH & Co.KG, Karlsruhe, Germany
FcR blocking reagent	Miltenyi Biotec GmbH, Bergisch Gladbach, Germany
Fetal bovine serum (FBS)	Merck KGaA, Darmstadt, Germany
IL-12, human recombinant	STEMCELL Technologies, Grenoble, France
IL-18, human recombinant	InvivoGen, Toulouse, France
IL-2, human recombinant	Novartis Pharma GmbH, Nuremberg, Germany
IL-2, mouse recombinant	reprokine Ltd., Rehovot, Israel
Ionomycin	Merck KGaA, Darmstadt, Germany
Isoflurane	Forene® 100% Abbott GmbH & Co. KG Wiesbaden, Germany
MACS BSA stock solution	Miltenyi Biotec GmbH, Bergisch Gladbach, Germany
MACS rinsing solution	Miltenyi Biotec GmbH, Bergisch Gladbach, Germany
Monensin Solution (1000X)	BioLegend, Coblenz, Germany
Penicillin-Streptomycin (10,000 U penicillin and 10 mg/ml streptomycin in 0.9% NaCl)	Sigma-Aldrich Inc., St. Louis, USA
Phorbol-12-myristate 13-acetate (PMA)	InvivoGen, Toulouse, France
Red blood cell (RBC) lysis buffer	c.c. pro GmbH, Oberdorla, Germany
RPMI medium 1640 L-glutamin	Corning Inc., Corning, USA
Sodium azide (NaN ₃)	Carl Roth GmbH & Co.KG, Karlsruhe, Germany
Sodium pyruvate	Merck KGaA, Darmstadt, Germany
Trypsin-EDTA	Sigma-Aldrich Inc., St. Louis, USA

2.3. Buffers, media and solutions

MACS buffer: 1450 ml MACS rinsing solution
75 ml MACS BSA stock solution
> sonicated for 15 min to degas buffer

Splenocyte culture medium: 500 ml RPMI-1640
10% (v/v) FBS
1% (v/v) Penicillin-Streptomycin
50 µM 2-Mercaptoethanol

FACS-buffer: 1x DPBS
1% (v/v) heat-inactivated FBS
2 mM EDTA
0.05% Sodium azide

2.4. Antibodies

Table 3: Fluorochrome-conjugated mononuclear antibodies for surface staining of murine peripheral blood immune cells for flow cytometric analysis.

Antigen	Fluorochrome	Isotype	Clone	Concentration [$\mu\text{g/ml}$]	Company
CD3e	PerCP	Hamster IgG1, κ	145-2C11	100.00	BD Biosciences Inc.
Ly-6G	BV510	Rat IgG2a, κ	1A8	50.00	BD Biosciences Inc.
Ly-6C	BV605	Rat IgM, κ	AL-21	200	BD Biosciences Inc.
KLRG1	BV421	Hamster IgG2, κ	2F1	50.00	BD Biosciences Inc.
CD8a	Alexa Fluor 700	Rat IgG2a, κ	53-6.7	100.00	BD Biosciences Inc.
CD4	PE-Cy	Rat IgG2a, κ	RM4-5	100.00	BD Biosciences Inc.
CD45	FITC	Rat IgG2b, κ	30F11	150.00	Miltenyi Biotec GmbH
CD27	PE	Hamster IgG	LG.3A10	30.00	Miltenyi Biotec GmbH
CD127	PE-Vio770	Rat IgG2a κ	A7R 34	30.00	Miltenyi Biotec GmbH
CD335 (NKp46)	APC	Rat IgG2a κ	29A1.4.9	150.00	Miltenyi Biotec GmbH
CD161 (NK1.1)	PE-Vio770	Mouse IgG2a κ	PK136	150.00	Miltenyi Biotec GmbH
CD122 (IL-2R β)	PE-Vio770	Rat IgG2b κ	TM- β 1	30.00	Miltenyi Biotec GmbH
CD94	APC-Vio770	Rat IgG2a κ	18d3	30.00	Miltenyi Biotec GmbH
CD69	PE	Hamster IgG1	H1.2F3	30.00	Miltenyi Biotec GmbH
CD314 (NKG2D)	PE-Vio770	Rat IgG1 κ	CX5	30.00	Miltenyi Biotec GmbH
CD62L	PE	Rat IgG2a κ	MEL14- H2.100	30.00	Miltenyi Biotec GmbH
Ly-49C/F/I/H	APC-Vio770	Hamster IgG	14B11	30.00	Miltenyi Biotec GmbH
CD244.2 (2B4 C57BL/6 alloantigen)	PE-Vio770	Recombin ant human IgG1	REA388	30.00	Miltenyi Biotec GmbH
CD19	APC-Vio770	Rat IgG2a κ	6D5	30.00	Miltenyi Biotec GmbH
CD11b	VioBlue	Recombin ant human IgG1	M1/70.15.1 1.5	33.00	Miltenyi Biotec GmbH
CD49b	PE	Rat IgM κ	DX5	30.00	Miltenyi Biotec GmbH

Table 4: Fluorochrome-conjugated mononuclear antibodies for surface staining of human peripheral blood mononuclear cells for flow cytometric analysis.

Antigen	Fluoro-chrome	Isotype	Clone	Concentration [µg/ml]	Company
CD2	APC-H7	Mouse IgG1, κ	RPA-2.10	25.00	BD Biosciences Inc.
CD3	VioGreen	Mouse IgG2a, κ	BW264/56	44.00	Miltenyi Biotec GmbH
CD4	BV605	Mouse IgG1, κ	RPA-T4	50.00	BD Biosciences Inc.
CD8	PE	Mouse IgG1, κ	RPA-T8	6.25	BD Biosciences Inc.
CD14	FITC	Mouse IgG2b, κ	MφP9	25.00	BD Biosciences Inc.
CD16	VioBlue	Human IgG1	REA423	55.00	Miltenyi Biotec GmbH
CD19	PE-Vio770	Mouse IgG1, κ	LT19	50.00	Miltenyi Biotec GmbH
CD25	PE-CF594	Mouse IgG1, κ	M-A251	50.00	BD Biosciences Inc.
CD27	PE	Hamster IgG, κ	LG.3A10	22.00	Miltenyi Biotec GmbH
CD56	APC	Human IgG1, κ	REA196	2.20	Miltenyi Biotec GmbH
CD57	BV 605	Mouse IgM, κ	NK-1	100.00	BD Biosciences Inc.
CD62L	PE-CF594	Mouse IgG1, κ	DREG-56	50.00	BD Biosciences Inc.
CD69	BV605	Mouse IgG1, κ	FN50	100.00	BioLegend Inc.
CD107a	PE	Mouse IgG1, κ	H4A3	3.00	BD Biosciences Inc.
CD158a (KIR2DL1)	PE-Vio770	Human IgG1, κ	REA284	88.00	Miltenyi Biotec GmbH
CD158b1/b2 (KIR2DL2/DL3)	PE	Mouse IgG2a, κ	DX27	27.50	Miltenyi Biotec GmbH
CD158e/k (KIR3DL1/DL2)	PE	Mouse IgG1, κ	5.133	77.00	Miltenyi Biotec GmbH
CD158i (KIR2DS4)	PE-Vio770	Mouse IgG1, κ	JJC11.6	88.00	Miltenyi Biotec GmbH
CD159a (NKG2A)	PE-Vio770	Human IgG1, κ	REA110	44.00	Miltenyi Biotec GmbH
CD159c (NKG2C)	PE	Human IgG1, κ	REA205	55.00	Miltenyi Biotec GmbH
CD161 (NK1.1)	BV605	Mouse IgG1, κ	HP-3G10	100.00	BioLegend Inc.
CD226 (DNAM-1)	BV605	Mouse IgG1, κ	DX11	200.00	BD Biosciences Inc.
CD244 (2B4)	PE-Cy7	Mouse IgG1, κ	C1.7	200.00	BioLegend Inc.
CD279 (PD-1)	BV605	Mouse IgG1, κ	EH12.2H7	100.00	BioLegend Inc.
CD314 (NKG2D)	PE-Vio615	Human IgG1, κ	REA797	100.00	Miltenyi Biotec GmbH

Antigen	Fluoro-chrome	Isotype	Clone	Concentration [µg/ml]	Company
CD328 (Siglec-7)	PE	Mouse IgG1, κ	6-434	50.00	BioLegend Inc.
CD335 (NKp46)	PE-Vio615	Human IgG1, κ	REA808	16.50	Miltenyi Biotec GmbH
CD336 (NKp44)	PE-Vio770	Mouse IgG1, κ	2.29	16.50	Miltenyi Biotec GmbH
CD337 (NKp30)	PE-Vio615	Human IgG1, κ	REA823	5.00	Miltenyi Biotec GmbH
NKp80 (KLRF1)	PE-Vio615	Human IgG1, κ	REA845	37.50	Miltenyi Biotec GmbH
TIGIT (VSTM3)	BV605	Mouse IgG2a, κ	A15153G	200.00	BioLegend Inc.

Table 5: Fluorochrome-conjugated monoclonal antibodies for intracellular staining of human peripheral blood mononuclear cells for flow cytometric analysis.

Antigen	Fluorochrome	Isotype	Clone	Concentration [µg/ml]	Company
TRAIL (CD253)	PE	mouse IgG1κ	RIK-2.1	55.00	Miltenyi Biotec GmbH
IFN-γ	PE-Cy7	Mouse IgG1, κ	4S.B3	200.00	BD Biosciences Inc.
Granzyme B	Alexa Fluor 700	Mouse IgG1, κ	GB11	200.00	BD Biosciences Inc.
Granzyme A	FITC	Mouse IgG1, κ	CB9	25.00	BD Biosciences Inc.
EOMES	PE	Mouse IgG1, κ	WD1928	50.00	Thermo Fisher Scientific Inc.
T-bet	PE-Cy7	Mouse IgG1, κ	4B10	200.00	BioLegend Inc.
Perforin	PE-CF594	Mouse IgG2b, κ	δG9	50.00	BD Biosciences Inc.
Blimp-1	DyLight 488	Mouse IgG1	3H2-E8	600.00	Invitrogen, Thermo Fisher Scientific Inc.

2.5. Kits

Table 6: Kits.

Kit	Company
Inside Stain Kit	Miltenyi Biotec GmbH, Bergisch Gladbach, Germany
Multiplex Immunoassay Kit (High Sensitivity 5-Plex Mouse ProcartaPlex™ Panel)	Thermo Fisher Scientific Inc., Darmstadt, Germany
NK Cell Isolation Kit, human/mouse	Miltenyi Biotec GmbH, Bergisch Gladbach, Germany

2.6. Cell lines

Table 7: Cell lines.

Name	Species	Type	Culture	Supplier
CT26.WT	Mouse	Colorectal adenocarcinoma cells	Adherent	ATCC, LGC Standards GmbH, Wesel, Germany
DLD-1	Human	Colorectal adenocarcinoma cells	Adherent	Sigma-Aldrich Inc., St. Louis, USA
K562	Human	Myelogenous leukemia cells	Suspension	Kindly provided by Prof. Roland Jacobs, Department of Clinical Immunology and Rheumatology, Hannover Medical School, Hannover, Germany
MCF-7	Human	Mammary adenocarcinoma cells	Adherent	Kindly provided by Dr. Matthias Bache, Department of Radiation Oncology, University Hospital Halle (Saale), Halle (Saale), Germany
NK-92	Human	Natural killer lymphoma cells (Interleukin-2-dependent)	Suspension	Kindly provided by Prof. Roland Jacobs, Department of Clinical Immunology and Rheumatology, Hannover Medical School, Hannover, Germany

2.7. Mouse strain

Strain	Nomenclature	Haplotype	Company
C57BL/6	C57BL/6NCrl	H-2 ^b	Charles River Laboratories Inc., Wilmington, USA

2.8. Animal diets

Table 8: Animal diets.

Diet	Company
Rodent diet with 10 kcal% fat (D12450J): 3.85 kcal/g 4.3 g fat/100 g (10 kcal% fat) 19.2 g protein/100g (20 kcal% protein) 67.3 g carbohydrate/100g (70 kcal% carbohydrate)	Research Diets Inc., New Brunswick, USA
Rodent diet with 60 kcal% fat (D12492): 5.24 kcal/g 34.9 g fat/100 g (60 kcal% fat) 26.2 g protein/100g (20 kcal% protein) 26.3 g carbohydrate/100g (20 kcal% carbohydrate)	Research Diets Inc., New Brunswick, USA
Standard-chow 1324	Altromin Spezialfutter GmbH & Co. KG, Lage, Germany

2.9. Software

Table 9: Software.

Software	Company
FACS Diva Version 7.0	Becton Dickinson GmbH, Heidelberg, Germany
Flowlogic Version 700.2A	Miltenyi Biotec GmbH, Bergisch Gladbach, Germany
FlowJo Version 8.7	FlowJo LLC, Ashland, USA
Graphpad Prism Version 6.07	GraphPad Software Inc., La Jolla, USA
Procartaplex-analyst 1.0 software	Affymetrix, eBioscience, San Diego, USA
RTCA Data Analysis Software Version 1.0	ACEA Biosciences Inc., San Diego, USA

3 Methods

3.1. Cell lines and cell culture

The human breast adenocarcinoma cell line MCF-7 was originally isolated from a 69-year-old woman with metastatic breast adenocarcinoma [148]. MCF-7 cells express low amounts of MHC class I molecules on their surface [149]. The human DLD-1 colorectal adenocarcinoma cell line was originally derived from a 45-year-old man with adenocarcinoma of the sigmoid colon [150]. DLD-1 cells lack MHC class I expression [151]. The K562 cell line was originally isolated from 53-year-old women with chronic myeloid leukemia in blast crisis [152]. This cell line is devoid of MHC class I molecules [105]. The NK-92 cells were originally isolated from a 50-year-old man with non-Hodgkin's lymphoma [153] and are characterized by a CD56^{bright}CD16⁻ phenotype, similar to the minor human NK cell subset in peripheral blood [154]. The CT26.WT murine colon carcinoma cell line was originally derived from BALB/c mice with chemically induced colon carcinoma [155]. CT26.WT cells express MHC class I molecules (H-2^d) [156].

The adherent target cell lines MCF-7, DLD-1 and CT26.WT were cultured in 75 cm² cell culture flasks with RPMI 1640 supplemented with 10% of heat-inactivated fetal bovine serum (FBS), 1% penicillin/streptomycin (10,000 U/ml penicillin; 10 µg/ml streptomycin) and 1% sodium-pyruvate (100 mM), further referred to as complete RPMI (cRPMI). Equally cultured with cRPMI were the K562 and NK-92 suspension cell lines. NK-92 cells were additionally supplemented with 200 U/ml recombinant human IL-2 (hIL-2). All cell lines were maintained under standard cell culture conditions (37 °C, humidified atmosphere, 5% CO₂) and were regularly tested for mycoplasma contamination. Passaging of adherent cells was performed at 80% to 90% of confluent monolayer using 0.05% trypsin/ethylenediaminetetraacetic acid (EDTA) solution after a washing step with 1x Dulbecco's Phosphate Buffered Saline (DPBS). The reaction was stopped by adding fresh media. After a centrifugation step for 5 min at 300 x g, the cell pellet was resuspended in 1 ml media, followed by cell counting (see 3.2). The respective volumes of cell suspension were used both for passaging the cells in a new flask and for seeding target cells in wells of the E-plates of the real-time cell analysis (RTCA) system (see 3.11). Suspension cells were passaged twice a week by mixing the resuspended pellet after a centrifugation step (5 min, 300 x g) in a ratio of 1:4 with fresh medium. The fourth and fifth passages of cells after thawing were used for further experiments, i.e. cell proliferation assays. After exceeding a passage number of 20 after thawing, target cell lines were discarded and new cells were thawed and cultured.

3.2. Cell count and viability determination

Cell yield and cell viability were consistently determined using an automated fluorescence cell counter LUNA-FL™. Cells were stained at an 1:11 ratio with acridine orange/propidium iodide (AO/PI) to label and distinguish live and dead cells.

3.3. Mouse husbandry, feeding regimes and experimental setup

Six weeks old male C57BL/6 mice (N = 34) were maintained on a 12 h light/12 h dark cycle with free access to pelleted food and water under controlled conditions at 23 ± 2 °C and $55 \pm 5\%$ relative humidity. Water was replaced twice a week and the cages were cleaned once a week. After one week of acclimatization under *ad libitum* feeding with regular rodent chow, mice were randomized into four groups (see Figure 3) and subsequently housed individually. Mice received either a normal-fat diet (NFD, 4% fat, 19% protein, 67% carbohydrate and 3.9 kcal/g metabolizable energy; D12450J), or to induce obesity, a high-fat diet (HFD, 35% fat, 26% protein, 26% carbohydrate and 5.2 kcal/g metabolizable energy; D12492 – matches the sucrose calories in D12450J) for 18 weeks (for diet compositions: see also Materials 2.8). Additionally, mice were fed the particular diet either *ad libitum* or they received 90% of the daily food intake of the corresponding *ad libitum* group (restrictive feeding regime). The restrictive feeding occurred every day at the same time – at the beginning of the active phase of mice.

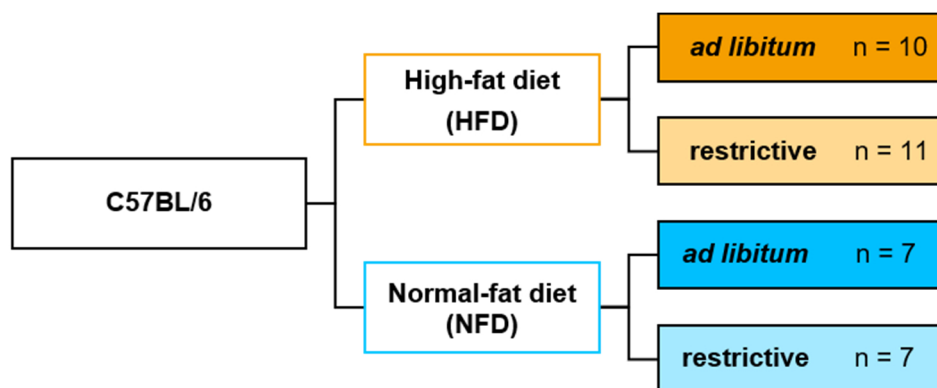


Figure 3: Diets and feeding regimes of mice with sample sizes per group.

Food intake was documented daily and the respective food amount for the restrictive fed groups was calculated. Daily intake of energy, fat, protein, and carbohydrate was calculated using the daily food intake and data of diet composition given by the manufacturer. Body weight was determined every week. All research and animal care procedures were approved by the local Animal Care Committee of the “Landesverwaltungsamt Halle” (reference number 42502–2-1341 MLU). Matthias Emde, Martin Allweyer and Wiebke Naujoks performed the animal handling and Dr. Julia Spielmann and Dr. Ina Bähr supervised the experiment and performed the animal killing.

3.4. Mouse anesthesia, sacrificing and probe sampling

Seventeen weeks after starting the feeding with NFD or HFD, final body weight was determined. Animals were sacrificed under general isoflurane inhalation anesthesia (1.5-2.0% v/v in O₂) by puncture of the cardiac ventricle and exsanguination. Blood was withdrawn, mixed with 10 µl EDTA anticoagulant and stored on crushed ice. A fraction of blood (~500 µl) was treated with red blood cell (RBC) lysis buffer (155 mM NH₄Cl, 10 mM KHCO₃ and 0.01% EDTA) to remove RBCs and to obtain leukocytes for following cytometric analysis (see 3.9.2). For plasma extraction, remaining fractions of blood were centrifuged for 10 min at 1200 x g and supernatant was stored at -80 °C for cytokine analysis (see 3.5). Visceral fat, spleen, liver, lung, heart, kidneys, brain, pancreas, skeletal muscle, small intestine, colon, abdominal aorta and thyroid gland were removed and visceral fat mass as well as organ weights were determined. Spleens of mice were kept in splenocyte culture medium (see 2.3) at 37 °C. Spleens were used immediately for further analysis (see 3.10). Tissue samples of VAT and organs including aorta, small and large intestine were either immediately frozen in liquid nitrogen and stored at -80 °C or preserved in 4% (v/v) formaldehyde (4 °C) for fixation and kept at 4 °C.

3.5. Multiplex immunoassay of murine plasma cytokines

Multiplex immunoassays enable the simultaneous determination of multiple protein targets, such as plasma cytokines in a single sample. It is based on the antibody-analyte-antibody complex principle of a sandwich ELISA (enzyme-linked immunosorbent assay) combined with the Luminex® xMAP® technology. The Luminex® xMAP® technology is based on paramagnetic beads that are internally dyed with two fluorophores of differing intensities. Furthermore, antigen-specific capture antibodies are bound to the beads, which bind the analyte-antigen. The subsequent attachment of labeled detection antibody to another analyte-antigen generates the measurable signal [157]. In this thesis, a 5-plex immunoassay was used to detect and quantify IL-2, IL-4, IL-6, IFN-γ and TNF-α in plasma samples of C57BL/6 mice of the different experimental groups.

Sample preparation and measurements were performed according to the manufacturer's instructions. In brief: First, antigen standards were prepared by serial dilutions for each cytokine and a 96-well-plate was pre-loaded with the antibody magnetic beads. Next, 25 µl of the provided universal assay buffer was added in each well, followed by 25 µl of prepared standards or plasma samples into the dedicated wells. For wells designated as blanks additional 25 µl buffer was added. After 30 min of shaking, an overnight incubation at 4 °C in the dark and another 30 min shaking step, the plate was washed three times and 25 µl of detection antibody solution was added to each well. After 30 min of incubation on a shaker and three wash steps, 50 µl streptavidin-PE solution was added to each well. After the same incubation and washing steps as before, 120 µl reading

buffer was added. Finally, the plate was incubated for 5 min on the shaker and subsequently ran on a Luminex instrument. Data were analyzed using the Procartaplex-analyst 1.0 software.

3.6. Buffy coat sample acquisition from human blood donors

A buffy coat (BC) is a by-product of a whole blood donation. It contains most of the leukocytes and platelets. Leukocyte-enriched BCs of 46 male blood donors were collected and provided by the Department of Transfusion Medicine at the University Hospital Halle (Saale). Before blood donation, each donor had to sign an agreement that allowed the use of blood for research purposes. Subjects were divided into three groups according to their body mass index (BMI: kg/m²) – normal weight with BMI 18.5 – 24.9 kg/m² (n = 14), overweight with BMI 25 – 29.9 kg/m² (n = 16) and obese with BMI ≥ 30 kg/m² (n = 16). Subjects suffering from any acute infection, immunosuppression or known malignant tumors were excluded by previous anamnesis.

3.7. Separation of peripheral blood mononuclear cells (PBMCs) from human buffy coats

At first, three different isolation procedures (direct overlay of BC on Biocoll separating solution, usage of SepMate™ tubes from StemCell Technologies and LeukoSep™ tubes from Miltenyi Biotec, both in combination with Biocoll solution) as well as procedure conditions were tested and compared to obtain the highest possible number of PBMCs from BCs equipped with high viability and low RBC and platelet contaminations. As a result of these experiments (data comparisons are not shown in this work), the PBMCs were isolated from BCs using LeukoSep™ tubes according to the manufacturer's instructions. In brief, 16 ml room-temperature (RT) Biocoll separating solution was preloaded in a 50 ml LeukoSep™ tube by centrifugation for 30 s at 1000 x g. The BC samples were diluted with equal volumes of RT DPBS and 25 ml of the diluted BC was added to a preloaded LeukoSep™ tube. The separating tubes were centrifuged for 10 min at 1000 x g without braking at RT. The PBMC-containing interphase was collected and washed twice with cold (4 °C) DPBS supplemented with 1% heat-inactivated FBS for 10 min at 350 x g at 4 °C, followed by a third washing and centrifugation step at 200 x g to get rid of platelets. To remove erythrocytes residues, the PBMC pellets were resuspended with 5 ml RBC lysis buffer and incubated for 5 min on ice followed by adding 15 ml DPBS supplemented with 1% heat-inactivated FBS, and a centrifugation step at 300 x g for 6 min at 4 °C. Before cell counting (see 3.2), the pellets were resuspended in 1 ml heat-inactivated FBS.

3.8. Cryopreservation and thawing of human PBMCs

Both cryopreservation as well as thawing of PBMCs of all donors were carried out according to a self-established and further standardized protocol based on experiments conducted by

Duske *et al.* 2011 [158], which minimized and normalized impairment of cell activity and viability due to those processes. Aliquots of purified PBMCs were cryopreserved and stored in liquid nitrogen. A freezing medium containing 90% heat-inactivated FBS and 10% dimethyl sulfoxide (DMSO) was freshly prepared and kept at 4 °C. Following centrifugation, the PBMCs were gently resuspended in freezing medium and aliquoted into cryovials with $\sim 5 \times 10^7$ PBMCs/vial. Cryovials were immediately transferred into a freezing container and stored at -80 °C for 24 h before being stored in liquid nitrogen until further analyzed.

For further analysis, the cryopreserved PBMCs were thawed in a 37 °C water bath until the liquid phase of the cell suspension was almost completely melted. Each cell suspension was transferred into a 50 ml tube and 10 ml cold (4 °C) cRPMI medium was added drop-wise within 60 s under constant mixing. Afterwards, the cells were centrifuged at 250 x g for 10 min at 4 °C. In the next washing step, after aspiration of the supernatant, the cell pellet was gently resuspended in 1 ml cold cRPMI before it was filled up to a 10 ml end volume and centrifuged under the same conditions as before. In the final washing step, the PBMCs were resuspended in 10 ml cold DPBS supplemented with 1% heat-inactivated FBS and centrifuged at 300 x g for 10 min at 4 °C. Thereafter, the washed PBMCs were counted (see 3.2) and subsequently used either for flow cytometric analysis (see 3.9.3) or NK cell isolation (see 3.10).

3.9. Flow cytometric analysis

3.9.1. Principles of flow cytometry

Flow cytometry provides a rapid analysis of various characteristics of individual cells in a high throughput rate. The information given is both quantitative and qualitative by simultaneously measuring and analyzing the cells optical and fluorescence properties. For this purpose, cells are labeled with fluorochrome-conjugated monoclonal antibodies, which bind specific proteins on cell membranes or inside cells. The fluorescently labeled cells are excited by a laser leading to light scattering and fluorescence emission.

The recorded scattered light is subdivided into forward-scattered light (FSC) and side-scattered light (SSC). The FSC is proportional to the cell surface area or size, whereas the SSC is proportional to the internal cell complexity or cell granularity. By FSC/SSC gating it is possible to differentiate between different cell types in a heterogeneous cell population.

The more fluorochrome-conjugated antibodies bind to their antigen on or in the cell, the more fluorescence is emitted and the higher the fluorescence intensity. By using different-colored lasers and the use of different fluorochromes, which differ in their wavelengths of the emitted fluorescence light, it is possible to detect different subpopulations as well as different surface markers on a specific cell population in a mixed cell suspension. In addition to the fluorochrome-

conjugated antibodies, fluorescent chemical compounds, such as propidium iodide (PI) and 7-aminoactinomycin-D (7-AAD), are used as fluorescence markers. Both compounds penetrate into dead and damaged cells and stable intercalate into the DNA. Therefore, they are used to exclude nonviable cells in flow cytometric analysis.

FSC, SSC and each different fluorescence emission intensities are recorded individually for each event. The measured data can be visualized by using different types of representative plots. In this study, dot and density plots, dot-plots with pseudo color and contour plots and histograms were chosen for illustration. In the dot plot, a two-dimensional data visualization, two different parameters are plotted – one along the X-axis and the other along the Y-axis. Each cell is plotted as a dot based on the measured values of the two parameters. In the density plot, the frequency of events in the different areas of a dot plot is made visible by color coding. The dot plot with pseudo color and contour plot allows the visualization of the frequency of events in lines and not in individual points, except for events (cells) outside the frequency ranges of given regions. Events with the same characteristics can be enclosed to a populations or subset by setting gates and the percentages of the specific population can be determined. The histogram shows only one parameter at a time. Here, the fluorescence intensity detected in a single channel (X-axis) is plotted against the number of events (the cell count; Y-axis) [159, 160].

In this thesis, flow cytometric analysis was used for the immunophenotyping of murine and human NK cells.

3.9.2. Multicolor flow cytometry of murine peripheral blood immune cells

The flow cytometric analysis was used to determine and quantify specific cell populations in the collected samples of murine whole blood, in particular leukocytes, lymphocytes, monocytes, granulocytes, B cells, T cells and T cell subsets, NK cells and NK cell subsets and to characterize the phenotype of the murine NK cells. PD Dr. habil. Dagmar Quandt kindly performed the gating of the murine data and provided the obtained flow cytometric results for further statistical analysis.

3.9.2.1. Surface staining and determination of extracellular markers

Heparinized murine whole blood was stained with an appropriate combination of fluorochrome-conjugated monoclonal antibodies as master mixes to analyze different leukocyte subsets and NK cell receptor surface expression by flow cytometry. The flow cytometry panel used in this study is listed in Table 10. Initially, 70 μ l of whole blood was mixed with 50 μ l antibody master mix and incubated for 15 min at RT protected from light. Next, RBC lysis was conducted by adding 980 μ l RBC lysis buffer and incubated for 10 min at RT. Samples were washed twice by adding 150 μ l FACS (fluorescence activated cell sorting) buffer and centrifugation at 4 °C, 250 x g for 5 min. After a final washing step, all samples were resuspended in 300 μ l FACS buffer and kept

at 4 °C in the dark until flow cytometric analysis. In order to clearly distinguish the different immune cell populations in each tube and to identify only specific surface molecules on NK cells, a backbone antibody staining was used in each panel. This backbone antibody staining consisted of specific antibodies against leukocytes (CD45), T lymphocytes (CD3) and NK cells (CD335). Tube 8 contained only these three antibodies and served as Fluorescence Minus One (FMO) control, which is essential in multicolor analysis.

For determining absolute counts of leukocytes in murine blood, Trucount tubes with a known number of fluorescent beads were used, instead of normal FACS tubes, followed by identical steps as mentioned above. Here, after addition of 600 µl RBC lysis buffer no additional step was needed prior to analysis.

Table 10: Panel description and specification of antigens, fluorochromes and quantity of antibodies used for surface staining of murine whole blood in 120 μ l.

Tube/Panel	Antigen	Fluorochrome	Antibody amount [μ l]
1	Backbone*		
	CD8	Alexa Fluor 700	1.00
	Ly-6G	BV510	1.00
	Ly-6C	BV605	1.00
	CD19	APC-Vio770	6.66
	CD4	PE-Cy7	1.00
	CD49b	PE	4.00
	CD11b	VioBlue	4.00
2	Backbone*		
	CD127	PE-Cy7	6.66
	CD11b	VioBlue	4.00
	CD27	PE	6.66
3	Backbone*		
	Ly-49C/F/I/H	APC-Vio770	6.66
	CD11b	VioBlue	4.00
	CD161 (NK1.1)	PE-Vio770	6.66
	CD27	PE	6.66
4	Backbone*		
	CD314 (NKG2D)	PE-Vio770	6.66
	CD11b	VioBlue	4.00
	CD27	PE	6.66
5	Backbone*		
	CD11b	VioBlue	4.00
	CD27	PE	6.66
6	Backbone*		
	CD94	APC-Vio770	6.66
	KLRG1	BV421	1.00
	CD122	PE-Vio770	6.66
	CD69	PE	6.66
7	Backbone*		
	CD244.2	PE-Vio770	6.66
	CD62.L	PE	6.66
8	CD335 (NKp46)	APC	4.00
	CD45	FITC	4.00
	CD3	PerCP	1.00
Backbone-staining*/ Fluorescence Minus One (FMO) control			

*Backbone-staining with CD335-APC, CD45-FITC and CD3-PerCP with same antibody amounts present in tubes 1 to 7. Volumes of tubes less than 50 μ l were adjusted to 50 μ l with FACS buffer.

3.9.3. Multicolor flow cytometric analysis of human PBMCs

The flow cytometric analysis was used to determine and quantify specific cell populations of human PBMCs, in particular monocytes and lymphocytes, and to characterize the phenotype of NK cells, especially of the two main NK cell subsets CD56^{bright}CD16^{dim} and CD56^{dim}CD16^{bright} NK cells.

3.9.3.1. Surface staining and determination of extracellular markers

Live, unstimulated human PBMCs of blood donors of three different BMI groups were stained with an appropriate combination of fluorochrome-conjugated monoclonal antibodies to analyze NK cell receptor surface expression by flow cytometry. Therefore, eight antibody panel tubes of differently fluorescently labeled monoclonal antibodies were prepared in a volume of 50 μ l each per donor (see Table 11). Tube 1 was used to differentiate immune cell populations within PBMCs. For this purpose, specific antibodies against antigens of T lymphocytes (CD3), T helper cells (CD4), cytotoxic T cells (CD8), NKT cells (CD3 and CD16), monocytes (CD14), B lymphocytes (CD19) and NK cells (CD16 and CD56) were used. The tubes 2 to 8 included fluorochrome-conjugated antibodies to stain for specific surface NK cell markers. In order to clearly distinguish the different immune cell populations in each tube and to identify only specific surface molecules on NK cells, a backbone antibody staining was used in each panel. This backbone antibody staining consisted of specific antibodies against T lymphocytes (CD3), monocytes (CD14) and NK cells (CD16 and CD56). Tube 9 contained only these four antibodies and served as FMO control, which is essential in multicolor analysis. FMO control is required for accurately discriminating positive from negative signals [161]. For surface staining, 1×10^6 PBMCs in 50 μ l FACS buffer per tube and donor were used. 1×10^7 PBMCs (required cell number for 9 tubes plus reserve) were resuspended in 80 μ l FACS buffer supplemented with 20 μ l FcR blocking reagent and incubated for 10 min on ice to block non-specific FcR-binding. Next, the samples were adjusted to a volume of 500 μ l by adding FACS buffer. The PBMC suspension was transferred into nine FACS tubes and incubated with the respective antibody mix (50 μ l per tube) for 15 min at 4 $^{\circ}$ C protected from light. After washing with 1 ml FACS puffer and a centrifugation step (300 x g, 4 $^{\circ}$ C, 5 min), the pellets were resuspended in 250 μ l FACS buffer. All samples were stained with 2.5 μ l 7-AAD prior to analysis. Until measurement, the samples were stored at 4 $^{\circ}$ C in the dark.

Table 11: Panel description and specification of antigens, fluorochromes and quantity of antibodies used for surface staining of peripheral blood mononuclear cells (PBMCs) in 100 μ l.

Tube	Antigen	Fluorochrome	Antibody amount [μ l]
1 PBMC immunophenotyping	Backbone*		
	CD4	BV605	2.00
	CD8	PE	8.00
	CD19	PE-Vio770	2.00
2 NK cell immunophenotyping	Backbone*		
	CD107a	PE	10.00
	CD336 (NKp44)	PE-Vio770	7.00
	CD337 (NKp30)	PE-Vio615	10.00
	TIGIT	BV605	4.00
3 NK cell immunophenotyping	Backbone*		
	CD57	BV605	1.50
	CD159a (NKG2A)	PE-Vio770	9.09
	CD159c (NKG2C)	PE	9.09
	CD314 (NKG2D)	PE-Vio615	5.00
4 NK cell immunophenotyping	Backbone*		
	CD2	APC-H7	2.50
	CD25	PE-CF594	5.00
	CD158a (KIR2DL1)	PE-Vio770	9.09
	CD158b (KIR2DL2/DL3)	PE	9.09
	CD279 (PD-1)	BV605	2.00
5 NK cell immunophenotyping	Backbone*		
	CD69	BV605	2.00
	CD158i (KIR2DS4)	PE-Vio770	7.00
	NKp80 (KLRF1)	PE-Vio615	3.00
6 NK cell immunophenotyping	Backbone*		
	CD62L	PE-CF594	2.50
	CD158e/k (KIR3DL1/DL2)	PE	9.09
	CD226 (DNAM-1)	BV605	2.50
	CD244 (2B4)	PE-Cy7	2.50
7 NK cell immunophenotyping	Backbone*		
	CD27	PE	7.00
	CD161 (NK1.1)	BV605	5.00
	CD295 (LEPR)	PE-Vio770	9.09
	CD335 (NKp46)	PE-Vio615	5.00
8 NK cell immunophenotyping	Backbone*		
	CD328 (Siglec-7)	PE	7.50
9 Backbone-staining* / Fluorescence Minus One (FMO) control	CD3	VioGreen	9.09
	CD14	FITC	5.00
	CD16	VioBlue	5.00
	CD56	APC	5.00

*Backbone-staining with CD3-VioGreen, CD14-FITC, CD16-VioBlue and CD56-APC with same antibody amounts present in tubes 1 to 8. Volumes of tubes less than 50 μ l were adjusted to 50 μ l with FACS buffer.

3.9.3.2. Intracellular staining and IFN- γ detection

Freshly thawed PBMCs of blood donors of three different BMI groups were resuspended in pre-warmed cRPMI, cell numbers and cell viability were determined by AO/PI staining. PBMCs were seeded with a density of 2×10^6 cells/ml per well in a 24-well plate. PBMCs were stimulated either with 10 ng/ml interleukin-12 (IL-12) in combination with 50 ng/ml interleukin-18 (IL-18) overnight at 37 °C under 5% (v/v) CO₂ or with 50 ng/ml phorbol-12-myristate-13-acetate (PMA) and 1 μ g/ml ionomycin on the next morning for 4 h. Prior to the 4 h incubation, 10 μ g/ml brefeldin A was added to the cells to inhibit secretion of IFN- γ . Unstimulated PBMCs served as controls. After 4 h of stimulation, samples were washed, incubated with FcR blocking reagent and stained with the following extracellular staining antibodies: CD3 conjugated with VioGreen, CD16 conjugated with VioBlue, CD56 conjugated with APC and CD14 conjugated with APC-Vio770. This backbone-staining served for negative (CD3 and CD14) and positive (CD16 and CD56) NK cell selection for later analysis. Live/Dead Fixable Yellow was added to all sample tubes to allow discrimination between live and dead cells. The extracellular staining was performed for 15 min at 4 °C in the dark. Afterwards, cells were washed, followed by fixation and staining for intracellular markers via the inside stain kit according to manufacturer's instructions. Briefly, cells were fixated with inside fix buffer for 20 min in the dark at RT. After centrifugation (300 x g, 5 min), the supernatant was discarded. The cells were resuspended with inside perm buffer, followed by centrifugation (300 x g, 5 min). Subsequently, stimulated and unstimulated PBMCs were intracellularly stained for 20 min at RT protected from light with the respective fluorochrome-conjugated antibody panel listed in Table 12. After washing with inside perm, cells were resuspended in 250 μ l FACS buffer and kept cold and protected from light until measurement. Unstimulated PBMCs were also stained extra- and intracellularly and served as negative controls as well as for the determination of intracellular expression of EOMES, T-bet, perforin and Blimp-1.

Table 12: Panel description of intracellular staining of human peripheral blood mononuclear cells (PBMCs) in 100 μ l inside perm buffer with extracellular staining for lineage differentiation.

Tube/Panel	Treatment	Antigen	Fluorochrome	Antibody amount [μ l]
1a	Unstimulated	CD3	VioGreen	9.09
		CD14	FITC	5.00
		CD16	VioBlue	5.00
		CD56	APC	5.00
1b	Unstimulated	Backbone*		
		TRAIL (CD253)	PE	9.09
		IFN- γ	PE-Cy7	0.25
		Granzyme B	AlexaFuor700	1.00
		Granzyme A	FITC	20.00
1c	Unstimulated	Backbone*		
		EOMES	PE	8.00
		T-bet	PE-Cy7	1.25
		Perforin	PE-CF594	5.00
		Blimp-1	DyLight488	1.33
2a	IL-12+IL-18	Backbone*		
2b	IL-12+IL-18	Backbone*		
		TRAIL (CD253)	PE	9.09
		IFN- γ	PE-Cy7	0.25
		Granzyme B	AlexaFuor700	1.00
		Granzyme A	FITC	20.00
3a	PMA+ionomycin	Backbone*		
3b	PMA+ionomycin	Backbone*		
		TRAIL (CD253)	PE	9.09
		IFN- γ	PE-Cy7	0.25
		Granzyme B	AlexaFuor700	1.00
		Granzyme A	FITC	20.00

*Backbone-staining (extracellular) with CD3-VioGreen, CD14-FITC, CD16-VioBlue and CD56-APC with same antibody amounts present in tubes 1a-c, 2a-b, 3a-b.

Tubes 2a, 2b: Treatment of human PBMCs with 10 ng/ml IL-12 plus 50 ng/ml IL-18 overnight.

Tubes 3a, 3b: Treatment of human PBMCs with 50 ng/ml Phorbol-12-myristate 13-acetate (PMA) plus 1 μ g/ml ionomycin for 4 h.

3.9.3.3. CD107a degranulation assay

CD107a expression on NK cells was measured to analyze NK cell degranulation. PBMCs stimulated overnight with 10 ng/ml IL-12 plus 50 ng/ml IL-18 were washed and treated afterwards either with K562 cells with an effector-to-target (E:T) ratio of 15:1 or without target cells in 500 μ l cRPMI. The E:T ratio of 15:1 was assessed as the optimal ratio by pretests. Additionally, IL-12 plus IL-18-untreated PBMCs were co-incubated with K562 cells with an E:T ratio of 15:1 to analyze the impact of pre-priming on effector cells in context with CD107a expression. Furthermore, PBMCs stimulated only with PMA (50 ng/ml) plus ionomycin (1 μ g/ml) served as positive controls for CD107a expression. Prior to 4 h incubation CD107a-PE antibody and secretion inhibitors monensin (5 μ g/ml) and brefeldin A (5 μ g/ml) were added directly into the

medium. For every condition, CD107a-unstained controls were present as well as unstimulated samples to detect spontaneous degranulation. After 4 h of incubation at 37 °C and 5% CO₂, samples were washed and extracellular backbone immunofluorescence staining was performed as described above (see 3.9.3.1).

3.9.4. Flow cytometric measurements and gating strategies

All samples (murine and human) were measured by using the flow cytometry analyzer BD LSRFortessa™. This device has four excitation lasers with wavelengths of 355, 405, 488, and 640 nm, which stimulate the fluorochromes conjugated to the specific antibodies. Measured data were analyzed using the analyzers internal BD FACS Diva™ software version 7.0 or external software - Flowlogic™ version 700.2A or FlowJo version 8.7.

Due to the fact that emission spectra of fluorochromes can overlap, compensation was performed prior to all measurements. This procedure allows the correction of signal overlaps (spillovers) of fluorochromes detected in other channels than their respective channel. Thus, a falsification of the measurement can be prevented. For compensation, all fluorochromes used in this study were tested. Since they were several antibodies conjugated to identical fluorochromes, one of them was representatively chosen. Therefore, a more abundant antigen was selected to ensure good signals for the subsequent compensation. The compensation of the overlapping fluorescence spectra was carried out directly in the FACS Diva 7.0 software. This procedure was performed for each experiment separately (murine surface stainings, human surface and intracellular stainings). In particular: For immunophenotyping of murine whole blood cells, compensation was conducted by staining 30 µl of murine whole blood with 70 µl of the respective fluorochrome-conjugated antibody diluted in FACS buffer according to the protocol in chapter 3.9.2, except that no 7-AAD was added to the probes prior to analysis. For immunophenotyping of human PBMCs by extra- and intracellular staining, 250,000 PBMCs and 500,000 PBMCs, respectively, were stained with the respective fluorochrome-conjugated antibody according to the protocols for surface staining (see 3.9.3.1) and intracellular staining (see 3.9.3.2), except that no 7-AAD or Live/Dead Fixable Yellow dyes were added prior to analysis.

For the immunophenotyping of primary murine blood NK cells 50,000 – 100,000 events were measured per panel. The NK cell phenotyping of extracellular markers was based on the gating strategy illustrated in Figure 4.

For the immunophenotyping of primary human NK cells by flow cytometric analysis 100,000 events were measured per panel. The NK cell phenotyping of extra- and intracellular markers was based on the gating strategies depicted in Figure 5 and Figure 6, respectively.

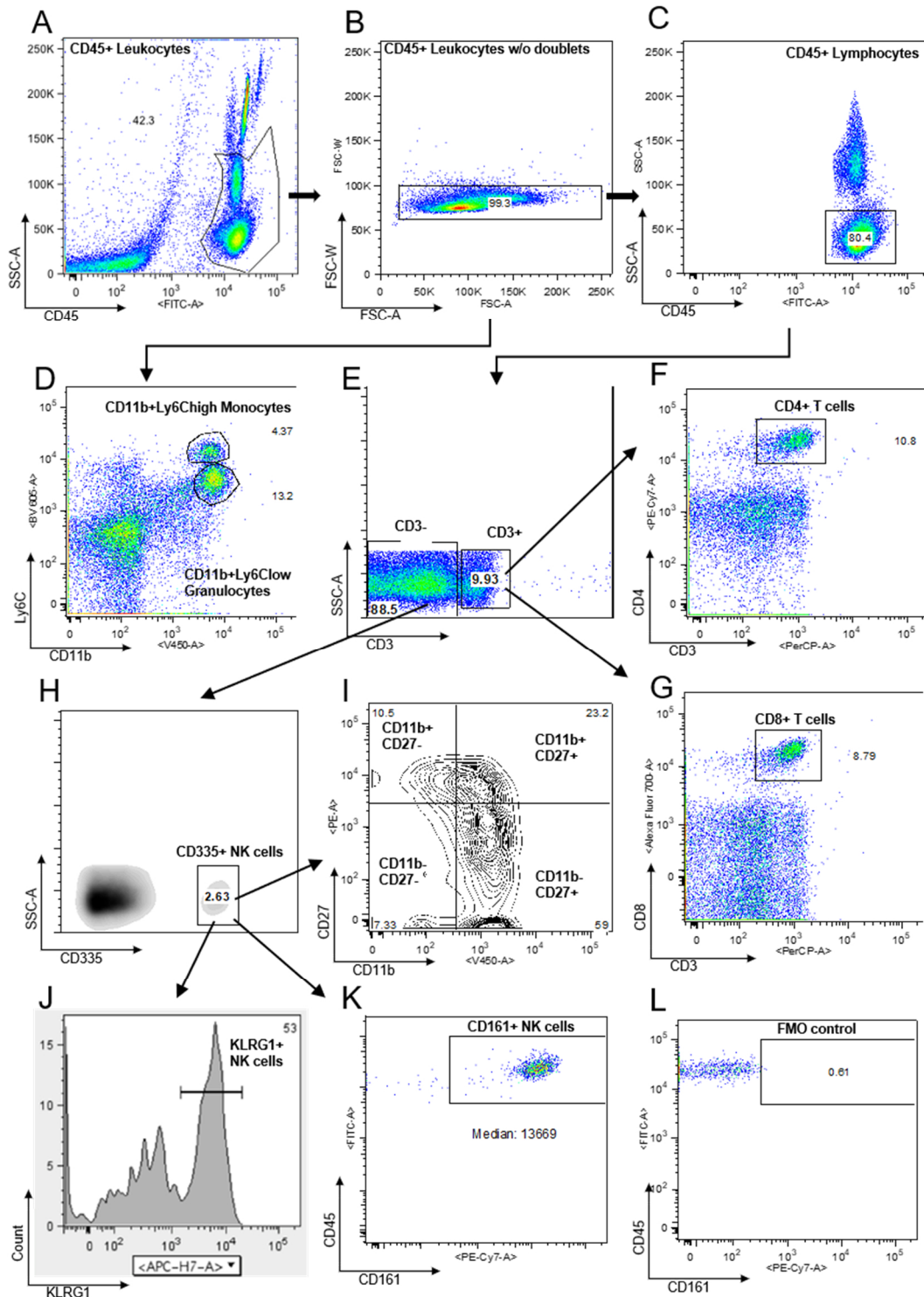


Figure 4: Gating strategy used to identify immune cell populations, NK cell subsets and NK cell surface marker expression from CD57BL/6 mice. Lymphocytes were identified by their size and granularity in the FSC/SSC dot plot (A), followed by doublet exclusion (B), and gating of CD45⁺ leukocytes (C). Based on the single cell lymphocyte gate CD11b⁺Ly6C^{high} monocytes and CD11b⁺Ly6C^{low} granulocytes (D) were classified. Based on the lymphocyte gate, CD3⁻ and CD3⁺ lymphocytes (E) were classified. CD3⁺CD4⁺ helper T cells (F) and CD3⁺CD8⁺ cytotoxic T cells (G) were selected from the CD3⁺ fraction. CD335⁺ NK cells were selected from the CD3⁻ fraction (H). On the basis of the expression of CD11b and CD27, the total NK cell population was further differentiated into the four murine NK cell subsets (I). The expression of each NK cell marker was assessed on the CD335⁺ NK cell fraction – here represented by histogram analysis of KLRG1 expression (J) and CD161 median fluorescent intensity (K). FMO control was used to determine positive staining (L). The above plots are representative.

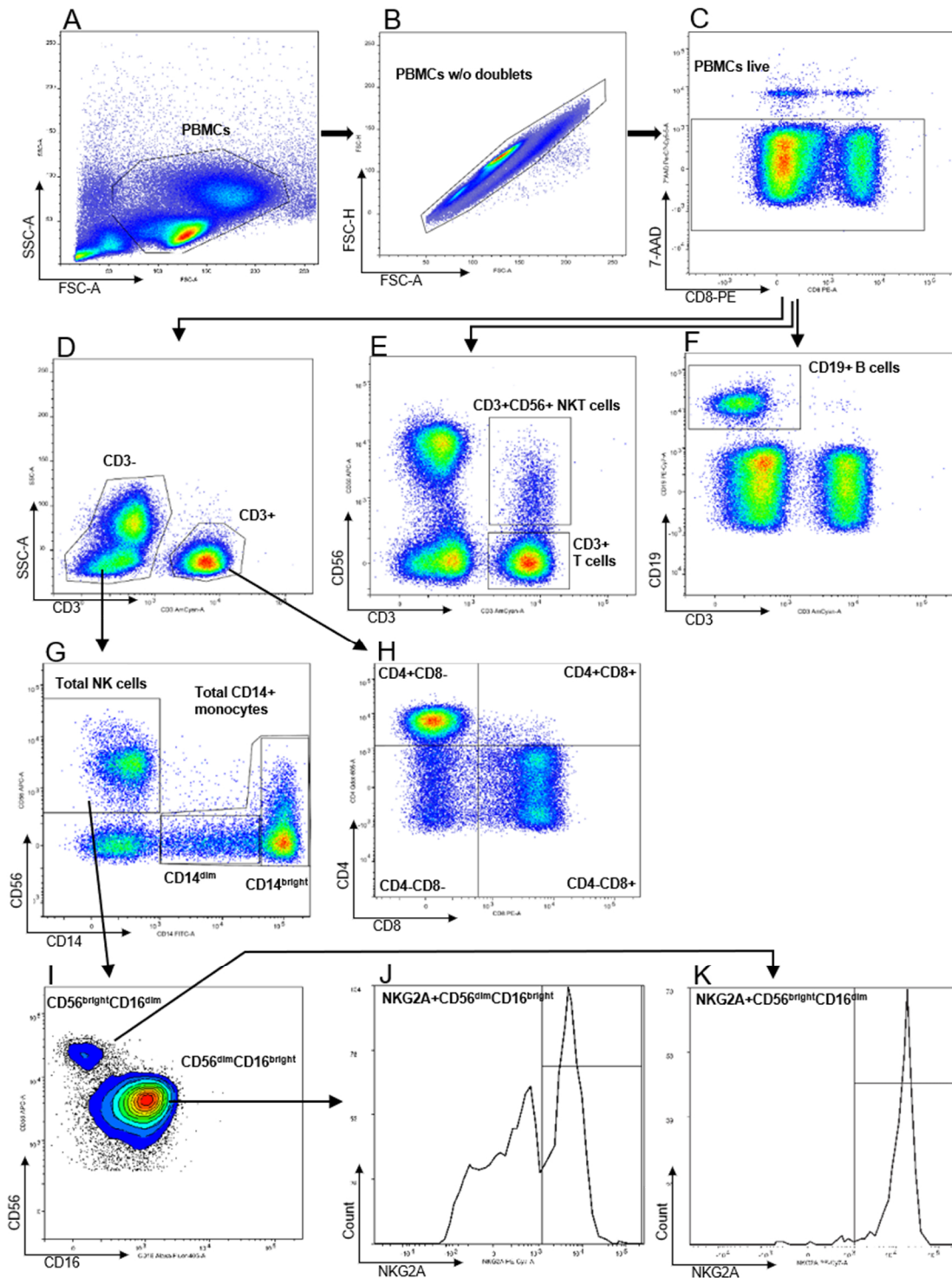


Figure 5: Gating strategy to identify T cells, B cells, NKT cells, monocytes and NK cells isolated from buffy coats of human blood donors. Lymphocytes were identified by their size and granularity in the FSC/SSC dot plot (A), followed by doublet exclusion (B) and gating of viable cells (C). Based on the lymphocyte live gate, CD3⁺ and CD3⁻ cells (D), T cells (CD3⁺CD56⁻) and NKT cells (CD3⁺CD56⁺) (E) as well as B cells (CD19⁺, F) were classified. Monocytes (CD14⁺) and NK cells (CD56⁺) were selected from the CD3⁻ fraction (G). CD4⁺ T helper cells and CD8⁺ cytotoxic T cells were selected from the CD3⁺ fraction (H). On the basis of the expression of CD56 and CD16, the NK cell population was further identified and differentiated into the CD56^{bright}CD16^{dim} and CD56^{dim}CD16^{bright} NK cell subsets (I). The expression of each NK cell marker was assessed on both CD56^{dim}CD16^{bright} (J) and CD56^{bright}CD16^{dim} (K) NK cell subsets (here represented by histogram analysis of NKG2A expression for both subsets). FMO control was used to determine positive staining. The above plots are representative.

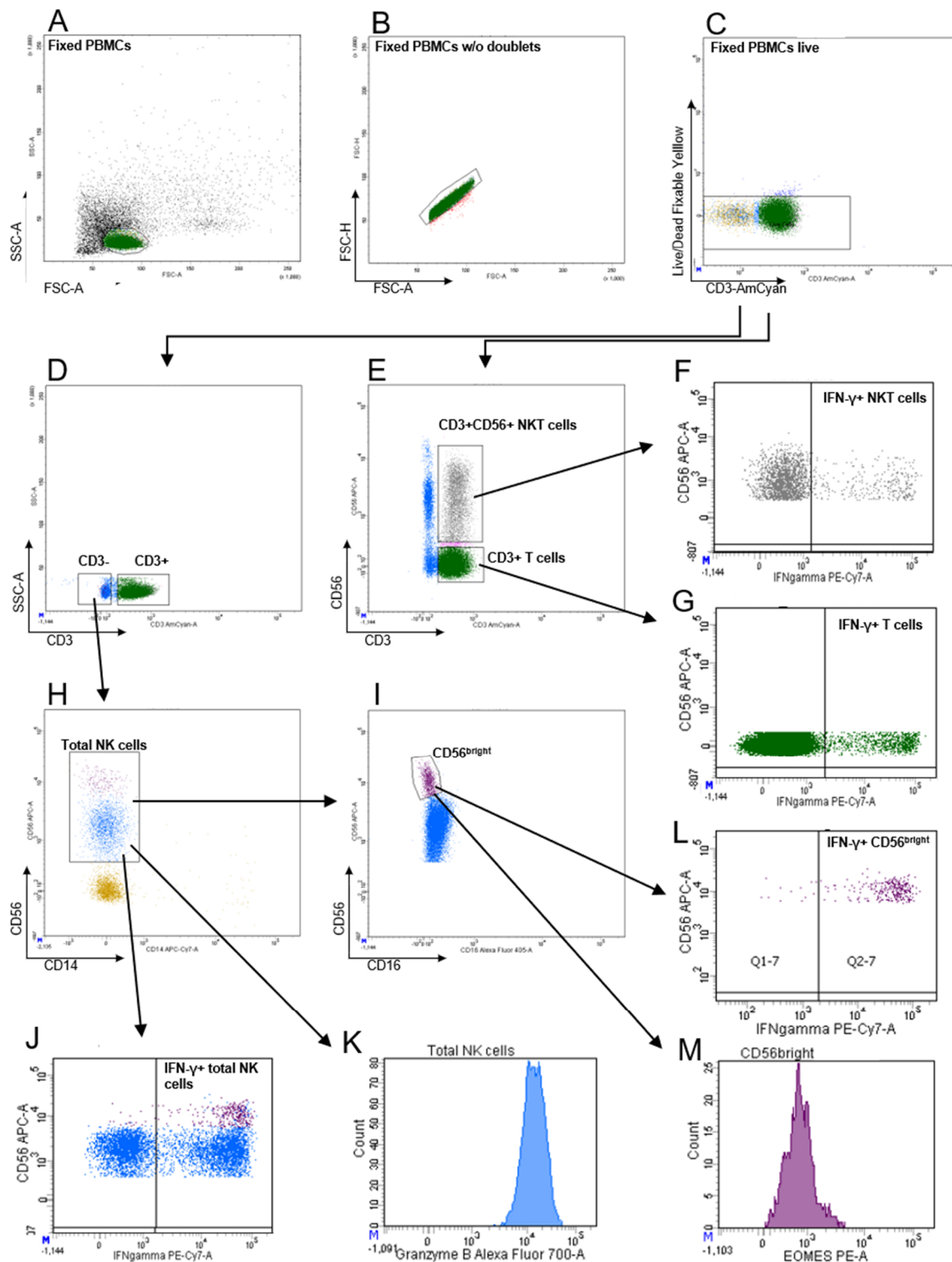


Figure 6: Gating strategy to identify T cells, NKT cells, and NK cells from buffy coats of human blood donors for the determination of intracellular markers. Lymphocytes were identified by their size and granularity in the FSC/SSC dot plot (A), followed by doublet exclusion (B) and gating of viable cells (C). Based on the lymphocyte live fraction, cells were further divided into CD3⁻ and CD3⁺ cells (D), T cells (CD3⁺CD56⁻) and NKT cells (CD3⁺CD56⁺, E). Total NK cells were selected from the CD3⁻ fraction (H) and further differentiated and identified into the CD56^{bright} NK cell subset. Representative density plots to demonstrate discrimination between positive and negative population for the presence of intracellular IFN- γ in NKT cells (F), T cells (G), total NK cells (J) and CD56^{bright} NK cells (L). Representative histograms of total NK cell (K) and CD56^{bright} NK cell subset (M) populations to donate histogram analysis to determine MFI (mean fluorescence intensity) of intracellular NK cell markers (here: represented by granzyme B and EOMES). FMO control was used to determine positive staining.

3.10. Magnetic activated cell sorting (MACS)

MACS technology is a method for separation of specific immune cell populations from a mixed suspension based on their surface antigens (CD molecules). In this study, primary murine splenic NK cells and primary human peripheral blood NK cells were purified by immunomagnetic depletion of other immune cells (T cells, B cells, monocytes and others) using a murine and human NK Cell Isolation Kit from Miltenyi Biotec GmbH, respectively. Negative selection was performed as instructed by the manufacturer. The purity of NK cells (85 - 90%) was checked on a sample basis by flow cytometric analysis. CD3⁺ T cell contamination in purified NK cells was <1%.

Prior to the isolation of murine splenic NK cells, a single cell suspension of murine splenocytes from each mouse spleen was prepared. Therefore, spleens of mice, which were kept in splenocyte culture medium at 37 °C after organ dissection, were transferred in a petri dish and cut into fine pieces with a scalpel. MACS buffer was added to transfer the tissue into a 40 µm cell strainer placed in a centrifuge tube. Further homogenization of tissue was carried out by gentle mincing of tissue with a syringe plunger. Filter was washed several times with MACS buffer. After centrifugation (300 x g, 10 min, RT), pellet was washed with 5 ml MACS buffer and centrifuged again. The final pellet was resuspended in 1 ml MACS buffer and cell number was determined by A/O staining (see 3.2) and LUNA^{FL} automated counter.

3.11. Real-time cell analysis systems xCELLigence and iCELLigence

3.11.1. Principles of the real-time cell analysis system

The proliferation and cytotoxicity assays in this study were performed with the real-time cell analysis (RTCA) systems instruments obtained by the company ACEA Biosciences, Inc. In comparison to former commonly used standard end-point procedures such as radioactive chrome-release assay, this system provides a continuous real-time monitoring of cell proliferation and cytolytic activity. Additionally, it works in a label-free, non-invasive and automatic manner. These systems use the principle of cellular impedance. Adherent cells, used as target cells, grow on gold-microelectrode-coated E-plates and act as insulators. The adherent cells impeded the flow of a non-invasive alternating microampere electric current between electrodes (Figure 7). The changing electrical impedance signal is automatically measured, at a frequency defined by the user and displayed as a unit-less parameter called Cell Index (CI).

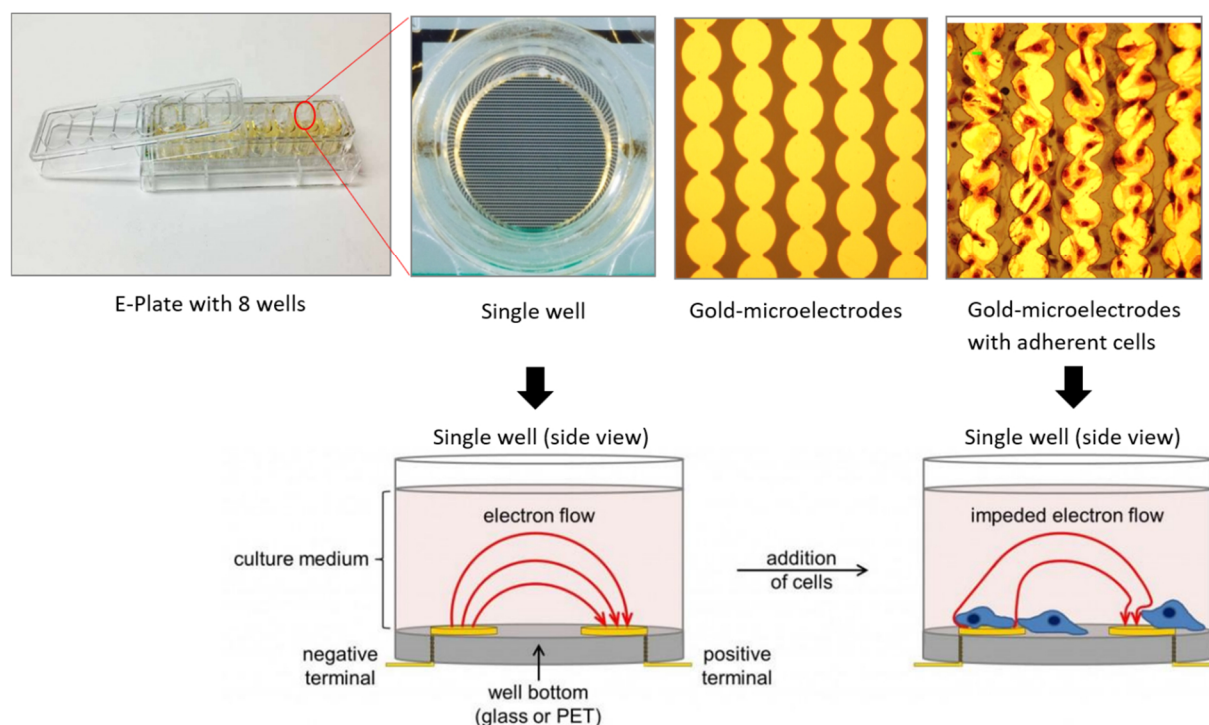


Figure 7: Composition and schematic view of the impedance-based real-time cell analysis system. An 8-well cell culture E-plate is shown with a closer top view on a single well with visible gold-microelectrodes without and with adherent cells. The schematic side view of a single well before and after adding of adherent cells is shown below. In the absence of cells, the electric current flows unimpeded in the media between the electrodes (negative and positive terminal). Due to the addition of cells, which adhere to and proliferate on the plate, the electron flow is impeded, resulting in a measurable impedance-changed signal. Modified from [162].

The CI value is dependent on morphology, number, size, and adhesion strength of the cells. Every cell line has its unique CI curve and maximum. Therefore, it can also be used as a quality measurement as well as a visual control of a good cell status during the experiments. In contrast to the adherent cancer target cells, the effector cells, e.g. NK cells, do not attach to the plate and therefore they do not produce an impedance signal. For this reason, the system cannot only be used to quantify proliferation, but also for analyzing cytolytic activity of effector cells. Figure 8 illustrates a generic real-time impedance trace. Over the course of time of an RTCA assay, changes in the impedance signal and therefore in the CI can vary in different degrees due to the different behavior of the adherent cells. Cell adhesion after addition of cells on the plate causes a rapid, exponential increase in CI; cell proliferation causes a slow, linear increase in CI; cell confluence causes stagnation of CI, and toxin addition caused a rapid decline in CI due to apoptosis and detachment of the cells.

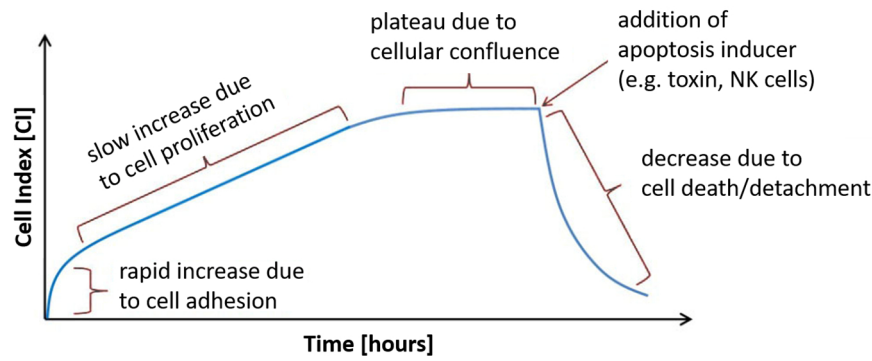


Figure 8: Generic real-time impedance trace of an apoptosis/cytotoxicity assay. The different behavior of the adherent cells and their induced apoptosis during the assay results in changing impedance signals, which are displayed in an increasing and decreasing CI curve. Modified from [162].

There were two products by ACEA Biosciences using the RTCA system: the xCELLigence™ and iCELLigence™ instruments, which have both been used in this study. Both RTCA instruments consisted of two elements – the RTCA station and the RTCA control unit. The station is placed in a standard CO₂ cell culture incubator and interfaces via WiFi® or a cable with the control unit (iPad® or laptop) that are housed outside the incubator. The iCELLigence product provided a RTCA station with two 8-well E-plates controlled via WiFi to an iPad. The xCELLigence product provided a RTCA station with three 16-well E-plates connected via cable with a laptop. An analyzing software was pre-installed on both RTCA control units.

Both RTCA instruments were initially used to determine the optimal cell seeding number of adherent cancer target cells (i.e. CT.26WT, DLD-1, MCF-7) by a titration-proliferation assay. The optimal cell number of cancer target cells was then used to perform cytotoxicity assays with effector cells, i.e. NK-92 cells, primary murine splenic NK cells and primary human peripheral blood NK cells. To quantify the lysis at specific time points, the data were exported from the control unit to Microsoft Excel. The percentage cytolytic activity of the effector cells at a given time point was determined by using the calculated normalized CI (NCI) according to the following formulas:

NCI in general:

$$NCI_{well_i}(t) = \frac{CI_{well_i}(t)}{CI_{well_i}(t_{normalization})}$$

with $CI_{well_i}(t_{normalization}) \neq 0$ and $i = 1, 2, \dots, n$

$NCI_{well_i}(t)$... normalized CI of well i at time point t

$CI_{well_i}(t)$... CI of well i at time point t

$CI_{well_i}(t_{normalization})$... CI of well i at normalization time point $t_{normalization}$

NCI for target cell control:

$$NCI_{target\ cell-ctrl_i}(t) = \frac{CI_{target\ cell_i-media}(t)}{CI_{target\ cell_i-media}(t_{normalization})}$$

NCI for E:T-ratio:

$$NCI_{E:T-Ratio_i}(t) = \frac{CI_{(E:T-Ratio_i)-(NK-cell-ctrl_i)-(media_i)}(t)}{CI_{(E:T-ratio_i)-(NK-cell-ctrl_i)-(media_i)}(t_{normalization})}$$

Cytolytic activity:

$$Cytolytic\ activity\ [\%] = \frac{NCI_{target\ cell-ctrl_i} - NCI_{E:T-ratio_i}}{NCI_{target\ cell-ctrl_i}} \cdot 100$$

All experiments described below were generally carried out under the following conditions: Before seeding of target cells, the blank value for each well was always measured with a defined volume of medium (iCELLigence: 200 μ l, xCELLigence: 100 μ l). Each probe was usually analyzed in double or triple determination, except for cytotoxicity assays with murine NK cells. Here, a single determination was made. The first well of each E-plate was constantly loaded with medium only and served as a medium control. The entire durations of measurements were 50 h up to 90 h. During this time, no media was replaced or added. All measurements were carried out under standard cell culture conditions and were subdivided into distinct steps (three to five steps), which were characterized by different durations and time intervals. The experimental procedure steps were set manually before starting each assay. The first three steps were always the same. The first step, the blank value measurement, was started manually and was pre-set with a running time and interval of one minute. After cell seeding, the second step followed by a manual start with a running time of 2 h and an interval of 1 min. Passing the 2 h, the third step started automatically with an interval of 1 h until the final duration time was achieved. For the cytotoxicity assays, this third step was stopped manually after 24 h to add the respective NK cells followed by a fourth step that collected data every minute. After the 2 h, an automatically started step followed with an interval of 10 to 15 min until the experiment was finally stopped.

3.11.2. Cell proliferation assays

The cell proliferation assays served as preliminary tests for the ensuing real-time cytotoxicity assays to determine the optimal cell seeding number of the different adherent cancer target cells, i.e. CT26.WT, DLD-1 and MCF-7. The aim was to determine the optimal cell seeding number at the pre-defined time point of effector cell addition (24 h post seeding). At this time point, a CI with a value of one third to two thirds of the maximum CI should be reached. For this

purpose, target cell suspensions with different cell numbers were prepared by using serial dilutions or later by preparing individual cell suspensions with a defined cell number. Target cells were seeded into the dedicated wells. After 30 min in which the cells were given time to settle evenly, the E-plates were inserted into the RTCA station and the measurement was started. After reaching the growth plateau the assay was stopped.

3.11.3. Cytotoxicity assays

The respective target cell seeding numbers of CT26.WT, DLD-1 and MCF-7 from the proliferation tests were used for the subsequently performed cytotoxicity assays with the different effector cells, i.e. primary murine splenic NK cells, NK-92 cells and primary human peripheral NK cells. The murine cytotoxicity assays were performed on the xCELLigence RTCA instrument, whereas the human cytotoxicity assays were performed on the iCELLigence RTCA instrument. In general, 24 h post-seeding of target cells the measurement was paused to add the respective NK cells at different E:T ratios. The effector cell number for each E:T ratio was calculated based on the initial target cell seeding number. Besides the medium control, NK cells alone served as controls for possible measurement interventions, target cells alone served as untreated growth controls and target cells with addition of NK cells served as treatment sample.

At first, preliminary cytotoxicity tests with murine and human NK cells (splenic NK cells from C57BL/6 mice and NK-92 cells, respectively) were performed to verify the optimal E:T ratio(s), but also to optimize the experimental setup in terms of duration, handling, and optimal target cell conditions at specific times of use. The final experiment settings for the main cytotoxicity assays are described below.

Primary splenic NK cells of C57BL/6 mice against CT26.WT colon cancer target cells

The murine target cells CT26.WT (15,000 cells/well) were seeded in 200 μ l splenocyte medium. The next day, single cell suspensions of spleens of C57BL/6 mice fed NFD or HFD in *ad libitum* or restrictive regimes over 18 weeks were prepared and were used to isolate the NK cells by MACS enrichment (see 3.10). The isolated splenic NK cells were counted and cell viability was determined. 24 h post-CT26.WT-seeding, the CI curve was checked and if positively validated of the optimum CI value the freshly isolated NK cells of each mice were added to the respective wells at different E:T ratios (70:1 or maximum possible number) in a volume of 100 μ l. In addition, 500 U/ml recombinant murine IL-2 (mIL-2) was added to each well to enhance and maintain NK cell mediated cytotoxicity. To ensure to have enough NK cells for the NK cell alone control, the remaining NK cells of all mice were mixed and added in the respective wells of the E-plates. No more than eight mice per day with similar distribution over groups were sacrificed and used for the cytotoxicity assay.

Primary human peripheral NK cells against human cancer target cells

The human target cells DLD-1 and MCF-7 were both seeded with a cell number of 40,000 cells/well in a volume of 400 μ l cRPMI on the E-plates. On the following day, primary human NK cells of one donor were isolated from PBMCs by MACS enrichment (see 3.10). Prior to addition of the NK cells, the CI curves of DLD-1 and MCF-7 were checked for the optimal CI values. After culturing target cells for 24 h, the freshly isolated NK cells were added at an E:T ratio of 15:1 in a volume of 100 μ l cRPMI in the dedicated wells. Per well, 200 U/ml hIL-2 was added.

3.12. Statistical analysis

All statistical analyses were performed using the GraphPad Prism software version 6.07. All data were examined for outliers followed by testing for normal distribution and homogeneity of variances. Student's *t* test was used to compare two groups (in detail overweight and obese BMI groups were compared to normal weight BMI control group), if data were normal distributed with equal variances; without equal variances the *t*-test with Welch's correction was used. The nonparametric Mann-Whitney *U* test was performed to compare two groups, if data were not normally distributed. One-way analysis of variance (ANOVA) with post-hoc Tukey's multiple comparison was used to compare the means of the normally distributed data of the human blood donor data (age, weight, height, BMI) of the three BMI groups. Two-way ANOVA with the main factors "diet" and "feeding regime" was performed to compare means of the four mouse groups with post-hoc Tukey's multiple comparison test. In animal experiments results are presented in bar graphs as means \pm standard error of the mean (SEM). Human flow cytometric data are presented as box and whisker plots with median \pm minimum to maximum values with additional dot plot representing individual donors. Real-time cell analysis results are presented as mean \pm SEM. $P < 0.5$ was considered to denote significance. Means with different letters (a, b, c, d) indicate significant differences between groups of mice according to post-hoc Tukey's multiple comparison test results ($P < 0.05$). *P* values are also indicated as follows: */# $P < 0.05$, ** $P < 0.01$ and *** $P < 0.001$.

4 Results

4.1. Murine study

4.1.1. Dietary intakes

In the used mice strain C57BL/6 both factors – the type of the diet and the feeding regime – had significant effects on food, energy and fat intakes as well as on carbohydrate and protein intakes. In both diets, the restrictive feeding regime displayed significantly lower values for all nutritional parameters compared to the *ad libitum* feeding regime (Figure 9A-E; except for the daily fat intake of NFD fed mice). Regardless of the feeding regime, the daily food intake of HFD fed mice was significantly lower compared to the corresponding NFD fed mice (Figure 9A). However, within the *ad libitum* feeding regime, the HFD fed group of C57BL/6 mice showed a significantly higher daily energy intake as the corresponding NFD fed group (Figure 9B). Nevertheless, mice with *ad libitum* access to the HFD displayed the significantly highest daily fat intake among all groups (Figure 9C). In consequence of the food compositions, all HFD fed mice had a significantly increased daily fat intake and a significantly decreased daily carbohydrate intake compared to the NFD fed mice (Figure 9C and D).

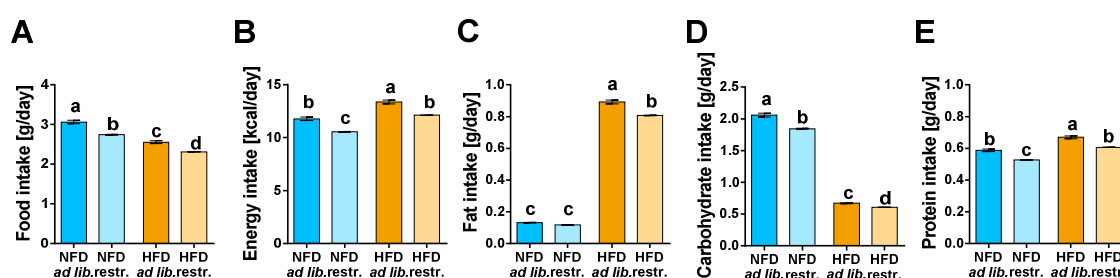


Figure 9: Nutritional data of daily dietary intakes of male C57BL/6 mice fed either a normal-fat diet (NFD) or high-fat diet (HFD) with *ad libitum* (*ad lib.*) and restrictive (*restr.*) feeding regimes for 18 weeks. Mean \pm SEM. Means with different letters are significantly different according to post-hoc Tukey's multiple comparison test results ($P < 0.05$).

4.1.2. Body weights, visceral fat masses and organ weights

The average body weights of seven-week-old male C57BL/6 mice at the start of the experiment (week 0) were $21.3 \text{ g} \pm 0.2 \text{ g}$. All mice increased their body weight over time (Figure 10A), with significant effects of the diet and the feeding regime (Figure 10D).

Ad libitum and restrictive HFD feeding significantly increased the body weight of C57BL/6 mice from week 3 onward compared to the respective NFD groups (Figure 10A). After 18 weeks of diet-induced obesity (DIO) feeding, mice with *ad libitum* access to HFD more than doubled their initial body weight (+55.2%), whereas the respective NFD group increased their body weight by about a quarter (+24.3%; Figure 10B). In accordance with the higher terminal body weight of the

HFD *ad libitum* fed group, the visceral fat mass was also significantly higher within this group compared to the NFD *ad libitum* fed group (Figure 10C). The average mass of visceral fat in C57BL/6 mice fed the HFD restrictive was significantly increased compared to the NFD restrictive fed group. For both analyzed parameters, the comparison between the feeding regimes within HFD and NFD showed only significant differences within the HFD groups (Figure 10B, C).

In summary, regardless of the feeding regime, HFD feeding of C57BL/6 mice resulted in significant higher terminal body weights and visceral fat mass compared to NFD feeding. The results of body weight and of visceral fat mass in C57BL/6 mice were additionally supported by the visual phenotypes of representative living and dead mice (Figure 10E, F).

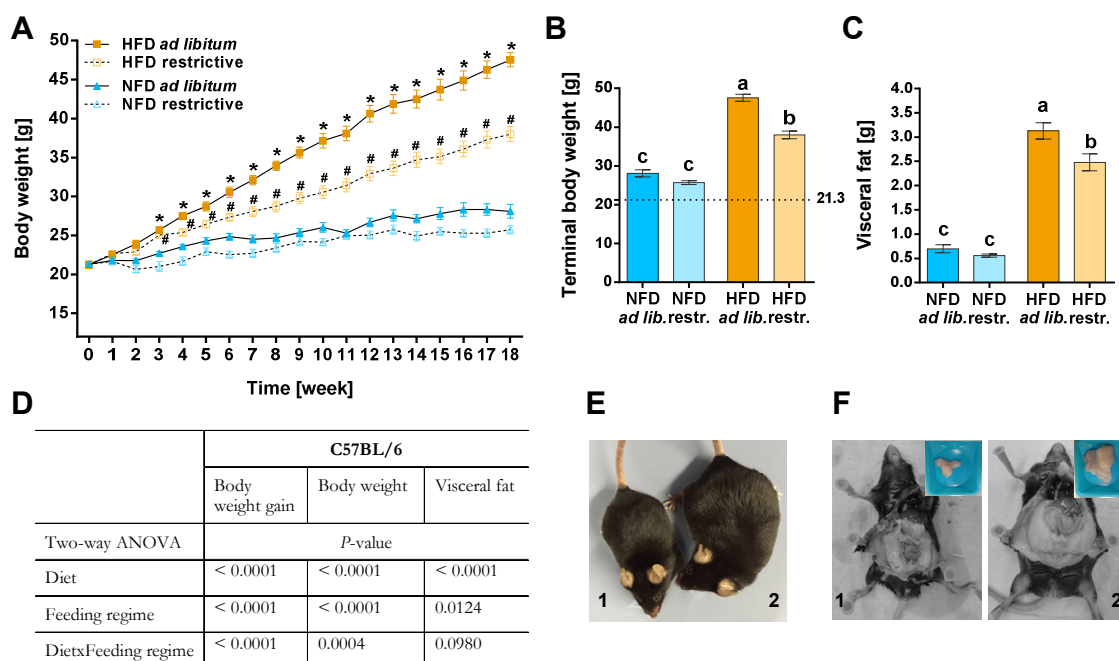


Figure 10: Effects of high-fat diet (HFD) and normal-fat diet (NFD) under *ad libitum* (*ad lib.*) and restrictive (*restr.*) feeding regimes on male C57BL/6 mice. Body weight gain (A) over 18 weeks, terminal body weight (B) with indication of initial body weight (dashed lines) at week 0, and visceral fat mass (C). Representative pictures of visual differences in body mass (E) and visceral fat mass (F) of C57BL/6 mice fed NFD *ad libitum* (1) vs. HFD *ad libitum* (2) after 18 weeks. * $P < 0.05$, HFD *ad libitum* compared to NFD *ad libitum* group. # $P < 0.05$, HFD restrictive compared to NFD restrictive group. Means with different letters are significantly different according to post-hoc Tukey's multiple comparison test results ($P < 0.05$). For two-way ANOVA P-values are shown for the main factors diet, feeding regime and the interaction of both main factors (D). Data are presented as mean \pm SEM.

The organ weights of C57BL/6 mice are illustrated in Figure 11. C57BL/6 mice fed the HFD *ad libitum* showed a significantly heavier spleen than NFD *ad libitum* fed mice, whereas no significant difference was observed between the restrictive groups (HFD and NFD). The liver in C57BL/6 mice were significantly heavier in the HFD *ad libitum* group compared to all other groups, with significant diet and feeding regime effects as well as the interaction effect of both factors (test

results not shown). However, no significant difference of liver weight was detected between both restrictive groups (NFD and HFD). The heart was significantly lighter in the NFD restrictive group compared to the HFD restrictive group. Two-way ANOVA showed significant influence of the diet on kidney weights of C57BL/6 mice. Independently from the regime, kidneys from HFD fed mice were significantly heavier compared to NFD fed mice. The significant diet factor effect also applied to the weight of pancreas. Here, mice of the HFD restrictive group showed a significantly increased weight of pancreas. Non-significant changes were observed in organ weights of lung, brain and thyroid gland.

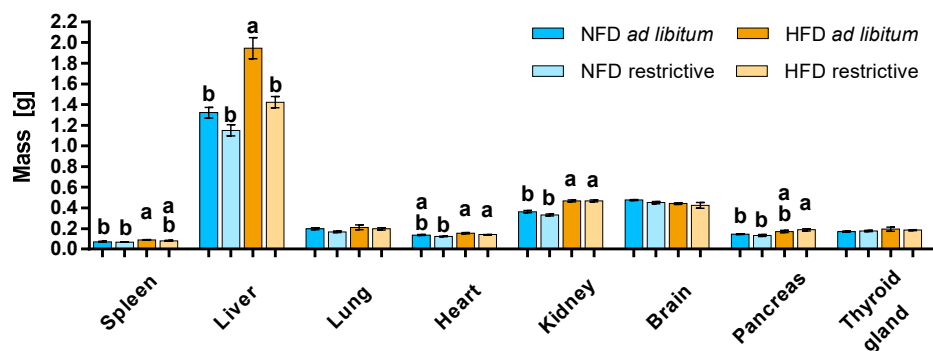


Figure 11: Physiological impact on organ weights by high-fat diet (HFD) and normal-fat diet (NFD) under *ad libitum* and restrictive feeding regimes in a C57BL/6 murine diet-induced obesity (DIO) model after 18 weeks. Mean \pm SEM. Means with different letters are significantly different according to post-hoc Tukey's multiple comparison test results ($P < 0.05$).

4.1.3. Cytokine plasma concentrations

Plasma levels of IL-6 increased threefold in C57BL/6 mice fed the HFD *ad libitum* compared to NFD *ad libitum*, whereas mice received the diets restrictive showed no differences in these cytokine plasma concentrations (Figure 12B). Plasma levels of IL-2 and TNF- α were not altered between C57BL/6 groups (Figure 12A, C). Although not significant, plasma IFN- γ was increased in the HFD *ad libitum* group compared to NFD *ad libitum* group (Figure 12D). Interestingly, two-way ANOVA showed a significant interaction of diet and feeding regime for TNF- α plasma levels in C57BL/6 mice.

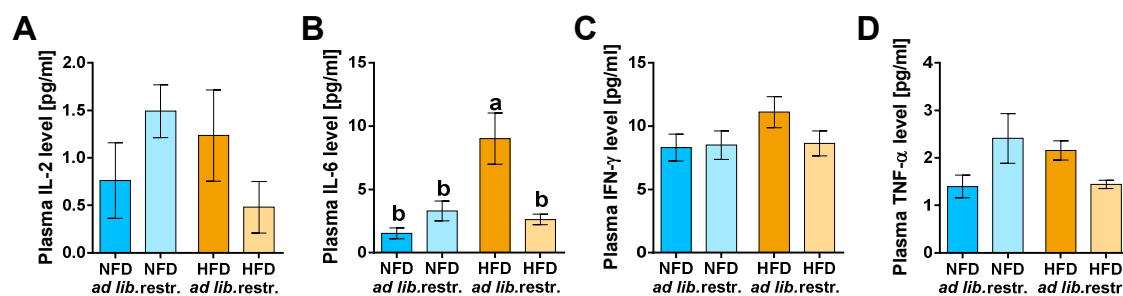


Figure 12: Blood plasma concentrations of interleukin (IL)-2 and IL-6 and chemokines interferon (IFN) γ and tumor necrosis factor (TNF)- α in C57BL/6 mice fed a high-fat diet (HFD) and normal-fat diet (NFD) under *ad libitum* (*ad lib.*) and restrictive (restr.) feeding regimes. Samples were analyzed by Luminex bead-based Multiplex assay. Mean \pm SEM. Means with different letters are significantly different according to post-hoc Tukey's multiple comparison test results ($P < 0.05$).

4.1.4. Immune cell populations in murine blood

Figure 13 shows the determined concentrations and frequencies of immune cell populations in HFD and NFD fed mice that received those diets *ad libitum* and restrictive. Analysis of blood leukocytes and lymphocytes revealed almost twice as high concentrations of circulating leukocytes, lymphocytes, CD11b⁺Ly6C^{high}Ly6G^{low} monocytes and CD19⁺ B lymphocytes of HFD fed mice compared to NFD fed mice regardless of the feeding regime (Figure 13A). The concentration of CD11b⁺Ly6C^{low}Ly6G⁺ granulocytes was significantly increased in HFD *ad libitum* fed mice compared to NFD restrictive fed mice. In addition, the cell count of total CD3⁺ T lymphocytes as well as CD3⁺CD4⁺ helper T cells and CD3⁺CD8⁺ cytotoxic T cells were slightly increased and significantly increased in the case of CD4⁺ T cells in HFD fed mice compared to NFD fed mice (Figure 13A).

Furthermore, the percentage of lymphocytes was slightly increased in HFD fed mice compared to NFD fed mice without being statistically significant (Figure 13B). The population of monocytes was significantly elevated in HFD fed mice compared to NFD fed mice with a significant difference between both *ad libitum* fed groups (Figure 13C). In contrast to the elevated cell counts of granulocytes in HFD fed mice, their percentages in the blood was slightly decreased in HFD fed mice (Figure 13D). The significantly increased cell count of B cells in HFD fed mice was also reflected in the percentages of B cells – HFD fed mice of both feeding regimes displayed significantly increased B lymphocytes compared to NFD fed mice of both feeding regime groups (Figure 13E). The slight increase in the T cell count of HFD fed mice compared to NFD fed mice was also mirrored in the population's frequencies (Figure 13F). Contrary to this results, both T cell subsets (CD4⁺ and CD8⁺ T cells) showed decreased frequencies in HFD fed animals compared to NFD fed animals, with over 20% lower frequencies between the corresponding HFD and NFD groups in both subsets (Figure 13G, H).

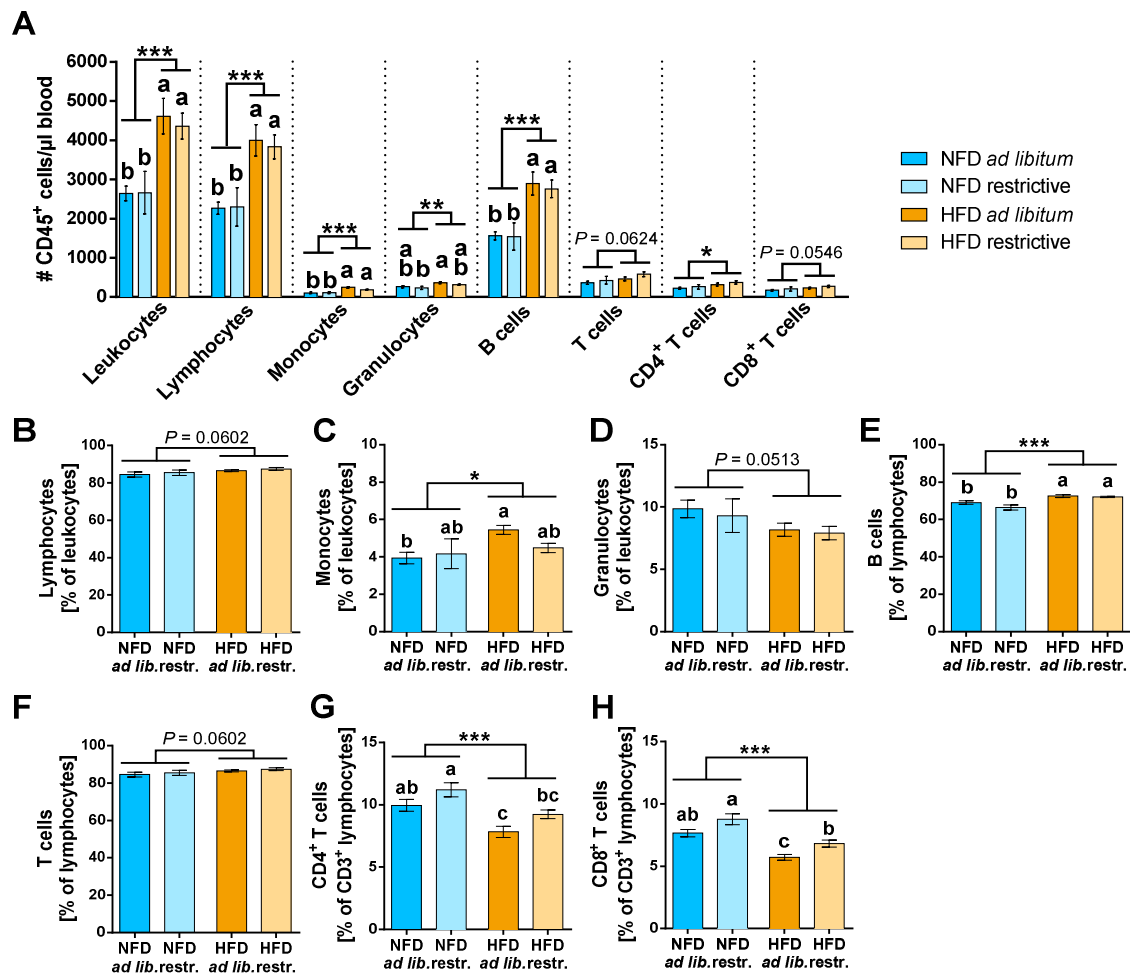


Figure 13: Concentrations, expressed as absolute cell number per μl blood, (A) and frequencies (B-H) of immune cell populations in whole blood samples of C57BL/6 mice fed either a high-fat diet (HFD) or normal-fat diet (NFD) under *ad libitum* (*ad lib.*) and restrictive (restr.) feeding regimes. Mean \pm SEM. Means with different letters are significantly different according to post-hoc Tukey's multiple comparison test results ($P < 0.05$). * $P < 0.05$ and exact P -values within $0.05 < P < 0.1$, two-way-ANOVA, NFD fed groups compared to HFD fed groups.

In addition to the mentioned immune cell populations above, the cell counts and frequencies of total primary murine NK cells were determined. The cell concentration of circulating NK cells was slightly increased in HFD fed mice compared to NFD fed mice, whereas the frequency of NK cells was significantly decreased in HFD fed mice (Figure 14A, B). Moreover, this decrease was also present between the corresponding HFD and NFD fed groups. In addition to the total NK cells, the frequencies of the four murine NK cell subsets CD11b⁻CD27⁻ (double negative), CD11b⁻CD27⁺, CD11b⁺CD27⁺ (double positive) and CD11b⁺CD27⁻ were analyzed. There were no significant differences in the frequencies of double negative and CD11b⁻CD27⁺ NK cell subsets between the examined diet groups (Figure 14C, D). In contrast, HFD fed mice showed significantly reduced frequencies of the double positive NK cell subset with a significant difference between HFD *ad libitum* and NFD restrictive fed mice (Figure 14E). In addition, the frequency of

the considered most mature stage, the CD11b⁺CD27⁻ NK cell subset, displayed an elevated frequency in HFD fed mice compared to NFD fed mice (Figure 14F).

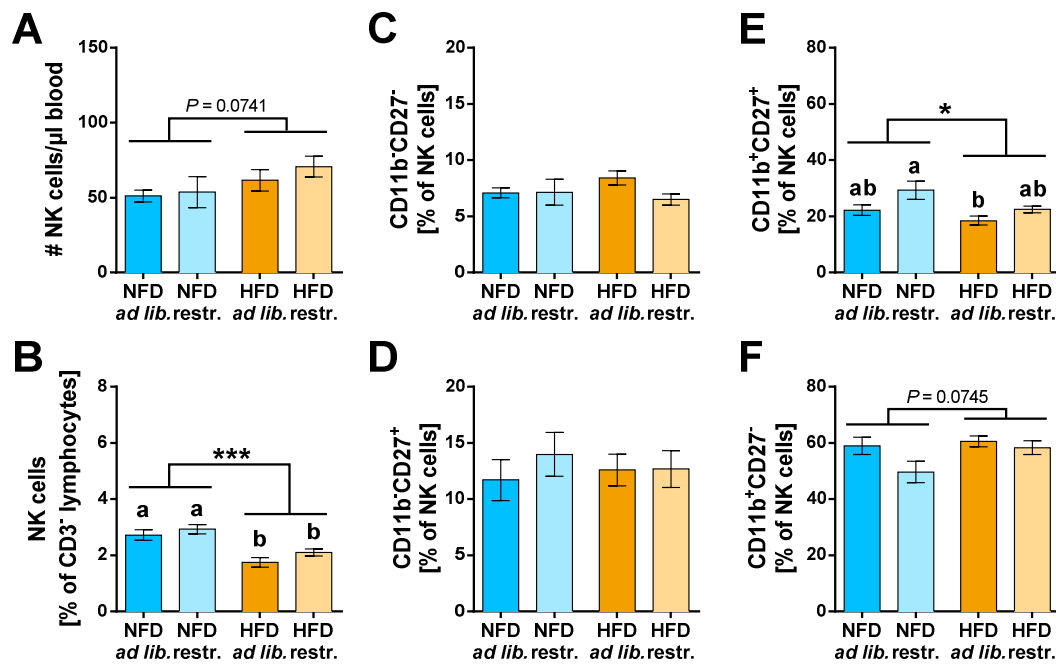


Figure 14: NK cells and NK cell subsets in whole blood samples of C57BL/6 mice fed either a high-fat diet (HFD) or normal-fat diet (NFD) under *ad libitum* (*ad lib.*) and restrictive (restr.) feeding regimes. Concentration of total NK cells (A), expressed as absolute cell number per μl , and percentages of total NK cells (B). Percentages of NK cell subsets with different surface expression profiles of CD11b and CD27 (C-F). Mean \pm SEM. Exact P-values within $0.05 < P < 0.1$, two-way-ANOVA, NFD fed groups compared to HFD fed groups. Means with different letters are significantly different according to post-hoc Tukey's multiple comparison test results ($P < 0.05$).

4.1.5. Phenotypes of primary murine peripheral blood NK cells

Figure 15 displays the expression of different surface markers on total primary NK cells. Regardless of the feeding regime, HFD fed mice showed significantly enhanced proportions of NK cells expressing KLRG1 on their surface compared to NK cells of NFD fed mice (Figure 15F). Furthermore and in regard of the feeding regime, the percentage of KLRG1⁺ NK cells was significantly higher in HFD *ad libitum* fed mice compared to NFD restrictive fed mice. In contrast and also regardless of the feeding regimes, the HFD led to significantly reduced percentages of CD127⁺ NK cells compared to the NFD (Figure 15G). No other significant changes in the expression patterns of examined surface receptors were found between the diet groups.

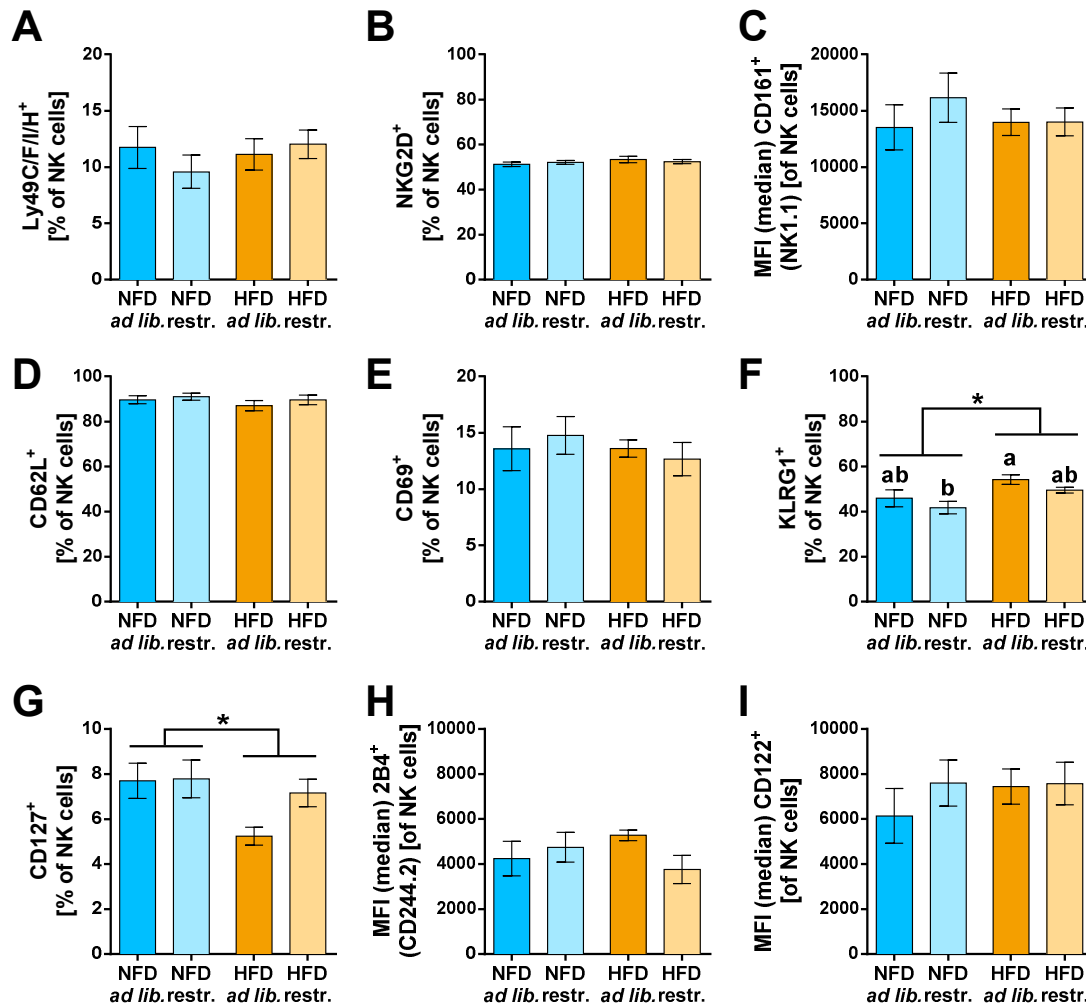


Figure 15: Frequencies or median fluorescent intensities (MFIs) of total NK cells of C57BL/6 mice expressing activating and inhibitory receptors (A-C), adhesion molecules (D), activation-associated markers (E), maturation markers (F, G) and co-stimulatory receptors (H, I). Mice were fed either a high-fat diet (HFD) or normal-fat diet (NFD) under *ad libitum* (*ad lib.*) or restrictive (*restr.*) feeding regimes. Mean \pm SEM. Means with different letters are significantly different according to post-hoc Tukey's multiple comparison test results ($P < 0.05$). * $P < 0.05$, two-way-ANOVA, NFD fed groups compared to HFD fed groups.

4.1.6. Determination of the optimal cell seeding number of CT26.WT target cells

Defining the ideal seeding density of the murine CT26.WT colon cancer target cells was essential to get the convenient CI (1/3 to 2/3 of CI_{max}) at the pre-defined time point of 24 h post seeding. This time point was set to add the primary murine effector NK cells in the subsequent cytotoxicity assays. Figure 16 shows the proliferation behavior of the CT26.WT cell line after titration and seeding cell numbers from 40,000 cells/well to 625 cells/well over an incubation period of 50 h. All cell curves show a similar growth pattern with a maximum CI of ~ 1.8 . The higher the seeding number, the faster the plateau phase with the CI_{max} was reached. At the defined time point 24 h, none of the CI curves showed the ideal 1/3 to 2/3 CI_{max} . The initially seeded cell numbers of 10,000 and 20,000 cells/well displayed either too low or too high CI values at 24 h post-seeding.

Therefore, the cell seeding number of CT26.WT was set to 15,000 cells/well for further experiments. This cell number/well was then confirmed in addition tests (data not shown).

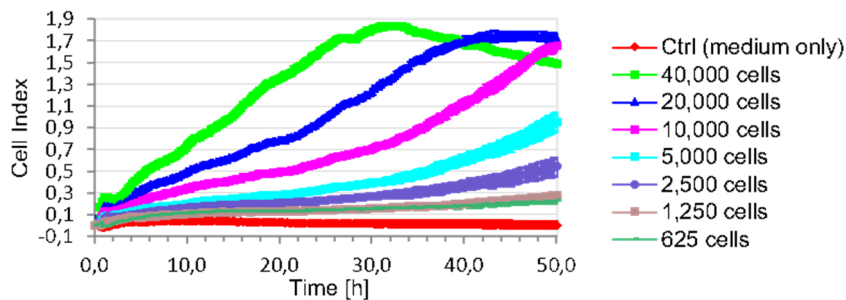


Figure 16: Representative figure of a cell proliferation assay to determine the optimal cell seeding number of the mouse colon cancer target cell line CT26.WT by impedance-based real-time cell analysis system xCELLigence. Cell numbers seeded per well are mentioned on the right side of the figure. Impedance was measured for 50 h. Medium only served as control (Ctrl). Analysis carried out in duplicates. Mean \pm SEM; N = 1.

4.1.7. Cytolytic activity of primary murine splenic NK cells against murine colon cancer cell line CT26.WT

These experiments aimed to analyze the cytolytic activity of freshly isolated NK cells from spleens of C57BL/6 mice fed an HFD or NFD with both *ad libitum* and restrictive feeding regimes.

At first and after defining the optimal cell seeding number of the CT26.WT target cells, preliminary cytotoxicity tests followed. The aim was on the one hand, to establish the assay procedure and on the other hand to explore feasible E:T ratios to receive evaluable data.

The review of literature about murine NK cell cytotoxicity assays revealed a broad spectrum of the used E:T ratios, reaching from 0.25:1 to 200:1 E:T ratio [163–169]. For that reason, isolated NK cells from spleens of three C57BL/6 mice were used with initially E:T ratios of 1:1, 4:1, 6:1, 12:1, 16:1, 25:1, 32:1 and 40:1 against the murine colon target cell line CT26.WT in individual experiments. Here, no cytolytic effect, visible in the form of no changes in cell index values after addition of splenic NK cells in comparison to target cells alone, was observed (data not shown). Therefore, a higher E:T ratio of 70:1 was applied. Due to time limitations and the fact, that isolated splenocytes were also used for other pretests, the isolated NK cell number of one mice spleen was not sufficient for the 70:1 E:T ratio. So, splenic NK cells of two C57BL/6 spleens were pooled to achieve the required NK cell number, followed by adding them 24 h post-target cell-seeding to the CT26.WT target cells. The cytolytic effect of splenic NK cells at 70:1 E:T ratio led to a decrease of the cell index (normalized to the time point of NK cell addition) 5 h after effector cell addition (Figure 17). As a result, it was decided to use 70:1 E:T ratio for the subsequent cytotoxicity assays with HFD and NFD fed C57BL/6 mice.

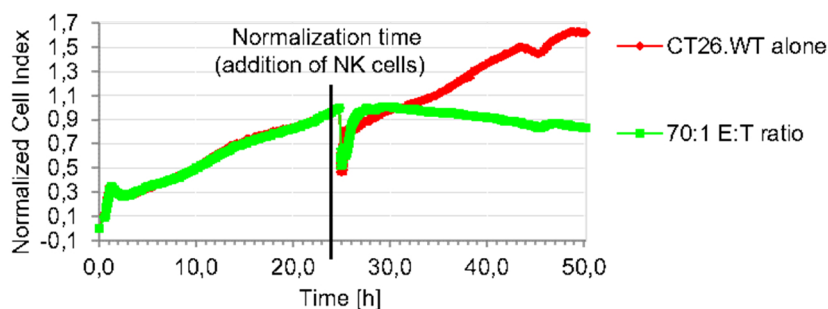


Figure 17: Representative figure of dynamic monitoring of cytolytic activity of pooled primary splenic NK cells (effector cells) isolated from two spleens of C57BL/6 mice against murine colon cancer cell line CT26.WT (target cells) by impedance-based real-time cell analysis system xCELLigence. Target cells were seeded at a density of 15,000/well. 24 h post-seeding effector cells were added at an E:T ratio of 70:1 to target cells and supplemented with 500 U/ml recombinant murine IL-2. Impedance at well bottoms was measured every 15 min for 50 h. Changes in impedance normalized to the normalization time (black line) are given as a dimensionless normalized cell index. Mean \pm SEM; N = 1.

In the preliminary tests, an E:T ratio of 70:1 exhibited a detectable cytolytic effect of the NK effector cells against CT26.WT target cells. However, as already indicated, it was challenging to achieve the required NK cell number from each mice spleen. Thus, it was only a small number of mice suitable to use their isolated NK cells with the pre-defined E:T ratio of 70:1. In accordance not to trash already isolated NK cells, also NK cells numbers applicable only for lower E:T ratios were used, ranging from 15:1 to 59:1 E:T ratio. However, in those cases no cytolytic effect was seen (data not shown). Due to the small sample size per group at an E:T of 70:1 it was not applicable to perform statistics between the four groups. Therefore, Figure 18 shows the obtained results without intergroup statistics. It is noticeable, even without intergroup comparison, a reduced cytolytic activity of NK cells from HFD *ad libitum* fed C57BL/6 is visible compared to the other groups. However, the performed two-way ANOVA displayed significant effects of the factor diet at different time points.

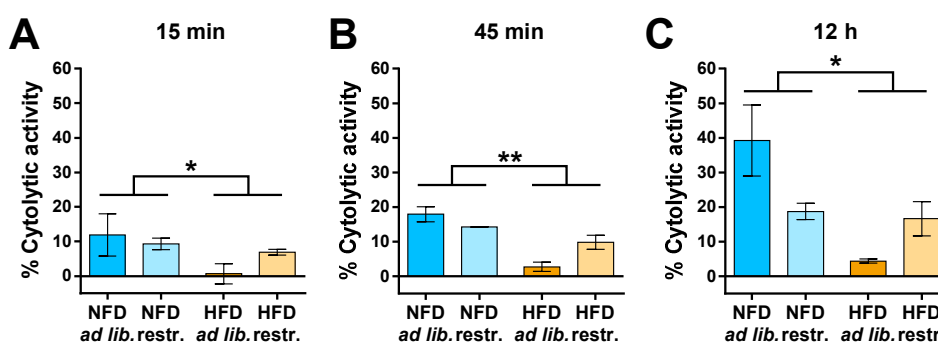


Figure 18: Cytolytic activity of primary splenic NK cells of C57BL/6 mice against the colon cancer target cell line CT26.WT at indicated time points after NK cell addition. Mice were fed a normal fat diet (NFD) or a high-fat diet (HFD) with both *ad libitum* (*ad lib.*) and restrictive (*restr.*) feeding regimes. Cytolytic activity was calculated from cell index data obtained by impedance-based real-time cell analysis system xCELLigence. Target cells were seeded at a density of 15,000 cells/well. Freshly isolated NK cells were added 24 h post-seeding at an E:T ratio of 70:1. *P < 0.05 and **P < 0.01 indicate results of two-way ANOVA for the main factor diet. Mean \pm SEM; n (per group) = 2 – 4.

4.2. Human study

4.2.1. Study population

The study population was composed of 46 subjects, which were divided into three groups according to the calculated BMI (based on the given information of body weight and height: $\text{BMI} = \text{kg}/\text{m}^2$): normal weight ($\text{BMI} 18.5 - 24.9 \text{ kg}/\text{m}^2$), overweight ($\text{BMI} 25 - 29.9 \text{ kg}/\text{m}^2$) and obese ($\text{BMI} \geq 30 \text{ kg}/\text{m}^2$) with a sample size of 14, 16 and 16, respectively. The study subjects were aged between 19 and 66 years. No significant differences were observed in age, height and human cytomegalovirus (HCMV) serostatus between the three BMI groups. In result of their classification into the BMI groups, body weight and BMI were significantly different between normal weight, overweight and obese individuals (Table 13).

Table 13: Characteristics of the human study population.

	Normal weight Mean \pm SEM (n = 14)	Overweight Mean \pm SEM (n = 16)	Obese Mean \pm SEM (n = 16)	One-way ANOVA F statistic (P-value)
Age (years)	37.7 \pm 3.9	47.3 \pm 3.6	49.6 \pm 3.6	0.1230
Height (cm)	182.9 \pm 1.8	178.4 \pm 1.1	178.8 \pm 2.6	0.2301
Weight (kg)	74.6 ^c \pm 1.9	87.5 ^b \pm 1.2	105.5 ^a \pm 4.3	< 0.0001
BMI ($\text{kg}\cdot\text{m}^{-2}$)	22.3 ^c \pm 0.4	27.5 ^b \pm 0.3	32.8 ^a \pm 0.5	< 0.0001
HCMV seronegative	5	4	5	0.8018
HCMV seropositive	9	12	11	

Means with different letters are statistically significantly different according to post-hoc Tukey's multiple comparison test results. Bold *P*-values mark statistical significance. ANOVA: Analysis of variance. BMI: Body mass index. HCMV: Human cytomegalovirus. SEM: Standard error of the mean.

4.2.2. Immune cell populations in peripheral blood mononuclear cells (PBMCs)

Figure 19 shows the determined frequencies of immune cell populations in PBMCs of normal weight, overweight and obese individuals. No significant differences were obtained in percentages of $\text{CD}14^+$ monocytes, $\text{CD}19^+$ B lymphocytes and $\text{CD}3^+$ T lymphocytes between overweight or obese in comparison to the normal weight control group (Figure 19A-C). Although not significant, a slight increase in percentage of $\text{CD}4^+$ T lymphocytes and a slight decrease in $\text{CD}8^+$ T lymphocytes of the overweight group compared to the normal weight control group were detected (Figure 19E, F). The obese group did not differ significantly to the normal weight control group in the percentages of $\text{CD}4^+$ and $\text{CD}8^+$ T lymphocytes. The percentage of the $\text{CD}3^+\text{CD}56^+$ NKT cell population in PBMCs was significantly increased in the obese group compared to the normal weight group (Figure 19D), whereas no significant difference was seen between overweight and normal weight groups.

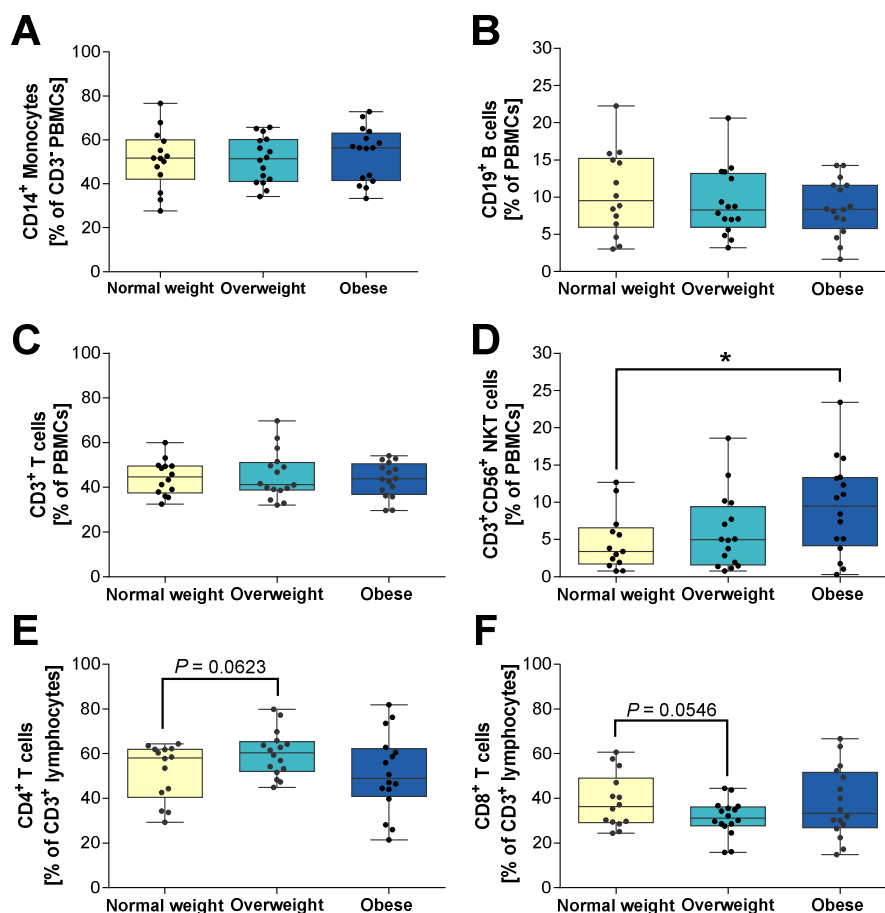


Figure 19: Frequencies of immune cell populations in peripheral blood mononuclear cells (PBMCs) isolated from normal weight, overweight and obese healthy blood donors. CD14⁺ Monocytes (A) as percentage of CD3⁺ lymphocytes. Percentage of CD19⁺ B lymphocytes (B), CD3⁺ T lymphocytes (C) and CD3⁺CD56⁺ natural killer T (NKT) cells (D) within viable PBMCs. CD4⁺ helper T lymphocytes (E) and CD8⁺ cytotoxic T lymphocytes (F) as percentage of CD3⁺ T lymphocytes. Graphs are box and whisker plots with median \pm minimum to maximum value; with additional dot plot representing individual donors. Overweight and obese groups were compared to normal weight control group. Statistical significance is indicated as: * $P < 0.05$; exact P-values within $0.05 < P < 0.1$ are indicated.

In addition to the mentioned immune cell populations above, the frequency of the CD3⁺CD56⁺ NK cells were determined. The NK cell percentages did not significantly differ between BMI groups (Figure 20A). In accordance to the underlying objectives of this study, NK cells were further gated and classified in their two main subsets – the more cytokine-producing CD56^{bright}CD16^{dim} NK cells and the more cytotoxic CD56^{dim}CD16^{bright} NK cells, depending on their amount of CD56 and CD16 expression (see gating strategy in 3.9.4). There was no significant difference in the percentage of CD56^{bright}CD16^{dim} NK cells in NK cells between the three BMI groups (Figure 20B). However, the percentage of CD56^{dim}CD16^{bright} NK cells in NK cells of the obese group was significantly increased compared to the normal weight control group (Figure 20C). Without being significant, a slight increase was determined in the percentage of CD56^{dim}CD16^{bright} NK cells of the overweight group in comparison with the normal weight control group (Figure 20C).

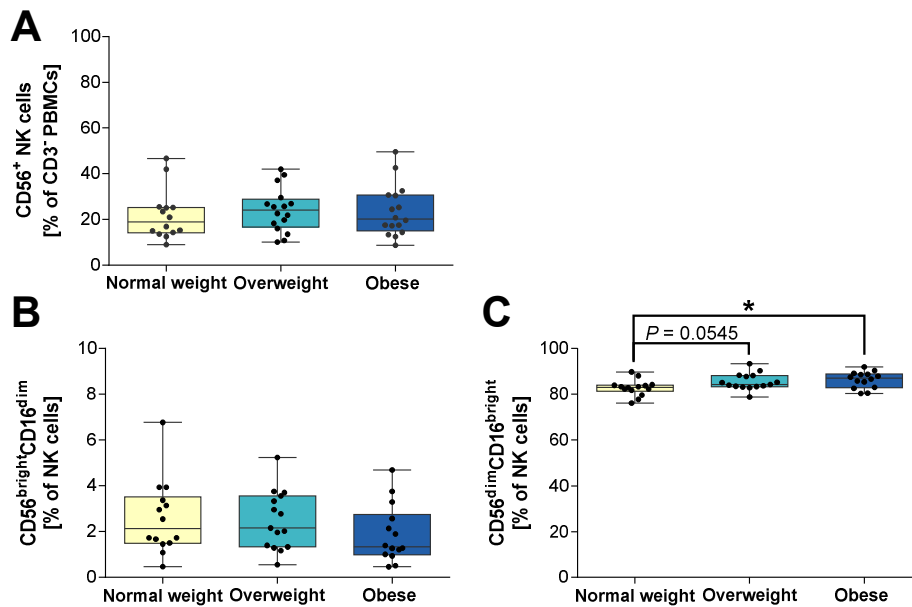


Figure 20: Frequencies of NK cells and NK cell subsets in peripheral blood mononuclear cells (PBMCs) isolated from normal weight, overweight and obese healthy blood donors. Percentage of CD56⁺ NK cells in CD3⁺ cells (A). Percentage of CD56^{bright}CD16^{dim} NK cells (B) and CD56^{dim}CD16^{bright} NK cells (C) in NK cells. Graphs are box and whisker plots with median \pm minimum to maximum value; with additional dot plot representing individual donors. Overweight and obese groups were compared to normal weight control group. Statistical significance is indicated as: * $P < 0.05$; exact P -values within $0.05 < P < 0.1$ are indicated.

4.2.3. Expression of killer-cell immunoglobulin-like receptors (KIRs) on NK cells

Figure 21 displays the expression of inhibitory and activating KIRs on total NK cells and on the two NK cell subsets. In general, the proportion of KIR-expressing CD56^{dim}CD16^{bright} NK cells was 10 to 20 times higher than that of CD56^{bright}CD16^{dim} NK cells; however, it was independent from the BMI (Figure 21; comparison of medians). In the case of the activating KIR CD158i, a significantly reduced proportion of total NK cells and of both subsets expressing this molecule were detected in the obese group compared to the normal weight control group (Figure 21A-C). Additionally, a slight reduction of CD158a⁺ and CD158b1/b2⁺ CD56^{bright}CD16^{dim} NK cells was observed in the obese group compared to the normal weight group (Figure 21B).

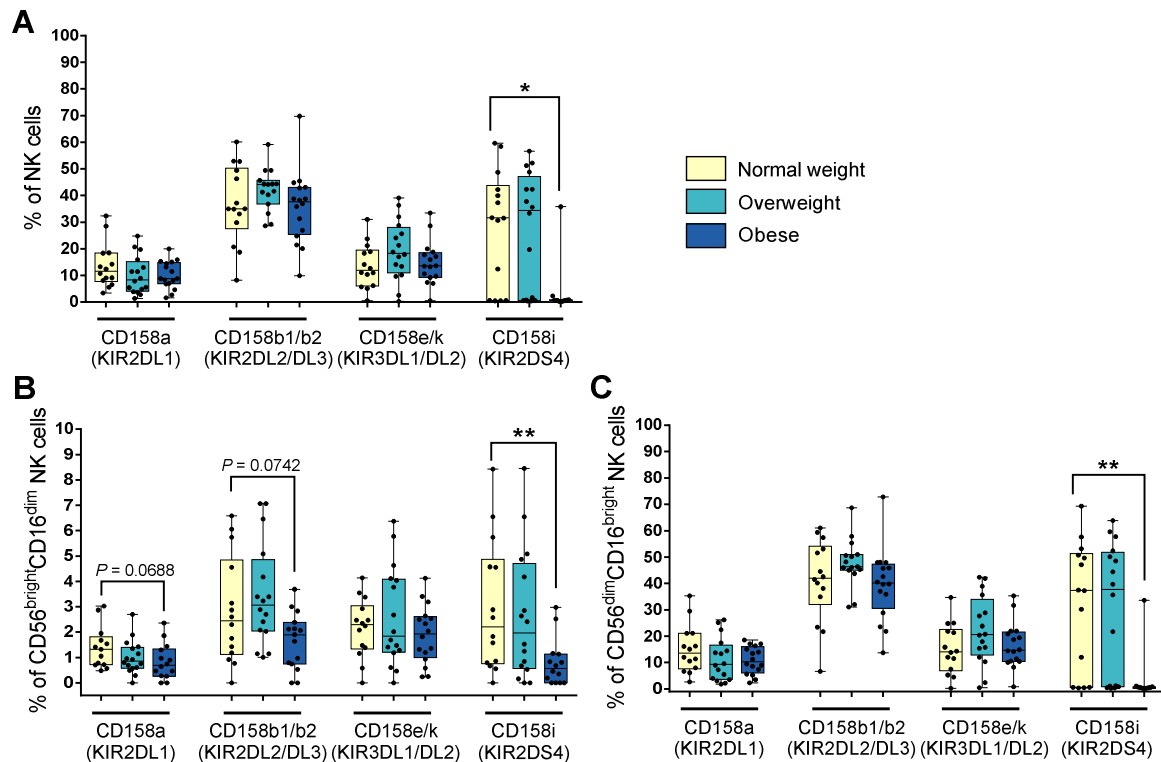


Figure 21: Frequencies of NK cells and NK cell subsets expressing killer-cell immunoglobulin-like receptors (KIRs) in peripheral blood mononuclear cells (PBMCs) isolated from normal weight, overweight and obese healthy blood donors. Percentage of KIR⁺ total NK cells (A), CD56^{bright}CD16^{dim} NK cells (B) and CD56^{dim}CD16^{bright} NK cells (C). KIRs named on X-axes are inhibitory (CD158a, CD158b1/b2, CD158e/k) and activating (CD158i) receptors on NK cells. Graphs are box and whisker plots with median \pm minimum to maximum value; with additional dot plot representing individual donors. Overweight and obese groups were compared to normal weight control. Statistical significance is indicated as: * $P < 0.05$; ** $P < 0.01$; exact P-values within $0.05 < P < 0.1$ are indicated.

4.2.4. Expression of natural cytotoxicity receptors (NCRs) on NK cells

The expression of the activating receptor NKp46 was highest among the three NCRs on CD56^{bright}CD16^{dim}, CD56^{dim}CD16^{bright} and total NK cells, whereas the proportion of activating receptor NKp44⁺ CD56^{bright}CD16^{dim}, CD56^{dim}CD16^{bright} and total NK cells was lowest, independent from the BMI group (Figure 22). No significant differences were detected between BMI groups and the level of NCR⁺ CD56^{bright}CD16^{dim}, CD56^{dim}CD16^{bright} and total NK cells. However, the number of NKp46-expressing CD56^{bright}CD16^{dim} NK cells in the obese group was slightly decreased compared to the normal weight control group (Figure 22A).

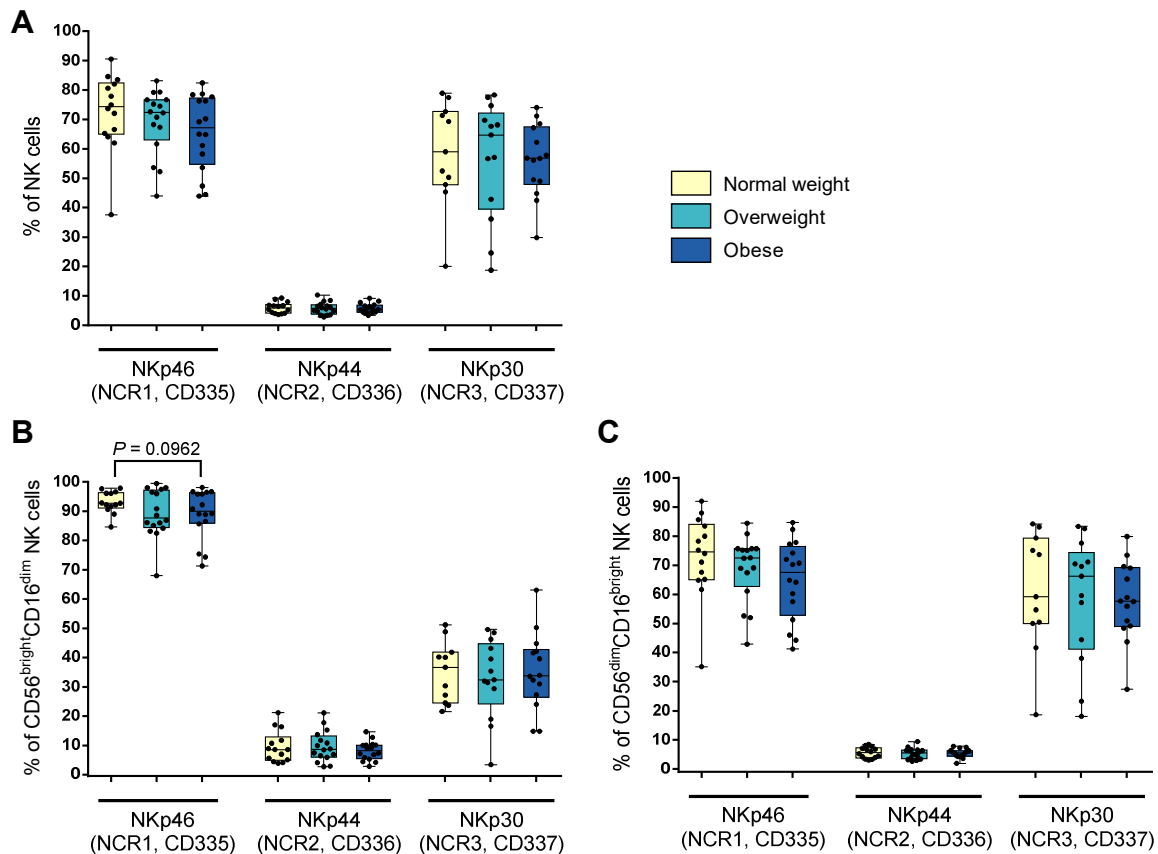


Figure 22: Frequencies of NK cells and NK cell subsets expressing natural cytotoxicity receptors (NCRs) in peripheral blood mononuclear cells (PBMCs) isolated from normal weight, overweight and obese healthy blood donors. Percentage of NCR⁺ total NK cells (A), CD56^{bright}CD16^{dim} NK cells (B) and CD56^{dim}CD16^{bright} NK cells (C). NCRs named on X-axes are activating receptors on NK cells. Graphs are box and whisker plots with median \pm minimum to maximum value; with additional dot plot representing individual donors. Overweight and obese groups were compared to normal weight control. Precise P-value within $0.05 < P < 0.1$ is indicated.

4.2.5. Expression C-type lectin-like NKG2 receptors on NK cells

Among all BMI groups, the proportion of total NK cells and CD56^{dim}CD16^{bright} NK cells expressing the activating NKG2D receptor was highest, while the proportion of the same populations expressing the inhibitory NKG2A receptor was almost 50% lower (Figure 23B). In contrast, the proportions of NKG2D⁺ and NKG2A⁺ CD56^{bright}CD16^{dim} NK cells was almost the same with mainly over 80% positive cells among all BMI groups (Figure 23A). Within total NK cells and NK cell subsets and among all BMI groups, the proportions of NKG2C⁺ cells were lowest compared to NKG2A⁺ and NKG2D⁺ cells.

The proportion of NKG2A⁺ CD56^{bright}CD16^{dim} NK cells was significantly higher in overweight individuals compared to normal weight individuals (Figure 23 A). Furthermore, the level of CD56^{dim}CD16^{bright} and total NK cells expressing the activating NKG2C receptor was slightly decreased in the overweight group compared to the normal weight group (Figure 23B, C).

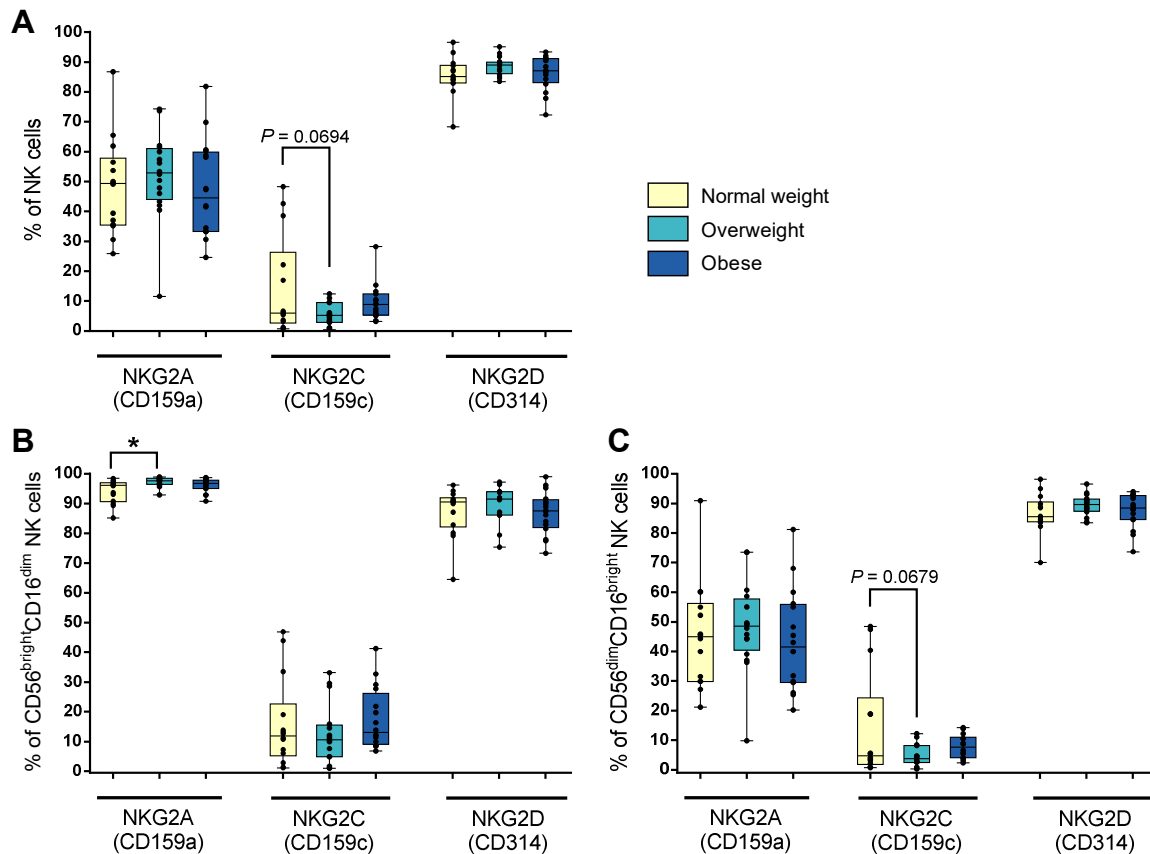


Figure 23: Frequencies of NK cells and NK cell subsets expressing C-type lectin receptors (CTLRs) in peripheral blood mononuclear cells (PBMCs) isolated from normal weight, overweight and obese healthy blood donors. Percentage of CLR⁺ total NK cells (A), CD56^{bright}CD16^{dim} NK cells (B) and CD56^{dim}CD16^{bright} NK cells (C). CTLRs named on X-axes are inhibitory (NKG2A) and activating (NKG2C, NKG2D) receptors on NK cells. Graphs are box and whisker plots with median \pm minimum to maximum value; with additional dot plot representing individual donors. Overweight and obese groups were compared to normal weight control group. Statistical significance is indicated as: * $P < 0.05$; P values within $0.05 < P < 0.1$ are indicated with precise P -value.

4.2.6. Expression of other inhibitory and activating receptors and adhesion molecules on NK cells

The expression analysis of the inhibitory receptor CD161 revealed similar fractions of CD56^{bright}CD16^{dim}, CD56^{dim}CD16^{bright} and total NK cells bearing this receptor. Furthermore, non-significant differences were found between BMI groups within the investigated NK cell populations (Figure 24A-C, left). However, a slight increase was detected in CD161⁺ CD56^{dim}CD16^{bright} NK cells of the overweight group compared to the normal weight control group (Figure 24B, left). Additionally, analysis of the median fluorescent intensity (MFI) of the level of CD161 expression on the NK cell populations was determined due to the similar level of CD161⁺ NK cell fractions; however, with no significant differences between the BMI groups (Figure 24A-C, right).

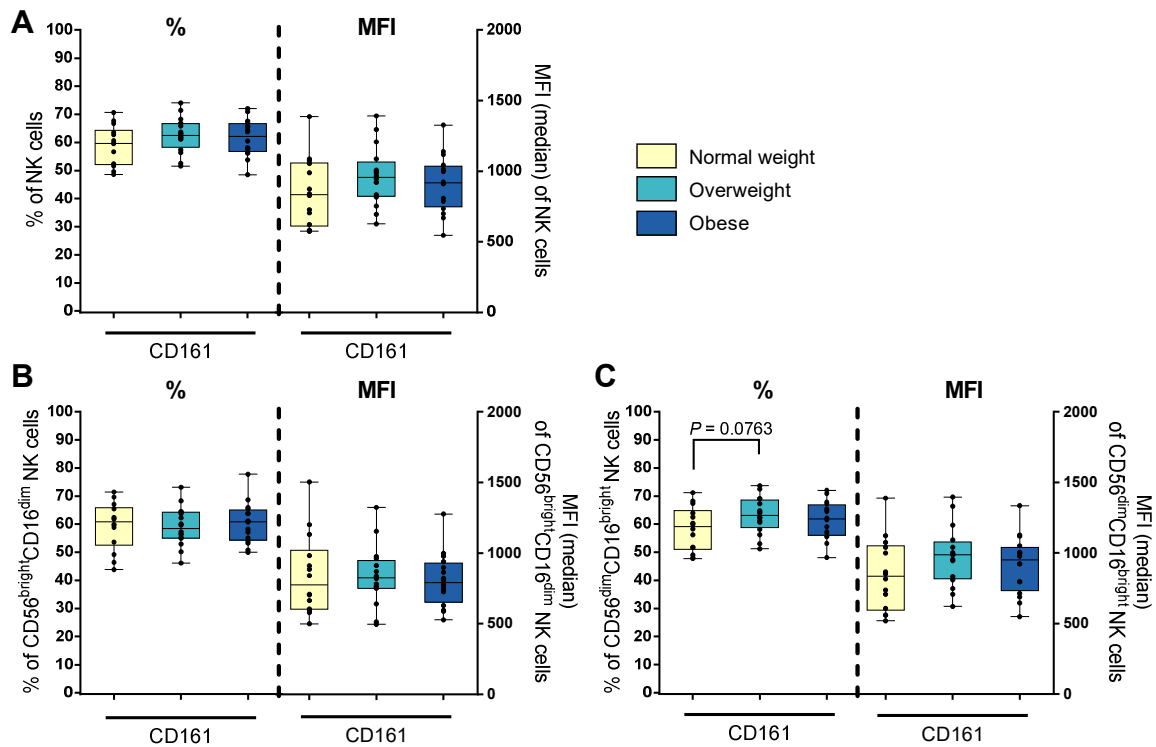


Figure 24: Frequencies of NK cells and NK cell subsets expressing inhibitory receptor CD161 in peripheral blood mononuclear cells (PBMCs) isolated from normal weight, overweight and obese healthy blood donors. Percentage (left) and median of fluorescent intensity (MFI; right) of CD161⁺ total NK cells (A), CD56^{bright}CD16^{dim} NK cells (B) and CD56^{dim}CD16^{bright} NK cells (C). Graphs are box and whisker plots with median \pm minimum to maximum value; with additional dot plot representing individual donors. Overweight and obese groups were compared to normal weight control group. Precise P values within $0.05 < P < 0.1$ are indicated.

The majority of NK cells in total and of both subsets expressed the inhibitory receptor Siglec-7 (Figure 25A-C, left). A slight increase in the proportion of Siglec-7⁺ CD56^{dim}CD16^{bright} NK cells of the overweight group was detected compared to the normal weight control group, without significant difference (Figure 25C, left). The same result applied for the total NK cell population of the overweight group (Figure 25A, left). Due to the high level of Siglec-7-expressing NK cells, the MFI of positive cells was analyzed. No BMI-related effect was found on the Siglec-7 expression level on the NK cell subsets. However, the MFI value of Siglec-7 molecules expressed on CD56^{bright}CD16^{dim} NK cells was half as high as the MFI value on CD56^{dim}CD16^{bright} NK cells and total NK cells (Figure 25B vs. A and C, right, respectively).

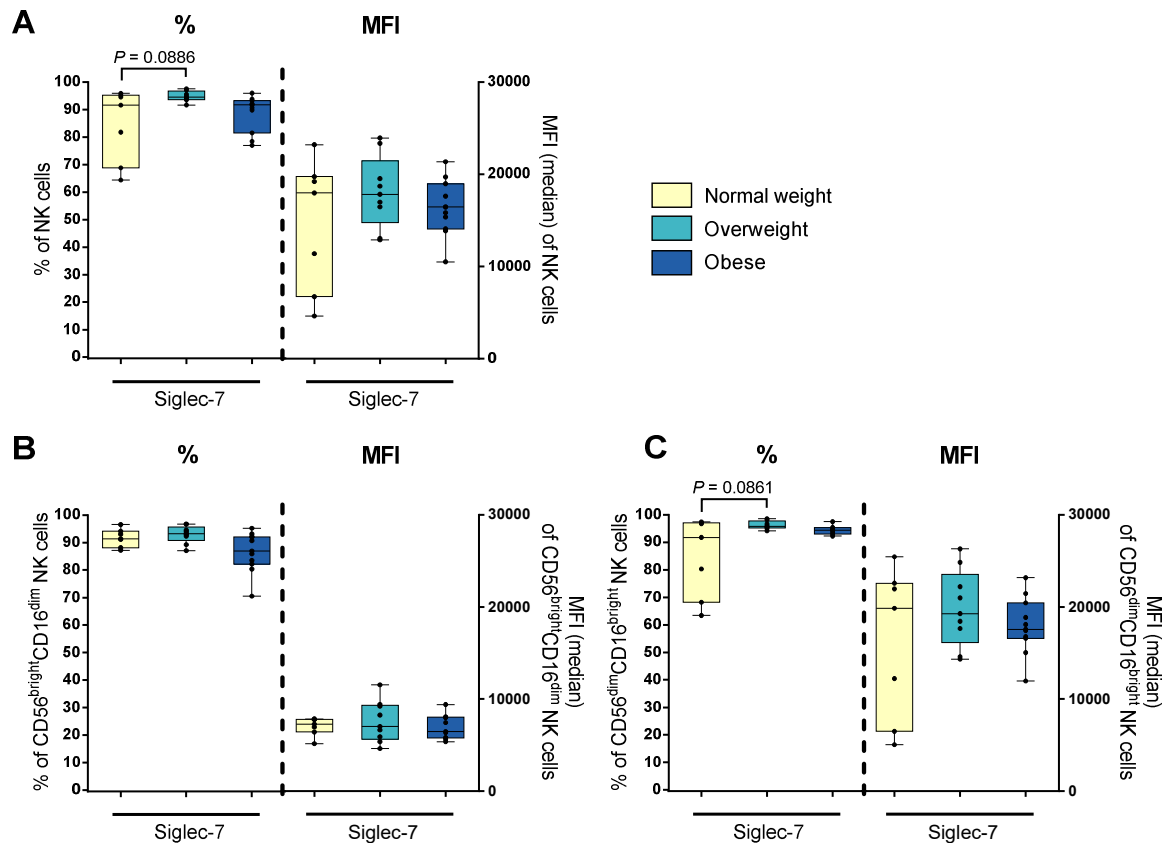


Figure 25: Frequencies of NK cells and NK cell subsets expressing inhibitory receptor Siglec-7 in peripheral blood mononuclear cells (PBMCs) isolated from normal weight, overweight and obese healthy blood donors. Percentage (left) and median of fluorescent intensity (MFI; right) of Siglec-7⁺ total NK cells (A), CD56^{bright}CD16^{dim} NK cells (B) and CD56^{dim}CD16^{bright} NK cells (C). Graphs are box and whisker plots with median \pm minimum to maximum value; with additional dot plot representing individual donors. Overweight and obese groups were compared to normal weight control group. P values within $0.05 < P < 0.1$ are indicated with precise P-value.

The adhesion molecules, CD2 and CD62L, were both higher expressed by the CD56^{bright}CD16^{dim} NK cell subset (> 90% and > 50%, respectively) compared to the CD56^{dim}CD16^{bright} NK cell subset and total NK cells (Figure 26A-C, left, and D-F, respectively).

Between the BMI groups, no significant differences have been revealed within the investigated CD2⁺ NK cell populations. However, a significantly reduced MFI of CD2⁺ CD56^{dim}CD16^{bright} NK cells was detected (Figure 26C, right). Interestingly, the proportion of CD56^{dim}CD16^{bright} NK cells expressing CD62L was significantly reduced in the obese and overweight groups compared to the normal weight control group ($P < 0.05$; Figure 26F). This significant difference was more pronounced in the proportion of CD62L⁺ total NK cells between obese and normal weight individuals ($P < 0.01$), whereas the reduction of CD62L-bearing NK cells of overweight individuals compared to normal weight individuals was not significant in the total NK cell population (Figure 26D).

Due to the highly expressed DNAM-1 (CD226) adhesion molecule on all investigated NK cell populations in all BMI groups (nearly 100% each, data not shown), the MFI was determined. The number of fluorescent-conjugated monoclonal antibody per cell for the adhesion molecule DNAM-1 was nearly equal on the surface of all three investigated NK cell populations of all BMI-groups. No significant differences were observed between the BMI-groups (Figure 26G-I).

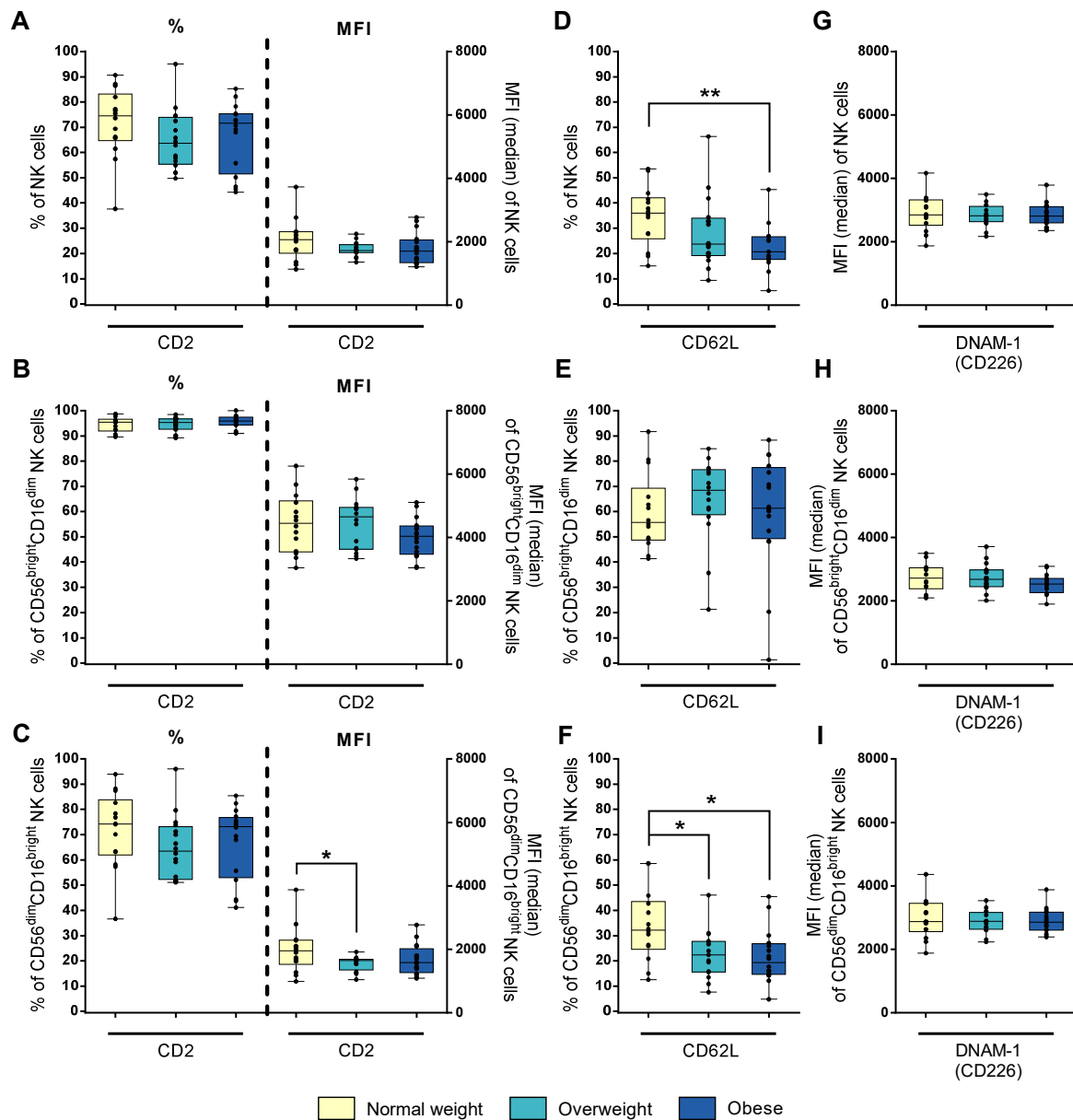


Figure 26: Frequencies and median fluorescent intensities (MFIs) of NK cells and NK cell subsets expressing the adhesion molecules CD2, CD62L and DNAM-1 (CD226) in peripheral blood mononuclear cells (PBMCs) isolated from normal weight, overweight and obese healthy blood donors. Percentage (left) and MFI (right) of CD2⁺ total NK cells (A), CD56^{bright}CD16^{dim} NK cells (B) and CD56^{dim}CD16^{bright} NK cells (C). Percentages of CD62L⁺ total NK cells (D), CD56^{bright}CD16^{dim} NK cells (E) and CD56^{dim}CD16^{bright} NK cells (F). MFI of DNAM-1⁺ total NK cells (G), CD56^{bright}CD16^{dim} NK cells (H) and CD56^{dim}CD16^{bright} NK cells (I). Graphs are box and whisker plots with median \pm minimum to maximum value; with additional dot plot representing individual donors. Overweight and obese groups were compared to normal weight control group. Statistical significance is indicated as: *P < 0.05; **P < 0.01.

4.2.7. Expression of functional markers on NK cells

The basal fraction levels and MFIs of the three NK cell populations expressing the activation-associated receptors CD25 and CD69 have been determined (Figure 27).

In general, CD56^{bright}CD16^{dim} NK cells expressed CD25 at a slightly higher level than CD56^{dim}CD16^{bright} and total NK cells among all BMI groups. In the obese study group elevated frequencies of CD56^{bright}CD16^{dim} NK cells were CD25⁺ compared to the normal weight control group, although the difference was not significant (Figure 27B, left). In contrast, the determined MFI showed a significantly higher proportion of CD25⁺ within the CD56^{bright}CD16^{dim} subset in the overweight group, but not in the obese group, compared to the control group (Figure 27B, right). The proportion of CD25⁺ CD56^{dim}CD16^{bright} and total NK cells showed equal levels in comparison to each other and among the BMI groups for each NK cell population (Figure 27A, C).

CD69 displayed the same expression level on all investigated NK cell populations and among all BMI groups (Figure 27D-F). No significant differences have been observed analyzing the proportion or MFI of CD69 expression in total NK cells as well as the two NK cell subsets (Figure 27D-F).

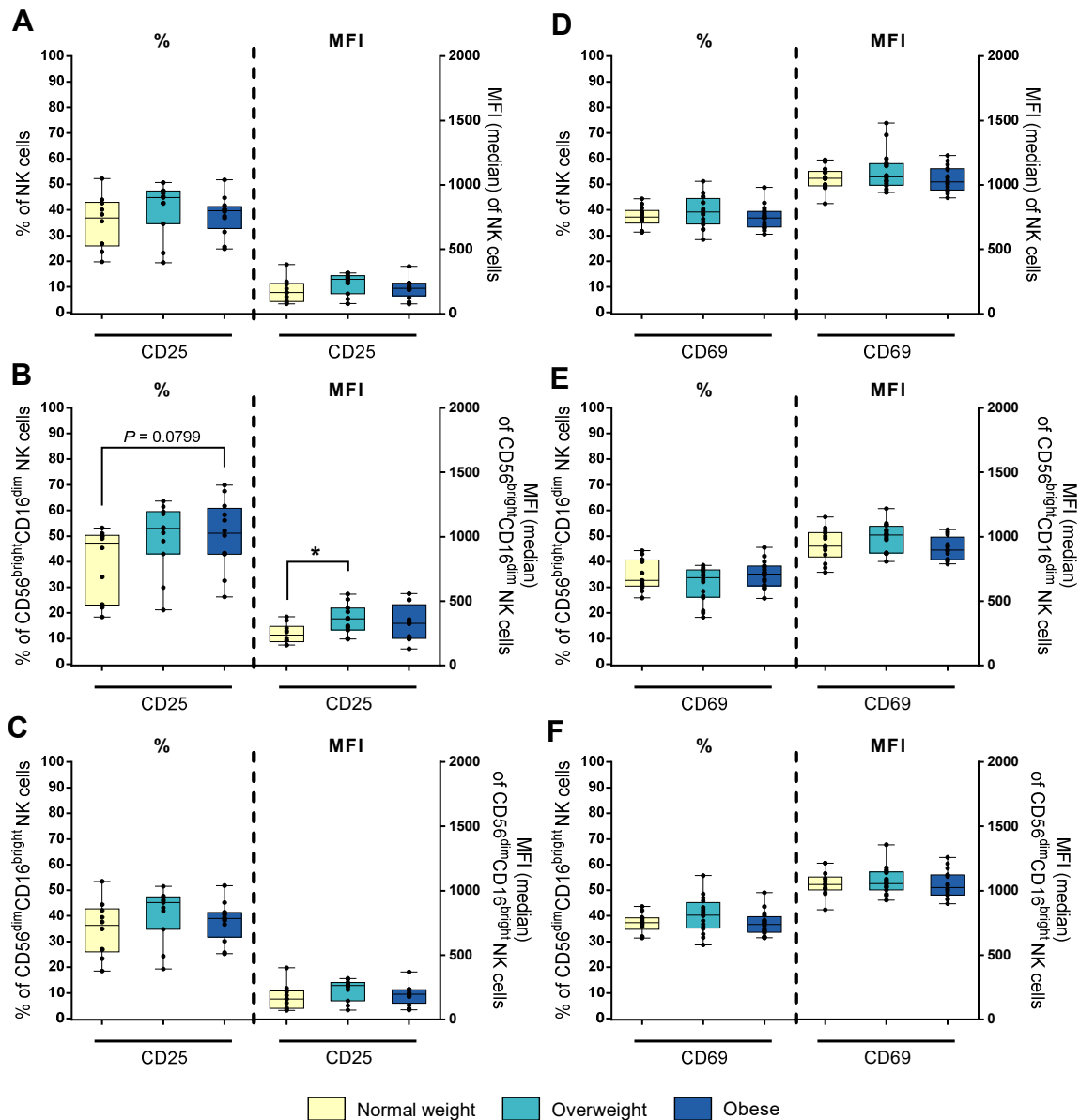


Figure 27: Frequencies and median fluorescent intensities (MFIs) of NK cells and NK cell subsets expressing the activation-associated receptors CD25 and CD69 in peripheral blood mononuclear cells (PBMCs) isolated from normal weight, overweight and obese healthy blood donors. Percentage (left) and MFI (right) of CD25⁺ total NK cells (A), CD56^{bright}CD16^{dim} NK cells (B) and CD56^{dim}CD16^{bright} NK cells (C). Percentages and MFI of CD69⁺ total NK cells (D), CD56^{bright}CD16^{dim} NK cells (E) and CD56^{dim}CD16^{bright} NK cells (F). Graphs are box and whisker plots with median \pm minimum to maximum value; with additional dot plot representing individual donors. Overweight and obese groups were compared to normal weight control group. Statistical significance is indicated as: * $P < 0.05$; P value within $0.05 < P < 0.1$ is indicated with precise P-value.

CD27 and CD57 represent markers to characterize the maturation and differentiation status of NK cells.

Regardless of the BMI group, the comparison between the CD56^{bright}CD16^{dim} and CD56^{dim}CD16^{bright} NK cell subsets revealed major differences in their proportion of CD27⁺ cells. The frequency of CD56^{bright}CD16^{dim} NK cells expressing CD27 was around ten times higher than the frequency of CD27⁺ CD56^{dim}CD16^{bright} NK cells (Figure 28B vs. C, left). Due to the same CD27

expression level on all NK cells as on CD56^{dim}CD16^{bright}, the previously described result also applied to the comparison between CD56^{bright}CD16^{dim} and all NK cells (Figure 28B vs. A, left). No significant differences were detected between BMI groups in the proportion of CD27⁺ CD56^{bright}CD16^{dim} NK cells. However, analyses of the MFI of this subset revealed an increased amount of CD27 molecules per NK cell in the overweight and obese group compared to the normal weight control group ($P < 0.05$ and $P = 0.0687$, respectively; Figure 28B, right).

Slightly reduced proportions of CD27⁺ CD56^{dim}CD16^{bright} and total NK cells were observed in the overweight group compared to the control group, without differences in the MFIs (Figure 28B). Furthermore, a significantly diminished frequency of total NK cells bearing the CD27 surface marker was observed in the obese group compared to the normal weight group, without differences in the MFIs (Figure 28C).

Similarly to CD27, the comparison between the CD56^{bright}CD16^{dim} and CD56^{dim}CD16^{bright} NK cell subsets showed also major differences in their proportion of CD57⁺ cells. But, in contrast to CD27, the frequency of CD56^{bright}CD16^{dim} NK cells expressing CD27 was around eight times lower than the frequency of CD27⁺ CD56^{dim}CD16^{bright} NK cells and also than the frequency of CD27⁺ total NK cells (Figure 28B vs. C and A, left, respectively). For the proportions and MFIs of the investigated CD57⁺ NK cell populations no differences were detected between the BMI groups (Figure 28D-F). Additionally to the general CD57 expression on the NK cell populations, the proportions of CD57^{high} CD56^{bright}CD16^{dim}, CD56^{dim}CD16^{bright} and total NK cells were determined. The comparison between CD56^{bright}CD16^{dim} and CD56^{dim}CD16^{bright} NK cell subsets showed a huge difference: the percentage of CD57^{high} CD56^{bright}CD16^{dim} NK cells was $> 0.6\%$ while the percentage of CD57^{high} CD56^{dim}CD16^{bright} was 100 times higher (about 60% positive cells; data not shown). However, the comparisons between BMI groups within each NK cell population in frequencies and MFIs revealed no differences (data not shown).

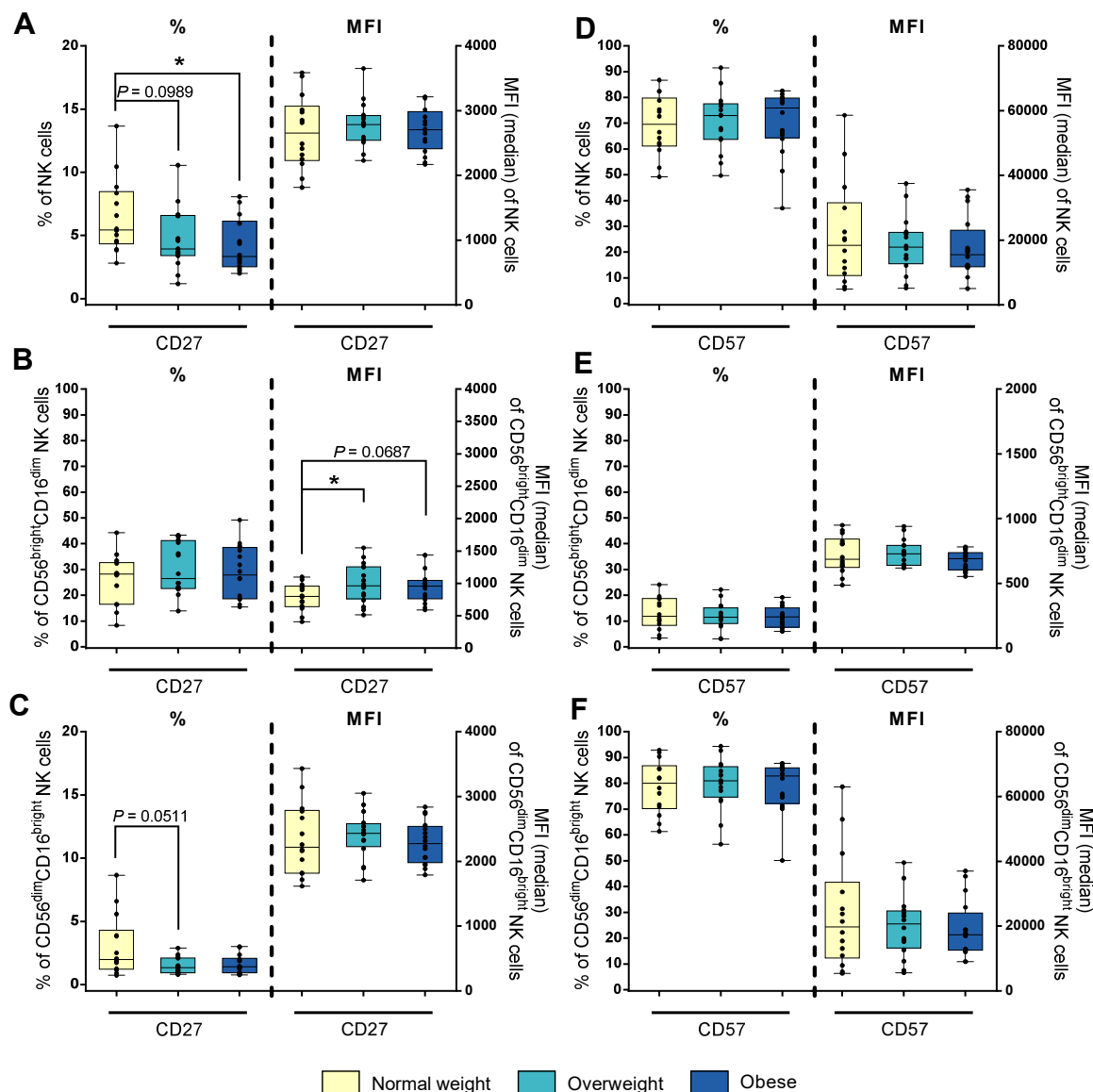


Figure 28: Frequencies and median fluorescent intensities (MFIs) of NK cells and NK cell subsets expressing the maturation and differentiation markers CD27 and CD57 in peripheral blood mononuclear cells (PBMCs) isolated from normal weight, overweight and obese healthy blood donors. Percentage (left) and MFI (right) of CD27⁺ total NK cells (A), CD56^{bright}CD16^{dim} NK cells (B) and CD56^{dim}CD16^{bright} NK cells (C). Percentages and MFI of CD57⁺ total NK cells (D) CD56^{bright}CD16^{dim} NK cells (E) and CD56^{dim}CD16^{bright} NK cells (F). Graphs are box and whisker plots with median \pm minimum to maximum value; with additional dot plot representing individual donors. Overweight and obese groups were compared to normal weight control. Statistical significance is indicated as: *P < 0.05; P values within 0.05 < P < 0.1 are indicated with precise P-value.

Additionally to all other already mentioned NK cell markers, the four co-signaling markers 2B4, NKp80, TIGIT and PD-1 (either co-stimulatory or co-inhibitory) were analyzed (Figure 29 and Figure 30).

Due to the highly expressed 2B4 activating co-receptor on all investigated NK cell populations in all BMI groups (nearly 100% each, data not shown), the MFI was determined (Figure 29A-C). Highly significantly elevated fractions of 2B4⁺ total NK cells and CD56^{dim}CD16^{bright} NK cells in the obese compared to the normal weight control group were detected (Figure 29A, C). The MFI

of the 2B4⁺ CD56^{bright}CD16^{dim} NK cell subset showed no differences between the BMI groups (Figure 29B).

For NKp80, the total NK cell population as well as both NK cell subsets displayed > 80% positive cells bearing this activating co-receptor regardless of the BMI group (Figure 29D-F), however, with a significantly increased fraction of NKp80⁺ total NK cells in the overweight group compared to the normal weight group (Figure 29D). The MFI levels of NKp80 exhibited no differences between BMI groups and within the NK cell populations (data not shown).

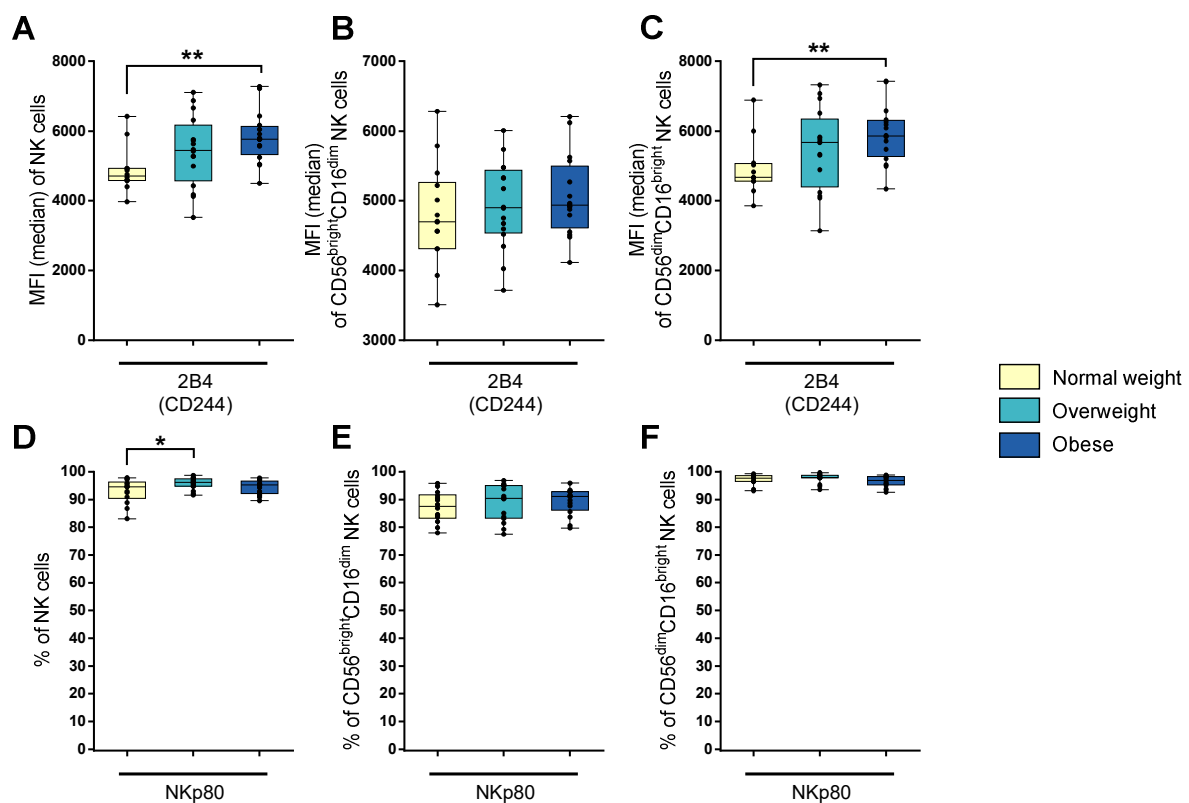


Figure 29: Median fluorescent intensities (MFIs) or frequencies of NK cells and NK cell subsets expressing the co-activating markers 2B4 and NKp80 in peripheral blood mononuclear cells (PBMCs) isolated from normal weight, overweight and obese healthy blood donors. MFI of 2B4⁺ total NK cells (A) CD56^{bright}CD16^{dim} NK cells (B) and CD56^{dim}CD16^{bright} NK cells (C). Percentage of NKp80⁺ total NK cells (D), CD56^{bright}CD16^{dim} NK cells (E) and CD56^{dim}CD16^{bright} NK cells (F). Graphs are box and whisker plots with median \pm minimum to maximum value; with additional dot plot representing individual donors. Overweight and obese groups were compared to normal weight control group. Statistical significance is indicated as: **P < 0.01; *P < 0.05.

Regardless of the BMI group, about two-third of total NK cells and CD56^{dim}CD16^{bright} NK cells expressed the inhibitory co-signaling receptor TIGIT and a bit more than half of the CD56^{bright}CD16^{dim} NK cell subset was TIGIT⁺. The frequencies of the investigated NK cell populations presented no differences for the expression of TIGIT between the three BMI groups (Figure 30G-I, left). In addition, no significant differences have been observed in the determined MFIs of TIGIT⁺ CD56^{dim}CD16^{bright} and total NK

cells (Figure 30C, A, right, respectively). However, a slightly increased MFI of the TIGIT⁺ CD56^{bright}CD16^{dim} subset of the overweight group compared to the normal weight group was determined (Figure 30B, right).

The fractions of the inhibitory co-receptor PD-1⁺ NK cells within all investigated NK cell populations revealed no differences in the percentage and MFIs of positive cells for each population (~ 30%) as well as no differences between the three BMI groups (Figure 30D-F).

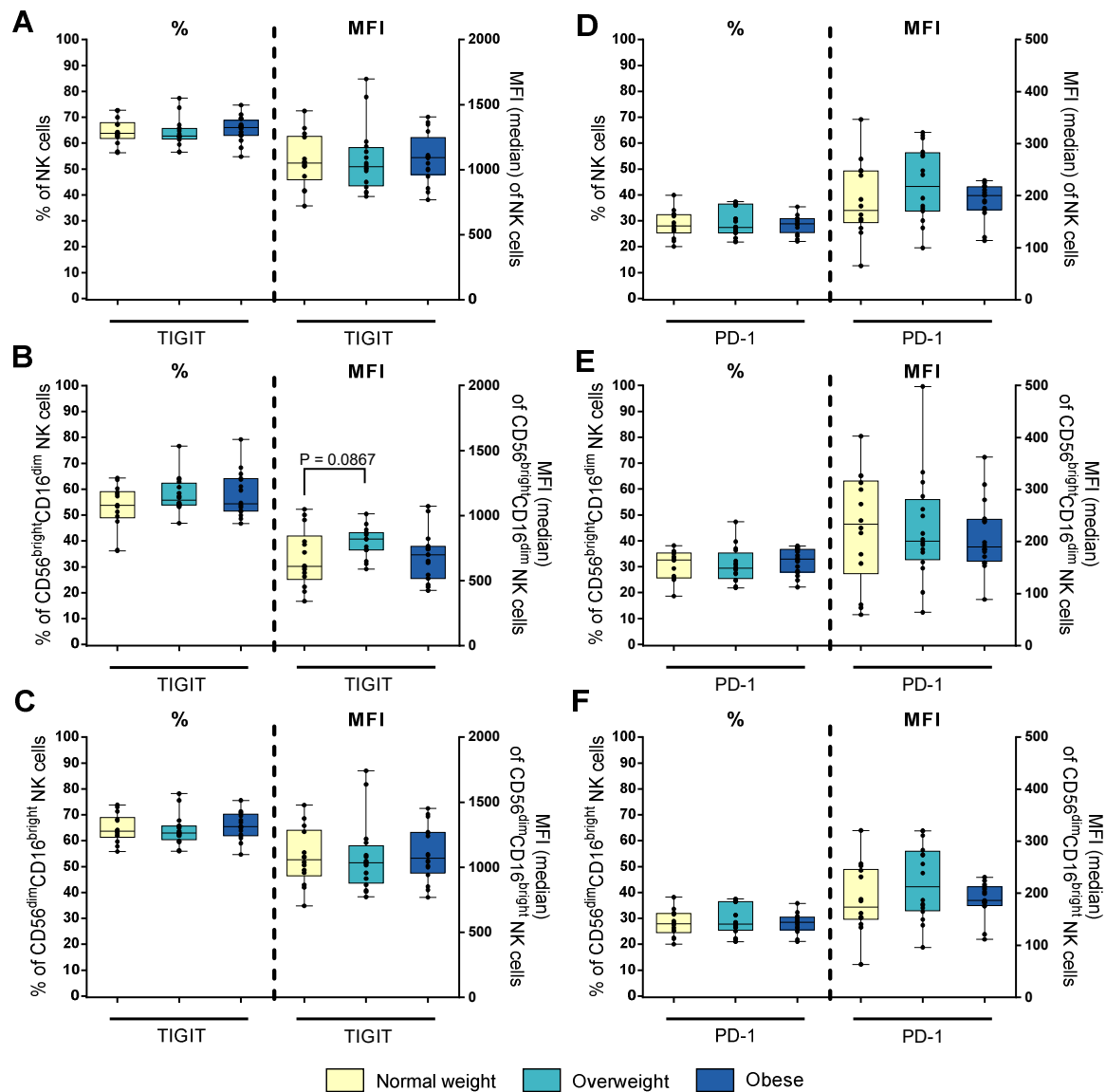


Figure 30: Frequencies and/or median fluorescent intensities (MFIs) of NK cells and NK cell subsets expressing the co-inhibitory markers TIGIT and PD-1 in peripheral blood mononuclear cells (PBMCs) isolated from normal weight, overweight and obese healthy blood donors. Percentage (left) and MFI (right) of TIGIT⁺ total NK cells (A), CD56^{bright}CD16^{dim} NK cells (B) and CD56^{dim}CD16^{bright} NK cells (C). Percentage (left) and MFI (right) of PD-1⁺ total NK cells (D), CD56^{bright}CD16^{dim} NK cells (E) and CD56^{dim}CD16^{bright} NK cells (F). Graphs are box and whisker plots with median \pm minimum to maximum value; with additional dot plot representing individual donors. Overweight and obese groups were compared to normal weight control group. P value within 0.05 < P < 0.1 is indicated with precise P-value.

4.2.8. Co-expression analysis of different NK surface markers

Figure 31 displays the frequencies of total NK cells and CD56^{dim}CD16^{bright} NK cells co-expressing different variations of interesting NK cell receptors. To note, the co-expression analysis was limited to the surface markers stained together in one flow cytometric multi-color panel and additionally displayed four populations in the analysis (double negative, single positives and double positive). Here, analysis was considered reasonable only of total NK cells and CD56^{dim}CD16^{bright} NK cell subset, because the number of events of co-expressing CD56^{bright}CD16^{dim} NK cell subset was too low for statistical evaluation.

The proportions of double-positive CD158a⁺CD158b1/b2⁺ and double-positive NKG2A⁺NKG2C⁺ total and CD56^{dim}CD16^{bright} NK cells were not different between the BMI groups (Figure 31A, E). However, obese individuals showed a slight but statistically not significant decrease in the proportion of double-positive CD62L⁺CD158e/k⁺ total NK cells compared to the normal weight individuals (Figure 31B, left). Furthermore, the proportions of total NK cells and CD56^{dim}CD16^{bright} NK cells co-expressing the maturation marker CD57 and the inhibitory receptor NKG2A were increased in the overweight group compared to the normal weight group, without being statistically significant (Figure 31C). A significant increase in the frequency of total NK cells co-expressing CD57 and the activating receptor NKG2C was determined in the obese group compared to the normal weight control group (Figure 31D, left). This increase was also observed in the frequency of CD56^{dim}CD16^{bright} NK cell subset comparing the same BMI groups, but without statistical significance (Figure 31D, right).

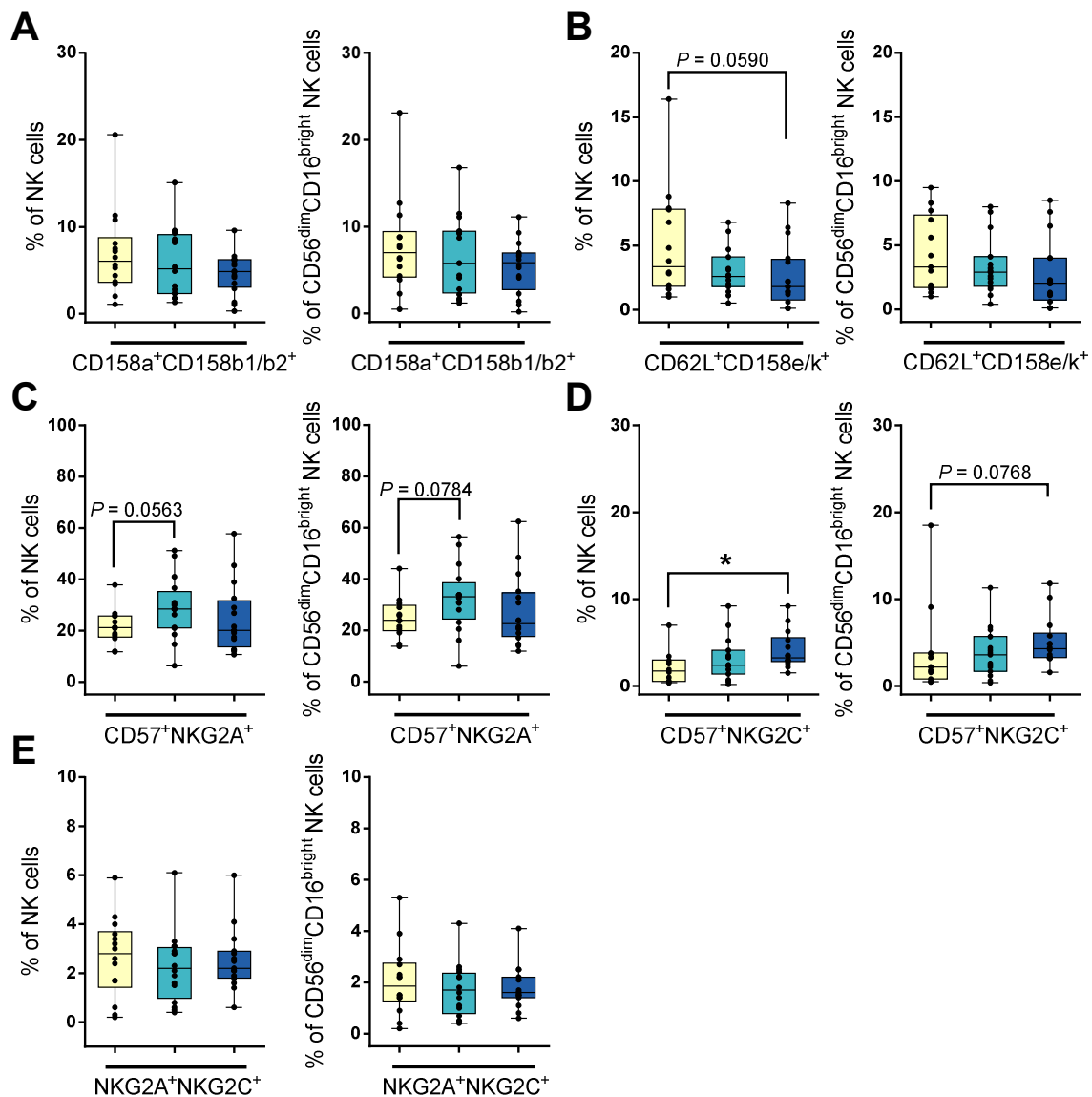


Figure 31: Frequencies of total NK cells (left) and CD56^{dim}CD16^{bright} NK cells (right) co-expressing inhibitory KIR receptors (A), adhesion molecule CD62L and inhibitory KIR receptor CD158e/k (B), maturation marker CD57 and inhibitory receptor NKG2A (C), CD57 and activating receptor NKG2C (D) and NKG2A and NKG2C (E). Graphs are box and whisker plots with median \pm minimum to maximum value; with additional dot plot representing individual donors. Overweight and obese groups were compared to normal weight control group. Statistical significance is indicated as: * $P < 0.05$. P values within $0.05 < P < 0.1$ are indicated with precise P-values.

4.2.9. Expression of intracellular NK cell markers

In addition to the analyzed NK cell surface markers, intracellular NK cell markers were determined. In order to investigate the potential of NK cell populations to produce IFN- γ , PBMCs of donors were stimulated either with IL-12 plus IL-18 overnight or with PMA plus ionomycin for 4 h. Here, due to the stimulations, the usual analysis of the two NK cells subsets according to their CD56 and CD16 expression was not possible and was limited to the sole expression of CD56 molecules on the NK cells. This is related to the fact that NK cells reduce their expression of CD16

upon stimulation with the used stimulants [170, 171]. Since the fraction of CD56^{bright} NK cells was low and there were hardly any differences between CD56^{dim} and total NK cells, only the expression data of the CD56^{bright} and total NK cell populations were evaluated.

Both stimulations successfully promoted the IFN- γ production in NK cells, detectable by the increased fractions of IFN- γ ⁺ total NK cells and CD56^{bright} NK cells among all BMI groups compared to basal levels (unstimulated PBMCs; Figure 32A, B). CD56^{bright} NK cells, stimulated with IL-12 plus IL-18, showed a higher potential to produce INF- γ in comparison to the total NK cell population among all BMI groups (Figure 32B vs. A, > 80% vs. 50 – 60%, respectively). Furthermore, a slightly elevated level of IFN- γ ⁺ CD56^{bright} NK cells of the overweight group compared to the normal weight group was determined (Figure 32B). In contrast, the MFI of IFN- γ ⁺ CD56^{bright} NK cell subset revealed no differences between the BMI groups (Figure 32C). The stimulation with PMA plus ionomycin led to a slight decrease of the total NK cell fraction expressing IFN- γ (Figure 32A). Two-way ANOVA revealed a significant influence of the stimulation used on both NK cell populations, with significant differences between the two used stimulations and between unstimulated control and both stimulations (data not shown).

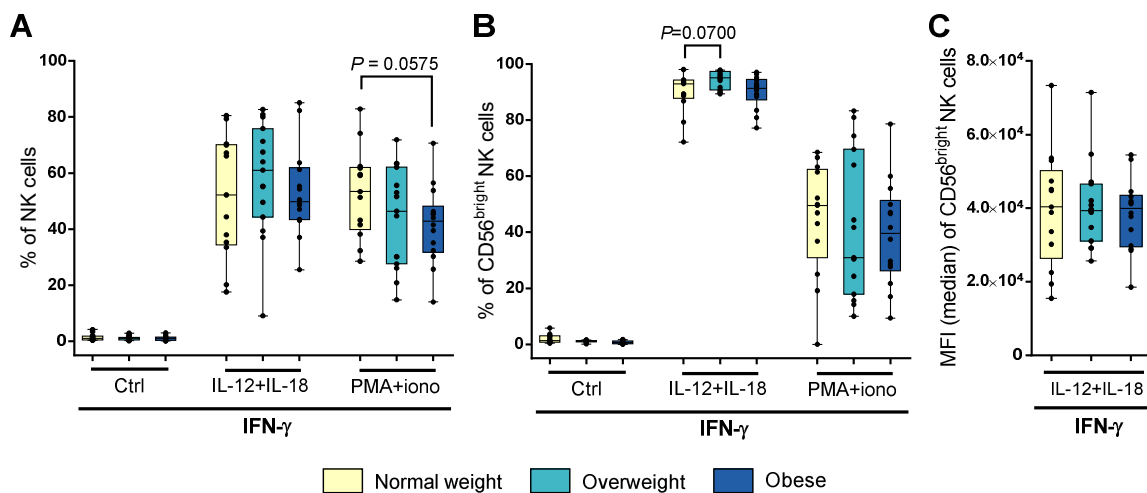


Figure 32: Stimulation of IFN- γ production in NK cell populations. PBMCs of blood donors with different body mass indexes were either stimulated with 10 ng/ml interleukin-12 (IL-12) in combination with 50 ng/ml interleukin-18 (IL-18) overnight or with 50 ng/ml phorbol-12-myristate-13-acetate (PMA) in combination with 1 μ g/ml ionomycin for 4 h. Percentage of IFN- γ ⁺ total NK cells (A) and CD56^{bright} NK cells (B). Median fluorescent intensity (MFI) of IFN- γ ⁺ CD56^{bright} NK cells (C). Graphs are box and whisker plots with median \pm minimum to maximum value; with additional dot plot representing individual donors. Overweight and obese groups were compared to normal weight control group within each stimulation setting. P values within 0.05 < P < 0.1 are indicated with precise P-value. Ctrl: unstimulated control.

Furthermore, the expression of the intracellular NK cell markers TRAIL, granzyme A, granzyme B and perforin were assessed on unstimulated as well as IL-12 plus IL-18 stimulated total NK and CD56^{bright} NK cells (Figure 33A-H).

The MFI of TRAIL expressing CD56^{bright} NK cells was three times higher than of total NK cells among all BMI groups (Figure 33B vs. A). Furthermore, the MFI of TRAIL⁺ unstimulated total NK cells of the obese group was significantly higher compared to the normal weight control group (Figure 33A).

The MFIs of granzyme A and granzyme B were nearly equal between total NK cells and CD56^{bright} NK cells. In addition, no differences were detected comparing the MFIs of granzyme A and granzyme B of the three BMI groups (Figure 33C-F). However, granzyme B⁺ stimulated CD56^{bright} NK cells showed a slightly reduced MFI in the obese group compared to the control group (Figure 33F).

The MFI value of perforin⁺ CD56^{bright} NK cells was two to four times lower compared to total NK cells, without differences among the BMI groups (Figure 33G-H).

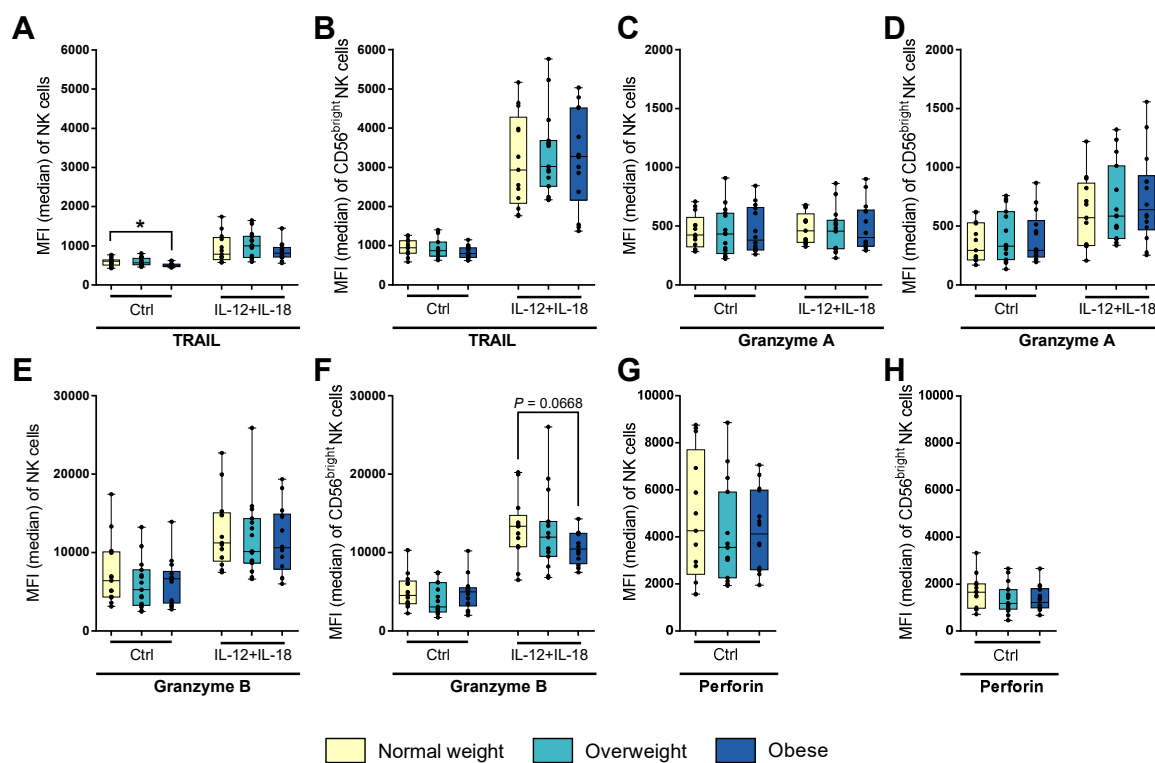


Figure 33: Median fluorescence intensity (MFI) of intracellular tumor necrosis factor–related apoptosis-inducing ligand (TRAIL), granzyme A, granzyme B and perforin in NK cells and CD56^{bright} NK cell subset. PBMCs of blood donors with different body mass indexes were either stimulated with 10 ng/ml interleukin-12 (IL-12) in combination with 50 ng/ml interleukin-18 (IL-18) overnight or remained untreated (perforin samples). MFI of TRAIL⁺ total NK cells (A) and CD56^{bright} NK cells (B). MFI of granzyme A⁺ total NK cells (C) and CD56^{bright} NK cells (D). MFI of granzyme B⁺ total NK cells (E) and CD56^{bright} NK cells (F). MFI of perforin⁺ total NK cells (G) and CD56^{bright} NK cells (H). Graphs are box and whisker plots with median \pm minimum to maximum value; with additional dot plot representing individual donors. Overweight and obese groups were compared to normal weight control group. Statistical significance is indicated as: * $P < 0.05$; P value within $0.05 < P < 0.1$ is indicated with precise P -value. Ctrl: unstimulated control.

The intracellular maturation and differentiation markers EOMES, T-bet and Blimp-1 revealed no differences, neither in total and CD56^{bright} NK cells nor among the BMI groups (Figure 34).

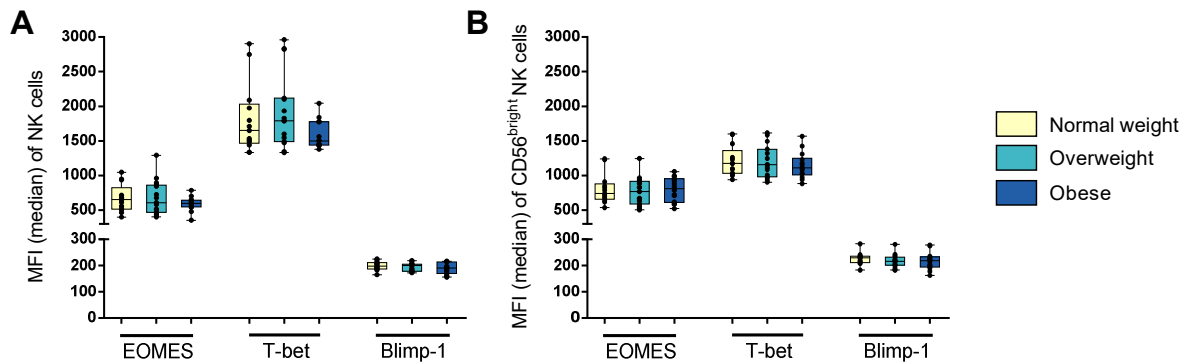


Figure 34: Median fluorescence intensity (MFI) of intracellular markers eomesodermin (EOMES), T-bet and Blimp-1 in total NK cells and CD56^{bright} NK cell subset. Unstimulated PBMCs of blood donors with different body mass indexes were stained with the respective fluorescent-conjugated antibodies. MFI of EOMES⁺, T-bet⁺, Blimp-1⁺ total NK cells (A) and CD56^{bright} NK cells (B). Graphs are box and whisker plots with median \pm minimum to maximum value; with additional dot plot representing individual donors. Overweight and obese groups were compared to normal weight control group.

4.2.10. CD107a degranulation

Figure 35 illustrates the results of the CD107a degranulation assay, performed on unstimulated and differently stimulated PBMCs, followed by CD107a surface staining on NK cells. Surface expression of CD107a was low on unstimulated NK cells (\sim 2%; Figure 35, Ctrl). Following stimulation with PMA plus ionomycin, CD107a surface expression on NK cells increased 20-fold. Stimulation with IL-12 plus IL-18 led to only a small increase in frequency of CD107a⁺ NK cells. Upon stimulation with K562 target cells, frequencies of CD107a⁺ total NK cells of all BMI groups were two times higher compared to IL-12 plus IL-18 stimulation. Furthermore, the proportion of CD107a⁺ total NK cells as well as the MFI was slightly reduced in the overweight group compared to the normal weight group after K562 stimulation (Figure 35, right). The combination of NK cell priming with IL-12 plus IL-18 overnight and MHC devoid K562 target cell challenge led to an increase in fractions of total NK cells bearing CD107a on their surface; even higher than the stimulation with PMA plus ionomycin alone. However, no differences between BMI groups were determined (Figure 35).

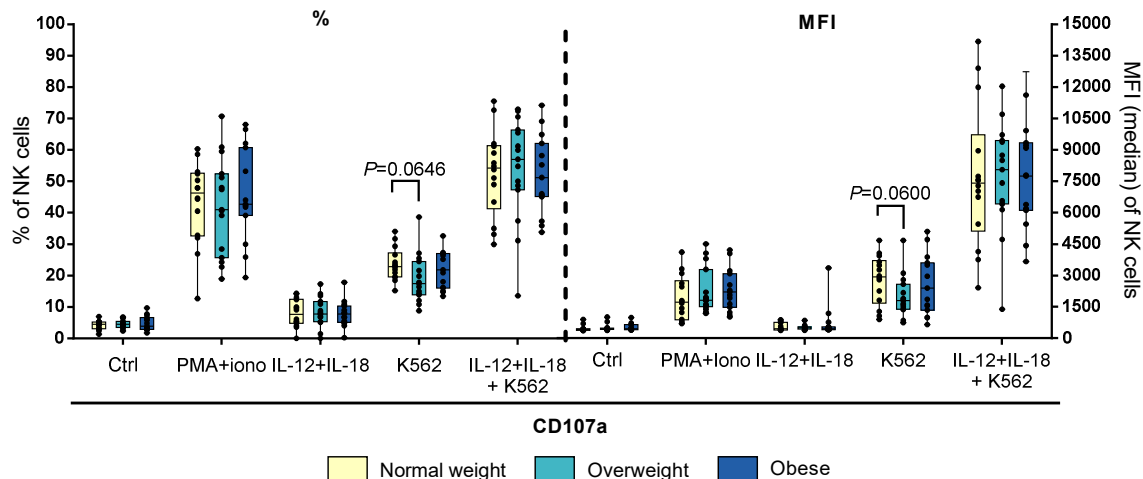


Figure 35: CD107a degranulation assay upon stimulation of PBMCs derived from blood donors with different body mass indexes either with 50 ng/ml phorbol-12-myristate-13-acetate (PMA) in combination with 1 μ g/ml ionomycin for 4 h or with 10 ng/ml interleukin-12 (IL-12) in combination with 50 ng/ml interleukin-18 (IL-18) overnight or stimulation with K562 target cells at 15:1 effector to target ratio for 4 h or with the combination of IL-12 plus IL-18 overnight followed by K562 challenge for 4 h prior to intracellular staining. Percentage and mean fluorescent intensity (MFI) of CD107a⁺ total NK cells are given. Graphs are box and whisker plots with median \pm minimum to maximum value; with additional dot plot representing individual donors. Overweight and obese groups were compared to normal weight control group within each stimulation setting. P values within $0.05 < P < 0.1$ are indicated with precise P-value. Ctrl: unstimulated control.

4.2.11. Determination of the optimal cell seeding number of the human cancer target cells DLD-1 and MCF-7

As mentioned in the introduction, overweight and obesity are associated with a higher risk for men to develop colon cancer and for woman to develop post-menopausal breast cancer. In this context, the commonly used human cancer cell lines DLD-1 (colon) and MCF-7 (breast) were used as target cells in this study. The optimal cell seeding numbers of both cell lines were determined by proliferations assays using the impedance-based real-time cell analysis system iCELLigence. In accordance with the pre-defined time point for addition of NK effector cells 24 h post-seeding, the optimal CI value at 24 h was searched for. Figure 36 shows the proliferation curves of DLD-1 (Figure 36A) and MCF-7 (Figure 36B) cells seeded with different cell numbers. Both cell lines showed a cell line specific curve progression independent of the corresponding cell seeding number. The DLD-1 cell line had a higher CI_{max} value than the MCF-7 cell line (CI_{max} values: ~ 11 and ~ 6 , respectively). The required two third of the maximum CI at the time point 24 h post-seeding was nearly hit by the DLD-1 cells initially seeded with 40,000 cells/well and exactly hit by the MCF-7 cells initially seeded with the same cell number. It was decided to use a cell number

of 50,000 cells/well of DLD-1 cells and 40,000 cells/well of MCF-7 cells for later experiments with NK-92 effector cells to achieve the two third of maximum CI at 24 h post-seeding.

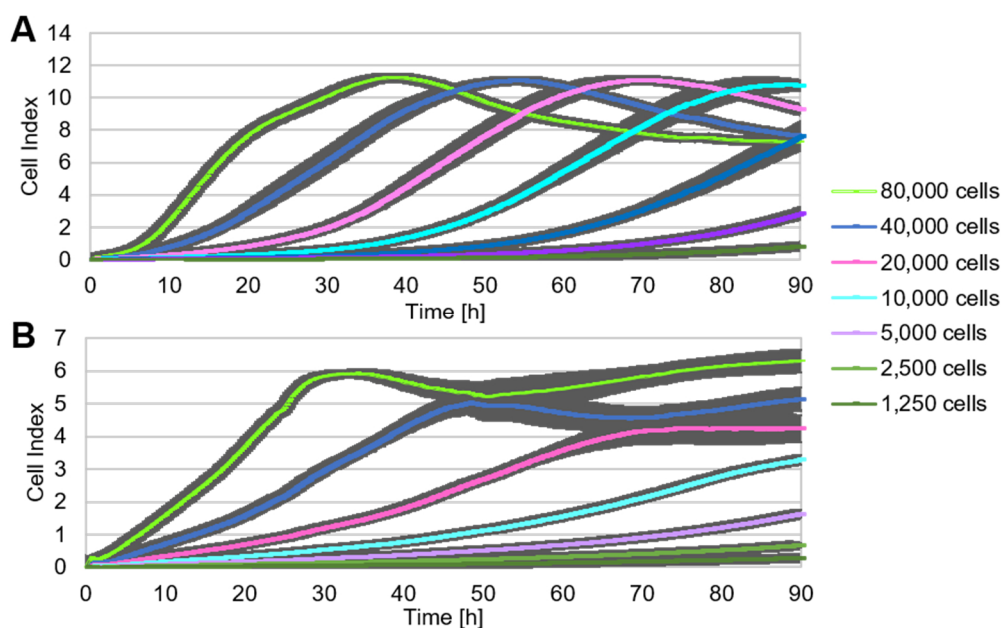


Figure 36: Cell proliferation assay of human colon cancer target cell line DLD-1 (A) and human breast cancer target cell line MCF-7 (B) by impedance-based real-time cell analysis system iCELLigence. Determination of optimal target cell seeding numbers for further cytolytic experiments. Starting with a stock cell suspension of 80,000 cells/200 μ l medium, a serial dilution down to 1,250 cells/200 μ l was prepared. Impedance was measured for 90 h. Impedance changes over time are given as cell index (CI) values. Mean \pm SEM; N (DLD-1, MCF-7) = 3.

4.2.12. Determination of the appropriate effector to target (E:T) ratio

Initially, NK-92 cells were used as effector cells to establish the impedance-based cytotoxicity assay system iCELLigence for later analysis with primary human NK cells from blood donors with different body mass indexes. Based on the results of the proliferation assays with DLD-1 and MCF-7, target cells were seeded at the defined densities and NK-92 cells were added 24 h later at different E:T ratios (Figure 37). Due to the highly cytotoxic potential of NK-92, a relatively low and small range of E:T ratios with 1:1 to 16:1 were chosen after initial experiments with E:T ratios of 50:1, 25:1 and 12:1 (data not shown). Both, DLD-1 and MCF-7, were killed effectively by NK-92 at all E:T ratios over time. It is notable that MCF-7 lysis induced by NK-92 was time-delayed in comparison to DLD-1 lysis. More than 50% of DLD-1 cells were lysed at all E:T ratios after 5 h post-NK-92 addition, whereas the same cytolytic effect was observed not until 10 h for MCF-7 (Figure 37B, D). In DLD-1 cell lysis, almost no difference was seen between 16:1, 8:1 and 4:1 E:T ratios. At the same E:T ratios in MCF-7 cell lysis, an increase in the cell index was seen initially starting 8 h after NK-92 cell addition with a continued decrease 15 h later (Figure 37C, D). Unfortunately, the reason for this effect remains unknown. Morphological analysis showed no alterations of MCF-7 co-cultured with NK-92 cells at different E:T ratios. In summary, the best

results for both target cell lines were obtained at 16:1 E:T ratio which gave an orientation for further experiments with primary human NK cells.

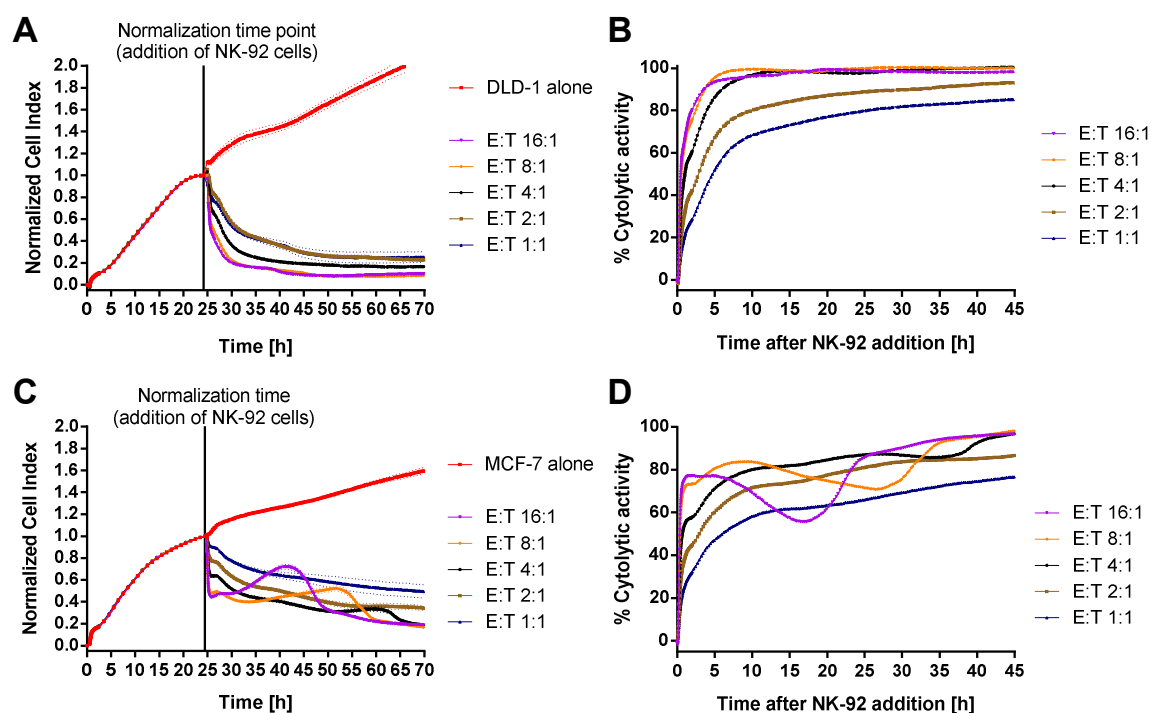


Figure 37: Real-time monitoring of NK-92-mediated target cell lysis against colon cancer cell line DLD-1 (A, B) and against breast cancer cell line MCF-7 (C, D) by the iCELLigence system. Human target cells were seeded with a density of 50,000 DLD-1/well and 40,000 MCF-7/well. (A, C) Human NK-92 were added at different E:T ratios (16:1 – 1:1) at normalization time point (indicated by full line). Impedance was measured every 15 min for 70 h. Changes in impedance normalized to the normalization time are given as dimensionless normalized cell index. Target cells alone served as controls. Based on the cell index data, percentage of cytolytic activity of NK-92 cells against DLD-1 (B) and MCF-7 (D) cells at different E:T ratios was calculated and displayed over time of 29 h after NK cell addition. Mean \pm SEM; n = 2 for each condition; N = 3 for both experiments.

Before the cytotoxicity assays with the primary human NK cells started, a new, more precise evaluation of an optimal target cell seeding number was performed to ensure an improved experimental setting (data not shown). In those tests, after 24 h post-seeding, the two third of maximum CI was achieved by both cell lines DLD-1 and MCF-7 with the initial cell seeding numbers of 40,000 cells/well. Therefore, this cell number was used for both cell lines in the subsequent cytotoxicity assays with primary human (phu) NK cells isolated from blood donors with different BMIs.

4.2.13. Cytolytic activity of primary human NK cells against the human colon cancer cell line DLD-1

To investigate a possible BMI-dependent impact on human NK cell functionality, cytotoxicity assays were performed. The cytolytic activity of phuNK effector cells, freshly isolated from PBMCs of blood donors with different BMIs, against the DLD-1 colon carcinoma target cell line was

analyzed at an E:T ratio of 15:1. The determination of the optimal E: T ratio of 15: 1 was based on the results of NK-92 cells and additional pre-tests with phuNK cells against DLD-1 and MCF-7 target cells (data not shown). Figure 38A displays the total trend of the time-dependent cytotoxicity of DLD-1 target cells by phuNK cells of the normal weight, overweight and obese groups over 45 h after NK cell addition. Figure 38B illustrates the cytotoxic activity of phuNK cells of the three BMI groups at different time points after NK cell addition. After 4 h no significant difference in the cytotoxic NK cell activity was detected. However, 8, 12, 16, 24 and 40 h after NK cell addition, the cytotoxicity of DLD-1 cells in the obese group was significantly reduced compared to the normal weight control group ($P < 0.05$; Figure 38B). At 40 h after NK cell addition, the difference of cytotoxic activity was 24% between the obese and normal weight group. In contrast to the obese group, the overweight group showed no significant differences in their cytotoxic NK activity at 4, 8, 12, 16 h after NK cell addition compared to the control group. However, 12 and 16 h after NK cell addition a slight reduction of cytotoxic activity was detected (Figure 38B) in the overweight group compared to the normal weight group. At 24 h and 40 h after NK cell addition, this difference between the overweight group and the normal weight group was statistically significant with a difference of 21% between those groups after 40 h (Figure 38B).

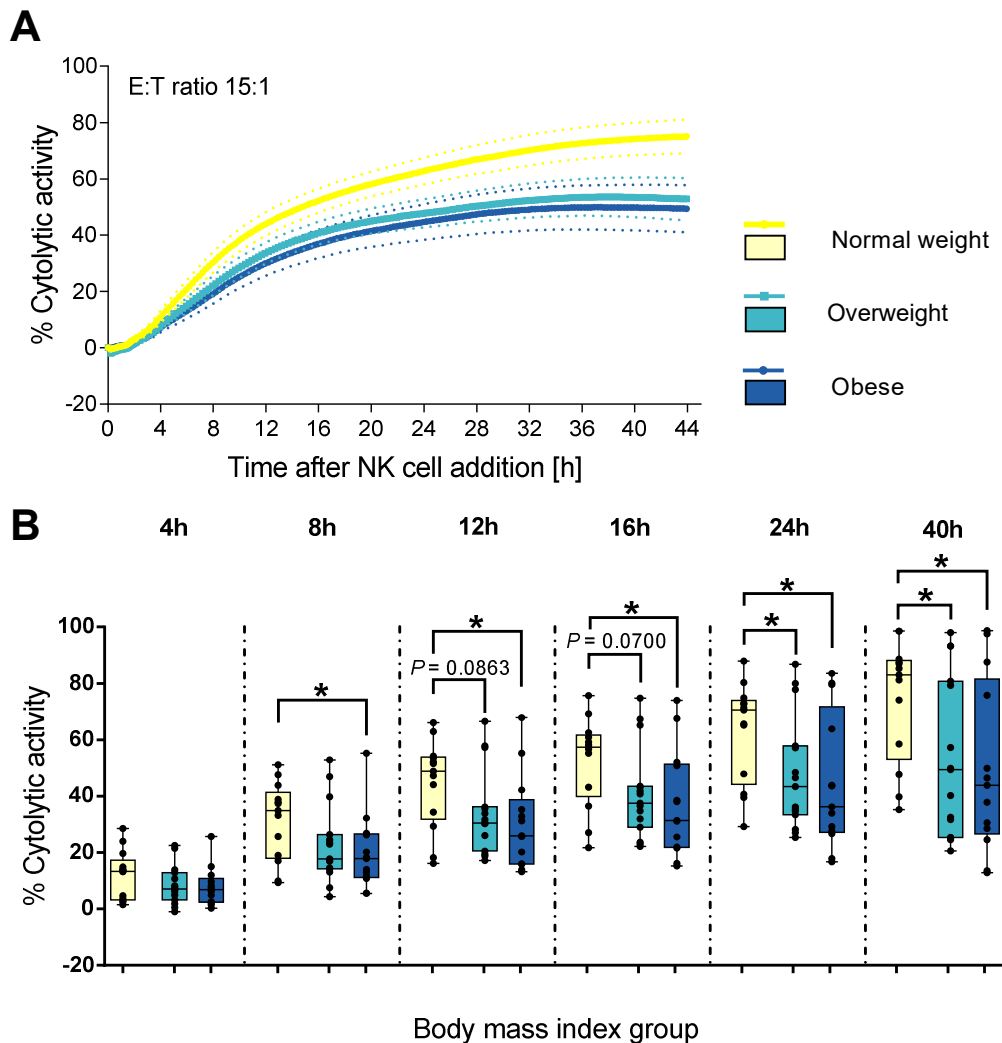


Figure 38: Cytolytic activity of primary human natural killer cells, isolated from blood donors with different BMIs, against human colon carcinoma cell line DLD-1. Target cells were seeded with a density of 40,000 cells/well. After 24 h freshly isolated human NK cells were added at 15:1 E:T ratio. Impedance was measured at well-bottoms every 15 min for 45 h. Changes in impedance were given as dimensionless cell index. Targets cells alone served as control. Based on CI values of target cells and target cells treated with NK cells, the percentage of cytolytic activity was calculated. (A) Total trend of time dependent cytolytic activity after NK cell addition. Mean \pm SEM (B) Specific cytolytic activity of primary human NK cells against DLD-1 target cells at different time points after NK cell addition. Graphs are box and whisker plots with median \pm minimum to maximum value; with additional dot plot representing individual donors. Overweight and obese groups were compared to normal weight control group. Statistical significance is indicated as: * $P < 0.05$; P values within $0.05 < P < 0.1$ are indicated with precise P -value.

4.2.14. Cytolytic activity of primary human NK cells against the human breast cancer cell line MCF-7

Similar to the cytotoxicity assay of the puNK cells of blood donors with different BMIs against the DLD-1 targets cell line, cytotoxicity assays with the same puNK cells against the breast cancer target cell line MCF-7 were performed. Figure 39A displays the total trend of the time-dependent cytotoxicity of MCF-7 target cells by puNK cells of the normal weight, overweight and obese groups over 45 h after NK cell addition. Figure 39B illustrates different time points after NK cell addition.

In contrast to the cytotoxicity assays with DLD-1 as target cells, no significant differences of cytolytic NK cell activity against the MCF-7 cells were determined between the three BMI groups (Figure 39B). However, at 16, 24 and 40 h post-NK-addition, a slight reduction in cytolytic activity of phuNK cells derived from overweight donors was determined compared to NK cells derived from normal weight donors (Figure 39B). At time point 40 h after NK cell addition, the difference in cytolytic activity of phuNK cells was 13.4% between the obese and normal weight groups.

In the period from 0 h to about 8-9 h in three BMI groups, a negative cytolytic activity was calculated. These negative values arised due to the behavior of the MCF-7 cells after addition of the phuNK cells and the resulting impedance changes, which were represented as CI. An increase in the CI over the MCF-7 growth control (untreated cells) occurred for about 8 h after addition of phuNK cells. After 8 h, the CI decreased and fell below the CI of the MCF-7 growth control. After decreasing below the MCF-7 growth control, positive values of % cytolytic activity were calculated.

As already observed with NK-92 as effector cells, the lysis of MCF-7 cells by the phuNK cells was time-delayed compared to the DLD-1 cytotoxicity assays. Furthermore, the cytolytic activity of phuNK cells was more pronounced against the colon cancer DLD-1 cells than against the breast cancer MCF-7 cells at all times.

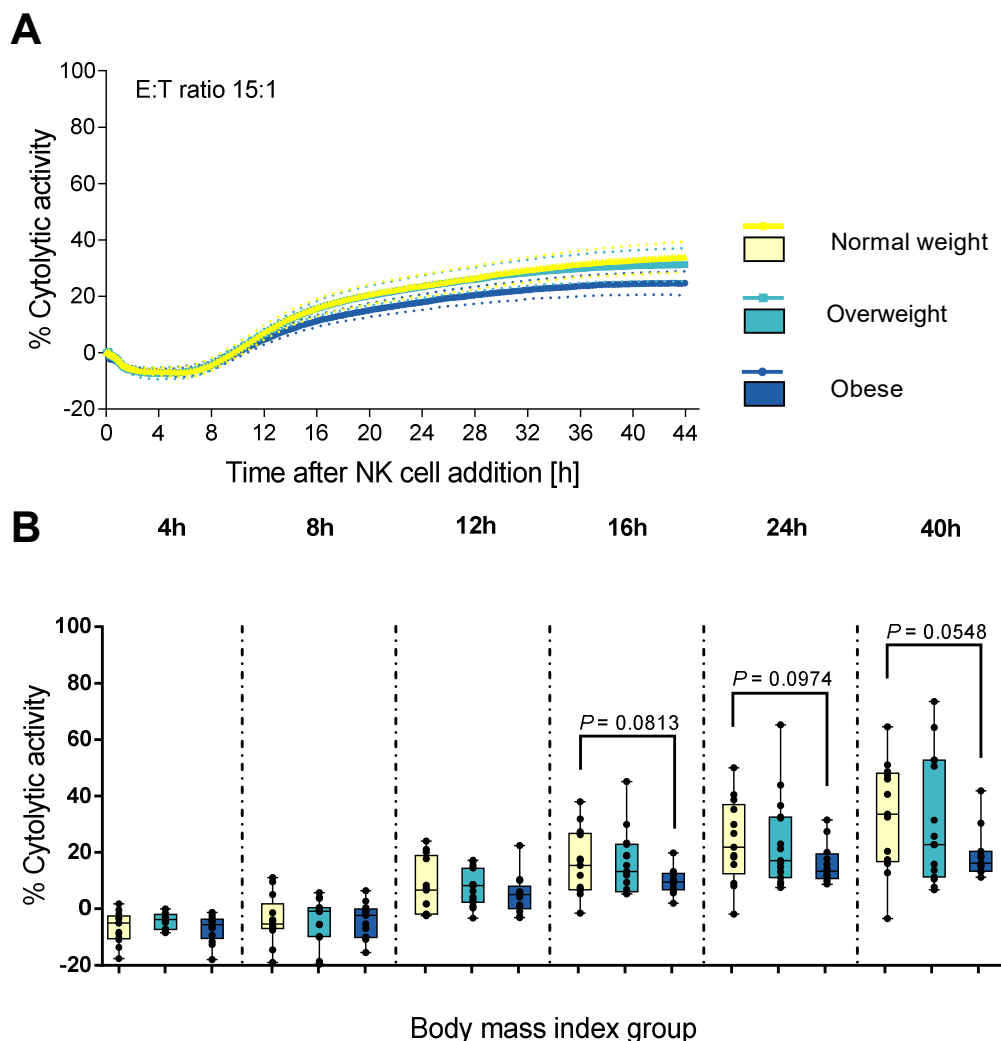


Figure 39: Cytolytic activity of primary human natural killer cells, isolated from blood donors with different BMIs, against human mamma carcinoma cell line MCF-7. Target cells were seeded with a density of 40,000 cells/well. After 24 h freshly isolated human NK cells were added at 15:1 E:T ratio. Impedance was measured at well-bottoms every 15 min for 45 h. Changes in impedance were given as dimensionless cell index. Targets cells alone served as control. Based on CI values of target cells and target cells treated with NK cells, the percentage of cytolytic activity was calculated. (A) Total trend of time dependent cytolytic activity after NK cell addition. Mean \pm SEM (B) Specific cytolytic activity of primary human NK cells against MCF-7 target cells at different time points after NK cell addition. Graphs are box and whisker plots with median \pm minimum to maximum value; with additional dot plot representing individual donors. Overweight and obese group were compared to normal weight control group. P values within $0.05 < P < 0.1$ are indicated with precise P-value.

5 Discussion

The prevalence of obesity and overweight among adults and children is rapidly rising worldwide and displays a major health problem due to the adverse health effects and costs, affecting both industrialized and developing countries [1]. Excess body weight is associated with numerous chronic non-communicable diseases, including diabetes mellitus type 2, cardiovascular diseases, fatty liver disease and neurodegenerative disorders [8–11]. Moreover, excess body fat increases the susceptibility to infections and the risk to develop certain types of malignancies, including esophageal adenocarcinoma, kidney and liver cancer as well as postmenopausal breast cancer and colorectal cancer [14, 15]. Obese individuals are 40% more likely to die from cancer than non-obese individuals [172]. All these findings led to the assumption that obesity contributes to an immunodeficient state. It is now generally accepted that obesity causes immune dysregulation [124, 173]. Nevertheless, the link between obesity and cancer susceptibility is still elusive. Several previous animal and human studies have demonstrated an impairment of NK cell functionality in obese subjects, which has been associated with an increased incidence of cancer [37, 39, 40, 124–126, 132, 137, 138]. However, the available data on the meaning of functional NK cell receptors in dependence on body weight is insufficient. There are some studies analyzing the impact of obesity on NK cells in animals demonstrating an altered NK cell phenotype and functionality in obese rats and mice. In contrast, there are only a few studies analyzing NK cell characteristics in human obese individuals. Especially, studies with a focus on NK cell subsets in overweight and obese individuals are rare. Therefore, the present study aims to fill these gaps.

5.1. Diet-induced obesity in C57BL/6 mice

Experimental mouse models provide a good opportunity to conquer genetic heterogeneity and various environmental factors that affect obesity and its associated disorders. In this study, a murine model was used to perform a systematic cross-sectional study of body weight gain on a high-fat diet (HFD) compared to the corresponding control normal-fat diet (NFD). Furthermore, the influence of two feeding regimes – *ad libitum* vs. restrictive – on the experimental outcome on this model was investigated. For this purpose, the widely used C57BL/6 mouse strain was applied in this study. Especially the used substrain C57BL/6NCrl is suggested to be highly susceptible to DIO [174]. Nevertheless, there are controversial studies about a partial obesity-resistance of C57BL/6 mice [174–176]. Therefore, a higher number of mice in both HFD fed groups were chosen to receive a sufficient number of obese animals in the respective groups. In addition to being a proper model for DIO, this strain is also commonly used as a mouse cancer model to address questions of cancer research. Obesity is associated with an elevated risk for men to develop colorectal cancer and for postmenopausal women to develop breast cancer. The C57BL/6 strain

is a sensitive model for the induction of colorectal cancer [177], and predicted to be used in a future project with a colorectal cancer model with DIO male C57BL/6 mice. Therefore, male C57BL/6 mice were used in the present study.

5.1.1. Dietary phenotypes

As expected, HFD *ad libitum* fed C57BL/6 mice showed increased weight gain, terminal body weight and visceral fat mass compared to all other groups. Furthermore, despite the supposed occurrence of obesity-resistant mice, all HFD fed mice became obese. In contrast and as expected, NFD restrictive fed C57BL/6 mice displayed the lowest weight gain, terminal body and visceral fat mass as well as the lightest weights of most organs among all groups. Regardless of the feeding regime, body weight of NFD fed C57BL/6 mice increased only moderately over time with signs of stagnation in the last weeks of the experiment, whereas HFD fed C57BL/6 mice continuously gained body weight in a linear, steep mode until the end of the experiment. Furthermore, three weeks were required to detect significant differences in body weights between *ad libitum* fed HFD and NFD mouse groups. The same was true for the restrictively fed HFD and NFD mouse groups. However, already one week on HFD either *ad libitum* or restrictive was sufficient to increase body weight to a greater extent than the corresponding NFD. This is in line with other studies [178].

Interestingly, only the restrictive group of HFD fed mice showed a significantly reduced terminal body weight and visceral fat mass compared to the HFD *ad libitum* group, while NFD restrictive and NFD *ad libitum* groups did not differ significantly in these parameters to each other. Considering the nutritional parameters, the fat intake is the only parameter in which HFD and NFD groups differ from each other between the two feeding regimes. The fat intake is the same for both feeding regime groups of NFD fed mice, while all other parameters differ significantly. In contrast, for HFD fed mice, all parameters differ significantly between *ad libitum* and restrictive feeding regime groups. This leads to the assumption that the different dietary fat intake led to the significant differences between the two feeding regimes in the HFD fed mice, which was not the case in the NFD fed mice between the two regimes. This suggestion is supported by a recent study by Hu *et al.*, which reported that dietary fat intake and not carbohydrate or protein intakes causes obesity in mice [179].

As expected, HFD *ad libitum* and restrictive fed C57BL/6 mice consumed significantly less food than the NFD groups, but showed significantly higher energy intakes due to the 60% kcal fat content in the HFD. However, only the HFD *ad libitum* feeding led to severely increased liver organ weights compared to all other groups, whereas HFD restrictive feeding protected mice to develop a fatty liver as no significant difference was detected compared to the NFD groups. Development of increased liver weights under HFD feeding are well known, thus, the present results corresponds

to other studies [178, 180, 181] As already mentioned, the non-alcoholic fatty liver disease is a common comorbidity associated with obesity [11]. Intriguingly, a study by Hatori and colleagues reported that a time restricted HFD feeding of mice for 8 h during their active phase without an reduction in caloric intake protected mice to develop an obese phenotype with hepatic steatosis [180].

Beside heavier liver weights under HFD *ad libitum* feeding, the spleens were also significantly heavier in this feeding group compared to all other groups. Furthermore, kidney weights were significantly elevated in both feeding regime groups of HFD fed mice compared to both NFD fed groups. Both latter organs are also related to an obese phenotype in mice and humans [182–185]. Especially, nephromegaly in obesity is related to chronic kidney disease [186].

5.1.2. DIO-impact on cytokine plasma levels

IL-6, a marker of systemic inflammation, is well known to be elevated in the plasma of obese subjects [187, 188]. It is secreted mainly by adipocytes and AT-macrophages, but also by skeletal muscles [189]. IL-6 is seen as a major contributor of the obesity associated chronic state of low-grade inflammation [187]. In accordance with the literature, HFD *ad libitum* feeding led to significantly increased IL-6 plasma levels in C57BL/6 mice in the present study. Remarkably, this increase was prevented by restrictive feeding.

In this study, no significant differences were found in plasma levels of IL-2, IFN- γ and TNF- α when comparing the diets and feeding regimes. Although TNF- α plasma levels were not altered (not decreased) in the present study, the unchanged levels of IL-2 and IFN- γ as well as the significant increase in IL-6 levels are in agreement with findings in HFD fed C57BL/6N mice compared to control mice by Fenton *et al.* [190].

5.1.3. DIO-impact on immune cell populations

Analysis of blood leukocytes and lymphocytes populations revealed significantly enhanced cell concentrations of each population in both HFD fed groups compared to their corresponding NFD fed group. Furthermore, all HFD fed mice displayed elevated or significantly increased cell counts in all examined cell types. Similar and even higher increases in leukocyte and lymphocyte cell counts in the bone marrow and consequently in the peripheral blood of HFD fed mice compared to control mice were described by Trottier *et al.* [191]. The determined increases in HFD fed mice in the present study are probably mainly caused by the significantly increased cell concentrations of B lymphocytes. Appropriately, the percentages of B cells in both groups of HFD fed mice were significantly elevated compared to their corresponding NFD fed group. In several studies, B cells – central players in humoral immunity – have been described as regulators in the inflammatory process of AT in obesity [192, 193]. However, Kosaraju *et al.* reported significantly

decreased cell concentrations and percentages of B cells in the bone marrow of HFD fed mice [36], which can probably be transferred to peripheral sites. Another animal study described no changes in percentages of B cells in DIO rats [137]. Therefore, more research work is needed to clarify these discrepancies.

Circulating monocyte cell numbers were also significantly increased in both HFD groups compared to their NFD counterparts. That was also mirrored in their frequencies in HFD *ad libitum* fed mice compared to NFD *ad libitum* fed mice. These results are consistent with previous reports [191, 194, 195]. It has been demonstrated in mice and humans that large numbers of circulating monocytes highly infiltrate AT in obesity [196, 197], where they differentiate into macrophages [198]. Thereby, the obesity-related AT-microenvironment leads to a polarization of the differentiation to pro-inflammatory M1 macrophages instead of anti-inflammatory M2 macrophages, causing and enhancing AT inflammation [199, 200]. A high level of M1 macrophages is associated with the promotion of insulin resistance in obese individuals [197].

Furthermore, leukocyte numbers in HFD mice maybe increased due to elevated numbers of granulocytes in those mice. Granulocytes are comprised of different cell types including neutrophils as the most abundant with more than 90% [201]. Several studies describe increased cell counts of neutrophils in HFD fed mice, indicating that the elevated numbers of granulocytes may be caused by an increased number of neutrophils in the present study [191, 201]. Interestingly, regardless of the feeding regime, HFD fed mice showed slightly reduced frequencies of granulocytes; probably attributable to a decreased percentage of circulating neutrophils. Neutrophils are considered to be the first type of cells rapidly recruited to sites of inflammation and they are capable to recruit monocytes and facilitate their infiltration into tissues [202]. A previous study reported a primary increased recruitment of neutrophils in AT of HFD fed mice, which preceded the infiltration by monocytes/macrophages [203].

Regardless of the feeding regime, HFD feeding caused a slightly elevated cell number and frequency of T cells. The subdivision in helper CD4⁺ T cells and cytotoxic CD8⁺ T cells revealed significantly increased and slightly increased cell numbers in HFD fed mice, respectively. Intriguingly, the frequencies of both T cell subsets showed significantly reduced proportions in HFD *ad libitum* fed mice compared to NFD *ad libitum* fed mice. In addition, the restrictive feeding on HFD mice led to a significant decreased proportion of both T cell subsets compared to the corresponding NFD restrictive group, but not compared to the NFD *ad libitum* group. To the author's knowledge, these data are the first of its kind. This is supported by a review by Ip *et al.* describing that T cells and T cell subsets, among others, have not yet been elucidated in the systemic circulation of obese mice compared to lean mice [204]. One study reported significantly decreased frequencies of CD4⁺ T cells and significantly increased frequencies of CD8⁺ T cells in DIO

rats [137], which is partly consistent with the present results. However, a lot of studies reported enhanced recruitment and infiltration of CD4⁺ and CD8⁺ T cells into AT in DIO mice and obese humans [205–207]. Additionally, and similar to macrophages, CD4⁺ T cells can be further divided into pro-inflammatory T helper 1 cells (Th1) and anti-inflammatory T helper 2 cells (Th2), whereas both exhibit different cytokines secretion profiles [208]. In obesity, the balance of Th1/Th2 is shifted to Th1 cells accompanied with elevated secretion of pro-inflammatory IFN- γ [35]. It has been demonstrated that CD8⁺ T cells promote macrophage M1 polarization in AT of DIO mice [209].

In sum, the obtained results about blood cell concentrations indicate an enhanced hematopoiesis in HFD fed mice as declared and confirmed by Trottier *et al.* [191]. Furthermore, the altered percentages of immune cell populations in HFD fed mice are in good agreement with previous studies. However, in some aspects, it is shown that a restricted intake of HFD already protected mice from significantly adverse effects of a high-fat consumption under *ad libitum* regime.

5.1.4. DIO-impact on murine NK cell population and NK cell subsets

As in previous studies, the results of the present study confirmed that the frequency of circulating NK cells is significantly decreased in HFD *ad libitum* fed mice compared to the corresponding NFD group [124, 210]. Furthermore, HFD mice fed restrictively displayed also a significantly diminished frequency of NK cells compared to the corresponding group. Interestingly, the number of peripheral blood NK cells showed a slight, but not significant, increase in HFD fed mice compared to NFD fed mice, regardless of the feeding regime. No significant differences in blood NK cell numbers between HFD and NFD fed C57BL/6 mice were described previously [211, 212]. Further classification and analysis of the four murine NK cell subsets – based on their expression of the differentiation and maturation markers CD11b and CD27 – showed a slight increase in the proportion of the most mature NK cell subset (CD11b⁺CD27⁻) in HFD fed mice compared to NFD fed mice, regardless of the feeding regime. This is further supported by a decreased proportion of the stage before, the early mature NK cell subset (CD11b⁺CD27⁺), in HFD fed mice in comparison to NFD fed mice, again, regardless of the feeding regime. In comparison to the double-positive NK cell subset, the CD11b⁺CD27⁻ NK cell subset is considered to be less proliferative and exhibit reduced effector function [213, 214]. In contrast, the double-positive NK cell subset is reported to show higher levels of cytokine production and cytotoxicity. Furthermore, the two stages before, CD11b⁻CD27⁻ and CD11b⁻CD27⁺ NK cell subsets, were unchanged between the diet groups. These findings suggest that HFD feeding may play a role in regulating peripheral NK cell differentiation and maturation. Furthermore, some studies described increased proportions of CD11b⁺CD27⁺ NK cell subset and contemporarily diminished

proportion of the terminally differentiated, or most mature, NK cell subset in restrictively fed mice compared to *ad libitum* fed mice [215, 216]. This is reflected in the present results, even if only partial, probably due to lower percental restriction of feeding regime referred to other studies.

5.1.5. DIO-impact on receptor profiles of murine NK cells

The effector function of murine NK cells is orchestrated by various activating and inhibitory receptors as well as by adhesion molecules. After 18 weeks of HFD feeding, C57BL/6 mice displayed significantly enhanced proportions of circulating KLRG1⁺ NK cells compared to NFD fed mice and regardless of the feeding regime. Thereby, HFD *ad libitum* fed mice showed the highest proportion of KLRG1⁺ NK cells and NFD restrictive fed mice the lowest, whereby this difference was significant. The expression of the inhibitory KLRG1 receptor is associated with a most terminal differentiated status of murine NK cells and is therefore predominantly expressed on the CD11b⁺CD27⁻ NK cell subset [113, 213]. Thus, the higher proportion of KLRG1⁺ NK cells seem to be in accordance with the observation of the slightly increased frequency of the most mature CD11b⁺CD27⁻ NK cell subset in HFD fed mice as discussed previously. KLRG1 expression on NK cells is further associated with decreased cytotoxicity and IFN- γ secretion, NK cell senescence and increased apoptosis [113, 217, 218]. Additionally, NK cells of HFD fed mice demonstrated significantly reduced expression of the CD127 (IL-7R α), a marker for immature NK cells [219]. Interestingly, CD127⁺ murine NK cells are considered to have homology to the human CD56^{bright}CD16^{-/dim} NK cell subset, because of their immunoregulatory properties – due to high cytokine production and low cytotoxicity [51]. A study by Theurich *et al.* 2017 reported unchanged expression levels (MFI) of KLRG1 on blood NK cells of obese C57BL/6 mice compared to control mice [212]. This study also described no alteration in expression levels of Ly49C/I/H, NKG2D and NKp46 as well as the proportion of CD69⁺ NK cells in obese mice compared to control mice, which is in accordance to the present study.

Based on the alteration of receptor expression in the present study, HFD feeding of mice appears to lead to NK cell proportions that are based less immunoregulatory, less cytotoxic and terminally differentiated, indicating an adverse impact on the NK cell functionality.

There are only very few studies investigating the impact of DIO on murine NK cell receptor expression. An animal study reported significantly reduced relative splenic mRNA (messenger ribonucleic acid) expression of NKG2D and NKp46 and also a reduced relative mRNA expression of NKp30 in the liver of DIO rats compared to controls [137]. Another study by Spielmann *et al.* described also significantly lower relative splenic mRNA concentrations of NKp46 in DIO rats [138].

5.1.6. DIO-impact on cytolytic activity of murine NK cells

As reported by several studies, obesity is linked to a higher incidence and mortality rate for colorectal cancer, especially in men [18]. In the present study, immunophenotyping of primary murine NK cells by flow cytometric analysis revealed altered expression of several receptors and markers on NK cells from obese mice compared to control mice. These findings lead to the assumption that the NK cytolytic functionality may therefore be impaired in obese mice. Hence, impacts of these alterations on the NK cell activity to lyse cancer cells have been investigated. For the first time, the cytolytic activities of these primary murine NK cells from HFD and NFD fed male mice under restrictive and *ad libitum* feeding regimes were analyzed against the murine colorectal cancer cell line CT26.WT by the real-time cell analysis system xCELLigence. Despite the fact that the number of mice per group was too low for representative statistics, however, NK cells isolated from HFD fed mice revealed remarkably reduced NK cell mediated target cell lysis of colorectal tumor cells compared to NFD fed mice. The highest cytolytic activity was present in NFD *ad libitum* fed mice and the lowest cytolytic activity in HFD *ad libitum* fed mice at all time points. These results are in general agreement with previous findings in obese mice and obese rats [38, 133, 137]. However, the current findings expand and support the prior works.

5.1.7. Summary I

The C57BL/6NCrl strain is an appropriate model for studies on immunometabolic effects of diet-induced obesity. Male mice react sensitive to HF and NF diets and the *ad libitum* and restrictive feeding regimes; with different and appropriate dietary phenotypes, including increased body weight gain, visceral fat masses and fatty liver in HFD mice. HFD fed feeding reveals significant impacts on numbers and frequencies of immune cell populations in peripheral blood of mice with elevated cell counts of the immune cell populations (including leukocytes, lymphocytes, monocytes, granulocytes, B cells, T cells and NK cells). Especially frequencies of monocytes and B cells are elevated, whereas frequencies of CD4⁺ and CD8⁺ T cells and NK cells are reduced in HFD fed mice. Furthermore, NK cells of HFD fed mice display a more mature state due to reduced frequency of CD11b⁺CD27⁺ NK cells subset and slightly more CD11b⁺CD27⁻ NK cell subset. Moreover, the frequency of NK cells expressing the maturation marker and inhibitory receptor KLRG1 is increased in HFD fed mice. In addition, the frequency of NK cells expressing the immature marker CD127 is reduced. This expression pattern could indicate a terminal differentiated status of NK cells, which is associated with less effector functionality of the NK cells. This assumption is partly confirmed by the reduced cytolytic activity of NK cells from HFD fed mice against the colorectal cancer cells CT26.WT.

5.2. Human study: Impact of the human body weight on NK cell receptor profiles and NK cell functionality

5.2.1. Study population

All study subjects were blood donors at the Department of Transfusion Medicine at the University Hospital Halle (Saale). Due to anamnesis prior to the blood donation, it can be excluded that subjects suffered from any acute infection, immunosuppression or known malignant tumors. The information about body weight, body height, age and HCMV serostatus were given by the University Hospital and used to calculate the individual BMI of each subject. Therefore, each subject was classified in either normal weight, overweight or obese. The BMI is the most commonly used diagnostic measure to characterize overweight and obesity in humans and the easiest to use. However, it has its limitations due to the lack of considering age, gender and body composition [220]. There are other methods to estimate excess body fat, i.e. bioelectrical impedance analysis (BIA) or the determination of waist and hip circumferences to calculate the waist-to-hip ratio [221, 222]. The advantage of these methods is the better estimation of body fat distribution, but the purchase of a BIA device is expensive and the accurate determination of waist and hip circumferences is time consuming and error-prone [223]. In addition, the WHO recommends the BMI as the most useful measure of overweight and obesity [1].

In this study, the three BMI groups differed only significantly in body weight and BMI, but not in body height, age and HCMV serostatus. It is known that age and CMV seropositivity may have impacts on immune cell populations, e.g. T cells, B cells and NK cells [224–226]. The seroprevalence of CMV infection increases steadily with age. The global seroprevalence in adult population is estimated of about 89%; 66% in WHO European regions [227]; 57% in Germany [228]. A one-to-one matching of all parameters of donors would have been optimal. However, due to the limited time period of buffy coat acquisition, a sufficient number of voluntary blood donors could not be obtained. Interestingly to note, it was even difficult to obtain enough buffy coats from normal weight donors, because of the predominance of overweight and obese donors. For data protection reasons, additional parameters, e.g. smoking, nutrition and fitness status, which also may influence the immune system and metabolism of donors, could not be considered in this study. The total number of 46 individuals in this study is considered to be sufficient to address the considered objectives and for giving initial and important insights. Nevertheless, for even more specific investigations and statements, larger studies with higher numbers of subjects and under consideration of the confounders will be necessary in the future to confirm the results obtained here. However, this is a common limitation of human studies.

In this study, only buffy coats from male blood donors were used for analysis. An important reason is the exclusion of the possible influences of hormonal fluctuations in women during the

menstrual cycle on immune cells and especially the NK cells. It is known that estrogen has negative effects on NK cell activity [229, 230]. Various studies have shown that the incidence for breast cancer is elevated in postmenopausal obese women [19, 147, 231]. It is suspected that adipose tissue-derived endogenous estrogen, produced by the enzyme aromatase, plays an important role as the BMI is positively correlated with high levels of estrogen [232]. Furthermore, AT is the primary source of estrogen after menopause [233]. Therefore, elevated estrogen levels are presumable involved in the higher risk of breast cancer development in postmenopausal women [234]. Although the risk of breast cancer is significantly higher in women, there is also a risk for men to develop breast cancer [235]; which is also increased with high BMI [20]. By contrast, men have a higher risk of colorectal cancer than women [236], and in terms of the analysis of the cytolytic activity of the primary NK cells against the colorectal DLD-1 cells, this was another reason to involve male donors. An additional reason for the involvement of male donors was the simultaneous measurement of cytolytic activity of NK cells from identical donors against tumor cells of two different tumor entities (colorectal and mammary cancers) with regard to providing information about differences in cytolytic activity and its time course.

5.2.2. Altered distribution of immune cell populations in obese subjects

Buffy coats are leukocyte-enriched by-products of a whole blood donation in the transfusion medicine, which are obtained by centrifugation. Thus, it was possible to isolate PBMCs and to determine percentages of blood leukocyte populations from the total amount of PBMCs. An analysis of total cell counts in relation to total blood volume, as done in the murine study, was not possible due to the previous processing of blood donations.

Results of the present study demonstrate a significant increase of NKT cells in obese subjects compared to subjects with normal weight. NKT (CD3⁺CD56⁺) cells are an innate-like lymphocyte population and exhibit phenotypic and functional characteristics of both NK cells (CD56⁺) and T lymphocytes (CD3⁺) [237]. The literature reports controversial results about the role of NKT cells in obesity as former studies showed no changes of NKT cells in obese women [238] or a decline in the proportion of NKT cells in obese individuals [239, 240]. In accordance with the results of this study, an animal study showed an increase in the proportion of NKT cells in obese rats. Additionally, the DIO rats displayed a higher colorectal tumor burden. These findings indicate an impaired NKT cell-mediated response to tumor cells in obese individuals [137].

Although no significant differences were obtained in the frequencies of T lymphocytes and the two T cell subsets between the BMI groups, a slight increase of helper T cells (CD4⁺) and a slight decrease of cytotoxic T cells (CD8⁺) were determined in overweight subjects compared to normal weight subjects, but not in obese subjects. Interestingly, previous studies report inconsistent results

on T lymphocyte subsets in obesity [209, 241, 242]. CD4⁺ T cells were reported to positively correlate with BMI in humans [242], but only in circulating CD4⁺ counts. In contrast, percentage of CD4⁺ T cells displayed similar results between obese and normal weight individuals, which is consistent with the present results [243, 244]. Some studies described decreased percentages of CD8⁺ T cells in obesity [242, 244], whereas others described no difference [238].

In this study, the total NK cell population and the CD56^{bright}CD16^{dim} NK cell subset showed no significant differences in their frequencies between the BMI groups. These results confirm the results of earlier studies in obese humans and animals [37, 39, 137, 145]. Interestingly, obese subjects displayed a significantly increased frequency of their cytolytic CD56^{dim}CD16^{bright} NK cell subset. In addition, a slight increase was also observed in overweight subjects compared to normal weight subjects. To the knowledge of the author, these results are the first of its kind. This may be explained by the fact that very few of these studies have specifically distinguished the two main populations of NK cells for their analysis. However, a study by Bähr *et al.* reported increased proportions of CD56^{bright} NK cells and reduced proportions of CD56^{dim} NK cells in obese subjects compared to normal weight subjects [125]. This contrary result compared to the present study may be explained by a different number of subjects and the NK cell differentiation in CD56^{bright} and CD56^{dim} NK cell subsets, which is less specific than the here performed classification into the CD56^{bright}CD16^{dim} and CD56^{dim}CD16^{bright} NK cell subsets.

5.2.3. Altered NK cells phenotypes in overweight and obese subjects

NK cells express a variety of receptors on their surface that enables them to distinguish healthy cells from infected, stressed or malignant transformed cells and subsequently eliminate the latter ones. To perform their effector functions, NK cells are equipped with multiple inhibitory and activating receptors, but also adhesion molecules and functional extra- and intracellular markers [62]. The expression profile of these receptors is different on the two main human subpopulations CD56^{dim}CD16^{bright} and CD56^{bright}CD16^{dim}-NK cells, and characterizes the effector functional properties. For instance, the cytotoxicity of these two NK cell subpopulations is determined by the different level of expression of divers receptors [51, 245]. Despite this knowledge, only a few publications exist that deal with individual receptors or receptor subclasses, adhesion molecules as well as functional markers and their expression on the two mentioned NK cell subsets. The available data regarding altered receptor expressions in both NK cell subpopulations in dependence of an increased body weight are limited.

In this study, a comprehensive screening was performed to investigate the impact of the human body weight on the expression of the majority of known inhibitory and activating receptors as well as adhesion molecules and functional markers on both NK cell subpopulations for the first time.

Activating and inhibitory NK cell receptors

As described in the introduction, KIRs represent one of the important NK cell receptor families with mainly inhibitory function in NK cell responses. As expected and in accordance with the literature, all four analyzed KIRs in this study were higher expressed on the CD56^{dim}CD16^{bright} NK cell subset than on the CD56^{bright}CD16^{dim} NK cell subset, independent of the BMI group [246, 247]. Excitingly, obese individuals showed significantly reduced frequencies of the activating CD158i (KIR2DS4) receptor-positive cells in total NK cells and both subsets compared to individuals with normal weight. This indicates a less activatable state of NK cells and NK cell subsets in obese individuals, which may contribute to a higher susceptibility to infections and tumors. Additionally, CD158i KIR expression within the BMI groups was highly variable among all examined NK cell populations, except for the obese group, that predominantly lack CD158i expression. This noticeable separation within the BMI groups may be explained by different KIR haplotypes of the donors. Two kinds of KIR haplotype have been defined based upon gene content and are termed as A and B. In general, haplotype A is composed of several inhibitory KIR genes and one activating gene (*KIR2DS4*), whereas haplotype B has at least one other activating KIR gene in addition to *KIR2DS4* [248]. Interestingly, it has been demonstrated that A haplotypes have null variants of *KIR2DS4* resulting in no surface expression, e.g. on NK cells [248, 249]. One study already reported that the donor's CMV serostatus has no influence on the KIR expression [250]. The present results about different CD158i expression patterns among different BMI groups are the first of its kind. To evaluate if the obese donors are mainly null-expressors of the A haplotype or the downregulation of CD158i⁺ NK cells is influenced by the body weight, further studies need to be done for elucidation.

The expression analysis of the activating NCRs NKp46, NKp44 and NKp30 on the different NK cell populations revealed no significant differences among the BMI groups. However, a slightly reduced frequency of NKp46-expressing CD56^{bright}CD16^{dim} NK cells was observed in obese subjects compared to normal weight subjects. This corresponds roughly to results by Viel and colleagues, who described decreased expression of NKp46 on circulating NK cells from obese subjects, which additionally correlated with an increasing BMI [39]. Another study by Bähr *et al.* demonstrated *in vitro* significantly reduced NKp46 relative mRNA expression on human NK-92 cells incubated with leptin compared to untreated NK-92 cells [137]. Interestingly, NK-92 cells feature phenotypically characteristics of the human CD56^{bright}CD16^{dim} NK cell subset [154], which displayed a tendency of NKp46 reduction in the present study. Furthermore, NK-92 cells treated with leptin were significantly less effective in killing colorectal cancer cells than untreated NK-92 cells. Hence, it was concluded, that a decreased expression of the potent activating NKp46 may be associated with a reduction in NK cell response against tumor cells, thus increasing the risk to

develop cancer [137]. The same study revealed no altered relative mRNA expression of NKp30 on NK-92 cells. This supports findings of another study that did not find altered expressions of NKp30 as well as of NKp44 on circulating NK cells from obese subjects compared to normal weight subjects [251]. These findings are consistent with the present results. Additionally, NKp44 is known to be expressed only on activated NK cells [74]. The present results display unstimulated, basal levels of NKp44, NKp46 and NKp30 receptors.

As expected, and in line with the literature, the inhibitory receptor NKG2A was higher expressed on CD56^{bright}CD16^{dim} NK cells, whereas the activating NKG2D was stronger represented on CD56^{dim}CD16^{bright} NK cells [56]. Interestingly, overweight subjects, but not obese subjects, showed a significantly higher expression of NKG2A on CD56^{bright}CD16^{dim} NK cells in comparison to normal weight subjects. Aside of this, expression of the activating counterpart NKG2C was slightly decreased on CD56^{dim}CD16^{bright} and total NK cells in the overweight group compared to the normal weight control group. Both receptors, NKG2A and NKG2C, specifically recognize HLA-E, which is important in antiviral responses [252].

The data of this study indicate that the cytokine producing NK cell subset is more active in overweight subjects, whereas the cytotoxic function may be partly decreased due to the less activated status of CD56^{dim}CD16^{bright} subset. Little research has been done so far investigating the role of both these receptors in the context of overweight and obesity. Thus, the present results provide an initial insight.

In the present study, no significant differences were found regarding NKG2D expression within the NK cell populations between the BMI groups. In contrast, other studies demonstrated altered NKG2D expression in obese individuals, although with conflicting results. *In vitro* studies reported that human NK-92 cells expressed lower NKG2D relative mRNA levels after incubation with high levels of leptin [137]. Furthermore, DIO rats showed significantly decreased relative mRNA expression of NKG2D in splenic tissues, that was accompanied with cancer development and metastases [137, 138]. In humans, O'Rourke *et al.* found significantly more NKG2D-expressing NK cells in VAT [140]. However, other human studies reported unaltered frequencies of NKG2D expression within circulating total NK cell populations of obese subjects compared to lean subjects [125, 251]. However, despite the unaltered frequency of NKG2D-expressing total NK cells, the frequency of NKG2D⁺ CD56^{bright} NK cells was significantly increased, whereas the frequency of NKG2D⁺ CD56^{dim} NK cells was decreased [125].

The CD161 receptor has been shown to be expressed on the majority of NK cells [97], which is in good agreement with the present results. Rosen *et al.* demonstrated that LLT-1 ligand-expressing target cells reduced the capability of CD161⁺ NK cells to kill them. Furthermore, ligand binding of CD161 to LLT-1 led to reduced cytokine production of NK cells [253]. In the present

study, expression analysis of the inhibitory receptor CD161 revealed no significant differences on the examined NK cell populations and among BMI groups. However, the frequency of CD56^{dim}CD16^{bright} NK cell subset bearing CD161 was slightly increased in overweight subjects compared to normal weight subject. To date, only one other study investigated the expression of CD161 on NK cells in dependence on body weight, but without declaring the result [39].

The frequencies of inhibitory receptor Siglec-7-positive NK cells was comparable among the examined NK cell populations, with no distinct differences between BMI groups. This result confirms the results of a previous study on human blood donors with different BMIs [145].

Adhesion molecules

Adhesion molecules, such as CD2, CD62L and CD226 (DNAM-1), participate in interactions of NK cells with other immune cells and virus-infected or malignant transformed cells and thus play a crucial role in generating an effective NK cell-mediated immune response [254].

The literature describes a higher expression of the adhesion molecules CD2 and CD62L on the CD56^{bright}CD16^{dim} NK cell subset in comparison to the CD56^{dim}CD16^{bright} subset, which could be confirmed in this study [57, 255]. Despite of no differences in the proportion of CD2⁺CD56^{dim}CD16^{bright} NK cells among the BMI-groups, those NK cells showed significantly less CD2 molecules per cell in the overweight group compared to the normal weight group. CD2 is described to be an important molecule for membrane nanotube forming between NK cell and target cell upon CD2-ligand interaction [87]. The nanotube formation is of functional importance to facilitate NK cell cytotoxic activity [256]. Therefore, a reduction of CD2 molecules on the NK cells may lead to less nanotube forming and as a consequence, the co-stimulatory signal for NK cell activation would be less intense, so that inhibitory signals gain the upper hand. This could lead to a reduced cytotoxicity and cytokine production in overweight individuals.

In the present study, the frequencies of total NK cells and CD56^{dim}CD16^{bright} NK cells bearing CD62L on their surfaces were significantly reduced in the obese group. Moreover, overweight subjects displayed reduced CD62L expression on the CD56^{dim}CD16^{bright} NK cell subset. A previous study investigating CD62L reported a downregulation of this molecule on both NK cell subsets after *in vitro* stimulation with immunomodulatory cytokines, which are shown to be elevated in obesity [257, 258]. Furthermore, overweight and obesity are accompanied by increased levels of C-reactive protein (CRP) possibly as a result of stimulation by AT-derived IL-6 [259, 260]. CRP is an acute-phase inflammatory marker produced mainly in the liver but also in AT and CRP level rises with increasing BMI [261–263]. A study by Cottam *et al.* suggests that high CRP levels downregulate CD62L expression on leukocytes including NK cells and therefore disable them to migrate to sites of infection and inflammation [264]. As mentioned in the introduction, CD62L is essential for extravasation of NK cells to sites of inflammation through blood-vessel walls [91].

Thus, a reduced expression of CD62L on NK cells, as in the current study, may explain the increased risk for infections and cancer in overweight and obese individuals. At the same time, due to the possible restriction to leave the blood stream through the reduced CD62L expression on CD56^{dim}CD16^{bright} NK cells subset, this could be a possible reason for the increased frequency of the same subset in obese subjects in the present study.

Functional markers

To investigate functional parameters of NK cells in dependence of body weight, the expression of the activation-associated markers CD25 and CD69 were investigated in this study. Significantly more activation-associated CD25 molecules per cell were observed on CD56^{bright}CD16^{dim} NK cells in the overweight group compared to the normal weight group. However, the same BMI group displayed no difference in their proportion of CD25⁺ CD56^{bright}CD16^{dim} NK cells. Although not significant, the obese group showed a slightly increased proportion of CD25⁺ CD56^{bright}CD16^{dim} NK cell subset. As initially mentioned, CD25 is a crucial component of the high-affinity IL-2 receptor and constitutively expressed by CD56^{bright} NK cells [100, 102].

Furthermore, the early activation marker CD69 revealed no distinct differences between the examined NK cell populations and among the BMI groups. Previous studies provide contradictory results comparing CD69 expression between obese and normal weight subjects. Viel *et al.* described increased levels of CD69 on NK cells in association with high BMI [39]. They concluded that chronic stimulation in obesity admittedly leads to an activated NK cell status, but those persistently activated NK cells are incapable to kill target cells. In contrast, Bähr *et al.* determined decreased CD69 expression on total NK cells and on the CD56^{dim} NK cell subset [125]. Moreover, Cottam *et al.* reported no changes in CD69 expression on NK cells between normal weight and obese subjects [264], which is identical to the present results. The different results in the mentioned studies may vary due to differences in the number, sex, age and BMI levels of the examined subjects.

In accordance with results from other studies, present data showed lower CD27 expression of the CD56^{dim}CD16^{bright} NK cell subset than of the CD56^{bright}CD16^{dim} NK cell subset [265]. Within the scope of this study, total NK cells of obese subjects presented significantly decreased expression of CD27 compared to normal weight subjects. Furthermore, slightly decreased proportions of CD27⁺ CD56^{dim}CD16^{bright} and total NK cells were determined in the overweight subjects compared to subjects with normal weight. It has been observed that decreased CD27 expression on NK cells and specifically on CD56^{dim}CD16^{bright} NK cells is associated with high cytolytic activity and decreased cytokine production. In contrast, higher CD27 expression, especially on CD56^{bright} NK cells, was found to be associated with more IFN- γ secretion [266]. Thus, it has been suggested that CD27 can serve as an additional marker to discriminate human

NK cell subsets, comparably to mouse NK cell subset discriminations [265]. Interestingly, in the current study, CD27 expression per cell was significantly upregulated on the CD56^{bright}CD16^{dim} NK cell subset in overweight subjects, and slightly upregulated in obese subjects on the same subset, compared to normal weight subjects.

The expression analysis of CD57, defined as the terminal differentiation and maturation marker of NK cells, showed no alterations among BMI groups of the examined NK cell populations. In accordance with the introduced literature about the maturation and differentiation stages of human NK cells, the given results show that CD56^{dim}CD16^{bright} NK cells were clearly more CD57⁺ than CD56^{bright}CD16^{dim} NK cells. Previous studies declared that CD57 expression on NK cells is accompanied with a higher cytolytic activity, particularly when stimulated by CD16 crosslinking, and reduced responsiveness to cytokines [111]. Additionally, percentage of circulating CD57⁺ NK cells has been shown to rise with CMV infection and aging [267]. To the author's knowledge, no study has so far investigated the impact of human body weight on the expression of CD57 on NK cells and NK cell subsets. For the first time it could be shown that CD57 is apparently regulated independently from the human body weight.

Previous studies demonstrated that human 2B4 can effectively co-stimulate activating NK cell receptors, such as NKp46, NKp30, NKG2D, CD16 and others, thus, activating non-MHC-restricted NK cell-mediated cytotoxicity [268, 269]. 2B4 engagement with its ligand CD48, which is expressed on all hematopoietic cells, also induces IFN- γ and TNF- α secretion by NK cells [92]. Interestingly, a prolonged triggering of 2B4 results in downregulation of 2B4 mRNA expression, reduced 2B4 surface expression and a reduced NK cell activation and cytotoxicity [270, 271]. Furthermore, 2B4-mediated activating signaling in NK cells can be totally blocked by co-engagement of inhibitory receptors, e.g. CD158a (KIR2DL1) or CD94/NKG2A, probably ensuring self-tolerance of NK cells [272]. In the present study, although, frequencies of 2B4-expressing NK cells of examined NK cell populations were not altered among the BMI groups, significantly upregulated expression in numbers of 2B4 molecules per cell on total NK cell population as well as on the CD56^{dim}CD16^{bright} subset was detected in the obese group compared to the normal weight group. This indicates an improved ability of each CD56^{dim}CD16^{bright} NK cell to be activated by 2B4 engagement. As no other studies are available investigating the impact of body weight on the 2B4 co-activating receptor, the present results are the first of its kind.

Similar to 2B4, NKp80 co-stimulates activation of NK cell-mediated cytotoxicity and promotes the release of the proinflammatory cytokines IFN- γ and TNF- α [93, 273]. Results of the present study showed a significantly increased proportion of total NK cells expressing NKp80 in overweight subject compared to normal weight subjects. Despite this significant difference, NKp80 is expressed on almost all NK cells in high frequencies, which confirms results of previous

studies [93]. Freud *et al.* reported that NKp80 expression also marks mature NK cells and thus contributes to full NK cell functionality [274]. The present results show for the first time to what extent the human body weight impacts NKp80 expression.

The expression of the co-inhibitory receptor TIGIT revealed similar frequencies of TIGIT⁺ NK cells among all examined NK cell populations and among the BMI groups. Wang *et al.* described a wide variation in expression levels of TIGIT on NK cells of healthy subjects [275]. This is not confirmed in the present study, but this is probably due to the lower number of 46 donors in the present study compared to 199 donors in the mentioned study. Interestingly, and comparable to the results of 2B4 in the present study, no differences were determined in frequencies of TIGIT⁺ NK cells on examined populations, however, a slight increase in the number of TIGIT molecules per NK cell was detected within the CD56^{bright}CD16^{dim} subset in the overweight group compared to the normal weight group. High TIGIT expression is associated with a reduced ability of NK cells to release cytokines, to degranulate and to kill target cells, as demonstrated by Wang *et al.* [275]. The present work shows for the first time whether and to what extent overweight and obesity influence the expression of TIGIT on NK cells and the two main NK cell subsets.

Analysis of the second co-inhibitory receptor PD-1 demonstrated no alterations in the examined NK cell populations and among the BMI groups. Functional studies demonstrated that an increase in PD-1 expression on NK cells is associated with a decline in NK cell-mediated tumor defense and with a poorer prognosis in digestive cancers [276]. Another study reported higher levels of PD-1 expression upon stimulation in obese children compared to normal weight counterparts. In addition, this was accompanied by a reduced NK cell-mediated killing of target cells [126]. The discrepancy to the present study may result from the difference between juvenile and adult subjects.

Co-expression analysis

Co-expression analysis revealed significantly increased percentages of double-positive CD57⁺NKG2C⁺ total NK cells in the obese group compared to the normal weight group. The percentage of the CD56^{dim}CD16^{bright} NK cell subset co-expressing CD57 and NKG2C was slightly, but not significantly, increased in the obese group compared to the normal weight counterpart. Interestingly, individual analysis of both receptors (CD57 and NKG2C) on total NK cells and CD56^{dim}CD16^{bright} NK cells showed no differences between these groups. It has been described that the simultaneous presence of both these receptors on NK cells is evoked by inflammatory processes and HCMV infection [277]. Since there is no significant difference in CMV seropositivity between donor groups, it can be hypothesized that the difference is due to a possible obese-associated low grade inflammation in the obese individuals compared to normal weight individuals. Moreover, CD57⁺NKG2C⁺ NK cells are considered as terminally matured [278]. Furthermore,

total NK cells as well as CD56^{dim}CD16^{bright} NK cells co-expressing CD57 and inhibitory receptor NKG2A showed slightly increased proportions in the overweight group compared to the normal weight group. This co-expression indicates an intermediate state in the differentiation process, in which NKG2A⁺CD57⁻KIR⁻ NK cells represent the early stages, whereas NKG2A⁻CD57⁺KIR⁺ represent the most differentiated [112]. Thus, overweight and obese individuals seem to have a higher proportion of NK cells, which show advanced differentiation and maturation stages compared to the normal weight individuals.

Expression of intracellular markers

IFN- γ is one of the most important immunoregulatory cytokine predominantly produced by activated NK cells upon infection [279]. According to Cooper *et al.*, CD56^{bright} NK cells are the main source of IFN- γ production – in response to stimulation with monocyte-derived cytokines (monokines), such as IL-12 and IL-18 [51]. Analogous to the finding of Cooper *et al.*, CD56^{bright} NK cells in the present study showed higher proportions of IFN- γ ⁺ cells after IL-12 plus IL-18 stimulation compared to the total NK cell population. Moreover, the comparison of the kind of stimulation with either IL-12 plus IL-18 or PMA plus ionomycin displayed lower percentages of IFN- γ ⁺ CD56^{bright} NK cells following stimulation with PMA plus ionomycin, which is also consistent with the results of Cooper *et al.* [51]. Comparison between obese and overweight subjects to normal weight subjects demonstrated no significant changes in the proportions of IFN- γ ⁺ NK cells in the examined NK cell populations. However, a slight decrease was determined in the frequency of IFN- γ ⁺ CD56^{bright} NK cells in the overweight group compared to the normal weight group upon IL-12 plus IL-18 stimulation. In addition, PMA plus ionomycin stimulated total NK cells displayed slightly reduced percentages of IFN- γ ⁺ cells in the obese group compared to the normal weight group. Previous NK cell studies provide heterogeneous data about IFN- γ production and expression in obesity [37, 39, 145, 244]. The present results tend to confirm a previous study that reported higher amounts of IFN- γ expressing CD56^{bright} NK cells in obese humans compared to normal weight counterparts [125]. In contrast, Viel *et al.* described less IFN- γ production in obese individuals, additionally accompanied with lower degranulation capacity [39]. These results obtained by Viel *et al.* could be explained by the high mean BMI of 40 of obese subjects included in their study. Interestingly, Wrann *et al.* showed that long-term exposure to leptin revealed reduced IFN- γ production of human NK cells from healthy donors [132]. The obesity-associated systemic low-grade inflammation is, among other aspects, attributed to the IFN- γ secretion by NK cells, which contributes to activation and polarization of monocytes towards proinflammatory M1 type macrophages [280].

Previous animal studies have demonstrated that pre-activation, also called priming, of NK cells with combinations of IL-12 and IL-18 enhance the expression of cytolytic molecules, such

as TRAIL and granzyme B, and that NK cell priming is required to exhibit full NK cell effector activity [281, 282].

Surface-bound TRAIL induces apoptosis in virus-infected and malignant cells and constitutes a direct-killing effector mechanism of NK cells [116]. Interestingly, a significant reduction in numbers of intracellular TRAIL molecules in total NK cells was determined in the obese group of unstimulated NK cells compared to the normal weight group. Upon stimulation, no differences were obtained among groups. Regardless of the BMI group, stimulation with IL-12 plus IL-18 demonstrated elevated expression of TRAIL molecules in CD56^{bright} NK cells. Besides the kind of stimulation, this phenomenon could also have been promoted by the higher proportion of IFN- γ ⁺ CD56^{bright} NK cells, because IFN- γ is found to be a potent inducer of TRAIL expression [116]. This result is comparable to findings of Huebner *et al.* showing higher expression of TRAIL on CD56^{bright} NK cells compared to CD56^{dim} NK cells [283]. Other studies demonstrated either no differences between obese and normal weight subjects or lower percentages of TRAIL⁺ total NK cells in obesity [37, 125]. In contrast to the present study, the latter studies investigated basal surface expression of TRAIL and not intracellular expression after cytokine stimulation.

Concerning the expression quantity of granzyme A and perforin, no significant differences were observed between the BMI groups. These findings are in line with other studies reporting no alterations in the expression of granzyme A [37, 125, 132] and perforin [39, 132] in human obesity. However, a recent study by Michelet *et al.* describes reduced mRNA and protein levels of perforin in obese compared to lean subjects [124]. A possible reason for this discrepancy may be that the number of obese donors investigated by Michelet *et al.* was much higher ($n = 45$) compared to the other studies ($n = 4 - 16$). Thus, obesity-associated effects regarding the expression of perforin may be pronounced with higher sample size. Furthermore, the same study by Michelet *et al.* reported reduced granzyme B⁺ NK cells in obesity. On the contrary, another study published increased levels of granzyme B in obese individuals compared to normal weight individuals [39]. In the present study, regardless of the BMI group, both stimulated NK cell populations showed a significantly increased quantity of granzyme B molecules compared to unstimulated cells. Interestingly, the serine protease granzyme B was slightly decreased in its numbers of protein in CD56^{bright} NK cells of obese subjects compared to normal weight subjects upon stimulation.

The maturation and differentiation of NK cells are regulated by intrinsic signals of transcription factors, particularly EOMES, T-bet and Blimp-1 [284]. No significant differences concerning the quantity of expression of the above-mentioned transcription factors were observed in the present study. To the author's knowledge, no other study has investigated at these transcription factors in regards of different BMIs.

CD107a degranulation assay

CD107a, also called lysosomal-associated membrane protein-1 (LAMP-1), lines the membrane of cytolytic granules within NK cells and becomes accessible for detection antibodies upon NK cell activation followed by degranulation [285]. Although one study suggests that CD107a protects NK cells from degranulation-associated apoptosis [286], the role of CD107a in NK cell biology remains widely unknown [287]. Several studies have demonstrated that CD107a detection on NK cells correlated with target cell lysis and cytokine production [105, 106]. Thus, CD107a is considered as an appropriate candidate and functional marker to evaluate NK cell cytotoxic activity.

In line with previous *ex vivo* studies, unstimulated NK cells displayed very low levels of CD107a expression, whereas stimulation with IL-12 plus IL-18 as well as PMA plus ionomycin significantly increased the percentages of CD107a⁺ NK cells [37, 105, 251]. As expected, the highest CD107a expression was determined after cytokine-priming and K562 target cell co-culture, which mirrors results obtained by Aktas *et al.* [106]. In contrast to expectations about the CD107a degranulation assay in the present study, no significant differences between the BMI groups were identified within the different stimulation types. Only slight decreases of CD107a⁺ NK cells and a slight down-regulation in the number of CD107a molecules on the surface of NK cells were determined following co-culture with K562 cells in the overweight group compared to the normal weight group. Some studies investigating obesity-related impacts on NK cells obtained reduced basal levels of CD107a expression on NK cells of obese subjects, but without significance [37, 251]. Other studies did not find any difference in CD107a expression on NK cells of obese individuals compared to normal weight counterparts [125]. Investigations by Viel *et al.* reported an adverse correlation of the frequency of CD107a⁺ NK cells with increasing BMI after NK cell co-culture with K562 cells [39]. The inconsistent results could be explained by the different sample sizes of subjects and in the case of Viel *et al.* the inclusion of subjects with severe obesity with a BMI of > 40 kg/m².

5.2.4. Real-time cytotoxicity assays of primary human NK cells against colon and breast cancer cells

NK cells play an important role in the early detection and elimination of virus-infected and malignant transformed cells [49]. After recognition of target cells through a large repertoire of receptors, NK cells are able to perform the elimination via two main cytolytic mechanisms in parallel – granule-dependent and death ligand-induced cytotoxicity [118]. Several studies in animals and humans revealed alterations in NK cell receptor expression profiles due to an increased body weight that was associated with elevated tumor risk and tumor burden [37, 39, 124, 137, 138, 145]. A previous study on primary human NK cells from normal weight blood donors have shown that

the NK cells specific lysis against DLD-1 colon cancer cells is significantly reduced after NK cells were incubated with high levels of leptin [137].

In the present study, immunophenotyping of primary human NK cells by flow cytometric analysis revealed altered expression of several receptors and markers on NK cells from overweight and obese subjects compared to normal weight subjects. Subsequently, impacts of these alterations on the NK cell activity to lyse cancer cells have been investigated. For the first time, the cytolytic activity of these primary human NK cells was analyzed against the commonly used human colorectal cancer cell line (DLD-1) and breast cancer cell line (MCF-7) in relation to the body weight by the real-time cell analysis system iCELLigence.

Results of the cytotoxicity assay against the colorectal cancer cell line DLD 1 showed a significantly reduced cytolytic activity of puNK cells isolated from obese donors compared to those isolated from normal weight donors. The first significant difference was determined at 8 h post NK cell addition and continued until the last time point determined. Interestingly, puNK cells from overweight donors also displayed a slightly reduced cytolytic activity at the first time points and became as well significant at 24 h post-NK cell addition compared to the normal weight group until the last time point. These data provide convincing evidence of a strong correlation between increased body weight and reduced NK cell activity and a resulting higher risk of colorectal cancer.

In contrast to the cytotoxicity assay with DLD-1 cells, puNK cell confronted with MCF-7 cells showed no distinct differences between obese and overweight donors compared to normal weight donors. However, noticeable is a slight reduction in the cytolytic activity of puNK cells from obese donors compared to normal weight donors at later time points – similar to the DLD-1 challenge. A comparison of the cytolytic activity of puNK cells against DLD-1 and MCF-7 cancer cell lines revealed a 50% reduction rate of lysis by puNK cell of same donors against MCF-7 cells compared to DLD-1 cells. The reduced cytolysis was also confirmed in pre-test with the human NK-92 cell line, which also displayed lower cytolytic activity against MCF-7 cells compared to DLD-1 cells. In addition, puNK cell cytolytic activity against MCF-7 cells was found to start 6 – 10 h later than against DLD-1 cells. These observations may be explained by biological characteristics of the MCF-7 cell line. On the one hand, MCF-7 cells express moderate levels of MHC-I molecules [149], which may belongs to a immune escape strategy of those cancer cells, whereas DLD-1 cells are devoid of MHC-I [151]. Binding of some MCF-7 expressed MHC-I molecules by inhibitory NK cell receptors may contribute to a lower activating signaling within the NK cell. On the other hand, MCF-7 cells are caspase-3 deficient [288]. Caspase-3 is an essential mediator of programmed cell death. It is crucial for apoptotic chromatin condensation and DNA fragmentation as well as for other processes associated with cell degradation and formation of

apoptotic bodies [289, 290]. Additionally to caspase-3, there are two other caspases, caspase-6 and -7, which mediate apoptosis [291]. However, NK cell mediated granule-dependent induction of target cell apoptosis is mainly restricted to the activation of caspase-3 by granzyme B in the target cell [291]. The second killing mechanism, that induces apoptosis involves binding of death ligands FasL and TRAIL expressed on NK cells to the corresponding death receptors expressed on the surface of target cells, that activates downstream caspases-3, -6 and -7 [118]. However, studies have shown that MCF-7 cells express low levels of Fas receptor [292] and are resistant to TRAIL-induced apoptosis [293]. Nevertheless, NK cells can mediate lysis by a caspase-independent cell death pathway inducible by granzyme A [294]. Taken together, the observed reduced NK cell mediated lysis of MCF-7 cells compared to DLD-1 cells may have been due to a combination of the mentioned aspects above. This is further supported by studies describing that MCF-7 cells required a prolonged co-incubation time with NK cells to be lysed [295]. Other studies suggest that MCF-7 cells are less sensitive or even resistant to NK cell mediated lyses, but often they determined lysis rates already after 4 h [296, 297], which seems to be too short-timed in the case of MCF-7 cells. The advantage of a non-end-point cytotoxicity assay, as applied in the present study by the real time cell analysis system iCELLigence, is particularly evident here in order to determine the time-dependent NK cell activity against cancer target cells. Nevertheless, the present results concerning phuNK cell-mediated lysis of MCF-7 cells are encouraging and should be validated in a larger cohort of blood donors. Taken altogether, the presented data provide further evidence that the used target cell line has a considerable impact on the outcome of NK cell-mediated cytotoxicity, as previously reported by Lamas and colleagues [298].

An interesting side finding was that the results obtained by the direct functional assessment of the cytolytic activity of phuNK cells against cancer cells did not match the results obtained by the indirect assessment through the CD107a degranulation assay. According to the results of the degranulation assay, no altered cytolytic activities should have been detected between the BMI groups. Nevertheless, the cytotoxicity assay revealed adverse effects of an elevated human body weight on the NK cell ability to lyse DLD-1 cells. Actually, determining degranulation of NK cells through CD107a expression is often used to analyze the functional capacity of NK cells instead of using direct cytotoxicity assays, due to its advantage to identify the specific effector cells with cytotoxic ability instead of dead or apoptotic target cells [299]. This discrepancy between degranulation and lytic effector function could be related to the differentially used target cells – K562 for degranulation and DLD-1/MCF-7 for direct cytotoxicity. In future work, it would be beneficial to perform both assays with the same target cells.

5.2.5. Summary II

PBMCs isolated *ex vivo* from healthy obese and overweight blood donors exhibit alterations in a variety of the examined immunological parameters – including immune cell populations, expression profiles of NK cells, CD56^{bright}CD16^{dim} and CD56^{dim}CD16^{bright} NK cell subsets and functional NK cell analysis against tumor cells, compared to normal weight donors. Obese subjects display significantly increased percentages of NKT cells and of the cytolytic CD56^{dim}CD16^{bright} NK cell subset, whereas no changes are observed in other immune cell populations. Overweight subjects display a slight, but not significant, increase in CD4⁺ helper T cells and a slight decrease in CD8⁺ cytotoxic T cells. Additionally, obese and overweight subjects present an altered immunophenotype of circulating NK cells and both NK cell subsets. Furthermore, the majority of changes in receptor expression profiles are detected on total NK cells and CD56^{dim}CD16^{bright} NK cells in obese subjects, characterized by a significantly reduced expression of the activating receptor CD158i (KIR2DS4) and the adhesion molecule CD62L as well as significantly increased expression of co-stimulatory receptor molecules 2B4 per cell. Furthermore, the proportion of total NK cells expressing the maturation marker CD27 is decreased. The primarily cytokine producing NK cell subset CD56^{bright}CD16^{dim} shows only reduced expression of CD158i in obese subjects. In contrast, overweight subjects present increased proportions of NKp80⁺ total NK cells and decreased proportions of CD62L⁺ CD56^{dim}CD16^{bright} NK cells as well as a decline in the level of adhesion molecules CD2 per cell on the same subset. However, CD56^{bright}CD16^{dim} NK cells of overweight subjects show increased frequencies of the inhibitory NKG2A receptor and higher expression levels of the CD27 maturation marker and activation-associated marker CD25. The co-expression analysis reveals an increase in the frequency of CD57⁺NKG2C⁺ total NK cells. Stimulated total NK cells isolated from obese donors show a slight, but not significant, decrease in IFN- γ production. Apart from an increased proportion of unstimulated total NK cells positive for TRAIL expression, no differences are found in the expression of other examined intracellular markers, such as granzyme A and B, perforin, EOMES, T-bet and Blimp-1. Degranulation of CD107a as a common marker for indirect assessment of NK cell functionality exhibits no differences among the BMI groups and examined NK cell groups. Remarkably, the direct assessment of the ability of the isolated primary NK cells of obese and overweight subjects reveals significantly reduced cytolytic NK cell activity against the colon cancer cell line DLD-1 compared to NK cells isolated from normal weight donors. In contrast, the cytolytic NK cell activity against the breast cancer cell line MCF-7 is only slightly reduced in the obese groups compared to the normal weight group. The present data indicate that the human body weight has a modifying impact on the receptor profiles of the two main NK cell subsets and on total NK cells. The reduced NK cell activity in obese and overweight subjects to lyse colon cancer target cells implies that the

detected modifications in receptor and marker expression profiles on NK cells and NK cell subsets in those subjects may have an impairing effect on their NK cell functionality.

5.3. Comparison between mice and man

Taken together, diet-induced obesity in C57BL/6 mice and overweight and obesity in male human blood donors suggest having a great impact on immune cell populations, especially NK cells and NK cell receptor expression profiles as well as on NK cell functionality to kill tumor cells. In more detail: In contrast to overweight and obese human subjects, the feeding of a HFD to mice shows a more comprehensive influence on the investigated immune cell populations, especially on cell numbers in the blood. In humans, only the proportion of NKT cells is significantly increased in obese subjects compared to normal weight subjects. Due to the focus on the main immune cell populations in mice and the restricted panel design, murine NKT cells (CD3⁺NK1.1⁺TCRβ⁺) could not be classified in the present study. Therefore, the murine flow cytometric panel design should be extended to also include murine NKT cell analysis in further studies. Moreover, the possibility to collect whole blood samples from the human donors would enable to determine the immune cell counts as done in the murine model for further comparisons. A possible reason for the observed variations in immune cell populations might be species-specific differences between mice and humans. Furthermore, individual parameters of the human blood donors, such as smoking and exercise habits, nutrition, ethnicity, and blood glucose and cholesterol levels can also have an influence on the obtained results. Those factors are widely excluded in the murine study with genetically identical mice under laboratory conditions. In addition, in human studies the BMI measurement is the most common tool to determine overweight and obesity, whereas body fat mass determination is commonly used in mice. There is no definition of murine obesity based on BMI [300]. Due to the doubled body weight of HFD *ad libitum* fed mice compared to the NFD counterparts after 18 weeks, it could be assumed that HFD *ad libitum* fed mice might be better comparable to severe obese humans than to the current 'mild' obese blood donors (since the average obese BMI here is < 35 kg/m²). The present results in obese mice display a stronger effect of obesity on the investigated parameters due to the direct induction of DIO, whereas the results obtained in the human study display weaker effects of the human body weight. However, in humans other factors as mentioned earlier may have also their impact. In future projects, it would also be interesting to study severely obese subjects, treated in obesity centers of hospitals. Nevertheless, analysis of the frequency of NK cell subsets in mice and humans reveal a similar pattern. The NK cells seem to be more mature and differentiated in both obese study subjects due to higher frequencies of CD11b⁺CD27⁻ murine NK cells and of CD56^{dim}CD16^{bright} human NK cells. This is further supported by a lower proportion of CD27⁺ total NK cells in obese mice

and humans. Additionally, NK cells of obese mice and obese as well as overweight humans are impaired in their effector function to kill colon cancer cells, although the sample size in the murine model is low in the cytotoxicity assay. The used DIO model is a convenient model to better understand human obesity and to further analyze the obesity-cancer link. As performed in the present study, it is beneficial to investigate potential phenotypical and functional differences in NK cells without any intervention on the basis of the feeding diet in combination with the feeding regime.

5.4. Conclusion and outlook

In this study, a comprehensive screening has yielded into additional and some completely new findings. In detail, obesity and even overweight in healthy humans leads to changes in the expression of a large number of surface receptors and functional markers on primary human total NK cells as well as on CD56^{dim}CD16^{bright} and CD56^{bright}CD16^{dim} NK cells subsets. Similarly, DIO mice present altered receptor expression levels on their total NK cell population. Those phenotypical NK cell alterations were accompanied by a decreased cytolytic NK cell activity against colon cancer cells. As NK cells are major effector components to eliminate cancer cells, the present results provide further important insights to elucidate mechanisms underlying the known obesity-associated increased cancer risk. Figure 40 illustrates and summarizes the connections between an impaired NK cell functionality and the obesity-cancer link.

For future projects, the comparable data between mouse and human support that the murine DIO model using C57BL/6 mice is appropriate to study obesity under controlled conditions and to transfer the obtained results to human obesity. In future studies, this strain could be used to investigate in vivo the impact of a disturbed NK cell functionality on the development of colorectal cancer in obese mice. The obtained results in humans are encouraging and should be validated in a larger cohort, particularly due to the more individual variations in human materials. In order to additionally confirm the results of this work with other methods, gene expression analyses for the determination of mRNA levels using real-time qRT-PCR (quantitative reverse transcription polymerase chain reaction) on primary NK cells from blood donors of different BMI groups and on DIO mice could be performed in the future. This method could provide information about changes in the transcription of different NK cell-relevant genes. Further functional assays, e.g. receptor blockade by monoclonal antibodies (mAb), could be carried out to characterize the functional role of the altered NK cell receptors, especially on the NK cell subsets, in obesity with regard to NK cell cytotoxicity. Moreover, genetic knockout mouse models could be used to study the role of those receptors in obesity. Furthermore, cytolytic NK cell activity could be explored against cancer cells of other obesity-related tumor entities. For example, in addition to DLD 1 and

MCF 7 cancer target cells, other breast cancer cells like MDA-MB-231 or other colon cancer cells like HT 29, or the pancreatic cancer cell line Capan-1 or the cervical cancer cell line HeLa could be used. To study NK cell functionality under conditions of other obesity-associated cancer types in mice, other mouse strains could be used in future studies – such as female BALB/c mice, susceptible to DIO and a common mouse model for breast cancer research.

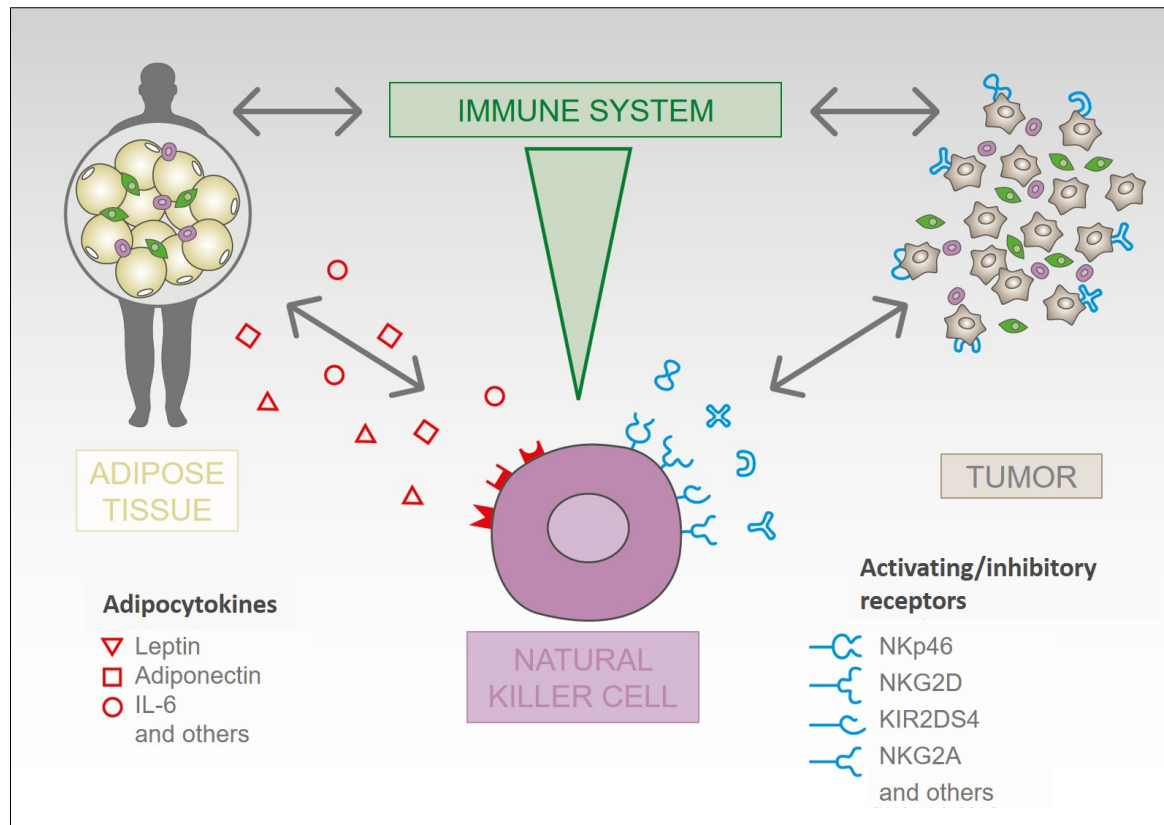


Figure 40: Summarized illustration of the interactions in the obese organism that directly and indirectly affect the function of NK cells. It further demonstrates the interplay with developing and existing tumors (adapted from [301]).

References

1. World Health Organization. Overweight and obesity. 2016. http://www.who.int/gho/ncd/risk_factors/overweight/en/. Accessed 4 Jul 2018.
2. Global Burden of Disease Collaborative Network. Global Burden of Disease Study 2015 (GBD 2015) Obesity and Overweight Prevalence 1980-2015. Seattle, United States: Institute for Health Metrics and Evaluation (IHME). 2017.
3. Afshin A, Forouzanfar MH, Reitsma MB, Sur P, Estep K, Lee A, *et al*. Health Effects of Overweight and Obesity in 195 Countries over 25 Years. *N Engl J Med*. 2017;377:13–27. doi:10.1056/NEJMoa1614362.
4. Robert Koch Institut. Gesundheit in Deutschland: Robert Koch-Institut; 2015.
5. Kelly T, Yang W, Chen C-S, Reynolds K, He J. Global burden of obesity in 2005 and projections to 2030. *Int J Obes (Lond)*. 2008;32:1431–7. doi:10.1038/ijo.2008.102.
6. Lenz M, Richter T, Mühlhauser I. The morbidity and mortality associated with overweight and obesity in adulthood: a systematic review. *Dtsch Arztebl Int*. 2009;106:641–8. doi:10.3238/arztebl.2009.0641.
7. Abdelaal M, Le Roux CW, Docherty NG. Morbidity and mortality associated with obesity. *Ann Transl Med*. 2017;5:161. doi:10.21037/atm.2017.03.107.
8. Abdullah A, Peeters A, Courten M de, Stoelwinder J. The magnitude of association between overweight and obesity and the risk of diabetes: A meta-analysis of prospective cohort studies. *Diabetes Res Clin Pract*. 2010;89:309–19. doi:10.1016/j.diabres.2010.04.012.
9. Guh DP, Zhang W, Bansback N, Amarsi Z, Birmingham CL, Anis AH. The incidence of comorbidities related to obesity and overweight: A systematic review and meta-analysis. *BMC Public Health*. 2009;9:88. doi:10.1186/1471-2458-9-88.
10. Singh-Manoux A, Dugravot A, Shipley M, Brunner EJ, Elbaz A, Sabia S, Kivimaki M. Obesity trajectories and risk of dementia: 28 years of follow-up in the Whitehall II Study. *Alzheimers Dement*. 2018;14:178–86. doi:10.1016/j.jalz.2017.06.2637.
11. Fabbrini E, Sullivan S, Klein S. Obesity and nonalcoholic fatty liver disease: Biochemical, metabolic, and clinical implications. *Hepatology*. 2010;51:679–89. doi:10.1002/hep.23280.
12. Reyes C, Leyland KM, Peat G, Cooper C, Arden NK, Prieto-Alhambra D. Association Between Overweight and Obesity and Risk of Clinically Diagnosed Knee, Hip, and Hand Osteoarthritis: A Population-Based Cohort Study. *Arthritis & rheumatology (Hoboken, N.J.)*. 2016;68:1869–75. doi:10.1002/art.39707.
13. Herrington WG, Smith M, Bankhead C, Matsushita K, Stevens S, Holt T, *et al*. Body-mass index and risk of advanced chronic kidney disease: Prospective analyses from a primary care cohort of 1.4 million adults in England. *PLoS One*. 2017;12:e0173515. doi:10.1371/journal.pone.0173515.
14. Dobner J, Kaser S. Body mass index and the risk of infection - from underweight to obesity. *Clin Microbiol Infect*. 2018;24:24–8. doi:10.1016/j.cmi.2017.02.013.
15. Behrens G, Gredner T, Stock C, Leitzmann MF, Brenner H, Mons U. Cancers Due to Excess Weight, Low Physical Activity, and Unhealthy Diet. *Dtsch Arztebl Int*. 2018;115:578–85. doi:10.3238/arztebl.2018.0578.
16. Wolin KY, Carson K, Colditz GA. Obesity and cancer. *Oncologist*. 2010;15:556–65. doi:10.1634/theoncologist.2009-0285.
17. Bray F, Ferlay J, Soerjomataram I, Siegel RL, Torre LA, Jemal A. Global cancer statistics 2018: GLOBOCAN estimates of incidence and mortality worldwide for 36 cancers in 185 countries. *CA Cancer J Clin*. 2018;68:394–424. doi:10.3322/caac.21492.
18. Ma Y, Yang Y, Wang F, Zhang P, Shi C, Zou Y, Qin H. Obesity and risk of colorectal cancer: A systematic review of prospective studies. *PLoS One*. 2013;8:e53916. doi:10.1371/journal.pone.0053916.

19. Munsell MF, Sprague BL, Berry DA, Chisholm G, Trentham-Dietz A. Body mass index and breast cancer risk according to postmenopausal estrogen-progestin use and hormone receptor status. *Epidemiol Rev.* 2014;36:114–36. doi:10.1093/epirev/mxt010.
20. Brinton LA, Cook MB, McCormack V, Johnson KC, Olsson H, Casagrande JT, *et al.* Anthropometric and hormonal risk factors for male breast cancer: Male breast cancer pooling project results. *J Natl Cancer Inst.* 2014;106:djt465. doi:10.1093/jnci/djt465.
21. Park EJ, Lee JH, Yu G-Y, He G, Ali SR, Holzer RG, *et al.* Dietary and genetic obesity promote liver inflammation and tumorigenesis by enhancing IL-6 and TNF expression. *Cell.* 2010;140:197–208. doi:10.1016/j.cell.2009.12.052.
22. Patel A, Pathak Y, Patel J, Sutariya V. Role of nutritional factors in pathogenesis of cancer. *Food Quality and Safety.* 2018;2:27–36. doi:10.1093/fqsafe/fyx033.
23. McTiernan A. Mechanisms linking physical activity with cancer. *Nat Rev Cancer.* 2008;8:205–11. doi:10.1038/nrc2325.
24. Tsugane S, Inoue M. Insulin resistance and cancer: Epidemiological evidence. *Cancer Sci.* 2010;101:1073–9. doi:10.1111/j.1349-7006.2010.01521.x.
25. Coelho M, Oliveira T, Fernandes R. Biochemistry of adipose tissue: an endocrine organ. *Arch Med Sci.* 2013;9:191–200. doi:10.5114/aoms.2013.33181.
26. Magnuson A, Fouts J, Booth A, Foster M. Obesity-induced chronic low grade inflammation: Gastrointestinal and adipose tissue crosstalk. *Integr Obesity Diabetes* 2015. doi:10.15761/IOD.1000124.
27. Andersen CJ, Murphy KE, Fernandez ML. Impact of Obesity and Metabolic Syndrome on Immunity. *Adv Nutr.* 2016;7:66–75. doi:10.3945/an.115.010207.
28. Gesta S, Tseng Y-H, Kahn CR. Developmental origin of fat: Tracking obesity to its source. *Cell.* 2007;131:242–56. doi:10.1016/j.cell.2007.10.004.
29. Bjørndal B, Burri L, Staalesen V, Skorve J, Berge RK. Different adipose depots: Their role in the development of metabolic syndrome and mitochondrial response to hypolipidemic agents. *J Obes.* 2011;2011:490650. doi:10.1155/2011/490650.
30. Francisco V, Pino J, Gonzalez-Gay MA, Mera A, Lago F, Gómez R, *et al.* Adipokines and inflammation: Is it a question of weight? *Br J Pharmacol.* 2018;175:1569–79. doi:10.1111/bph.14181.
31. Francisco V, Pino J, Campos-Cabaleiro V, Ruiz-Fernández C, Mera A, Gonzalez-Gay MA, *et al.* Obesity, Fat Mass and Immune System: Role for Leptin. *Front. Physiol.* 2018;9:473. doi:10.3389/fphys.2018.00640.
32. Gregor MF, Hotamisligil GS. Inflammatory mechanisms in obesity. *Annu Rev Immunol.* 2011;29:415–45. doi:10.1146/annurev-immunol-031210-101322.
33. Wensveen FM, Jelencic V, Valentic S, Sestan M, Wensveen TT, Theurich S, *et al.* NK cells link obesity-induced adipose stress to inflammation and insulin resistance. *Nat Immunol.* 2015;16:376–85. doi:10.1038/ni.3120.
34. Castoldi A, Naffah de Souza C, Câmara NOS, Moraes-Vieira PM. The Macrophage Switch in Obesity Development. *Frontiers in Immunology.* 2015;6:637. doi:10.3389/fimmu.2015.00637.
35. Gerriets VA, MacIver NJ. Role of T cells in malnutrition and obesity. *Front. Immunol.* 2014;5:379. doi:10.3389/fimmu.2014.00379.
36. Kosaraju R, Guesdon W, Crouch MJ, Teague HL, Sullivan EM, Karlsson EA, *et al.* B Cell Activity Is Impaired in Human and Mouse Obesity and Is Responsive to an Essential Fatty Acid upon Murine Influenza Infection. *J Immunol.* 2017;198:4738–52. doi:10.4049/jimmunol.1601031.
37. Laue T, Wrann CD, Hoffmann-Castendiek B, Pietsch D, Hubner L, Kielstein H. Altered NK cell function in obese healthy humans. *BMC Obes.* 2015;2:1. doi:10.1186/s40608-014-0033-1.

38. Nave H, Mueller G, Siegmund B, Jacobs R, Stroh T, Schueler U, *et al.* Resistance of Janus kinase-2 dependent leptin signaling in natural killer (NK) cells: a novel mechanism of NK cell dysfunction in diet-induced obesity. *Endocrinology*. 2008;149:3370–8. doi:10.1210/en.2007-1516.
39. Viel S, Besson L, Charrier E, Marçais A, Disse E, Bienvenu J, *et al.* Alteration of Natural Killer cell phenotype and function in obese individuals. *Clin Immunol* 2016. doi:10.1016/j.clim.2016.01.007.
40. O'Shea D, Cawood TJ, O'Farrelly C, Lynch L. Natural killer cells in obesity: impaired function and increased susceptibility to the effects of cigarette smoke. *PLoS One*. 2010;5:e8660. doi:10.1371/journal.pone.0008660.
41. Eberl G, Colonna M, Di Santo JP, McKenzie ANJ. Innate lymphoid cells. *Innate lymphoid cells: A new paradigm in immunology*. *Science*. 2015;348:aaa6566. doi:10.1126/science.aaa6566.
42. Artis D, Spits H. The biology of innate lymphoid cells. *Nature*. 2015;517:293 EP -. doi:10.1038/nature14189.
43. Vivier E, Artis D, Colonna M, Diefenbach A, Di Santo JP, Eberl G, *et al.* Innate Lymphoid Cells: 10 Years On. *Cell*. 2018;174:1054–66. doi:10.1016/j.cell.2018.07.017.
44. Abel AM, Yang C, Thakar MS, Malarkannan S. Natural Killer Cells: Development, Maturation, and Clinical Utilization. *Frontiers in Immunology*. 2018;9:1869. doi:10.3389/fimmu.2018.01869.
45. Beaulieu AM. Memory responses by natural killer cells. *J Leukoc Biol*. 2018;104:1087–96. doi:10.1002/JLB.1RI0917-366R.
46. Hall LJ, Clare S, Dougan G. NK cells influence both innate and adaptive immune responses after mucosal immunization with antigen and mucosal adjuvant. *J Immunol*. 2010;184:4327–37. doi:10.4049/jimmunol.0903357.
47. Raulet DH. Interplay of natural killer cells and their receptors with the adaptive immune response. *Nat Immunol*. 2004;5:996–1002. doi:10.1038/ni1114.
48. Sun JC, Beilke JN, Lanier LL. Adaptive immune features of natural killer cells. *Nature*. 2009;457:557–61. doi:10.1038/nature07665.
49. Vivier E, Raulet DH, Moretta A, Caligiuri MA, Zitvogel L, Lanier LL, *et al.* Innate or adaptive immunity? The example of natural killer cells. *Science*. 2011;331:44–9. doi:10.1126/science.1198687.
50. Lysakova-Devine T, O'Farrelly C. Tissue-specific NK cell populations and their origin. *J Leukoc Biol*. 2014;96:981–90. doi:10.1189/jlb.1RU0514-241R.
51. Cooper MA. Human natural killer cells: A unique innate immunoregulatory role for the CD56bright subset. *Blood*. 2001;97:3146–51. doi:10.1182/blood.V97.10.3146.
52. van Acker HH, Capsomidis A, Smits EL, van Tendeloo VF. CD56 in the Immune System: More Than a Marker for Cytotoxicity? *Front. Immunol*. 2017;8:892. doi:10.3389/fimmu.2017.00892.
53. Yeap WH, Wong KL, Shimasaki N, Teo ECY, Quek JKS, Yong HX, *et al.* CD16 is indispensable for antibody-dependent cellular cytotoxicity by human monocytes. *Sci Rep*. 2016;6:34310 EP -. doi:10.1038/srep34310.
54. Amand M, Iserentant G, Poli A, Sleiman M, Fievez V, Sanchez IP, *et al.* Human CD56dimCD16dim Cells As an Individualized Natural Killer Cell Subset. *Frontiers in Immunology*. 2017;8:699. doi:10.3389/fimmu.2017.00699.
55. Michel T, Poli A, Cuapio A, Briquemont B, Iserentant G, Ollert M, Zimmer J. Human CD56bright NK Cells: An Update. *J Immunol*. 2016;196:2923–31. doi:10.4049/jimmunol.1502570.
56. Poli A, Michel T, Thérésine M, Andrès E, Hentges F, Zimmer J. CD56bright natural killer (NK) cells: An important NK cell subset. *Immunology*. 2009;126:458–65. doi:10.1111/j.1365-2567.2008.03027.x.
57. Cooper MA, Fehniger TA, Caligiuri MA. The biology of human natural killer-cell subsets. *Trends Immunol*. 2001;22:633–40. doi:10.1016/S1471-4906(01)02060-9.
58. Chiossone L, Chaix J, Fuseri N, Roth C, Vivier E, Walzer T. Maturation of mouse NK cells is a 4-stage developmental program. *Blood*. 2009;113:5488–96. doi:10.1182/blood-2008-10-187179.

59. Hayakawa Y, Andrews DM, Smyth MJ. Subset analysis of human and mouse mature NK cells. *Methods Mol Biol.* 2010;612:27–38. doi:10.1007/978-1-60761-362-6_3.
60. Kim S, Iizuka K, Kang H-SP, Dokun A, French AR, Greco S, Yokoyama WM. In vivo developmental stages in murine natural killer cell maturation. *Nat Immunol.* 2002;3:523–8. doi:10.1038/ni796.
61. Hayakawa Y, Huntington ND, Nutt SL, Smyth MJ. Functional subsets of mouse natural killer cells. *Immunol Rev.* 2006;214:47–55. doi:10.1111/j.1600-065X.2006.00454.x.
62. Vivier E, Ugolini S, Blaise D, Chabannon C, Brossay L. Targeting natural killer cells and natural killer T cells in cancer. *Nat Rev Immunol.* 2012;12:239–52. doi:10.1038/nri3174.
63. Inngjerdingen M, Kveberg L, Naper C, Vaage JT. Natural killer cell subsets in man and rodents. *Tissue Antigens.* 2011;78:81–8. doi:10.1111/j.1399-0039.2011.01714.x.
64. Ljunggren HG, Kärre K. In search of the 'missing self': MHC molecules and NK cell recognition. *Immunol Today.* 1990;11:237–44.
65. Raulet DH, Vance RE, McMahon CW. Regulation of the natural killer cell receptor repertoire. *Annu Rev Immunol.* 2001;19:291–330. doi:10.1146/annurev.immunol.19.1.291.
66. Barrow AD, Colonna M. Exploiting NK Cell Surveillance Pathways for Cancer Therapy. *Cancers (Basel)* 2019. doi:10.3390/cancers11010055.
67. Middleton D, Gonzelez F. The extensive polymorphism of KIR genes. *Immunology.* 2010;129:8–19. doi:10.1111/j.1365-2567.2009.03208.x.
68. Chester C, Fritsch K, Kohrt HE. Natural Killer Cell Immunomodulation: Targeting Activating, Inhibitory, and Co-stimulatory Receptor Signaling for Cancer Immunotherapy. *Frontiers in Immunology.* 2015;6:601. doi:10.3389/fimmu.2015.00601.
69. Farag SS, Fehniger TA, Ruggeri L, Velardi A, Caligiuri MA. Natural killer cell receptors: New biology and insights into the graft-versus-leukemia effect. *Blood.* 2002;100:1935–47. doi:10.1182/blood-2002-02-0350.
70. Konjević G, Vuletić A, Martinović KM, Džodić R. The Role of Activating and Inhibitory NK Cell Receptors in Antitumor Immune Response. In: Aribi M, editor. *Natural Killer Cells: InTech*; 2017. doi:10.5772/intechopen.69729.
71. Rahim MMA, Tu MM, Mahmoud AB, Wight A, Abou-Samra E, Lima PDA, Makrigiannis AP. Ly49 receptors: Innate and adaptive immune paradigms. *Front. Immunol.* 2014;5:145. doi:10.3389/fimmu.2014.00145.
72. Schenkel AR, Kingry LC, Slayden RA. The ly49 gene family. A brief guide to the nomenclature, genetics, and role in intracellular infection. *Front. Immunol.* 2013;4:90. doi:10.3389/fimmu.2013.00090.
73. Kruse PH, Matta J, Ugolini S, Vivier E. Natural cytotoxicity receptors and their ligands. *Immunol Cell Biol.* 2014;92:221–9. doi:10.1038/icb.2013.98.
74. Vitale M, Bottino C, Sivori S, Sanseverino L, Castriconi R, Marcenaro E, *et al.* NKp44, a Novel Triggering Surface Molecule Specifically Expressed by Activated Natural Killer Cells, Is Involved in Non-Major Histocompatibility Complex-restricted Tumor Cell Lysis. *J Exp Med.* 1998;187:2065–72. doi:10.1084/jem.187.12.2065.
75. Tremblay-McLean A, Coenraads S, Kiani Z, Dupuy FP, Bernard NF. Expression of ligands for activating natural killer cell receptors on cell lines commonly used to assess natural killer cell function. *BMC Immunol.* 2019;20:8. doi:10.1186/s12865-018-0272-x.
76. Walzer T, Blery M, Chaix J, Fuseri N, Chasson L, Robbins SH, *et al.* Identification, activation, and selective in vivo ablation of mouse NK cells via NKp46. *Proc Natl Acad Sci U S A.* 2007;104:3384–9. doi:10.1073/pnas.0609692104.
77. Moretta L, Montaldo E, Vacca P, Del Zotto G, Moretta F, Merli P, *et al.* Human natural killer cells: Origin, receptors, function, and clinical applications. *Int Arch Allergy Immunol.* 2014;164:253–64. doi:10.1159/000365632.

78. Pazina T, Shemesh A, Brusilovsky M, Porgador A, Campbell KS. Regulation of the Functions of Natural Cytotoxicity Receptors by Interactions with Diverse Ligands and Alterations in Splice Variant Expression. *Front. Immunol.* 2017;8:369. doi:10.3389/fimmu.2017.00369.
79. Lanier LL. NK cell recognition. *Annu Rev Immunol.* 2005;23:225–74. doi:10.1146/annurev.immunol.23.021704.115526.
80. Braud VM, Allan DS, O'Callaghan CA, Söderström K, D'Andrea A, Ogg GS, *et al.* HLA-E binds to natural killer cell receptors CD94/NKG2A, B and C. *Nature.* 1998;391:795–9. doi:10.1038/35869.
81. Vance RE, Kraft JR, Altman JD, Jensen PE, Raulet DH. Mouse CD94/NKG2A is a natural killer cell receptor for the nonclassical major histocompatibility complex (MHC) class I molecule Qa-1(b). *J Exp Med.* 1998;188:1841–8.
82. Farag SS, Caligiuri MA. Human natural killer cell development and biology. *Blood Rev.* 2006;20:123–37. doi:10.1016/j.blre.2005.10.001.
83. Radaev S, Sun PD. Structure and function of natural killer cell surface receptors. *Annu Rev Biophys Biomol Struct.* 2003;32:93–114. doi:10.1146/annurev.biophys.32.110601.142347.
84. Wensveen FM, Jelenčić V, Polić B. NKG2D: A Master Regulator of Immune Cell Responsiveness. *Front. Immunol.* 2018;9:441. doi:10.3389/fimmu.2018.00441.
85. Bauer S. Activation of NK Cells and T Cells by NKG2D, a Receptor for Stress-Inducible MICA. *Science.* 1999;285:727–9. doi:10.1126/science.285.5428.727.
86. Rosen DB, Araki M, Hamerman JA, Chen T, Yamamura T, Lanier LL. A Structural basis for the association of DAP12 with mouse, but not human, NKG2D. *J Immunol.* 2004;173:2470–8.
87. Comerci CJ, Mace EM, Banerjee PP, Orange JS. CD2 promotes human natural killer cell membrane nanotube formation. *PLoS One.* 2012;7:e47664. doi:10.1371/journal.pone.0047664.
88. Juelke K, Killig M, Luetke-Eversloh M, Parente E, Gruen J, Morandi B, *et al.* CD62L expression identifies a unique subset of polyfunctional CD56dim NK cells. *Blood.* 2010;116:1299–307. doi:10.1182/blood-2009-11-253286.
89. Seth S, Georgoudaki A-M, Chambers BJ, Qiu Q, Kremmer E, Maier MK, *et al.* Heterogeneous expression of the adhesion receptor CD226 on murine NK and T cells and its function in NK-mediated killing of immature dendritic cells. *J Leukoc Biol.* 2009;86:91–101. doi:10.1189/jlb.1208745.
90. Chen S, Kawashima H, Lowe JB, Lanier LL, Fukuda M. Suppression of tumor formation in lymph nodes by L-selectin-mediated natural killer cell recruitment. *J Exp Med.* 2005;202:1679–89. doi:10.1084/jem.20051473.
91. Ley K, Laudanna C, Cybulsky MI, Nourshargh S. Getting to the site of inflammation: The leukocyte adhesion cascade updated. *Nat Rev Immunol.* 2007;7:678–89. doi:10.1038/nri2156.
92. Claus M, Meinke S, Bhat R, Watzl C. Regulation of NK cell activity by 2B4, NTB-A and CRACC. *Front Biosci.* 2008;13:956–65.
93. Vitale M, Falco M, Castriconi R, Parolini S, Zambello R, Semenzato G, *et al.* Identification of NKp80, a novel triggering molecule expressed by human NK cells. *Eur J Immunol.* 2001;31:233–42. doi:10.1002/1521-4141(200101)31:1<233::AID-IMMU233>3.0.CO;2-4.
94. He Y, Peng H, Sun R, Wei H, Ljunggren H-G, Yokoyama WM, Tian Z. Contribution of inhibitory receptor TIGIT to NK cell education. *J Autoimmun.* 2017;81:1–12. doi:10.1016/j.jaut.2017.04.001.
95. Stanietsky N, Rovis TL, Glasner A, Seidel E, Tsukerman P, Yamin R, *et al.* Mouse TIGIT inhibits NK-cell cytotoxicity upon interaction with PVR. *Eur J Immunol.* 2013;43:2138–50. doi:10.1002/eji.201243072.
96. Hassan SS, Akram M, King EC, Dockrell HM, Cliff JM. PD-1, PD-L1 and PD-L2 Gene Expression on T-Cells and Natural Killer Cells Declines in Conjunction with a Reduction in PD-1 Protein during the Intensive Phase of Tuberculosis Treatment. *PLoS One.* 2015;10:e0137646. doi:10.1371/journal.pone.0137646.

97. Kurioka A, Cosgrove C, Simoni Y, van Wilgenburg B, Geremia A, Björkander S, *et al.* CD161 Defines a Functionally Distinct Subset of Pro-Inflammatory Natural Killer Cells. *Front. Immunol.* 2018;9:486. doi:10.3389/fimmu.2018.00486.
98. Rosen DB, Bettadapura J, Alsharifi M, Mathew PA, Warren HS, Lanier LL. Cutting Edge: Lectin-Like Transcript-1 Is a Ligand for the Inhibitory Human NKR-P1A Receptor. *J Immunol.* 2005;175:7796–9. doi:10.4049/jimmunol.175.12.7796.
99. Jandus C, Boligan KF, Chijioke O, Liu H, Dahlhaus M, Démoulin T, *et al.* Interactions between Siglec-7/9 receptors and ligands influence NK cell-dependent tumor immunosurveillance. *J Clin Invest.* 2014;124:1810–20. doi:10.1172/JCI65899.
100. Caldirola MS, Rodríguez Broggi MG, Gaillard MI, Bezrodnik L, Zwirner NW. Primary Immunodeficiencies Unravel the Role of IL-2/CD25/STAT5b in Human Natural Killer Cell Maturation. *Front. Immunol.* 2018;9:1429. doi:10.3389/fimmu.2018.01429.
101. Wang KS, Ritz J, Frank DA. IL-2 induces STAT4 activation in primary NK cells and NK cell lines, but not in T cells. *J Immunol.* 1999;162:299–304.
102. Rudnicka K, Matusiak A, Chmiela M. CD25 (IL-2R) expression correlates with the target cell induced cytotoxic activity and cytokine secretion in human natural killer cells. *Acta Biochim Pol.* 2015;62:885–94. doi:10.18388/abp.2015_1152.
103. Cibrián D, Sánchez-Madrid F. CD69: From activation marker to metabolic gatekeeper. *Eur J Immunol.* 2017;47:946–53. doi:10.1002/eji.201646837.
104. Fogel LA, Sun MM, Geurs TL, Carayannopoulos LN, French AR. Markers of nonselective and specific NK cell activation. *J Immunol.* 2013;190:6269–76. doi:10.4049/jimmunol.1202533.
105. Alter G, Malenfant JM, Altfeld M. CD107a as a functional marker for the identification of natural killer cell activity. *J Immunol Methods.* 2004;294:15–22. doi:10.1016/j.jim.2004.08.008.
106. Aktas E, Kucuksezzer UC, Bilgic S, Erten G, Deniz G. Relationship between CD107a expression and cytotoxic activity. *Cell Immunol.* 2009;254:149–54. doi:10.1016/j.cellimm.2008.08.007.
107. Freud AG, Caligiuri MA. Human natural killer cell development. *Immunol Rev.* 2006;214:56–72. doi:10.1111/j.1600-065X.2006.00451.x.
108. Yu J, Freud AG, Caligiuri MA. Location and cellular stages of natural killer cell development. *Trends Immunol.* 2013;34:573–82. doi:10.1016/j.it.2013.07.005.
109. Wu Y, Tian Z, Wei H. Developmental and Functional Control of Natural Killer Cells by Cytokines. *Front. Immunol.* 2017;8:930. doi:10.3389/fimmu.2017.00930.
110. Mace EM. Requirements for human natural killer cell development informed by primary immunodeficiency. *Curr Opin Allergy Clin Immunol.* 2016;16:541–8. doi:10.1097/ACI.0000000000000317.
111. Lopez-Vergès S, Milush JM, Pandey S, York VA, Arakawa-Hoyt J, Pircher H, *et al.* CD57 defines a functionally distinct population of mature NK cells in the human CD56dimCD16+ NK-cell subset. *Blood.* 2010;116:3865–74. doi:10.1182/blood-2010-04-282301.
112. Björkström NK, Riese P, Heuts F, Andersson S, Fauriat C, Ivarsson MA, *et al.* Expression patterns of NKG2A, KIR, and CD57 define a process of CD56dim NK-cell differentiation uncoupled from NK-cell education. *Blood.* 2010;116:3853–64. doi:10.1182/blood-2010-04-281675.
113. Huntington ND, Tabarias H, Fairfax K, Brady J, Hayakawa Y, Degli-Esposti MA, *et al.* NK cell maturation and peripheral homeostasis is associated with KLRG1 up-regulation. *J Immunol.* 2007;178:4764–70.
114. Sutlu T, Alici E. Natural killer cell-based immunotherapy in cancer: current insights and future prospects. *J Intern Med.* 2009;266:154–81. doi:10.1111/j.1365-2796.2009.02121.x.
115. Jenkins MR, Rudd-Schmidt JA, Lopez JA, Ramsbottom KM, Mannering SI, Andrews DM, *et al.* Failed CTL/NK cell killing and cytokine hypersecretion are directly linked through prolonged synapse time. *J Exp Med.* 2015;212:307–17. doi:10.1084/jem.20140964.

116. Smyth MJ, Cretney E, Kelly JM, Westwood JA, Street SEA, Yagita H, *et al.* Activation of NK cell cytotoxicity. *Mol Immunol.* 2005;42:501–10. doi:10.1016/j.molimm.2004.07.034.
117. Cullen SP, Martin SJ. Mechanisms of granule-dependent killing. *Cell Death Differ.* 2008;15:251–62. doi:10.1038/sj.cdd.4402244.
118. Chávez-Galán L, Arenas-Del Angel MC, Zenteno E, Chávez R, Lascurain R. Cell death mechanisms induced by cytotoxic lymphocytes. *Cell Mol Immunol.* 2009;6:15–25. doi:10.1038/cmi.2009.3.
119. Colditz GA, Peterson LL. Obesity and Cancer: Evidence, Impact, and Future Directions. *Clin Chem.* 2018;64:154–62. doi:10.1373/clinchem.2017.277376.
120. Brown KA, Simpson ER. Obesity and breast cancer: Progress to understanding the relationship. *Cancer Res.* 2010;70:4–7. doi:10.1158/0008-5472.CAN-09-2257.
121. Lauby-Secretan B, Scoccianti C, Loomis D, Grosse Y, Bianchini F, Straif K. Body Fatness and Cancer-Viewpoint of the IARC Working Group. *N Engl J Med.* 2016;375:794–8. doi:10.1056/NEJMs1606602.
122. Ackerman SE, Blackburn OA, Marchildon F, Cohen P. Insights into the Link Between Obesity and Cancer. *Curr Obes Rep.* 2017;6:195–203. doi:10.1007/s13679-017-0263-x.
123. Himbert C, Delphan M, Scherer D, Bowers LW, Hursting S, Ulrich CM. Signals from the Adipose Microenvironment and the Obesity-Cancer Link-A Systematic Review. *Cancer Prev Res (Phila).* 2017;10:494–506. doi:10.1158/1940-6207.CAPR-16-0322.
124. Michelet X, Dyck L, Hogan A, Loftus RM, Duquette D, Wei K, *et al.* Metabolic reprogramming of natural killer cells in obesity limits antitumor responses. *Nat Immunol.* 2018;19:1330–40. doi:10.1038/s41590-018-0251-7.
125. Bähr I, Jahn J, Zipprich A, Pahlow I, Spielmann J, Kielstein H. Impaired natural killer cell subset phenotypes in human obesity. *Immunol Res.* 2018;66:234–44. doi:10.1007/s12026-018-8989-4.
126. Tobin LM, Mavinkurve M, Carolan E, Kinlen D, O'Brien EC, Little MA, *et al.* NK cells in childhood obesity are activated, metabolically stressed, and functionally deficient. *JCI Insight* 2017. doi:10.1172/jci.insight.94939.
127. Lautenbach A, Wrann CD, Jacobs R, Muller G, Brabant G, Nave H. Altered phenotype of NK cells from obese rats can be normalized by transfer into lean animals. *Obesity (Silver Spring).* 2009;17:1848–55. doi:10.1038/oby.2009.140.
128. La Cava A, Matarese G. The weight of leptin in immunity. *Nat Rev Immunol.* 2004;4:371–9. doi:10.1038/nri1350.
129. Tilg H, Moschen AR. Adipocytokines: Mediators linking adipose tissue, inflammation and immunity. *Nat Rev Immunol.* 2006;6:772–83. doi:10.1038/nri1937.
130. Shah NR, Braverman ER. Measuring adiposity in patients: The utility of body mass index (BMI), percent body fat, and leptin. *PLoS One.* 2012;7:e33308. doi:10.1371/journal.pone.0033308.
131. Kobayashi T, Mattarollo SR. Natural killer cell metabolism. *Mol Immunol* 2017. doi:10.1016/j.molimm.2017.11.021.
132. Wrann CD, Laue T, Hubner L, Kuhlmann S, Jacobs R, Goudeva L, Nave H. Short-term and long-term leptin exposure differentially affect human natural killer cell immune functions. *Am J Physiol Endocrinol Metab.* 2012;302:E108-16. doi:10.1152/ajpendo.00057.2011.
133. Smith AG, Sheridan PA, Harp JB, Beck MA. Diet-induced obese mice have increased mortality and altered immune responses when infected with influenza virus. *J Nutr.* 2007;137:1236–43. doi:10.1093/jn/137.5.1236.
134. Zhao Y, Sun R, You L, Gao C, Tian Z. Expression of leptin receptors and response to leptin stimulation of human natural killer cell lines. *Biochem Biophys Res Commun.* 2003;300:247–52.
135. Yaqoob P, Newsholme EA, Calder PC. Inhibition of natural killer cell activity by dietary lipids. *Immunol Lett.* 1994;41:241–7.

136. Jeffery NM, Sanderson P, Newsholme EA, Calder PC. Effects of varying the type of saturated fatty acid in the rat diet upon serum lipid levels and spleen lymphocyte functions. *Biochim Biophys Acta*. 1997;1345:223–36.
137. Bähr I, Goritz V, Doberstein H, Hiller GGR, Rosenstock P, Jahn J, *et al*. Diet-Induced Obesity Is Associated with an Impaired NK Cell Function and an Increased Colon Cancer Incidence. *Journal of Nutrition and Metabolism*. 2017;2017:1–14. doi:10.1155/2017/4297025.
138. Spielmann J, Hanke J, Knauf D, Ben-Eliyahu S, Jacobs R, Stangl GI, *et al*. Significantly enhanced lung metastasis and reduced organ NK cell functions in diet-induced obese rats. *BMC Obes*. 2017;4:24. doi:10.1186/s40608-017-0161-5.
139. Lamas O, Martínez JA, Marti A. Energy restriction restores the impaired immune response in overweight (cafeteria) rats. *J Nutr Biochem*. 2004;15:418–25. doi:10.1016/j.jnutbio.2004.02.003.
140. O'Rourke RW, Gaston GD, Meyer KA, White AE, Marks DL. Adipose tissue NK cells manifest an activated phenotype in human obesity. *Metab Clin Exp*. 2013;62:1557–61. doi:10.1016/j.metabol.2013.07.011.
141. Imai K, Matsuyama S, Miyake S, Suga K, Nakachi K. Natural cytotoxic activity of peripheral-blood lymphocytes and cancer incidence: An 11-year follow-up study of a general population. *The Lancet*. 2000;356:1795–9. doi:10.1016/S0140-6736(00)03231-1.
142. Jahn J, Spielau M, Brandsch C, Stangl GI, Delank K-S, Bähr I, *et al*. Decreased NK cell functions in obesity can be reactivated by fat mass reduction. *Obesity (Silver Spring)*. 2015;23:2233–41. doi:10.1002/oby.21229.
143. Moulin CM, Marguti I, Peron JPS, Halpern A, Rizzo LV. Bariatric surgery reverses natural killer (NK) cell activity and NK-related cytokine synthesis impairment induced by morbid obesity. *Obes Surg*. 2011;21:112–8. doi:10.1007/s11695-010-0250-8.
144. Barra NG, Fan IY, Gillen JB, Chew M, Marcinko K, Steinberg GR, *et al*. High Intensity Interval Training Increases Natural Killer Cell Number and Function in Obese Breast Cancer-challenged Mice and Obese Women. *J Cancer Prev*. 2017;22:260–6. doi:10.15430/JCP.2017.22.4.260.
145. Rosenstock P, Horstkorte R, Gnanapragassam VS, Harth J, Kielstein H. Siglec-7 expression is reduced on a natural killer (NK) cell subset of obese humans. *Immunol Res* 2017. doi:10.1007/s12026-017-8942-y.
146. Lamas B, Nachat-Kappes R, Goncalves-Mendes N, Mishellany F, Rossary A, Vasson M-P, Farges M-C. Dietary fat without body weight gain increases in vivo MCF-7 human breast cancer cell growth and decreases natural killer cell cytotoxicity. *Mol Carcinog*. 2015;54:58–71. doi:10.1002/mc.22074.
147. Renehan AG, Tyson M, Egger M, Heller RF, Zwahlen M. Body-mass index and incidence of cancer: A systematic review and meta-analysis of prospective observational studies. *The Lancet*. 2008;371:569–78. doi:10.1016/S0140-6736(08)60269-X.
148. Soule HD, Vazquez J, Long A, Albert S, Brennan M. A human cell line from a pleural effusion derived from a breast carcinoma. *J Natl Cancer Inst*. 1973;51:1409–16.
149. Martin BK, Chin K-C, Olsen JC, Skinner CA, Dey A, Ozato K, Ting JP-Y. Induction of MHC Class I Expression by the MHC Class II Transactivator CIITA. *Immunity*. 1997;6:591–600. doi:10.1016/S1074-7613(00)80347-7.
150. Dexter DL, Barbosa JA, Calabresi P. N,N-dimethylformamide-induced alteration of cell culture characteristics and loss of tumorigenicity in cultured human colon carcinoma cells. *Cancer Res*. 1979;39:1020–5.
151. Imanishi T, Kamigaki T, Nakamura T, Hayashi S, Yasuda T, Kawasaki K, *et al*. Correlation between expression of major histocompatibility complex class I and that of antigen presenting machineries in carcinoma cell lines of the pancreas, biliary tract and colon. *Kobe J Med Sci*. 2006;52:85–95.
152. Lozzio CB, Lozzio BB. Cytotoxicity of a Factor Isolated From Human Spleen 2. *JNCI: Journal of the National Cancer Institute*. 1973;50:535–8. doi:10.1093/jnci/50.2.535.

153. Gong JH, Maki G, Klingemann HG. Characterization of a human cell line (NK-92) with phenotypical and functional characteristics of activated natural killer cells. *Leukemia*. 1994;8:652–8.
154. Suck G, Odendahl M, Nowakowska P, Seidl C, Wels WS, Klingemann HG, Tonn T. NK-92: an 'off-the-shelf therapeutic' for adoptive natural killer cell-based cancer immunotherapy. *Cancer Immunol Immunother*. 2016;65:485–92. doi:10.1007/s00262-015-1761-x.
155. Wang M, Bronte V, Chen PW, Gritz L, Panicali D, Rosenberg SA, Restifo NP. Active immunotherapy of cancer with a nonreplicating recombinant fowlpox virus encoding a model tumor-associated antigen. *J Immunol*. 1995;154:4685–92.
156. Castle JC, Loewer M, Boegel S, Graaf J de, Bender C, Tadmor AD, *et al*. Immunomic, genomic and transcriptomic characterization of CT26 colorectal carcinoma. *BMC Genomics*. 2014;15:190. doi:10.1186/1471-2164-15-190.
157. Thermo Fisher Scientific. ProcartaPlex Multiplex Immunoassay for Simplex Kits and Combinable Panels User Guide (Pub.No. MAN0016941 E.0 (37)). 2019.
158. Duske H, Sputtek A, Binder T, Kröger N, Schrepfer S, Eiermann T. Assessment of physiologic natural killer cell cytotoxicity in vitro. *Hum Immunol*. 2011;72:1007–12. doi:10.1016/j.humimm.2011.08.006.
159. BD Biosciences. Einführung in die Durchflusszytometrie. 2014. <http://www.bd.com/resource.aspx?IDX=31055>. Accessed 3 Mar 2019.
160. Givan AL. *Flow Cytometry: First Principles*. New York, USA: John Wiley & Sons, Inc; 2001.
161. BD Biosciences. Multicolor Flow Cytometry. 2011. https://www.bdbiosciences.com/documents/webinar_2011_07_MulticolorSetup.pdf. Accessed 3 Mar 2019.
162. ACEA Biosciences I. xCELLigence – Continuous, Label-Free, Real-Time Cell Analysis - Principles of Operation and Selected Applications -. 2016. <https://www.aceabio.com/products/icelligence/>. Accessed 28 May 2018.
163. Freund-Brown J, Choa R, Singh BK, Robertson TF, Ferry GM, Viver E, *et al*. Cutting Edge: Murine NK Cells Degranulate and Retain Cytotoxic Function without Store-Operated Calcium Entry. *J Immunol* 2017. doi:10.4049/jimmunol.1700340.
164. Pak-Wittel MA, Piersma SJ, Plougastel BF, Poursine-Laurent J, Yokoyama WM. Isolation of murine natural killer cells. *Curr Protoc Immunol*. 2014;105:3.22.1-9. doi:10.1002/0471142735.im0322s105.
165. Michel T, Poli A, Domingues O, Mauffray M, Thérésine M, Brons NHC, *et al*. Mouse lung and spleen natural killer cells have phenotypic and functional differences, in part influenced by macrophages. *PLoS One*. 2012;7:e51230. doi:10.1371/journal.pone.0051230.
166. Fehniger TA, Cai SF, Cao X, Bredemeyer AJ, Presti RM, French AR, Ley TJ. Acquisition of murine NK cell cytotoxicity requires the translation of a pre-existing pool of granzyme B and perforin mRNAs. *Immunity*. 2007;26:798–811. doi:10.1016/j.immuni.2007.04.010.
167. Kim S, Iizuka K, Aguila HL, Weissman IL, Yokoyama WM. In vivo natural killer cell activities revealed by natural killer cell-deficient mice. *Proc Natl Acad Sci U S A*. 2000;97:2731–6. doi:10.1073/pnas.050588297.
168. Punturieri A, Velotti F, Piccoli M, Herberman RB, Frati L, Santoni A. Overnight incubation of mouse spleen cells in recombinant IL-2 generates cytotoxic cells with NK characteristics from precursors enriched with or devoid of LGL. *Clinical and Experimental Immunology*. 1989;75:155–60.
169. Saxena RK, Saxena QB, Adler WH. Interleukin-2-induced activation of natural killer activity in spleen cells from old and young mice. *Immunology*. 1984;51:719–26.
170. Romee R, Foley B, Lenvik T, Wang Y, Zhang B, Ankarlo D, *et al*. NK cell CD16 surface expression and function is regulated by a disintegrin and metalloprotease-17 (ADAM17). *Blood*. 2013;121:3599–608. doi:10.1182/blood-2012-04-425397.

171. Grzywacz B, Kataria N, Verneris MR. CD56dimCD16+ NK cells downregulate CD16 following target cell induced activation of matrix metalloproteinases. *Leukemia*. 2007;21:356 EP -. doi:10.1038/sj.leu.2404499.
172. Agha M, Agha R. The rising prevalence of obesity: Part A: impact on public health. *Int J Surg Oncol (N Y)*. 2017;2:e17. doi:10.1097/IJ9.000000000000017.
173. O'Shea D, Hogan AE. Dysregulation of Natural Killer Cells in Obesity. *Cancers (Basel)*. 2019;11:573. doi:10.3390/cancers11040573.
174. Boi SK, Buchta CM, Pearson NA, Francis MB, Meyerholz DK, Grobe JL, Norian LA. Obesity alters immune and metabolic profiles: New insight from obese-resistant mice on high-fat diet. *Obesity (Silver Spring)*. 2016;24:2140–9. doi:10.1002/oby.21620.
175. Peyot M-L, Pepin E, Lamontagne J, Latour MG, Zarrouki B, Lussier R, *et al*. Beta-cell failure in diet-induced obese mice stratified according to body weight gain: Secretory dysfunction and altered islet lipid metabolism without steatosis or reduced beta-cell mass. *Diabetes*. 2010;59:2178–87. doi:10.2337/db09-1452.
176. Boulangé CL, Claus SP, Chou CJ, Collino S, Montoliu I, Kochhar S, *et al*. Early metabolic adaptation in C57BL/6 mice resistant to high fat diet induced weight gain involves an activation of mitochondrial oxidative pathways. *J Proteome Res*. 2013;12:1956–68. doi:10.1021/pr400051s.
177. Diwan BA, Blackman KE. Differential susceptibility of 3 sublines of C57BL/6 mice to the induction of colorectal tumors by 1,2-dimethylhydrazine. *Cancer Lett*. 1980;9:111–5.
178. Podrini C, Cambridge EL, Lelliott CJ, Carragher DM, Estabel J, Gerdin A-K, *et al*. High-fat feeding rapidly induces obesity and lipid derangements in C57BL/6N mice. *Mamm Genome*. 2013;24:240–51. doi:10.1007/s00335-013-9456-0.
179. Hu S, Wang L, Yang D, Li L, Togo J, Wu Y, *et al*. Dietary Fat, but Not Protein or Carbohydrate, Regulates Energy Intake and Causes Adiposity in Mice. *Cell Metabolism*. 2018;28:415 - 431.e4. doi:10.1016/j.cmet.2018.06.010.
180. Hatori M, Vollmers C, Zarrinpar A, DiTacchio L, Bushong EA, Gill S, *et al*. Time-restricted feeding without reducing caloric intake prevents metabolic diseases in mice fed a high-fat diet. *Cell Metabolism*. 2012;15:848–60. doi:10.1016/j.cmet.2012.04.019.
181. Park H, Kim M, Kwon GT, Lim DY, Yu R, Sung M-K, *et al*. A high-fat diet increases angiogenesis, solid tumor growth, and lung metastasis of CT26 colon cancer cells in obesity-resistant BALB/c mice. *Mol Carcinog*. 2012;51:869–80. doi:10.1002/mc.20856.
182. El-Aziz R, Naguib M, Rashed L. Spleen size in patients with metabolic syndrome and its relation to metabolic and inflammatory parameters. *Egypt J Intern Med*. 2018;30:78. doi:10.4103/ejim.ejim_86_17.
183. Strandberg L, Verdrengh M, Enge M, Andersson N, Amu S, Onnheim K, *et al*. Mice chronically fed high-fat diet have increased mortality and disturbed immune response in sepsis. *PLoS One*. 2009;4:e7605. doi:10.1371/journal.pone.0007605.
184. Glastras SJ, Chen H, Teh R, McGrath RT, Chen J, Pollock CA, *et al*. Mouse Models of Diabetes, Obesity and Related Kidney Disease. *PLoS One*. 2016;11:e0162131. doi:10.1371/journal.pone.0162131.
185. Tsuboi N, Okabayashi Y, Shimizu A, Yokoo T. The Renal Pathology of Obesity. *Kidney Int Rep*. 2017;2:251–60. doi:10.1016/j.ekir.2017.01.007.
186. Soheilipour F, Jesmi F, Rahimzadeh N, Pishgahroudsari M, Almassinokian F, Mazaherinezhad A. Configuring a Better Estimation of Kidney Size in Obese Children and Adolescents. *Iran J Pediatr*. 2016;26:e4700. doi:10.5812/ijp.4700.
187. Eder K, Baffy N, Falus A, Fulop AK. The major inflammatory mediator interleukin-6 and obesity. *Inflamm Res*. 2009;58:727–36. doi:10.1007/s00011-009-0060-4.

188. Yeste D, Vendrell J, Tomasini R, Broch M, Gussinyé M, Megia A, Carrascosa A. Interleukin-6 in obese children and adolescents with and without glucose intolerance. *Diabetes Care*. 2007;30:1892–4. doi:10.2337/dc06-2289.
189. Akira S, Taga T, Kishimoto T. Interleukin-6 in biology and medicine. *Adv Immunol*. 1993;54:1–78.
190. Fenton JI, Nuñez NP, Yakar S, Perkins SN, Hord NG, Hursting SD. Diet-induced adiposity alters the serum profile of inflammation in C57BL/6N mice as measured by antibody array. *Diabetes Obes Metab*. 2009;11:343–54. doi:10.1111/j.1463-1326.2008.00974.x.
191. Trottier MD, Naaz A, Li Y, Fraker PJ. Enhancement of hematopoiesis and lymphopoiesis in diet-induced obese mice. *Proc Natl Acad Sci U S A*. 2012;109:7622–9. doi:10.1073/pnas.1205129109.
192. DeFuria J, Belkina AC, Jagannathan-Bogdan M, Snyder-Cappione J, Carr JD, Nersesova YR, *et al*. B cells promote inflammation in obesity and type 2 diabetes through regulation of T-cell function and an inflammatory cytokine profile. *Proc Natl Acad Sci U S A*. 2013;110:5133–8. doi:10.1073/pnas.1215840110.
193. Nishimura S, Manabe I, Takaki S, Nagasaki M, Otsu M, Yamashita H, *et al*. Adipose Natural Regulatory B Cells Negatively Control Adipose Tissue Inflammation. *Cell Metabolism*. 2013;18:759–66. doi:10.1016/j.cmet.2013.09.017.
194. Manicone AM, Gong K, Johnston LK, Giannandrea M. Diet-induced obesity alters myeloid cell populations in naïve and injured lung. *Respir Res*. 2016;17:24. doi:10.1186/s12931-016-0341-8.
195. Wu H, Perrard XD, Wang Q, Perrard JL, Polsani VR, Jones PH, *et al*. CD11c expression in adipose tissue and blood and its role in diet-induced obesity. *Arterioscler Thromb Vasc Biol*. 2010;30:186–92. doi:10.1161/ATVBAHA.109.198044.
196. Weisberg SP, McCann D, Desai M, Rosenbaum M, Leibel RL, Ferrante AW. Obesity is associated with macrophage accumulation in adipose tissue. *J. Clin. Invest*. 2003;112:1796–808. doi:10.1172/JCI19246.
197. Xu H, Barnes GT, Yang Q, Tan G, Yang D, Chou CJ, *et al*. Chronic inflammation in fat plays a crucial role in the development of obesity-related insulin resistance. *J. Clin. Invest*. 2003;112:1821–30. doi:10.1172/JCI19451.
198. Italiani P, Boraschi D. From Monocytes to M1/M2 Macrophages: Phenotypical vs. Functional Differentiation. *Front. Immunol*. 2014;5:514. doi:10.3389/fimmu.2014.00514.
199. Chylikova J, Dvorackova J, Tauber Z, Kamarad V. M1/M2 macrophage polarization in human obese adipose tissue. *Biomed Pap Med Fac Univ Palacky Olomouc Czech Repub*. 2018;162:79–82. doi:10.5507/bp.2018.015.
200. Lee J. Adipose tissue macrophages in the development of obesity-induced inflammation, insulin resistance and type 2 diabetes. *Arch Pharm Res*. 2013;36:208–22. doi:10.1007/s12272-013-0023-8.
201. Talukdar S, Oh DY, Bandyopadhyay G, Li D, Xu J, McNelis J, *et al*. Neutrophils mediate insulin resistance in mice fed a high-fat diet through secreted elastase. *Nat Med*. 2012;18:1407–12. doi:10.1038/nm.2885.
202. Mraz M, Haluzik M. The role of adipose tissue immune cells in obesity and low-grade inflammation. *J Endocrinol*. 2014;222:R113–27. doi:10.1530/JOE-14-0283.
203. Elgazar-Carmon V, Rudich A, Hadad N, Levy R. Neutrophils transiently infiltrate intra-abdominal fat early in the course of high-fat feeding. *J Lipid Res*. 2008;49:1894–903. doi:10.1194/jlr.M800132-JLR200.
204. Ip BC, Hogan AE, Nikolajczyk BS. Lymphocyte roles in metabolic dysfunction: Of men and mice. *Trends Endocrinol Metab*. 2015;26:91–100. doi:10.1016/j.tem.2014.12.001.
205. Wu H, Ghosh S, Perrard XD, Feng L, Garcia GE, Perrard JL, *et al*. T-cell accumulation and regulated on activation, normal T cell expressed and secreted upregulation in adipose tissue in obesity. *Circulation*. 2007;115:1029–38. doi:10.1161/CIRCULATIONAHA.106.638379.

206. Strissel KJ, DeFuria J, Shaul ME, Bennett G, Greenberg AS, Obin MS. T-cell recruitment and Th1 polarization in adipose tissue during diet-induced obesity in C57BL/6 mice. *Obesity (Silver Spring)*. 2010;18:1918–25. doi:10.1038/oby.2010.1.
207. Duffaut C, Zakaroff-Girard A, Bourlier V, Decaunes P, Maumus M, Chiotasso P, *et al.* Interplay between human adipocytes and T lymphocytes in obesity: CCL20 as an adipochemokine and T lymphocytes as lipogenic modulators. *Arterioscler Thromb Vasc Biol*. 2009;29:1608–14. doi:10.1161/ATVBAHA.109.192583.
208. Huh JY, Park YJ, Ham M, Kim JB. Crosstalk between adipocytes and immune cells in adipose tissue inflammation and metabolic dysregulation in obesity. *Mol Cells*. 2014;37:365–71. doi:10.14348/molcells.2014.0074.
209. Nishimura S, Manabe I, Nagasaki M, Eto K, Yamashita H, Ohsugi M, *et al.* CD8⁺ effector T cells contribute to macrophage recruitment and adipose tissue inflammation in obesity. *Nat Med*. 2009;15:914–20. doi:10.1038/nm.1964.
210. Ramírez-Orozco RE, Franco Robles E, Pérez Vázquez V, Ramírez Emiliano J, Hernández Luna MA, López Briones S. Diet-induced obese mice exhibit altered immune responses to early Salmonella Typhimurium oral infection. *J Microbiol*. 2018;56:673–82. doi:10.1007/s12275-018-8083-6.
211. Lee B-C, Kim M-S, Pae M, Yamamoto Y, Eberlé D, Shimada T, *et al.* Adipose Natural Killer Cells Regulate Adipose Tissue Macrophages to Promote Insulin Resistance in Obesity. *Cell Metabolism*. 2016;23:685–98. doi:10.1016/j.cmet.2016.03.002.
212. Theurich S, Tsaousidou E, Hanssen R, Lempradl AM, Mauer J, Timper K, *et al.* IL-6/Stat3-Dependent Induction of a Distinct, Obesity-Associated NK Cell Subpopulation Deteriorates Energy and Glucose Homeostasis. *Cell Metabolism*. 2017;26:171-184.e6. doi:10.1016/j.cmet.2017.05.018.
213. Elpek KG, Rubinstein MP, Bellemare-Pelletier A, Goldrath AW, Turley SJ. Mature natural killer cells with phenotypic and functional alterations accumulate upon sustained stimulation with IL-15/IL-15 α complexes. *Proc Natl Acad Sci U S A*. 2010;107:21647–52. doi:10.1073/pnas.1012128107.
214. Hayakawa Y, Smyth MJ. CD27 dissects mature NK cells into two subsets with distinct responsiveness and migratory capacity. *J Immunol*. 2006;176:1517–24.
215. White MJ, Beaver CM, Goodier MR, Bottomley C, Nielsen CM, Wolf A-SFM, *et al.* Calorie Restriction Attenuates Terminal Differentiation of Immune Cells. *Front Immunol*. 2016;7:667. doi:10.3389/fimmu.2016.00667.
216. Clinthorne JF, Beli E, Duriancik DM, Gardner EM. NK cell maturation and function in C57BL/6 mice are altered by caloric restriction. *J Immunol*. 2013;190:712–22. doi:10.4049/jimmunol.1201837.
217. Müller-Durovic B, Lanna A, Covre LP, Mills RS, Henson SM, Akbar AN. Killer Cell Lectin-like Receptor G1 Inhibits NK Cell Function through Activation of Adenosine 5'-Monophosphate-Activated Protein Kinase. *J Immunol*. 2016;197:2891–9. doi:10.4049/jimmunol.1600590.
218. Robbins SH, Nguyen KB, Takahashi N, Mikayama T, Biron CA, Brossay L. Cutting edge: Inhibitory functions of the killer cell lectin-like receptor G1 molecule during the activation of mouse NK cells. *J Immunol*. 2002;168:2585–9. doi:10.4049/jimmunol.168.6.2585.
219. Di Santo JP. Natural killer cell developmental pathways: A question of balance. *Annu Rev Immunol*. 2006;24:257–86. doi:10.1146/annurev.immunol.24.021605.090700.
220. Nuttall FQ. Body Mass Index: Obesity, BMI, and Health: A Critical Review. *Nutr Today*. 2015;50:117–28. doi:10.1097/NT.0000000000000092.
221. Pietrobelli A, Rubiano F, St-Onge M-P, Heymsfield SB. New bioimpedance analysis system: Improved phenotyping with whole-body analysis. *Eur J Clin Nutr*. 2004;58:1479–84. doi:10.1038/sj.ejcn.1601993.
222. Gill T, Chittleborough C, Taylor A, Ruffin R, Wilson D, Phillips P. Body mass index, waist hip ratio, and waist circumference: Which measure to classify obesity? *Sozial- und Prventivmedizin/Social and Preventive Medicine*. 2003;48:191–200. doi:10.1007/s00038-003-2055-1.

223. Suchanek P, Kralova Lesna I, Mengerova O, Mrazkova J, Lanska V, Stavek P. Which index best correlates with body fat mass: BAI, BMI, waist or WHR? *Neuro Endocrinol Lett.* 2012;33 Suppl 2:78–82.
224. Koch S, Larbi A, Ozcelik D, Solana R, Gouttefangeas C, Attig S, *et al.* Cytomegalovirus infection: A driving force in human T cell immunosenescence. *Ann N Y Acad Sci.* 2007;1114:23–35. doi:10.1196/annals.1396.043.
225. Frasca D, Diaz A, Romero M, Landin AM, Blomberg BB. Cytomegalovirus (CMV) seropositivity decreases B cell responses to the influenza vaccine. *Vaccine.* 2015;33:1433–9. doi:10.1016/j.vaccine.2015.01.071.
226. Campos C, López N, Pera A, Gordillo JJ, Hassounch F, Tarazona R, Solana R. Expression of NKp30, NKp46 and DNAM-1 activating receptors on resting and IL-2 activated NK cells from healthy donors according to CMV-serostatus and age. *Biogerontology.* 2015;16:671–83. doi:10.1007/s10522-015-9581-0.
227. Zuhair M, Smit GSA, Wallis G, Jabbar F, Smith C, Devleeschauwer B, Griffiths P. Estimation of the worldwide seroprevalence of cytomegalovirus: A systematic review and meta-analysis. *Rev Med Virol.* 2019;29:e2034. doi:10.1002/rmv.2034.
228. Lachmann R, Loenenbach A, Waterboer T, Brenner N, Pawlita M, Michel A, *et al.* Cytomegalovirus (CMV) seroprevalence in the adult population of Germany. *PLoS One.* 2018;13:e0200267. doi:10.1371/journal.pone.0200267.
229. Curran EM, Berghaus LJ, Verneti NJ, Saporita AJ, Lubahn DB, Estes DM. Natural killer cells express estrogen receptor-alpha and estrogen receptor-beta and can respond to estrogen via a non-estrogen receptor-alpha-mediated pathway. *Cell Immunol.* 2001;214:12–20. doi:10.1006/cimm.2002.1886.
230. Stopińska-Gluszak U, Waligóra J, Grzela T, Gluszak M, Józwiak J, Radomski D, *et al.* Effect of estrogen/progesterone hormone replacement therapy on natural killer cell cytotoxicity and immunoregulatory cytokine release by peripheral blood mononuclear cells of postmenopausal women. *J Reprod Immunol.* 2006;69:65–75. doi:10.1016/j.jri.2005.07.006.
231. Picon-Ruiz M, Morata-Tarifa C, Valle-Goffin JJ, Friedman ER, Slingerland JM. Obesity and adverse breast cancer risk and outcome: Mechanistic insights and strategies for intervention. *CA Cancer J Clin.* 2017;67:378–97. doi:10.3322/caac.21405.
232. Schairer C, Fuhrman BJ, Boyd-Morin J, Genkinger JM, Gail MH, Hoover RN, Ziegler RG. Quantifying the Role of Circulating Unconjugated Estradiol in Mediating the Body Mass Index-Breast Cancer Association. *Cancer Epidemiol Biomarkers Prev.* 2016;25:105–13. doi:10.1158/1055-9965.EPI-15-0687.
233. Brown KA, Simpson ER. Obesity and breast cancer: Mechanisms and therapeutic implications. *Front Biosci (Elite Ed).* 2012;4:2515–24.
234. Bhardwaj P, Au CC, Benito-Martin A, Ladumor H, Oshchepkova S, Moges R, Brown KA. Estrogens and breast cancer: Mechanisms involved in obesity-related development, growth and progression. *J Steroid Biochem Mol Biol.* 2019;189:161–70. doi:10.1016/j.jsbmb.2019.03.002.
235. Miao H, Verkooyen HM, Chia K-S, Bouchardy C, Pukkala E, Larønningen S, *et al.* Incidence and outcome of male breast cancer: An international population-based study. *J Clin Oncol.* 2011;29:4381–6. doi:10.1200/JCO.2011.36.8902.
236. Kim S-E, Paik HY, Yoon H, Lee JE, Kim N, Sung M-K. Sex- and gender-specific disparities in colorectal cancer risk. *World J Gastroenterol.* 2015;21:5167–75. doi:10.3748/wjg.v21.i17.5167.
237. Wu L, van Kaer L. Natural killer T cells in health and disease. *Front Biosci (Schol Ed).* 2011;3:236–51.
238. Nieman DC, Henson DA, Nehlsen-Cannarella SL, Ekkens M, Utter AC, Butterworth DE, Fagoaga OR. Influence of obesity on immune function. *J Am Diet Assoc.* 1999;99:294–9. doi:10.1016/S0002-8223(99)00077-2.

239. Lynch L, O'Shea D, Winter DC, Geoghegan J, Doherty DG, O'Farrelly C. Invariant NKT cells and CD1d(+) cells amass in human omentum and are depleted in patients with cancer and obesity. *Eur J Immunol.* 2009;39:1893–901. doi:10.1002/eji.200939349.
240. Lynch L, Nowak M, Varghese B, Clark J, Hogan AE, Toxavidis V, *et al.* Adipose tissue invariant NKT cells protect against diet-induced obesity and metabolic disorder through regulatory cytokine production. *Immunity.* 2012;37:574–87. doi:10.1016/j.immuni.2012.06.016.
241. Tanaka S, Isoda F, Ishihara Y, Kimura M, Yamakawa T. T lymphopaenia in relation to body mass index and TNF-alpha in human obesity: Adequate weight reduction can be corrective. *Clin Endocrinol (Oxf).* 2001;54:347–54.
242. O'Rourke RW, Kay T, Scholz MH, Diggs B, Jobe BA, Lewinsohn DM, Bakke AC. Alterations in T-cell subset frequency in peripheral blood in obesity. *Obes Surg.* 2005;15:1463–8. doi:10.1381/096089205774859308.
243. Ilavská S, Horváthová M, Szabová M, Nemessányi T, Jahnová E, Tulinská J, *et al.* Association between the human immune response and body mass index. *Hum Immunol.* 2012;73:480–5. doi:10.1016/j.humimm.2012.02.023.
244. Lynch LA, O'Connell JM, Kwasnik AK, Cawood TJ, O'Farrelly C, O'Shea DB. Are natural killer cells protecting the metabolically healthy obese patient? *Obesity (Silver Spring).* 2009;17:601–5. doi:10.1038/oby.2008.565.
245. Nagler A, Lanier LL, Cwirla S, Phillips JH. Comparative studies of human FcRIII-positive and negative natural killer cells. *J Immunol.* 1989;143:3183–91.
246. Cossarizza A, Chang H-D, Radbruch A, Akdis M, Andrä I, Annunziato F, *et al.* Guidelines for the use of flow cytometry and cell sorting in immunological studies. *Eur J Immunol.* 2017;47:1584–797. doi:10.1002/eji.201646632.
247. Pesce S, Greppi M, Tabellini G, Rampinelli F, Parolini S, Olive D, *et al.* Identification of a subset of human natural killer cells expressing high levels of programmed death 1: A phenotypic and functional characterization. *J Allergy Clin Immunol.* 2017;139:335–346.e3. doi:10.1016/j.jaci.2016.04.025.
248. Hsu KC, Liu X-R, Selvakumar A, Mickelson E, O'Reilly RJ, Dupont B. Killer Ig-like receptor haplotype analysis by gene content: Evidence for genomic diversity with a minimum of six basic framework haplotypes, each with multiple subsets. *J Immunol.* 2002;169:5118–29. doi:10.4049/jimmunol.169.9.5118.
249. Ghanadi K, Shayanrad B, Ahmadi SAY, Shahsavari F, Eliasy H. Colorectal cancer and the KIR genes in the human genome: A meta-analysis. *Genom Data.* 2016;10:118–26. doi:10.1016/j.gdata.2016.10.010.
250. Gallez-Hawkins GM, Franck AE, Li X, Thao L, Oki A, Gendzekhadze K, *et al.* Expression of Activating KIR2DS2 and KIR2DS4 Genes after Hematopoietic Cell Transplantation: Relevance to Cytomegalovirus Infection. *Biol Blood Marrow Transplant.* 2011;17:1662–72. doi:10.1016/j.bbmt.2011.04.008.
251. Shoaie-Hassani A, Behfar M, Mortazavi-Tabatabaei SA, Ai J, Mohseni R, Hamidieh AA. Natural Killer Cells from the Subcutaneous Adipose Tissue Underexpress the NKp30 and NKp44 in Obese Persons and Are Less Active against Major Histocompatibility Complex Class I Non-Expressing Neoplastic Cells. *Front. Immunol.* 2017;8:1486. doi:10.3389/fimmu.2017.01486.
252. Saez-Borderias A, Romo N, Magri G, Guma M, Angulo A, Lopez-Botet M. IL-12-Dependent Inducible Expression of the CD94/NKG2A Inhibitory Receptor Regulates CD94/NKG2C+ NK Cell Function. *J Immunol.* 2009;182:829–36. doi:10.4049/jimmunol.182.2.829.
253. Aldemir H, Prod'homme V, Dumaurier M-J, Retiere C, Poupon G, Cazareth J, *et al.* Cutting edge: Lectin-like transcript 1 is a ligand for the CD161 receptor. *J Immunol.* 2005;175:7791–5. doi:10.4049/jimmunol.175.12.7791.
254. Robertson MJ, Caligiuri MA, Manley TJ, Levine H, Ritz J. Human natural killer cell adhesion molecules. Differential expression after activation and participation in cytotoxicity. *J Immunol.* 1990;145:3194–201.

255. Agrawal S, Tripathi P, Naik S. Roles and mechanism of natural killer cells in clinical and experimental transplantation. *Expert Rev Clin Immunol.* 2008;4:79–91. doi:10.1586/1744666X.4.1.79.
256. Chauveau A, Aucher A, Eissmann P, Vivier E, Davis DM. Membrane nanotubes facilitate long-distance interactions between natural killer cells and target cells. *Proc Natl Acad Sci U S A.* 2010;107:5545–50. doi:10.1073/pnas.0910074107.
257. Frey M, Packianathan NB, Fehniger TA, Ross ME, Wang WC, Stewart CC, *et al.* Differential expression and function of L-selectin on CD56bright and CD56dim natural killer cell subsets. *J Immunol.* 1998;161:400–8.
258. Schmidt FM, Weschenfelder J, Sander C, Minkwitz J, Thormann J, Chittka T, *et al.* Inflammatory cytokines in general and central obesity and modulating effects of physical activity. *PLoS One.* 2015;10:e0121971. doi:10.1371/journal.pone.0121971.
259. Dixon JB, Hayden MJ, Lambert GW, Dawood T, Anderson ML, Dixon ME, O'Brien PE. Raised CRP levels in obese patients: Symptoms of depression have an independent positive association. *Obesity (Silver Spring).* 2008;16:2010–5. doi:10.1038/oby.2008.271.
260. Visser M, Bouter LM, McQuillan GM, Wener MH, Harris TB. Elevated C-reactive protein levels in overweight and obese adults. *JAMA.* 1999;282:2131–5.
261. Blake GJ, Ridker PM. Inflammatory bio-markers and cardiovascular risk prediction. *J Intern Med.* 2002;252:283–94.
262. Guilleminault C, Kirisoglu C, Ohayon MM. C-reactive protein and sleep-disordered breathing. *Sleep.* 2004;27:1507–11. doi:10.1093/sleep/27.8.1507.
263. Anty R, Bekri S, Luciani N, Saint-Paul M-C, Dahman M, Iannelli A, *et al.* The inflammatory C-reactive protein is increased in both liver and adipose tissue in severely obese patients independently from metabolic syndrome, Type 2 diabetes, and NASH. *Am J Gastroenterol.* 2006;101:1824–33. doi:10.1111/j.1572-0241.2006.00724.x.
264. Cottam DR, Schaefer PA, Shaftan GW, Angus LDG. Dysfunctional immune-privilege in morbid obesity: Implications and effect of gastric bypass surgery. *Obes Surg.* 2003;13:49–57. doi:10.1381/096089203321136584.
265. Silva A, Andrews DM, Brooks AG, Smyth MJ, Hayakawa Y. Application of CD27 as a marker for distinguishing human NK cell subsets. *International Immunology.* 2008;20:625–30. doi:10.1093/intimm/dxn022.
266. Vossen MTM, Matmati M, Hertoghs KML, Baars PA, Gent M-R, Leclercq G, *et al.* CD27 defines phenotypically and functionally different human NK cell subsets. *J Immunol.* 2008;180:3739–45.
267. Nielsen CM, White MJ, Goodier MR, Riley EM. Functional Significance of CD57 Expression on Human NK Cells and Relevance to Disease. *Front. Immunol.* 2013;4:422. doi:10.3389/fimmu.2013.00422.
268. Sivori S, Parolini S, Falco M, Marcenaro E, Biassoni R, Bottino C, *et al.* 2B4 functions as a co-receptor in human NK cell activation. *Eur J Immunol.* 2000;30:787–93. doi:10.1002/1521-4141(200003)30:3<787::AID-IMMU787>3.0.CO;2-I.
269. Assarsson E, Kambayashi T, Persson CM, Chambers BJ, Ljunggren H-G. 2B4/CD48-mediated regulation of lymphocyte activation and function. *J Immunol.* 2005;175:2045–9. doi:10.4049/jimmunol.175.4.2045.
270. Mathew SO, Rao KK, Kim JR, Bambard ND, Mathew PA. Functional role of human NK cell receptor 2B4 (CD244) isoforms. *Eur J Immunol.* 2009;39:1632–41. doi:10.1002/eji.200838733.
271. Sandusky MM, Messmer B, Watzl C. Regulation of 2B4 (CD244)-mediated NK cell activation by ligand-induced receptor modulation. *Eur J Immunol.* 2006;36:3268–76. doi:10.1002/eji.200636146.
272. Watzl C, Stebbins CC, Long EO. NK cell inhibitory receptors prevent tyrosine phosphorylation of the activation receptor 2B4 (CD244). *J Immunol.* 2000;165:3545–8. doi:10.4049/jimmunol.165.7.3545.

273. Welte S, Kuttruff S, Waldhauer I, Steinle A. Mutual activation of natural killer cells and monocytes mediated by NKp80-AICL interaction. *Nat Immunol.* 2006;7:1334–42. doi:10.1038/ni1402.
274. Freud AG, Keller KA, Scoville SD, Mundy-Bosse BL, Cheng S, Youssef Y, *et al.* NKp80 Defines a Critical Step during Human Natural Killer Cell Development. *Cell Rep.* 2016;16:379–91. doi:10.1016/j.celrep.2016.05.095.
275. Wang F, Hou H, Wu S, Tang Q, Liu W, Huang M, *et al.* TIGIT expression levels on human NK cells correlate with functional heterogeneity among healthy individuals. *Eur J Immunol.* 2015;45:2886–97. doi:10.1002/eji.201545480.
276. Liu Y, Cheng Y, Xu Y, Wang Z, Du X, Li C, *et al.* Increased expression of programmed cell death protein 1 on NK cells inhibits NK-cell-mediated anti-tumor function and indicates poor prognosis in digestive cancers. *Oncogene.* 2017;36:6143–53. doi:10.1038/onc.2017.209.
277. Kared H, Martelli S, Tan SW, Simoni Y, Chong ML, Yap SH, *et al.* Adaptive NKG2C+CD57+ Natural Killer Cell and Tim-3 Expression During Viral Infections. *Front. Immunol.* 2018;9:686. doi:10.3389/fimmu.2018.00686.
278. Jin J, Ahn Y-O, Kim TM, Keam B, Kim D-W, Heo DS. The CD56bright CD62L+ NKG2A+ immature cell subset is dominantly expanded in human cytokine-induced memory-like NK cells; 2018.
279. Boehm U, Klamp T, Groot M, Howard JC. Cellular responses to interferon-gamma. *Annu Rev Immunol.* 1997;15:749–95. doi:10.1146/annurev.immunol.15.1.749.
280. Lumeng CN, Bodzin JL, Saltiel AR. Obesity induces a phenotypic switch in adipose tissue macrophage polarization. *J. Clin. Invest.* 2007;117:175–84. doi:10.1172/JCI29881.
281. Hüber CM, Doisne J-M, Colucci F. IL-12/15/18-preactivated NK cells suppress GvHD in a mouse model of mismatched hematopoietic cell transplantation. *Eur J Immunol.* 2015;45:1727–35. doi:10.1002/eji.201445200.
282. Chaix J, Tessmer MS, Hoebe K, Fuseri N, Ryffel B, Dalod M, *et al.* Cutting Edge: Priming of NK Cells by IL-18. *J Immunol.* 2008;181:1627–31. doi:10.4049/jimmunol.181.3.1627.
283. Huebner L, Engeli S, Wrann CD, Goudeva L, Laue T, Kielstein H. Human NK cell subset functions are differentially affected by adipokines. *PLoS One.* 2013;8:e75703. doi:10.1371/journal.pone.0075703.
284. Simonetta F, Pradier A, Roosnek E. T-bet and Eomesodermin in NK Cell Development, Maturation, and Function. *Frontiers in Immunology.* 2016;7:241. doi:10.3389/fimmu.2016.00241.
285. Penack O, Gentilini C, Fischer L, Asemissen AM, Scheibenbogen C, Thiel E, Uharek L. CD56dimCD16neg cells are responsible for natural cytotoxicity against tumor targets. *Leukemia.* 2005;19:835–40. doi:10.1038/sj.leu.2403704.
286. Cohnen A, Chiang SC, Stojanovic A, Schmidt H, Claus M, Saftig P, *et al.* Surface CD107a/LAMP-1 protects natural killer cells from degranulation-associated damage. *Blood.* 2013;122:1411–8. doi:10.1182/blood-2012-07-441832.
287. Krzewski K, Gil-Krzewska A, Nguyen V, Peruzzi G, Coligan JE. LAMP1/CD107a is required for efficient perforin delivery to lytic granules and NK-cell cytotoxicity. *Blood.* 2013;121:4672–83. doi:10.1182/blood-2012-08-453738.
288. Jänicke RU. MCF-7 breast carcinoma cells do not express caspase-3. *Breast Cancer Res Treat.* 2009;117:219–21. doi:10.1007/s10549-008-0217-9.
289. Jänicke RU, Sprengart ML, Wati MR, Porter AG. Caspase-3 is required for DNA fragmentation and morphological changes associated with apoptosis. *J Biol Chem.* 1998;273:9357–60. doi:10.1074/jbc.273.16.9357.
290. Porter AG, Jänicke RU. Emerging roles of caspase-3 in apoptosis. *Cell Death Differ.* 1999;6:99–104. doi:10.1038/sj.cdd.4400476.
291. Elmore S. Apoptosis: A review of programmed cell death. *Toxicol Pathol.* 2007;35:495–516. doi:10.1080/01926230701320337.

-
292. Danforth DN, Zhu Y. Conversion of Fas-resistant to Fas-sensitive MCF-7 breast cancer cells by the synergistic interaction of interferon-gamma and all-trans retinoic acid. *Breast Cancer Res Treat.* 2005;94:81–91. doi:10.1007/s10549-005-7491-6.
293. Zhang Y, Zhang B. TRAIL resistance of breast cancer cells is associated with constitutive endocytosis of death receptors 4 and 5. *Mol Cancer Res.* 2008;6:1861–71. doi:10.1158/1541-7786.MCR-08-0313.
294. Lieberman J. Granzyme A activates another way to die. *Immunol Rev.* 2010;235:93–104. doi:10.1111/j.0105-2896.2010.00902.x.
295. Hamilton G, Reiner A, Teleky B, Roth E, Kolb R, Spona J, Jakesz R. Natural killer cell activities of patients with breast cancer against different target cells. *J Cancer Res Clin Oncol.* 1988;114:191–6. doi:10.1007/BF00417836.
296. North J, Bakhsh I, Marden C, Pittman H, Addison E, Navarrete C, *et al.* Tumor-primed human natural killer cells lyse NK-resistant tumor targets: Evidence of a two-stage process in resting NK cell activation. *J Immunol.* 2007;178:85–94. doi:10.4049/jimmunol.178.1.85.
297. Taouk G, Hussein O, Zekak M, Abouelghar A, Al-Sarraj Y, Abdelalim EM, Karam M. CD56 expression in breast cancer induces sensitivity to natural killer-mediated cytotoxicity by enhancing the formation of cytotoxic immunological synapse. *Sci Rep.* 2019;9:8756. doi:10.1038/s41598-019-45377-8.
298. Lamas B, Goncalves-Mendes N, Nachat-Kappes R, Rossary A, Caldefie-Chezet F, Vasson M-P, Farges M-C. Leptin modulates dose-dependently the metabolic and cytolytic activities of NK-92 cells. *J Cell Physiol.* 2013;228:1202–9. doi:10.1002/jcp.24273.
299. Sudworth A, Dai K-Z, Vaage JT, Kveberg L. Degranulation Response in Cytotoxic Rat Lymphocytes Measured with a Novel CD107a Antibody. *Front. Immunol.* 2016;7:572. doi:10.3389/fimmu.2016.00572.
300. Yazdi FT, Clee SM, Meyre D. Obesity genetics in mouse and human: Back and forth, and back again. *PeerJ.* 2015;3:e856. doi:10.7717/peerj.856.
301. Spielmann J, Bähr I, Naujoks W, Kielstein H, Quandt D. Natürliche Killerzellen, Adipositas & Tumorgenese. *Adipositas - Ursachen, Folgeerkrankungen, Therapie.* 2019;13:36–42. doi:10.1055/a-0801-4014.

Abbreviations

7-AAD	7-amino-actinomycin D
<i>Ad lib.</i>	<i>Ad libitum</i>
ADCC	Antibody-dependent cellular cytotoxicity
ANOVA	Analysis of variance
AO	Acridine orange
APC	Allophycocyanin
AT	Adipose tissue
ATCC	American Type Culture Collection
BAT	Brown adipose tissue
BC	Buffy coat
BIA	Bioelectrical impedance analysis
Blimp-1	B lymphocyte-induced maturation protein-1
BMI	Body mass index
BV	Brilliant Violet
CD	Cluster of differentiation
CI	Cell index
CMV	Cytomegalovirus
CRC	Colorectal cancer
CRP	C-reactive protein
cRPMI	Complete RPMI
Ctrl	Control
DIO	Diet-induced obesity
DKFZ	German Cancer Research Center
DMSO	Dimethyl sulfoxide
DNA	Deoxyribonucleic acid
DNAM	DNAX accessory molecule
DPBS	Dulbecco's Phosphate Buffered Saline
e.g.	exempli gratia (for example)
E:T	Effector-to-target
EDTA	Ethylenediaminetetraacetic acid
ELISA	Enzyme-linked immunosorbent assay
EOMES	Eomesodermin
<i>et al.</i>	et alii (and others)
FACS	Fluorescence activated cell sorting
Fas-L	Fas ligand
FBS	Fetal bovine serum
Fc	Fragment crystallizable
FITC	Fluorescein isothiocyanate
FMO	Fluorescence minus one
FSC	Forward scatter
FSC-A	Forward scatter-area
FSC-H	Forward scatter-height
GM-CSF	Granulocyte-macrophage colony-stimulating factor
HCMV	Human cytomegalovirus
HFD	High-fat diet
HIIT	High intensity interval training
hIL	Human interleukin
HLA	Human leukocyte antigen
i.e.	id est (that is)
IFN- γ	Interferon- γ
Ig	Immunoglobulin
IL	Interleukin
ILC	Innate lymphoid cell
ITAM	Immunoreceptor tyrosine-based activation motif
ITIM	Immunoreceptor tyrosine-based inhibitory motif

kg	Kilogram
KIR	Killer cell immunoglobulin-like receptor
Klr	Killer cell lectin-like
KLRG1	Killer cell lectin-like receptor G1
LAMP	Lysosomal-associated membrane protein
LCR	Leukocyte receptor complex
LFA	Lymphocyte function-associated antigen
LLT	Lectin-like transcript
m	Meter
M.Sc.	Master of Science
MACS	Magnetic activated cell sorting
MFI	Median fluorescence intensity
MHC	Major histocompatibility complex
MICA and MICB	MHC-I chain related proteins A and B
mIL	Murine interleukin
min	Minute
MLU	Martin-Luther-University Halle-Wittenberg
mM	MilliMolar
mRNA	Messenger ribonucleic acid
NCAM	Neural cell adhesion molecule
NCD	Noncommunicable disease
NCI	Normalized cell index
NCR	Natural cytotoxicity receptor
NFD	Normal-fat diet
NK	Natural killer
NKG2	Natural killer group two
NKT	Natural killer T
PBMC	Peripheral blood mononuclear cell
PD-1	Programmed cell death receptor-1
PE	Phycoerythrin
pg/ml	Picogram per milliliter
phu	Primary human
PI	Propidium iodide
PMA	Phorbol-12-myristate 13-acetate
qRT-PCR	Quantitative reverse transcription polymerase chain reaction
RBC	Red blood cell
REA	Retinoic acid
Restr.	Restrictive
RPMI	Roswell Park Memorial Institute
RT	Room temperature
RTCA	Real-time cell analysis
SAT	Subcutaneous adipose tissue
SEM	Standard error of the mean
Siglec	Sialic acid binding immunoglobulin-like lectin
SSC	Side scatter
T-bet	T-cell associated transcription factor
Th	T helper
TIGIT	T-cell immunoreceptor with Ig and ITIM domains
TNF	Tumor necrosis factor
TRAIL	Tumor necrosis factor-related apoptosis-inducing ligand
v/v	Volume per volume
VAT	Visceral adipose tissue
w/o	without
WAT	White adipose tissue
WHO	World Health Organization

Lebenslauf

Persönliche Daten

Name Wiebke Naujoks
 Geburt: 15.10.1985 in Magdeburg
 Kontakt: naujow@posteo.de

Beruflicher Werdegang

08/2019 – 02/2020 Berufliche Qualifizierung und Weiterbildung im Life Science Management bei der ATV GmbH, Leipzig

01/2016 – 04/2019 Wissenschaftliche Mitarbeiterin an der Medizinischen Fakultät der Martin-Luther-Universität Halle-Wittenberg; Institut für Anatomie und Zellbiologie

2014 – 2015 Masterarbeit am Fraunhofer-Institut für Zelltherapie und Immunologie Leipzig

04/2011 – 08/2011 Projektassistenz am Europäischen Laboratorium für Molekularbiologie (EMBL) Grenoble

01/2011 – 04/2011 Projektassistenz am Kavli Institute for Systems Neuroscience and Centre for the Biology of Memory, NTNU Trondheim

08/2008 Projektassistenz an der Otto-von-Guericke Universität Magdeburg; Institut für Kognitionsbiologie

2005 – 2008 Berufliche Ausbildung zur Biologielaborantin am IDT Biologika GmbH, Dessau-Rosslau

Schulische & Akademische Ausbildung

01/2016 – 07/2020 Promotion an der Medizinischen Fakultät der Martin-Luther-Universität Halle-Wittenberg; Institut für Anatomie and Zellbiologie

2012 – 2015 Master of Science in Biological Sciences Major Disease Biology an der Universität Konstanz

2008 – 2012 Bachelor of Science in Biologie an der Technischen Universität Dresden

08/2010 – 12/2010 Auslandssemester an der Norwegian University of Science and Technology Trondheim

1996 – 2005 Abitur am Europagymnasium Gommern

LEIPZIG, DEN

.....

WIEBKE NAUJOKS

Publikationen

Spielmann, Julia; Bähr, Ina; **Naujoks, Wiebke**; Kielstein, Heike; Quandt, Dagmar (2019): Natürliche Killerzellen, Adipositas & Tumorgenese. In: Adipositas - Ursachen, Folgeerkrankungen, Therapie 13 (01), S. 36–42. DOI: 10.1055/a-0801-4014.

Naujoks, W.; Hauffe, A.; Spielmann, J.; Bähr, I.; Quandt, D.; Harth, J.; Kielstein, H. (2018): Influence of bodyweight on receptor expression and cytotoxicity of primary human natural killer cells against obesity-associated cancers. In: Ernährung 2018 – Ernährung ist Therapie und Prävention. Kassel: Georg Thieme Verlag KG (Aktuelle Ernährungsmedizin).

Konferenzen und Konferenzbeiträge

5th European Congress of Immunology (ECI) Amsterdam (2018, Poster)

W. Naujoks, A. Hauffe, J. Spielmann, I. Bähr, D. Quandt, J. Harth, H. Kielstein – Receptor expression and cytotoxicity of primary human NK cells is impaired in obesity

Ernährung 2018 Kongress Kassel (2018, Poster)

W. Naujoks, A. Hauffe, J. Spielmann, I. Bähr, D. Quandt, J. Harth, H. Kielstein – Influence of bodyweight on receptor expression and cytotoxicity of primary human natural killer cells against obesity-associated cancers

14th International Symposium on the Symposium "Tumor Immunology meets Oncology XIV Halle (Saale) (2018, Poster)

W. Naujoks, A. Hauffe, J. Spielmann, I. Bähr, D. Quandt, J. Harth, H. Kielstein – Influence of bodyweight on receptor expression and cytotoxicity of primary human NK cells against obesity-associated cancers

7th Translational Immunology School (TIS) Potsdam-Schwielowsee (2018)

27. Bilateral Symposium Poznan-Halle (2017, Poster)

W. Naujoks, A. Hauffe, J. Spielmann, I. Bähr, D. Quandt, J. Harth, H. Kielstein – Influence of bodyweight on cytotoxicity of primary human natural killer cells against obesity-associated cancers

XX. Lipid Meeting Leipzig (2017)

A. Hauffe, **W. Naujoks**, I. Bähr, J. Spielmann, H. Kielstein – Influence of bodyweight on cytotoxicity of primary human Natural Killer (NK) cells against obesity-associated cancers

4. Kongress für Doktorandinnen und Doktoranden Halle (Saale) (2017, Poster)

W. Naujoks, A. Hauffe, J. Spielmann, I. Bähr, D. Quandt, J. Harth, H. Kielstein – Einfluss des Körpergewichts auf die Rezeptorexpression und Zytotoxizität primärer humaner Natürlicher Killerzellen gegen humane Kolon- und Mammakarzinomzellen

NK Cell Symposium Düsseldorf (März 2017, Poster)

W. Naujoks, J. Spielmann, D. Quandt, M. Allweyer, M. Emde, H. Kielstein, I. Bähr – Influence of high fat feeding on NK cells in mice

1. Science Retreat (2016, Vortrag)

W. Naujoks, J. Spielmann, I. Bähr, H. Kielstein – iCELLigence: Zytotoxizitätsassays in Echtzeit

Danksagung

An dieser Stelle möchte ich mich ganz herzlich bei all denjenigen bedanken, die mich während der Durchführung und Anfertigung dieser Dissertation begleitet, motiviert und unterstützt haben.

Ich bedanke mich herzlichst bei Frau Prof.in Dr. Heike Kielstein für die Möglichkeit meine Dissertation in ihrer Arbeitsgruppe im Institut für Anatomie und Zellbiologie anfertigen zu können und für die Bereitstellung dieses spannenden Themas. Vielen Dank für die stete Unterstützung, auch bei der Realisierung von Kongressteilnahmen und Fortbildungen sowie natürlich für die Begutachtung meiner Dissertation.

Vielen Dank an Herrn Prof. Dr. Stefan Hüttelmaier für seine Unterstützung und die Übernahme des Erstgutachtens dieser Dissertation.

Weiterhin möchte ich mich bei Herrn Prof. Dr. Roland Jacobs von der Medizinischen Hochschule Hannover für die Übernahme des externen Gutachtens der vorliegenden Arbeit bedanken.

Besonderer Dank gilt meinen Betreuerinnen Frau Dr. Julia Spielmann und Frau Dr. Ina Bähr für ihre großartige Unterstützung, die spannenden Projekte, ihren steten Optimismus, ihr Vertrauen, die wertschätzende Atmosphäre, die hilfreichen fachlichen Anregungen und konstruktiven Kritiken, für das Korrekturlesen dieser Arbeit und die vielen leckeren Kaffees und Leckereien und die ein oder andere fröhliche Feier zusammen.

Ein ebenso besonderes Dankeschön möchte ich an Frau PD Dr. habil. Dagmar Quandt richten für ihre wissenschaftliche Expertise in sämtlichen „FACS“-Themen, die großartige, fröhliche Zusammenarbeit und ihre exzellente Unterstützung in der Durchführung und Auswertung der murinen und humanen durchflusszytometrischen Versuche.

Den bestehenden und teils ehemaligen Mitarbeiter*innen der AG Kielstein danke ich für ein tolles Arbeitsumfeld sowie ihre permanente Hilfs- und Diskussionsbereitschaft. Besonderen Dank gilt Susann Möschter und Franziska Knöfel für ihre freundliche Hilfe bei allen kleinen und großen Laborbelangen und vor allem für die zusätzlichen Hände bei der Bearbeitung der vielen BuffyCoats. Ein großer Dank gilt zudem Anja Hauffe für die großartige Zusammenarbeit im Labor, auch zu manch nächtlicher Stunde. Matthias Emde und Martin Allweyer danke ich für die gute Mausbetreuung. Ein weiter Dank gilt Dr. Tim Hohmann (AG Dehghani) für die freundliche Zurverfügungstellung des Hochleistungsrechners ohne dem die Auswertung der humanen Daten nicht möglich gewesen wäre.

Ebenso danke ich allen Kollegen*innen der gesamten Anatomie für die fachlichen und freundschaftlichen Gespräche im Büro, auf dem Flur, im Labor etc.

Der Einrichtung der Transfusionsmedizin des Universitätsklinikums Halle/Saale unter Leitung von Herrn Dr. Jörg Harth danke ich für die Bereitstellung der Buffy Coats.

Mein ganz großes Dankeschön gilt natürlich meiner Familie, insbesondere meinen Eltern, und meinen alten und neuen Freunden für den steten Glauben an mich, die stützenden Worte und Taten, die Geduld und das Verständnis für die Besonderheiten einer Dissertation. An dieser Stelle möchte ich mich auch nochmal besonders bei AABRAK bedanken. Ich wäre nie so weit gekommen.

Ein herausragender, besonderer Dank gilt Stephan, für seine stete Unterstützung in allen Lagen, seinem großen Verständnis und seinem unerschöpflichen Humor und Optimismus. Dankeschön. Ebenso danke ich seiner Familie für ihre stete Fröhlichkeit und dem unbeirrten Zuspruch und das Interesse an meiner Arbeit und dem erfolgreichen Abschluss. In stillem Gedenken an Bernd.